THE CILIOPATHY GENE *NPHP-2* FUNCTIONS IN MULTIPLE GENE NETWORKS AND REGULATES

CILIOGENESIS IN *C. ELEGANS*

By

SIMON ROBERT FREDERICK WARBURTON-PITT

A dissertation submitted to the

Graduate School – New Brunswick

and

The Graduate School of Biomedical Sciences

Rutgers, The State University of New Jersey

In partial fulfillment of the requirements

For the degree of

Doctor of Philosophy

Graduate Program in Molecular Genetics and Microbiology

Written under the direction of

Maureen M. Barr, PhD

And approved by

_____

_____

_____

_____

New Brunswick, New Jersey

January, 2015

ABSTRACT OF THE DISSERTATION

The ciliopathy gene *nphp-2* functions in multiple gene networks

and regulates ciliogenesis in *C. elegans*

By SIMON ROBERT FREDERICK WARBURTON-PITT

Dissertation Director: Maureen Barr

Cilia are hair-like organelles that function as cellular antennae. Cilia are conserved across

eukaryotes, and play a vital role in many biological processes including signal transduction,

signal cascades, cell-cell signaling, cell orientation, cell-cell adhesion, motility, interorganismal

communication, building extracellular matrix, and inducing fluid flow. In humans, cilia are

present in a majority of tissue types, and cilia dysfunction can lead to a range of syndromic

ciliopathies, including nephronopthisis (NPHP) and Meckel Syndrome (MKS).

Cilia have a microtubule backbone, the axoneme, and are composed of multiple

subcompartments, each with a specific function and composition: the transition zone (TZ)

anchoring to the axoneme to the membrane, the doublet region extending from the TZ, and in

some cilia types, the singlet region extending from the doublet region.

The nematode *C. elegans* is a well-established model of cilia biology, and possesses cilia

at the distal end of sensory dendrites. My work focused on exploring the role and function of

nphp-2, the *C. elegans* ortholog of mammalian *INVS/NPHP2,* and the relationships between

nphp-2, the TZ, and the doublet region. I found that TZ-associated genes can be grouped into

two redundant genetic modules that interact with *nphp-2* cell-type specific manner to regulate ciliogenesis and cilia placement. I also found that, like its ortholog Inversin (encoded by *INVS*), NPHP-2 localizes to the eponymous Inversin compartment, a subportion of the doublet region. *nphp-2* genetically interacts with other doublet region-associated genes; like TZ-associated genes, these interactions can also be organized into two redundant genetic modules. The doublet region modules regulate many aspects of cilia biology, including ciliogenesis, cilia placement, microtubule patterning, tubulin post-translational modification, and doublet region composition. Additionally, I characterized a positive and a negative regulator of the doublet region modules.

Together, these results help knit together data from mammalian models and *C. elegans*, and build a genetic framework between *nphp-2* and genes from multiple ciliary compartments, pulling together what were disparate threads to lead us to a better understanding of cilia biology.

Acknowledgments

This thesis was a very long time coming, and I'd like to thank everyone who supported me during these years. Thanks to my funding sources NIH and Waksman Institute for generously funding my research. Thank you to my colleagues Jinghua Hu, Ollie Blacque, Corey Williams, and Michel Leroux for reagents, advice, and good conversation at meetings. A big thanks to my thesis committee for making time for me and helping my project through some sticky spots. A huge thanks to the Barr Lab past and present, which has made coming to work a fun and amazing experience; you guys are such an amazing group of people and I've learned and changed (hopefully for the better!) from knowing all of you. I also apologize for going on a bit too much about Jurassic Park, which none of you are likely ever going to want to see again.

Thanks to my parents for never giving up on asking me when I was going to graduate, Julie for (PSST) never, ever letting it get too real, Brent for being a mathematical supergenius who introduced me to Elvira and drag queens, Becky for making me a Hippie, Natalia for endlessly (endless? :P) amazing conversation and hikes, dogs for existing, and Devin for being Devin. Also thanks to Square Enix, Namco, Bioware, Sony, Nintendo, Microsoft, the Vicar, Eddy and Patsy, Hyacinth, The Doctor, Matt Groening, Hideo Kojima, Stephen Baxter, Madonna, Lady Gaga, Exes, etc etc for keeping me sane and entertained.

And thank you to Maureen, without whom none of this would ever have happened, who never ran out of patience for my antics, who trusts me, and who let me be my own scientist.

Also, Devin again.

Table of Contents

Table of Figures

Table of Tables

Chapter 1: Cilia Biology and the Inversin Compartment

1.1 – Introduction to cilia

1.1.1 – Introduction

On the whole, cilia and flagella are amongst the most remarkable organelles, with wide-ranging structure and function, and define eukaryotes in the same manner as nuclei and mitochondria (Cavalier-Smith, 2002). Members of this class range from the simple thread-like mammalian primary cilia, bent by fluid flow in the renal lumen; to the willow-like chemosensory AWA, used by *Caenorhabditis elegans* to taste the environment; and to the pair of synchronously beating flagella used by *Chlamydomonas* to glide through pond water. In humans, cilia are fundamental to life. Their sweeping motion guides eggs through fallopian tubes towards flagella-driven sperm, enabling fertilization. During embryogenesis, cilia drive developmental signaling pathways, break left-right symmetry post-gastrulation, and regulate the development of most organs, including hearts and kidneys. After birth, cilia allow us to see, hear, smell, and taste the world. But for all their variety in role and purpose, a majority of cilia share a similar underlying logic in structure and composition.

1.1.2 – Abstract

Cilia are cellular antennae, a membrane-clad microtubule skeleton protruding from the cell surface. Cilia function in many fundamental processes, including sensation, motility, development, adhesion, and vesicle release. Cilia can be divided into several subcompartments with distinct compositions, structures, and roles. A recently discovered subcompartment is marked by the localization of Inversin, a protein that has been implicated in modulation of Wnt-signaling, cilia placement, and cilia assembly/disassembly. Other proteins have also been

found to localize to this "Inversin compartment", including Nek8, Nphp3, and Anks6. These

Inversin compartment components genetically and physically interact with numerous ciliary and

non-ciliary partners; this suggests that the Inversin compartment is intertwined with many

aspects of cilia biology. In this chapter, I discuss the biology of the Inversin compartment: its

characterization, composition, role in signaling pathways and signal transduction, and its

interactions with cilia base components, revealing the many facets of Inversin compartment

structure and function. The abundance of new evidence allowed us to explore many questions:

How do we define this proximal ciliary compartment? How is it established? What are its

structural features? What is its protein and lipid composition? How are these aspects

modulated? How are these features conserved across cilia types and organisms? And the

$64,000 question: What is the function of the Inversin Compartment?

1.2 – Brief Overview of Cilia Biology

1.2.1 – Cilia structure[1]

Defining the structure of cilia has taken many years and careers, though the task is not yet

complete (ultrastructure reviewed in Fisch and Dupuis-Williams, 2011). Mammalian renal tubule

primary cilia, a common cilia model, comprise a microtubule backbone clad with membrane,

anchored to the cell at the base (Figure 1). At this base lies the centriole-derived basal body,

composed of nine microtubule triplets. Nine microtubule doublets extend from these triplets

away from the cell, forming the transition zone (TZ). The TZ anchors the ciliary microtubule

---

[1] NB: Often, when specific ciliary sublocalization of a reporter cannot be determined (usually due to the absence of colabelling with known reporters), nonspecific terms are used. "Proximal cilium" refers to the portion of the cilium nearest the cell body/dendrite, encompassing any or all of the basal body, TZ, InvC, and doublet region; "distal cilium" refers to the portion of the cilium furthest from the cell body, encompassing the singlet region and distal tip.

structure—the axoneme—to the membrane through Y-links composed partly of MKS and NPHP

proteins. These membrane anchors pucker the outer ciliary membrane in a distinctive pattern

visible by electron microscopy, called the ciliary necklace due to its appearance (Gilula and Satir,

1972). The microtubule doublets of the TZ then extend much further, forming the ciliary shaft.

In some cilia types, microtubule singlets, in turn, extend from the doublets. This distal

microtubule singlet region can be permanent as in *C. elegans* amphid channel and phasmid cilia,

or transient, as in *Chlamydomonas*. While the above general arrangement holds true in most

cilia, in *C. elegans*, the basal body degenerates after ciliogenesis, leaving the TZ as the primary

anchor (Perkins et al., 1986) (Figure 1). In addition to the structural singlet and doublet

microtubules discussed above, there are often a number of microtubule singlets[2] that lie near

the center of the cilium and run along its entire length. These are required for motility in flagella

and motile cilia, but have an unknown function in sensory cilia.

A word of caution is warranted before moving forward, though. Though almost all literature,

including this dissertation, treats cilia as broadly comparable, it is important to remember that

there is no such thing as a "standard" cilium. All cilia are specialized for specific purposes, and

because of the diversity of these purposes, there are almost no universally common features.

Not all cilia have all subcompartments, cilia ultrastructures can be vastly different, many cilia

components play different roles in different in different cell types, and many components are

not universally conserved in ciliated and flagellated organisms. A brief description of the various

ciliary compartments follows (Figure 1).

Periciliary membrane. In general, the base of the cilium, including the periciliary membrane,

---

[2] These are henceforth referred to as "central singlets" to distinguish them from the nine structural
microtubule singlets. In standard cilia and flagella nomenclature, cilia and flagella re categorized as the
number of outer microtubules plus the number of central singlets, e.g., 9+2. *C. elegans* amphid cilia can
range from 9+0 to 9+5 (Perkins et al., 1986).

basal body, transition fibers, and transition zone function to regulate ciliary targeting and import of cilia components. The plasma membrane surrounding the cilia base plays a specialized role in cilia biology (Reviewed in Nachury Seeley 2010). This membrane compartment can be five or more times wider than the cilium itself, and is surrounded by a diffusion barrier (Hunnicutt et al., 1990; Vieira et al., 2006). This barrier may be formed by galectin-3 (Clare et al., 2014), Usher Syndrome proteins (Maerker et al., 2008), or Septin 2, the latter of which is required for localization of cilia membrane proteins and cilia function in the Sonic Hedgehog pathway (Hu et al., 2010) (See 1.5.1 – Signal Transduction and Amplification). Membrane composition may be defined solely by lipid rafts, though the actin cytoskeleton underlying the membrane may divide it into "nanocells", small patches of membrane to which transmembrane proteins are restricted (demonstrated in a series of papers from the Kusumi lab: Fujiwara et al., 2002; Morone et al., 2006; Nakada et al., 2003). Because the cilia and plasma membranes are divided, membrane proteins cannot freely travel between them. The periciliary region acts as a "landing strip" for vesicles from the rest of the cell loaded with ciliary cargo. These vesicles, laden with transmembrane cilia proteins, fuse to the membrane here, allowing the cilia proteins to be trafficked into the cilium through intraciliary trafficking pathways (Pazour and Bloodgood, 2008). The periciliary region is also the likely site of extracellular vesicle release in several ciliated cells, including the CEMs of male *C. elegans* (Wang et al., 2014). Rab8 and its activator Rabin8, which function together to target endosomes from the cell body to the cilia base, mediate some of these vesicular pathways (Molla-Herman et al., 2010; Moritz et al., 2001). The exocyst (not exorcist!) tethering complex regulates binding of these vesicles to the cilia membrane (modelled in Fogelgren et al., 2011). Both the polarized trafficking factors Rab8/Rabin8 and the exocyst complex are required for ciliogenesis and cilia function, and can lead to disease when disrupted (Fogelgren et al., 2011; Kaplan et al., 2010; Nachury et al., 2007; Zuo et al., 2009).

Distal dendrite. Because the cilia of *C. elegans* are found at the distal end of dendrites, they do not have a circular periciliary membrane patch surrounding them as mammalian cilia do. Instead, the dendritic tip constitutes the periciliary membrane, and can be distinguished from the rest of the dendrite by an enlarged diameter. The volume enclosed within the dendritic tip acts as a delivery and sorting center for ciliary traffic, connecting the ciliary traffic network to the dendritic microtubule traffic network. In addition to the functions described for the periciliary membrane described above, in amphid cilia, the distal dendrite is required for dendritic extension (Heiman and Shaham, 2009).

Ciliary pocket/pore. Much of what is known about the cilia pocket was established in the 1960s, but recent work has linked this region to ciliogenesis, and exocytosis/endocytosis at the cilia base (Sorokin, 1962; Sorokin, 1968; reviewed in Ghossoub et al., 2011). As the primary function of the cilium is as a liaison with the environment, the extracellular environment it lies in is critical to its function; mammalian and *C. elegans* cilia greatly differ in this respect. In mammalian cilia, most of the length of the cilium is directly exposed to the environment. Membrane around the cilia base is invaginated (shaped by the actin cytoskeleton) and the gap between the cilium and the plasma membrane is filled with extracellular matrix (Molla-Herman et al., 2010). The ciliary pocket of mammalian cilia is the site of active endocytosis*.*

C. elegans cilia, on the other hand, are completely buried within the ciliary pores, spaces contiguous with the external environment and wrapped by a sheath and a socket cell (Figure 2). This extracellular lumen is also filled with extracellular matrix (Perkins et al., 1986). Little is known about the composition of this matrix, though matrix proteins are present in ciliary-promoter-derived ciliomes and are upregulated in male ciliated neurons (Wang et al., 2014), and several transmembrane ciliary proteins have interaction domains (including protein-protein and glycosylated protein binding domains) on their external face (Bycroft et al.,

1999; Moy et al., 1996).

Basal Body. The basal body (BB) forms the "root" of the cilium, anchoring the cilium to the cytoskeleton and connecting the ciliary traffic network to the rest of the cell. The basal body is enriched in gamma-tubulin, suggesting that it is the site of active microtubule nucleation (e.g., Silflow et al., 1999). In mammalian cilia, the basal body is composed of the microtubule triplet centriole and centriolar associated protein (CEP) complex. The CEP is attached to the membrane through nine propeller-like transition fibers[3]. The transition fibers possibly attach to the membrane through Cep164 and ODF2 (Graser et al., 2007; Ishikawa et al., 2005). The transition fibers act as site for docking of intraflagellar transport (IFT) components, in a DYF-19/FBF1 specific manner, bound for the cilium (Wei et al., 2013).

The existence of a basal body in *C. elegans* cilia is contentious. After ciliogenesis (See 1.2.4 – Ciliogenesis), centrioles undock from the cilia base, leaving a portion of the CEP complex behind (including the ciliopathy protein HYLS-1 [Dammermann et al., 2009]); in *daf-19* mutants, which are missing the master ciliogenesis transcription factor, centrioles are found where the cilia base is expected to be (Perkins et al., 1986). This demonstrates that the centriole is present at the cilia base of *C. elegans* cilia for some portion of time. Some groups maintain that although the mature *C. elegans* cilia base does not contain a centriole (Perkins et al., 1986), the complex that is left behind constitutes a functionally conserved basal body (Williams et al., 2011). This hypothesis is supported by (1) localization of the centrioles in *daf-19* mutants (2) localization of the centriolar protein HYLS-1 to the cilia base in *C. elegans*, and (3) conservation of ultrastructural features (transition fibers). Both the BB and the *C. elegans* pseudo-BB[4] function

---

[3] Transition fibers may not exist in all cilia types. Detailed EM analyses in *C. elegans* suggest that "transition fibers" may be an EM artifact, and are actually splayed microtubule doublets that are not recognizable as such because the angle between the microtubules and the plane of the EM slices (Doroquez et al., 2014).
[4] In this work, we use the term "pseudo-BB" to represent the region of the *C. elegans* cilium analogous to

in regulation of traffic into and out of the cilium; IFT components are enriched in this compartment.

Transition Zone (TZ). The first compartment of the cilium proper is the transition zone: it is formed of microtubule doublets, and has a complex structure and multiple functions, including anchoring the cilium to the membrane and regulating ciliary traffic. It is described in detail below (and reviewed in Szymanska and Johnson, 2012).

Doublet region. The microtubule doublets of the transition zone extend to form the doublet region. In mammalian cilia, the doublet region constitutes the rest of the cilium; in *C. elegans* amphid and phasmid cilia the doublet region constitutes approximately half the length of the cilia shaft, giving the region its alternate name, the middle segment (Perkins et al., 1986). The doublet region has few known specific functions. In mammalian cilia, as it forms the largest ciliary compartment, it is the site of most signal transduction. In *C. elegans*, most signal transduction components localize to both the doublet and singlet regions, such that it is unknown whether the doublet region has specific signal transduction functions. The doublet region does contain passing cargo bound for and returning from the distal singlet region (Ou et al., 2005); this passing traffic can hypothetically be modulated by doublet region components. New evidence also suggests that the doublet region correlates to cilia shape (Malan Silva, Personal Communication).

Inversin Compartment (InvC). Unlike the other cilia regions described here, the Inversin compartment is actually a portion of another region of the cilium, the doublet region. This region is defined by the localization of Inversin (Shiba et al., 2009). The Inversin compartment is the main focus of this dissertation; the origin and possible function of the InvC are described in detail below, and in Chapters 3 and 5.

---

the mammalian basal body; this term reflects both the similarities and the differences between *C. elegans* and mammalian basal bodies.

Singlet region. Singlet microtubules extend from the microtubules of the doublet region into the distal region; in some cilia types, only one microtubule from each doublet extends (the B-tubule), whereas in other cilia types both microtubules from each doublet extend (A- and B-tubules) (Perkins et al., 1986), (Malan Silva, Personal Communication). There are exceptions to this: singlets of a few cilia, including CEP and amphid wing cilia (discussed in Chapter 3), are formed de novo (Doroquez et al., 2014; Perkins et al., 1986). The singlet region is often very specialized in shape and defines the function of a given cilium (Doroquez et al., 2014). In *C. elegans*, it is often the only portion of the cilium that is directly exposed to the environment and so is frequently linked to signal transduction pathways.

Distal tip. The distal tip of the cilium has no microtubules, and functions in vesicle release and turnaround of intraciliary trafficking components. The distal tip may also have a role regulating the length of the cilium.

1.2.3 – The ciliary transition zone

The ciliary transition zone lies at the base of the cilium between the basal body and the cilia shaft, and is so named because it is the transition between the cell and the cilium. The transition zone was first identified in TEM micrographs: it appeared as a circle of microtubule doublets held in place by an interior ring-like structure, linked to the membrane through 'Y' shaped protein links (Gibbons and Grimstone, 1960; Ringo, 1967). These Y-links are hypothesized to be composed in part of MKS and NPHP proteins. MKS and NPHP proteins may have other roles in addition to this structural function, although none have any predicted enzymatic domains, and instead contain a large amount of protein-protein, protein-lipid, and calcium binding domains. MKS and NPHP proteins/genes fall into physical and genetic modules (Garcia-Gonzalo et al., 2011; Sang et al., 2011; Warburton-Pitt et al., 2012; Williams et al., 2011). These include, to

date: the MKS module (MKS1, MKS6, B9D1/MKS9, B9D2/MKS10, TCTN1, TCTN2/MKS8), the first

NPHP module (NPHP1, NPHP4), and the second NPHP module[5] (NPHP5, NPHP6, Ataxin10). As

new TZ genes are identified, they can usually be grouped with one of these modules. While the

MKS and first NPHP modules are almost universally conserved, work in *C. elegans* identifies

MKS-5/NPHP-8 as both an MKS and NPHP module component (Williams et al., 2011), whereas

work in mammalian cell culture identifies RPGRIP1L/MKS5/NPHP8 as a physical component of

the first NPHP module (Sang et al., 2011). In *C. elegans*, MKS-5 functions to organize the

localization of the entire MKS physical module but not components of the NPHP module, which

would place it firmly as a member of the MKS module; however, *mks-5* genetically interacts with

both *mks* genes and *nphp-4*, which places outside of both modules (Williams et al., 2011). (For a

discussion of the unique genetic interactions between *mks-5* and *nphp-2*, see **Error! Reference**

ource not found.).

The TZ has many proposed functions, but all can be categorized as either gating or anchoring.

The first proposed function for the Y-links is anchoring the cilium to the membrane. Y-links

physically connect the microtubules of the axoneme to the membrane. Disruption of TZ links in

mutants has been linked to misplaced cilia in this and other work (Warburton-Pitt et al., 2014;

Warburton-Pitt et al., 2012; Williams et al., 2010). TZ anchoring is required for proper

ciliogenesis, as interactions between the TZ, basal body, and membrane are required during the

first step of ciliogenesis (See below, 1.2.4 – Ciliogenesis).

The second set of proposed functions relate to a gating function. As the Y-links physically fill the

TZ, they act as an occlusion mechanism, preventing large soluble molecules or membrane

components from freely diffusing into or out of the cilium (Awata et al., 2014; Cevik et al., 2013;

Huang et al., 2011; Kee et al., 2012). Disruption of the TZ leads to leakage of components in both

---

[5] Or the "JBTS module", coined by Szymanska and Johnson, 2012.

directions (Cevik et al., 2013; Huang et al., 2011; Williams et al., 2011). Startlingly, 3D reconstructions of TZ EMs reveals that gaps between neighboring Y-links are the exact same shape and size as IFT trains, implying that the TZ plays a critical role in regulation of IFT. The position of the TZ in the cilium necessitates its involvement in other ciliary trafficking pathways, including the nuclear pore-like Ran-importin system (Dishinger et al., 2010; see **Error! Reference ource not found.**) and the Unc119b protein shuttle (Wright et al., 2011; see Chapter 3, and 1.4.4 – Establishing the Inv Compartment), though how these intersect is completely unknown.

1.2.4 – Ciliogenesis

There are two primary methods of ciliogenesis (called here types A and B), which vary depending on cell type (Figure 3) (summarized in Williams et al., 2011).

> **Step One (Type A):** The centrosome protein complex is assembled around the centrioles, forming the proto-basal body. This complex then binds the ciliary vesicle, a step that may depend on the ciliopathy gene OFD1/JBTS10 and Talpid3 (Singla et al., 2010; Yin et al., 2009). The microtubules of the basal body then extend and impinge on the vesicle membrane, forming the proto-TZ. (The microtubule growth in this step is likely to be driven by tubulin diffusion, as IFT mutants still have this stunted cilium.) The microtubules of the proto-TZ bind to the vesicle membrane through Y-links. This ciliary vesicle complex then docks and fuses to the plasma membrane.

> **Step One (Type B):** After the centriolar protein complex is assembled, it docks directly with the plasma membrane. The microtubules of the basal body then extend, forming the TZ, which further anchors the cilium to the membrane.

> **Step Two (Types A and B):** IFT drives further extension of the cilium to its full length, and ciliary subregions are established through microtubule patterning pathways.

An important recent paper clarified several aspects of ciliogenesis in *C. elegans*, and tied them to distinct mechanisms (Williams et al., 2011). The first step is mediated in part by TZ complexes, described in the previous section; disruption of this step in severe TZ mutants may lead to knock-on defects in the second step of ciliogenesis. Targeting of the basal body to the plasma membrane can be controlled by Disheveled, a component of Wnt signaling pathways (Vladar and Axelrod, 2008) (See 1.5.1 – Signal Transduction and Amplification). The second step is driven by IFT and BBS complexes (described in the section below); during this step, the TZ functions primarily as a ciliary gate. The processes of the second step of ciliogenesis continue throughout the lifetime of the cilium, maintaining the cilium. Additional pathways also specifically regulate cilia maintenance, as described below. The division between the two steps of ciliogenesis and the different mechanisms driving each step is highlighted by the facts that defects in IFT mutants appear markedly different from TZ mutants, and that as a whole, TZ mutants tend to have relatively normal IFT rates.

1.2.2 – Intraflagellar Transport

Intraflagellar Transport (IFT) is the primary ciliary cargo transport mechanism, consisting of bidirectional movement of IFT particles along the length of the axoneme[6] (Figure 4). Cargo carried by IFT can include receptors and structural components (e.g., tubulins [Bhogaraju et al., 2013; Bhogaraju et al., 2013] and PKD-2 [Bae et al., 2006]). In *C. elegans*, anterograde transport (from the cilia base to the cilia tip) is mediated by two microtubule motors: heterotrimeric kinesin-II (KLP-11, KLP-20, KAP-1) and homodimeric OSM-3. Kinesin-II and OSM-3 function cooperatively in microtubule doublet cilia regions (the basal body, TZ, and doublet region), and OSM-3 alone functions in microtubule singlet regions (Ou et al., 2005). Retrograde transport

---

[6] In the context of this dissertation, cilia and flagella are synonymous terms

(from the cilia tip to the cilia base) is mediated by IFT dynein, which functions in all cilia regions. The IFT transport complex comprises two subcomplexes, IFT-A and IFT-B, which are linked by the BBSome. In some BBS mutants, the two IFT subcomplexes become separated and travel independently, leading to defects in ciliogenesis. Each of the two anterograde IFT motors is associated with a specific IFT particle: Kinesin-II is bound to IFT-A, and OSM-3 is bound to IFT-B. Though Kinesin-II and OSM-3 have different intrinsic velocities, because the entire IFT complex is bound together, the complex travels at an intermediate speed. Measurement of IFT particle velocity is often used to characterize trafficking and localization of cilia proteins and diagnosis specific defects in cilia mutants, as different cargo-motor associations or mutant defects yield characteristic velocity profiles (e.g., Table 2). IFT motor function and expression can be modulated in a cell specific manner, either by altering the ratio of motors (Evans et al., 2006) or by unlinking the two IFT subcomplexes (Mukhopadhyay et al., 2007). Secondary motors, such as kinesin KLP-6, can also bind to the IFT complex and modulate its velocity (Morsci and Barr, 2011). IFT is slightly modified in other cilia models: KIF17, the ortholog of OSM-3, functions as the primary IFT motor, whereas Kinesin-II functions to specialize cilia.

Although it was earlier believed that IFT complexes traveled along ciliary microtubules independently (as illustrated in the model in Figure 4), we now know that IFT particles travel along the axoneme in long multi-subunit trains. These trains have dynamic morphology dependent on both the direction of travel (anterograde trains are longer and narrow, while retrograde trains are short and compact [Pigino et al., 2009]) and length of cilium (the longer the axoneme, the shorter the trains, though the number of trains increases [Engel et al., 2009]). IFT trains are tightly associated with the flagellar membrane; this may be mediated via conserved membrane-binding domains in IFT peptides, interactions with ciliary proteins, (e.g., membrane associated ARL-13 and transmembrane MKS-3), or both.

1.3 – Ciliopathies and cystic kidney disease

Cystic kidney diseases are a large group of interrelated disorders, marked by abnormal

nephrodevelopment leading to the formation and progressive enlargement of cysts, often

comorbid with extrarenal manifestations including retinal degeneration, *situs inversus*, and

neurological disorders. This spectrum disorder includes Nephronophthisis (NPHP), Meckel

(MKS), Senior-Løken (SLS), and Joubert (JBTS) Syndromes, which in some instances share loci

(Reviewed in Baker and Beales, 2009). Initial studies of these disease genes revealed an

association between these cystic kidney diseases and the cilium; this class of disease is now also

known as the ciliopathies, diseases of the cilium (Figure 5).

Primary renal cilia lie at the root of most cystic kidney diseases. These cilia are thought to act as

mechanosensors of urine flow, indicating the onset of glomerular filtration; when development

has progressed to this point, the cilia precipitate a shift to a second nephrodevelopmental

pathway. Functional (e.g., mutations in mechanoreceptors and ion channels) and morphological

(e.g., mutations in ciliogenesis genes, maintenance genes) defects in the cilium break this

pathway and subsequently lead to abnormal proliferation, protein sorting, and cyst

development (Reviewed in Hildebrandt and Zhou, 2007).

Because a majority of human cell types possess cilia and require them for normal function,

ciliopathies have many secondary, extrarenal manifestations. As cilia of different cell types vary

in form, function, and basic biology, specific ciliary defects affect these different cell types in

different manners. This variety can yield a specific spectrum of symptoms. Clinicians group

ciliopathies depending on this set of symptoms: there are over 16 subtypes of

Nephronophthisis, 11 subtypes of Meckel Syndrome, and 20 subtypes of Joubert Syndrome

(Table 3). As specific subtypes are linked by broader symptoms, causative genes often function

in related pathways (e.g., described above, there is a MKS complex at the TZ composed, in part, of MKS1, MKS3, MKS5, and MKS6). Before the advent of large-scale ciliome screens, mapping mutations in ciliopathy patients was an extremely powerful method of identifying cilia genes and establishing their relationship to one another.

Caenorhabditis elegans is a powerful model for investigating these ciliopathies, including autosomal dominant polycystic kidney disease (ADPKD) and NPHP (Barr and Sternberg, 1999; Jauregui and Barr, 2005; Winkelbauer et al., 2005). Though lacking kidneys, *C. elegans* has functionally conserved cilia. Many cystic kidney disease genes are present and perform similar functions to higher fish and mammalian homologs. Novel ciliary genes have been identified in animal models of ciliopathies and subsequently found to be the causative agents in human cystic diseases of previously unknown etiology (e.g., in *C. elegans, bbs-5* has been linked to Bardet-Biedl Syndrome [Li et al., 2004], and in *Mus musculus, NEK8* linked to NPHP9 and *INVS* has been linked to NPHP2 [Otto et al., 2008]), illustrating that animal models provide fertile ground for novel research in this area. Additionally, cilia genes identified and characterized in *C. elegans* have later been found to be causative in newly classified ciliopathies (e.g., *mksr-1* in MKS9 and *mksr-2* in MKS10 [Dowdle et al., 2011; Hopp et al., 2011; Williams et al., 2008]).

1.4 – Characterizing the Inversin Compartment

1.4.1 – Discovering a proximal ciliary compartment

Definitions of the proximal cilium have often been confusing and incompatible. Originally, the term applied primarily to the first handful of microns of a given cilium or flagellum, but without specification to the number of microns or to where to begin measuring this distance. Eventually, it was found that a specialized compartment, with distinct structure, composition, and function

lay in this region. This compartment, the TZ, functions in protocilium-cilia vesicle-cell membrane interactions in early ciliogenesis, and in intraciliary trafficking in the mature organelle (Sorokin, 1962; Williams et al., 2011). The cilia shaft extends from the TZ, and can range in length from one to dozens of microns. However, further evidence emerged that the TZ did not constitute the entire proximal cilium.

In some models, the proximal and distal portions of the cilia shaft can exhibit distinct ultrastructure (Perkins et al., 1986; Reese, 1965). The proximal cilia shaft—the "middle segment" in *C. elegans* parlance—possesses microtubule doublets arranged about the center of the lumen, similarly to the whole of the flagellar shaft of *Chlamydomonas* and mammalian primary cilia. The distal portion of the cilia shaft—the "distal segment", in worm literature— possesses microtubule singlets arranged in a disorganized manner. In the early 1990s, the idea of a distinct post-TZ compartment appeared in *Chlamydomonas* literature, when it was discovered that the proximal half of *Chlamydomonas*' axoneme was associated with different dynein heavy chains than the distal portion (Piperno and Ramanis, 1991), and was specifically glutamylated (Fouquet et al., 1996).

Evidence for a proximal, post-TZ, ciliary compartment has also been found in *C. elegans*. In work characterizing intraflagellar transport (IFT), a microtubule motor based transport system that builds and maintains cilia and flagella, Jonathan Scholey's group demonstrated that *C. elegans* amphid channel cilia were built by two separate, but coordinated, kinesin motors (Snow et al., 2004). They found that while the motor OSM-3 was capable of building the entire cilium (TZ, doublet region, and singlet region), the second IFT motor Kinesin-II was only capable of building the TZ and doublet region (Perkins et al., 1986; Snow et al., 2004). In addition, the localization of Kinesin-II was restricted to this proximal region (Snow et al., 2004). This evidence from *Chlamydomonas* and *C. elegans* supported the idea of a distinct conserved, post-TZ ciliary

subcompartment, though the structure and composition appeared to differ between models, and the compartment had no identified function.

The floodgates opened in 2009 when the Yokoyama group published foundational work detailing the ciliary localization of a nephropathy-associated protein, Inversin (Shiba et al., 2009). Using immunogold antibodies, they demonstrated that in mammalian primary cilia Inversin strictly localized to a small ~2μm subcompartment directly distal to the TZ. Further work demonstrated that Inversin was required for the localization of multiple other proteins to this "Inversin compartment" (InvC), including Nphp3, Nek8, and Anks6 (Fukui et al., 2012; Hoff et al., 2013; Shiba et al., 2010). In *C. elegans*, multiple doublet region-restricted proteins in addition to Kinesin-II components were also found, including ARL-13, ARL-3, HDAC-6, UNC-119, and the Inversin homolog NPHP-2 (Cevik et al., 2010; Li et al., 2010; Warburton-Pitt et al., 2014; Warburton-Pitt et al., 2012); the doublet region was also found to be specifically glutamylated (O'Hagan et al., 2011).

1.4.2 – Defining the Proximal Cilium

The *C. elegans* doublet region is often understood to be analogous to the mammalian InvC, in part because of the partial-length localization patterns of several ciliary proteins (Blacque and Sanders, 2014; Cevik et al., 2010; Cevik et al., 2013; Warburton-Pitt et al., 2012; Wojtyniak et al., 2013). However, our recent work indicates that *C. elegans* possesses a conserved InvC that is distinct from the doublet region (Warburton-Pitt et al., 2014). This assessment is strongly supported by evidence demonstrating several *C. elegans* doublet region proteins, including the Kinesin-II components KLP-11 and KLP-20, the histone deacetylase HDAC-6, and the small GTPase ARL-13, have full length ciliary localization in the primary cilia of multiple mammalian cell types, including HEK293, MEF, IMCD3, RPE1, MDCK, and human fibroblasts (Fan et al., 2004;

Follit et al., 2009; Hori et al., 2008; Larkins et al., 2011; Lee et al., 2012; Pugacheva et al., 2007;

Sanchez de Diego et al., 2014; Satish Tammana et al., 2013; Wright et al., 2011; Wu et al., 2006;

Zhou et al., 2006). Furthermore, the doublet region-associated protein ARL-13 has been

demonstrated to have differing localization patterns in different larval stages (Cevik et al., 2013),

but the Inversin ortholog NPHP-2 is restricted to the proximal cilium in all larval stages

(Warburton-Pitt et al., 2014). This evidence confirms the hypothesis first proposed by Perkins *et
al.*: the *C. elegans* doublet region is analogous to the whole shaft of the primary cilium, and not

the InvC (Perkins et al., 1986). The *C. elegans* microtubule singlet region appears to be a

specialized ciliary compartment, not always present, and with widely varying morphology

(Doroquez et al., 2014). Other organisms also exhibit a microtubule singlet region, including

Chlamydomonas, in which a singlet region is present transiently during mating.

1.4.3 – The Inversin Complex

Fortuitously, the first InvC component characterized, Inversin, is relatively upstream in the

process that establishes the subcompartment—Inversin is strictly required for InvC localization

of most known InvC components, and the *C. elegans* ortholog *nphp-2* is required for localization

of TAX-2 and partially required for TAX-4. Inversin localizes to the InvC (Shiba et al., 2009),

physically interacts with itself (Wright et al., 2011), and both Inversin and NPHP-2 are possibly

membrane associated (Shiba et al., 2009; Warburton-Pitt et al., 2012); Inversin has also been

reported to localize to the basal body in addition to the InvC (Otto et al., 2003; Sang et al.,

2011). Very little is known about the localization dependencies of Inversin; it has been shown to

require the TZ protein B9d2 in zebrafish kinocilia, but these cilia do not possess a proximal InvC

(Zhao and Malicki, 2011). The MYND domain encoding *daf-25* is also required for *nphp-2*

expression or protein stability in *C. elegans* in several cilia types (Wojtyniak et al., 2013). DAF-25,

an ortholog of mammalian Ankmy2, localizes to cilia—though subciliary localization is unclear—

and regulates localization of a membrane-associated guanylyl cyclase (Jensen et al., 2010).

Inversin requires its ankyrin repeat-containing N-terminal region (Mochizuki et al., 1998;

Morgan et al., 1998) for cilia targeting and import, and requires a C-terminal ninein homology

domain for restriction to the InvC (Shiba et al., 2009). The Inversin C-terminal region also

contains a calmodulin-binding IQ domain that is required for localization and function (Morgan

et al., 2002; Otto et al., 2003; Yasuhiko et al., 2001). The calmodulin that physically interacts

with Inversin, CALM2, localizes along the entire cilium and at the basal body (Otto et al., 2005;

Shiba et al., 2009). The ankyrin repeat region of NPHP-2 also appears to be required for

targeting to the cilium in AWB neurons (Wojtyniak et al., 2013), but the C-terminal ninein

homology and IQ domains do not appear to be conserved. However, NPHP-2 does encode a

predicted Ca^{2+} binding EF-hand which may function analogously to the IQ domain of Inversin

(Warburton-Pitt et al., 2012); this EF hand is required for ciliary targeting in amphid channel and

phasmid cilia (Warburton-Pitt et al., 2014).

Physical interaction studies have identified a physical complex of Inversin-associated proteins,

including Nek8, Nphp3, and Anks6 (Bergmann et al., 2008; Fukui et al., 2012; Hoff et al., 2013;

Mahjoub et al., 2005; Shiba et al., 2010). These three proteins require Inversin for restriction to

the InvC (Hoff et al., 2013; Shiba et al., 2010), but not for ciliary import (Nakata et al., 2012).

Unsurprisingly, the N-terminal portion of Inversin is insufficient for InvC restriction of Nek8

(Shiba et al., 2010). It has been speculated that Nek8 and Anks6 bind Inversin through Inversin's

ankyrin repeat region (Hoff et al., 2013; Shiba et al., 2010). Anks6 stabilizes the InvC complex by

enhancing Inversin-Nek8 binding (Hoff et al., 2013). Nek8 and Anks6 themselves physically

interact, though they do not require each other for localization; this interaction is mediated by

an ankyrin-region hydroxylated arginine of Anks6 and the kinase domain of Nek8 (Hoff et al.,

2013). Like Anks6, Inversin contains a strongly conserved hydroxylation motif in its Ankyrin

repeat region (Hoff et al., 2013; Warburton-Pitt et al., 2014), which could plausibly play a similar

role in Invesin-Nek8 physical interactions. The hydroxylase that physically interacts with Anks6

and Inversin, HIF1AN (Rual et al., 2005), is not restricted to the InvC (Hoff et al., 2013).

Nek8 requires its catalytic kinase domain for InvC localization, but it alone is not sufficient for

ciliary targeting. Nek8 with a T162E mutation in the kinase activation loop is hyperactive and

seems to lose InvC restriction, but not cilia targeting (Zalli et al., 2012). Nek8 also contains an

RCC (remodeling of condensed chromatin) domain that is required for InvC restriction but not

ciliary targeting (Sohara et al., 2008). These disparate targeting motifs suggest against a

common InvC signal, and the data indicates that Inversin is the earliest known progenitor of the

compartment. Further proteins have been identified as physical interactors of the Inv complex,

including Ahi1 (Wright et al., 2011), Anks3, Sdha, Nek7, Sptbn1, Eef1d, and Vdac2 (Hoff et al.,

2013), though of these, only Ahi1 has a known relevance to cilia biology.

The localization requirements of Nphp3 have also been clearly characterized. Nphp3 localizes to

the InvC in a three step process (Nakata et al., 2012). First, a coiled-coil region targets Nphp3 to

the basal body. Second, Nphp3 translocates into the cilium in a manner dependent on its

N-terminal myristoyl side chain; deletion of the myristoylatable residue results in cilia base

accumulation of Nphp3. Third, residues 202-595 interact with Inversin, which restricts Nphp3 to

the InvC (Nakata et al., 2012; Shiba et al., 2010). Similarly to the case of Nek8, the N-terminal

portion of Inversin is not sufficient to restrict Nphp3 to the InvC (Shiba et al., 2010).

1.4.4 – Establishing the Inv Compartment

Little is known about how the InvC is initially established in any system, despite repeated

attempts. A quick note regarding the interpretation of localization data: it's difficult. If in a given

gene knockdown an InvC protein is only restricted to the InvC in half of cilia observed, is that

gene required for InvC targeting? It clearly is not, because the protein can target and be

restricted to the InvC compartment. But on the other hand, it clearly is, as the protein is no

longer restricted properly in many cilia. It has been the case where the same data has supported

opposite conclusions based on how incomplete penetrance is regarded (Wojtyniak et al., 2013

vs Blacque and Sanders, 2014).

Though IFT is required both to build the unelaborated cilium and to specialize cilia, IFT seems

not to play a critical role in establishing the InvC. Neither NPHP-2, UNC-119, nor TAX-2/TAX-4—

which colocalize with NPHP-2 in some cell types—have been reported to move along the

axoneme in an IFT-associated manner (Warburton-Pitt et al., 2012; Wojtyniak et al., 2013;

Warburton-Pitt et al., 2014). The localization of TAX-2/TAX-4 is not restored following

photobleaching, also indicating that these proteins are not IFT trafficked (Wojtyniak et al.,

2013). Inversin has not been found to directly bind to any IFT polypeptide, though it may

interact indirectly (Zhao and Malicki, 2011). In *C. elegans*, *osm-3* mutants can localize TAX-2 in

AWB and ASK cilia and TAX-4 in ASK cilia (Wojtyniak et al., 2013). The kinesin-II component

klp-11 is also not required for NPHP-2 and UNC-119 proximal cilium targeting in phasmid cilia

(Warburton-Pitt et al., 2014), and the Kinesin-II component *kap-1* is not required for TAX-2

ciliary targeting in AWB cilia (Wojtyniak et al., 2013). However, Kinesin-II does play some role in

localization, if not trafficking, as in Kinesin-II mutants NPHP-2 and UNC-119 both mislocalize to

the BB, and TAX-2 expression is reduced (Warburton-Pitt et al., 2014; Wojtyniak et al., 2013).

Recent work indicates that an Unc119b-based shuttle system may be responsible for the

myristoyl-dependent translocation of Nphp3 into the cilium (Figure 6) (Wright et al., 2011).

Briefly, Unc119b binds lauroylated and myristoylated proteins at the BB/TZ ciliary traffic staging

area (Zhang et al., 2011), and the complex translocates into the cilium proper. Here, the

GTP-bound form of Arl3 binds Unc119b (Veltel et al., 2008). RP2 binds the Arl3-Unc119b

complex and triggers Arl3 to hydrolyze its GTP (Grayson et al., 2002; Veltel et al., 2008), and Arl3

in turn triggers conformational changes in Unc119b that cause the release of acylated cargo into

the cilium (Ismail et al., 2012; Wright et al., 2011). Unc119b is then bound by C5orf30—which

prevents reassociation of Unc119b and cargo—and then exits the cilium (Wright et al., 2011).

One of the cargoes of Unc119b is Nphp3, which binds Unc119b through its myristoyl side chain

(Wright et al., 2011). Without Unc119b or the myristoyl side chain, Nphp3 cannot localize to the

cilium, and remains at the TZ (Nakata et al., 2012; Wright et al., 2011). Multiple components of

the Unc119b shuttle localize to the InvC, including Unc119b itself and C5orf30 (Wright et al.,

2011), though other components, including RP2 (Hurd et al., 2010; Hurd et al., 2011) and Arl3

(Wright et al., 2011; Zhou et al., 2006) do not. It remains untested whether Unc119b or C5orf30

require Inversin for localization, or vice versa. The Unc119b shuttle is tightly linked to

membrane biology. The myristoylated and palmitoylated RP2 is membrane associated (Chapple

et al., 2000; Chapple et al., 2002), Arl3-GTP binds membranes specifically (Ismail et al., 2012;

Wright et al., 2011), Unc119b can extract proteins from membranes (Zhang et al., 2011), and

known cargoes are all membrane associated (Wright et al., 2011; Zhang et al., 2011).

Additionally, casual observation indicates that Inversin/NPHP-2 itself may be membrane

associated (Shiba et al., 2009; Warburton-Pitt et al., 2012). The Unc119b shuttle is not sufficient

for InvC restriction of shuttled proteins; as described above, Inversin is strictly necessary.

C. elegans possesses orthologs of Unc119 (*unc-119*) (Higashide and Inana, 1999), Arl3 (*arl-3*) (Li

et al., 2004), RP2 (*rpi-2*) (Williams et al., 2011), PDE6d (*pdl-1*) (Hukema et al., 2006), Arl13b

(*arl-13*) (Cevik et al., 2010; Li et al., 2010), and INPP5E (*cil-1*) (Bae et al., 2009), but it is unknown

if the shuttle systems themselves are conserved. UNC-119 localizes to the proximal cilium in

amphid and phasmid neurons (Warburton-Pitt et al., 2014), and *unc-119* is required for the

localization of the myristoylated receptors ODR-3 and GPA-13 (Zhang et al., 2011). *C. elegans* UNC-119 is structurally conserved enough to rescue Unc119b-/- defects when expressed in mammalian cell culture models (Wright et al., 2011). Unc119b shuttle components also have other roles in *C. elegans* ciliogenesis: *unc-119* is required for singlet region biogenesis (Ou et al., 2007), *arl-3* plays a role in IFT regulation and ciliogenesis (Li et al., 2010), and *arl-3* depletion suppresses *unc-119* ciliary defects (Warburton-Pitt et al., 2014). Additionally, *unc-119* appears to be required to traffic NPHP-2, as mutants display an accumulation of dendritic NPHP-2 and a shortened InvC, but *nphp-2* is not required for UNC-119 localization (Warburton-Pitt et al., 2014). Curiously, *nphp-2* and *unc-119* genetically interact in ciliogenesis, resulting in additive defects, suggesting that they function in parallel pathways (Warburton-Pitt et al., 2014).

A large body of work describes amino acid motifs, domains, and post-translational modifications that function to target proteins to the cilium; however, little is known about compartment specific targeting signals, and whether they even exist. Multiple ciliary proteins contain coiled-coils, including the proximally enriched/restricted components Nphp3 (Nakata et al., 2012), Inversin/NPHP-2 (Warburton-Pitt et al., 2012), TAX-4, CNG-3 (Wojtyniak et al., 2013), Evc/Evc2 (Caparros-Martin et al., 2013), LOV-1/PKD-2 (Barr and Sternberg, 1999) and transition zone components Cep290 (Nakata et al., 2012) and Cep164 (Graser et al., 2007), among others. Though Nphp3 requires the coiled-coil domain for TZ/BB targeting, Cep290 does not, indicating that this targeting motif is not universal; it is unknown whether this motif is required for localization of other InvC associated proteins (Nakata et al., 2012). As discussed above, acylation may also function to target proteins to ciliary membranes in a regulatable, reversible, possibly compartment specific manner (Godsel and Engman, 1999; Resh, 1999). In addition to abovementioned Nphp3, RP2, ODR-3, and GPA-13, there are several other myristoylated ciliary proteins, including the Unc119b-interacting cystin (Tao et al., 2009; Wright et al., 2011),

fibrocystin (Follit et al., 2010), Arl6, Tctn2, and the Kinesin-II Kif7 (Nakata et al., 2012), but none of these are restricted to the InvC (Cantagrel et al., 2008; Garcia-Gonzalo et al., 2011; Liem et al., 2009; Ward et al., 2003; Wiens et al., 2010; Yoder et al., 2002). Other ciliary targeting signals, including RVxP and Ax(S/A)xQ, are either not present in known InvC proteins, or not required for targeting (Wojtyniak et al., 2013). InvC restriction is most likely determined through physical interactions with other InvC components and not through a signal sequence or motif.

Finally, other proteins also appear to have proximal ciliary localization in some cilia types, including the Ofd1 interactor Lca5 (Coene et al., 2009; den Hollander et al., 2007), the Bug22 ortholog Gtl3 (Ishikawa et al., 2012), and CDKL5 in *Chlamydomonas* (Tam et al., 2013), though how they functionally, physically, and genetically interact with other InvC components is completely unknown.

1.4.5 – Membrane Dynamics of the Inv Compartment

Differential lipid composition of ciliary membranes has long been linked to specific ciliary localization of membrane-associated proteins. Several InvC-associated proteins possess membrane interaction motifs and localize to the membrane, suggesting the InvC regulates, or is regulated by, membrane interactions. However, little is known regarding characterization and regulation of its membrane biology. Lipid rafts are required for function and localization of CNG channel CNGA1, ortholog of *C. elegans* InvC component TAX-4, in photoreceptors, though these regions may not correspond to the InvC of other cilia (Brady et al., 2004; Ding et al., 2008). An Inversin physical interactor, Ahi1, is required for ciliary targeting and function of Rab8a, which is required for ciliary membrane trafficking; knockdown of Ahi1 itself leads to membrane and vesicle trafficking associated defects (Hsiao et al., 2009; Sang et al., 2011).

Protein acylation is an important mechanism for both membrane association and InvC targeting,

as seen in the case of the Unc119b shuttle (Nakata et al., 2012; Wright et al., 2011). A newly

described *C. elegans* protein, CIL-7, has been implicated in ciliary membrane and extracellular

vesicle (ECV) trafficking; CIL-7 is intriguing in that it is a myristoylated protein that requires

unc-119 for proper localization in a myristoyl side chain dependent manner (Julie Maguire,

Personal Communication). The InvC may also be linked to ciliary vesicular dynamics. Inversin

physically interacts with Clathrin, a membrane coat protein (Sang et al., 2011). CIL-7 functions in

regulation of ECV release (Julie Maguire, Personal Communication)

A more heavily characterized protein involved in ciliary membrane trafficking is the prenylated

INPP5E, which is translocated into the cilium by the Unc119b paralog PDE6d in an

Arl13b-specific manner (Figure 6) (Bae et al., 2009; Humbert et al., 2012). This shuttle system is

likely conserved in *C. elegans*, as described above. Interestingly, the *C. elegans* INPP5E homolog

cil-1 may genetically interact with *nphp-2,* indicating a link between the two acyl shuttles; *per*

contra, *nphp-2* does not appear to be required for PKD-2 trafficking (**Error! Reference source**

ot found.). However, subciliary localization of CIL-1 is unknown (Bae et al., 2009), and INPP5E

localizes to the entire cilium (Bielas et al., 2009; Humbert et al., 2012; Jacoby et al., 2009),

arguing against an InvC specific role in these cilia types.

The Unc119b shuttle components RP2 and Arl3 appear both to be regulated by membrane

interactions and to link membrane dynamics to the microtubule dynamics. Recent structural

studies suggest that Arl3-GTP has weaker affinity for the cholesterol and sphingolipid-enriched

ciliary membrane than other membranes. This weaker affinity allows Arl3 to dissociate from the

ciliary membrane, revealing physical moieties that mediate Unc119b binding. Arl3 can then

trigger Unc119b cargo release, as described above (Ismail et al., 2012). The Arl3 GAP RP2 is also

membrane-associated (Chapple et al., 2000; Chapple et al., 2002), and requires its myristoyl and

palmitoyl anchors for proper function (Rosenberg et al., 1999). Though both Arl3 and Rp2 are

primarily membrane-associated, both also have established functions in microtubule regulation. Arl3 has been reported to be physically associated with microtubules (Grayson et al., 2002), modulates IFT microtubule motor interactions (Li et al., 2010), and preferentially binds unmyristoylated, non-membrane-associated RP2 (Bartolini et al., 2002). RP2, in addition to functioning as an Arl3 GAP, also functions as a tubulin GAP (Bartolini et al., 2002). These results suggest that a proximal cilium specific membrane compartment is linked to the microtubule dynamics and drives trafficking specificity. However, no known lipid markers reveal such a distinct membrane compartment. A caveat is warranted, though: most cilia lipid markers were observed in *Paramecium* and *Tetrahymena*, which may not have a conserved InvC because they have no identifiable Inversin ortholog.

Several cargos of PDE6d have been identified, including INPP5E, RHEB, Rab28, rhodopsin kinase, and rod phosphodiesterase (Florio et al., 1996; Humbert et al., 2012; Ismail et al., 2011; Thomas et al., 2014; Zhang et al., 2004; Zhang et al., 2007), though these are not known to be InvC restricted.

1.4.6 – Ultrastructure and microtubule dynamics

Whereas the transition zone is marked by microtubule doublets attached to the ciliary membrane via MKS-NPHP protein Y-links, there are few ultrastructure details to distinguish the InvC from the rest of the ciliary shaft. The InvC is composed of microtubule doublets, which appear to be spatially associated with the membrane (Shiba et al., 2009); perturbation of this has been associated with ciliary mutants (Cevik et al., 2010). Additionally, Inversin physically interacts with β-tubulin (Otto et al., 2003). However, tubulin post-translational modifications (PTMs) have been linked genetically and physically to the InvC, and Inversin itself associates with microtubules in a polymerization-state dependent manner (Nurnberger et al., 2004). Cilia of

Inv-/- mice have superficially wild-type ultrastructure (Shiba et al., 2009); however, *nphp-2*

worms have disorganized Y-links, overextended B-tubules, and misplaced cilia, which may be

due to TZ-anchoring failure (Warburton-Pitt et al., 2014). In worms absent *daf-25*—which has

been linked to *nphp-2* expression in some cell types—amphid channel cilia ultrastructure

appears normal (Jensen et al., 2010).

PTMs are small side chains added to microtubules after polymerization, altering their affinity to

binding partners, which in turn can modulate microtubule dynamics (Reviewed in Verhey and

Gaertig, 2007). Many PTMs have been identified to date, including acetylation,

polyglutamylation, detyrosination, polyglycylation, O-GlcNAcylation, phosphorylation,

palmitoylation, and removal of the two final C-terminal residues. Multiple modifications may be

present on the same tubulin subunit, allowing for combinatorial specificity (Redeker, 2010).

Microtubule stability has long been linked to PTMs. Most of these modifications have been

studied in the ciliary context, and acetylation and polyglutamylation have specifically linked to

InvC biology.

1.4.6.1 – Acetylation. Like other PTMs, acetylation is a marker for stabilized microtubules

(Palazzo et al., 2003). Though primary cilia are generally acetylated along their entire length

(Piperno et al., 1987), acetylation-associated enzymes, including the histone deacetylase Hdac6

(Hubbert et al., 2002), have been shown to be proximally enriched (Li et al., 2010), and

genetically interact with InvC components to control cilia integrity (Mergen et al., 2013;

Warburton-Pitt et al., 2014). (Another known tubulin deacetylase, Sirt2, doesn't seem to

function on axonemal microtubules [Li et al., 2010; North et al., 2003]). Acetylation has long

been associated primarily with alpha-tubulin residue K40 (L'Hernault and Rosenbaum, 1985).

However, the only *C. elegans* alpha tubulin with this residue, MEC-12, is not expressed in ciliated

neurons (Fukushige et al., 1999), anti-acetylated K40 antibodies do not label cilia (O'Hagan et al.,

2011; Warburton-Pitt et al., 2014), and the only known acetyltransferase that acetylates K40, MEC-17, has not been directly linked to cilia function (Akella et al., 2010). Because *hdac-6* functions in *C. elegans* ciliary stability, this suggests that *hdac-6* has other possible targets, though none have been identified (Li et al., 2010). Indeed, it has been recently found that β-tubulin also has an acetylatable K252 residue (Chu et al., 2011), and many tubulins are also included in the *Homo sapiens* acetylome (Choudhary et al., 2009), though it remains to be seen whether they have a role in ciliary dynamics.

Acetylation has also been tied to IFT components. Bbip10, a BBSome peptide, is required for both microtubule polymerization and acetylation in zebrafish. Acetylation is restricted to the proximal cilium in some, but not all, cell types. Intriguingly, Bbip10 and Hdac6 physically interact, and Hdac6 antagonizes Bbip10 acetylation function (Loktev et al., 2008). The *C. elegans* Bbip10 homolog is expressed in amphid and phasmid ciliated neurons, though has not been characterized (Kunitomo et al., 2005).

Unfortunately, the primary anti-acetylated tubulin antibody in use, 6-11B-1, is not actually specific to acetylat**ed** K40, labeling instead acetylat**able** tubulin, strongly curtailing the utility of acetylation data in many reports (Soppina et al., 2012).

1.4.6.2 – Glutamylation. Microtubule polyglutamylation is required for vertebrate and nematode ciliogenesis and function (O'Hagan et al., 2011; Pathak et al., 2007), and is regulated by TTLL (tubulin tyrosine ligase like) glutamylases and their converse deglutamylases (Reviewed in Verhey and Gaertig, 2007). Unlike acetylation, polyglutamylation has been associated with both an increase and decrease in microtubule stability, suggestive of cell type-specific regulatory activity, or a requirement for balance between stability and instability in normal cilia microtubule dynamics (O'Hagan et al., 2011; Wloga et al., 2010). Ciliary glutamylation is linked to the function of ciliopathy genes, including *nphp-2* in *C. elegans* and CEP41/JBTS15 in

mammalian models (Lee et al., 2012; Warburton-Pitt et al., 2014).

Over the years, polyglutamylated tubulin has been associated with the proximal cilium in many

models, including *Chlamydomonas* flagella (Fouquet et al., 1996), zebrafish pronephric cilia

(Pathak et al., 2007), *C. elegans* amphid channel and phasmid cilia (O'Hagan et al., 2011;

Warburton-Pitt et al., 2014), and human fibroblast cilia (Lee et al., 2012). Ciliary glutamylation

has also been associated with modulation of ciliary dynein (which functions in cilia movement),

though not IFT dynein, activity (Kubo et al., 2010; Suryavanshi et al., 2010). In a very suggestive

finding predating the discovery of the TTLL glutamylase and glycylase family (Janke et al., 2005),

Nphp3 was reported to have a TTL domain, though the function of this domain remains

completely uncharacterized (Olbrich et al., 2003). Additionally, Inversin physically interacts with

zebrafish TTC30B/Fleer (Zhao and Malicki, 2011), a cilia base protein, which—like Nphp3—

contains TPR repeats, and is required for tubulin polyglutamylation (Pathak et al., 2007) and

proper ciliary localization of Inversin (Zhao and Malicki, 2011). Besides these examples, very few

other genes are known to both regulate glutamylation and genetically interact with InvC

components. In *C. elegans*, the deglutamylase *ccpp-1* and glutamylase *ttll-4* function to regulate

amphid and phasmid ciliary glutamylation, but neither are reported to localize to the proximal

cilium (O'Hagan et al., 2011), and neither seem to be strictly required for localization of InvC

components, including NPHP-2, UNC-119, and TAX-2 (Warburton-Pitt et al., 2014; Wojtyniak et

al., 2013). Similarly, Cep41 is a basal body protein required for ciliary glutamylation; another

glutamylase, Ttll6, requires Cep41 for ciliary targeting but, similarly to Cep41, localizes to the

basal body (Lee et al., 2012). Recent work by our group has also demonstrated that *nphp-2*

mutants exhibit ectopic glutamylation and microtubule overstabilization; other proximal cilium

associated mutants, including *hdac-6* and *unc-119*, also have altered glutamylation patterns in

amphid and phasmid cilia. The actions of the proximal cilium associated genes appear to lie

upstream of the glutamylation apparatus (Warburton-Pitt et al., 2014).

Overall, studies of microtubule acetylation and glutamylation suggest that the InvC can

modulate cilia stability through microtubule acetylation and polyglutamylation, possibly in

response in environmental signals. As at least one TTLL protein is predicted to be myristoylated

(Tttl11b), and Nphp3 has a TTL domain and is myristoylated (Olbrich et al., 2003), it may be that

Unc119b and the InvC function to shuttle and localize the glutamylation apparatus in cilia, and

through this pathway, regulate microtubule patterning and ciliogenesis.

1.5 – The Function of the Inversin Compartment

The InvC has been implicated in virtually every cilia-associated pathway in recent years, with the

largest body of work exploring signal transduction and amplification. The InvC may also have

roles in ciliogenesis, cilia maintenance, cilia placement, cilia specialization, cilia length

regulation, IFT regulation, protein trafficking, and cilia motility. As wide ranging as this list is, it

neglects downstream and non-ciliary functions of these pathways, including cell cycle regulation

(Morgan et al., 2002; Simons and Walz, 2006), cellular motility (Werner et al., 2013), and DNA

damage repair (Chaki et al., 2012). I discuss several of these functions in turn.

1.5.1 – Signal Transduction and Amplification

Many signal transduction pathways have been linked to ciliary function, including Wnt,

Hedgehog, and Hippo, and signaling components such as CNGs, TRPVs, and Ca^{2+} channels.

1.5.1.1 – Wnt signaling. Wnt signaling is intimately tied into the function of the InvC. In the

canonical Wnt transduction cascade, Wnt ligand binds a Frizzled transmembrane receptor,

which then activates intracellular Disheveled. Disheveled then inhibits the activity of an

APC/GSK3β/CKI complex, which itself inhibits β-catenin function by targeting it to proteasomal

degradation. When the APC complex is inhibited by Disheveled, β-catenin can translocate into the nucleus and initiate transcription of Wnt effectors (Reviewed in Huang and He, 2008; MacDonald et al., 2009). The cilium as whole downregulates this pathway (He, 2008); knockout of kinesin Kif3A and Ofd1 results in cells with no cilia (Marszalek et al., 1999) and constitutive activation of Dishevelled (Corbit et al., 2008). Additionally, in ciliated cells, β-catenin accumulates at the cilia base, but in cilia knockdowns, β-catenin accumulates in the nucleus and constitutively activates Wnt-related transcription (Lancaster et al., 2011). This also implies the cilium is not required for canonical signaling, and that cilia retraction may actually potentiate the cell to receive future signals. Conversely, ciliogenesis does not require functional Wnt signaling (Kishimoto et al., 2008).

Inversin, Nphp3, Nek8, Hdac6, and the Inversin physical interactor Ahi1 (Sang et al., 2011), function in regulation of the ciliary Wnt response (Bergmann et al., 2008; Lancaster et al., 2011; Li et al., 2008; Simons et al., 2005) . Inversin has been misidentified as a basal body protein in the Wnt literature, which has led to confusion (Mahuzier et al., 2012; Simons et al., 2005). Inversin functions downstream from Frizzled, and is required for the recruitment of Dishevelled to the plasma membrane in response in Frizzled signaling (Lienkamp et al., 2010). Plasma membrane localization of Dishevelled has been associated with upregulation of an alternate Wnt pathway, the planar cell polarity (PCP) pathway (Axelrod et al., 1998). This change of localization is achieved by specific binding of Inversin to cytoplasmic Dishevelled, which is then targeted for degradation. Because this action also downregulates canonical Wnt signaling, Inversin has been called a switch between canonical Wnt and PCP signaling (Simons et al., 2005). In addition to indirectly upregulating PCP, Inversin also physically interacts with the PCP components Prickle and Van Gogh, suggesting that it also plays a direct role in this pathway (Das et al., 2004; Ross et al., 2005; Simons et al., 2005). However, more recent evidence contradicts

these results. In *inv-/-* mice, no upregulation of canonical Wnt signaling was observed, and

β-catenin did not accumulate in the nucleus as found previously (Sugiyama et al., 2011).

Additionally, the same group also found that overexpression of Inversin did not downregulate

canonical signaling (Sugiyama and Yokoyama, 2006). This discrepancy is suggested to be due to

differences between the earlier *in vitro* methods and the newer *in situ* data (Sugiyama et al.,

2011). Curiously, though Kif3a is best known as a requisite ciliary microtubule motor, it has also

been shown to regulate Wnt signaling in a non-ciliary pathway; this further confuses the role of

cilia in canonical Wnt signaling (Corbit et al., 2008). Thus, even though Inversin is known to

physically and genetically interact with Wnt components in multiple models, the role of Inversin

in Wnt signaling is now unclear. Disheveled function has been linked to basal body docking

during ciliogenesis; this echoes the role of *nphp-2* in cilia anchoring in *C. elegans* and may reflect

a conserved function of Wnt signaling (Vladar and Axelrod, 2008).

Not as much is known about the function of Nphp3 in Wnt signaling. Similarly to Inversin,

mutation and KO of Nphp3 both lead to PCP-associated defects in zebrafish development

(Bergmann et al., 2008; Zhou et al., 2010). The effects of Inversin and Nphp3 on Wnt signaling

are additive, suggesting that they function in parallel pathways (Bergmann et al., 2008).

Knockdown of Nek8 also results in *situs inversus* and other PCP-associated developmental

defects. Experimental evidence suggests that Nek8 functions downstream of Inversin, just as

Nek8 localization is dependent on Inversin (Fukui et al., 2012). However, such a model is

partially contradicted by the fact that knocking down both Inversin and Nek8 leads to an

increase in defects over the single knockdowns, which suggests that the genes function in

parallel pathways (Fukui et al., 2012).

Ahi1 has been demonstrated to physically interact with Inversin, and Ahi1 knockouts have

similar defects in epithelial cell polarization and organization as Nphp3 knockouts (Sang et al.,

2011). Ahi1 has also been shown to positively modulate canonical Wnt signaling in a cilium-specific manner, through regulation of β-catenin nuclear translocation (Lancaster et al., 2009; Lancaster et al., 2011). Disruption of Ahi1 localization in IFT knockout animals also perturbs canonical Wnt signaling (Lancaster et al., 2011). These results suggest that the Ahi1 cell polarization phenotype may be due to unopposed overactivation of the PCP pathway.

There are also several suggestive pieces of data that are currently difficult to fit together. Hdac6 has also been implicated in upregulating Wnt signaling, functioning to deacetylate β-catenin, a step required for nuclear translocation (Li et al., 2008). Though not shown in ciliated cells, yeast experiments indicate that Nphp3 physically interacts with Dysferlin, an Hdac6 inhibitor (Blandin et al., 2013; Di Fulvio et al., 2011); it is unknown whether this interaction functions to regulate Wnt signaling, microtubule acetylation, or other pathways.

1.5.1.2 – Hedgehog signaling. Hedgehog signaling is required for the development and patterning of organs, and unlike Wnt signaling, requires and is promoted by the primary cilium (Corbit et al., 2005; Huangfu et al., 2003). Hedgehog ligand binds to a Patch receptor, which then derepresses Smoothened (Humke et al., 2010; Tukachinsky et al., 2010). Smoothened translocates into the cilium and triggers the dissociation of the Sufu/Gli3 repressor complex; if Sufu/Gli3 cannot localize to the cilium tip, as in Kif3a, Kif7 and Ift88 knockdowns, it cannot be split (Haycraft et al., 2005; Huangfu et al., 2003; Humke et al., 2010; Liem et al., 2009; Tukachinsky et al., 2010). Finally, once separated from Sufu, Gli3 is no longer repressed and can activate transcription. TZ proteins have been shown to modulate Hedgehog signaling, including Rpgrip1l, which alters the ratio of repressed and active Gli3 (Vierkotten et al., 2007). The InvC interactor Arl13b has also been shown to mediate Hedgehog signaling (Caspary et al., 2007). Two physically interacting proteins, Evc and Evc2, localize to the proximal cilium and function in Hedgehog signaling (Caparros-Martin et al., 2013; Dorn et al., 2012). These proteins are required

for the Gli3 repressor complex to translocate to cilia tips—although not for ciliary localization of

Smoothened—and without them, Hedgehog signaling cannot be derepressed (Caparros-Martin

et al., 2013; Pusapati et al., 2014). Evc2 requires an N-terminal W-peptide for restriction to the

proximal cilium and deletion of this domain leads to Hedgehog signaling defects. This region is

also required for physical interactions with EFCAB7/IQCE, which anchors Evc/Evc2 to the

proximal cilium (Pusapati et al., 2014). EFCAB7 and IQCE both contain many calcium interacting

domains, thought the role of calcium in Hedgehog signal transduction and localization of these

components is unknown (Pusapati et al., 2014). Evc2 is not required for the localization of

Inversin, Arl13b, or IFT component IFT88 (Dorn et al., 2012). Interestingly, the Evc/Evc2 proximal

compartment is distinct from both the TZ and InvC, lying between, and partially overlapping,

both of them, and marks a novel ciliary subcompartment (Dorn et al., 2012).

1.5.1.3 – *Other signaling pathways.* Beyond the more general Wnt and Hedgehog signaling

pathways, proximal cilium components also function in more specific pathways. Crosstalk has

been demonstrated between Hippo and Wnt pathways (Varelas et al., 2010); Wnt components

Nek8 and Nphp3 both activate the Hippo intermediate TAZ, inhibiting the Hippo pathway (Frank

et al., 2013; Habbig et al., 2012); and Nek8 physically interacts with TGF-β pathway components

TGFBR and ACVR1 (Barrios-Rodiles et al., 2005). Recent evidence solidifies a link between Hippo

signaling and the cilium: the Hippo components MST1/2 and SAV1 antagonize ciliogenesis by

downregulating the AuroraA/HDAC6 pathway, associate with TZ proteins, and are required for

the ciliary targeting of some cargos (Kim et al., 2014).

In *C. elegans*, activation of the ODR-3 receptor—which requires UNC-119 for ciliary targeting—

leads to opening of the TAX-2 and TAX-4 CNG channels (Lans et al., 2004). These channels have

been demonstrated to be InvC localized in certain cell types, requiring full length NPHP-2 for

restriction (Wojtyniak et al., 2013); this is similar to the manner in which Inversin anchors InvC

components in primary cilia. Additionally, both TAX-2 and NPHP-2 require *daf-25* for expression

and localization in AWB cilia (Wojtyniak et al., 2013), though TAX-4 does not (Jensen et al.,

2010).

The polycystins have also been linked to the proximal cilium in multiple models.

Polycystin-1/PC1 has been reported to be localized to a restricted portion of the cilium, possibly

the InvC (Sengupta and Barr, 2014). It has also been suggested that PKD-2, the *C. elegans*

Polycystin-2/PC2 homolog, is enriched in the proximal portion of male-specific cilia of *C. elegans*

(Bae et al., 2006). PC1 and PC2 have been shown to physically interact (Newby et al., 2002),

though they functionally interact in a complex manner (Delmas et al., 2002; Geng et al., 2006;

Xu et al., 2003). Both PC1 and PC2 have also been linked to modulation of Wnt signaling

components and their downstream phenotypes (Bisgrove et al., 2005; Kim et al., 1999; McGrath

et al., 2003; Pennekamp et al., 2002), though some data is contradictory (Le et al., 2004; Miller

et al., 2011). In *C. elegans*, PKD-2 trafficking requires CIL-7, a myristoylated protein that interacts

with *unc-119* (Julie Maguire, Personal Communication), but does not require *nphp-2* (**Error!**

eference source not found.). In tubular epithelia primary cilia, Nek8 mutants exhibit ciliary

accumulation of PC1 and PC2 (Sohara et al., 2008), and PC2 is required for InvC-dependent

embryonic nodal signaling (Pennekamp et al., 2002). Other TRP family members have also been

associated with the proximal portion of the cilium, including the TRPV channels Nanchung and

Inactive in Drosophila (Gong et al., 2004; Lee et al., 2010). A related TRPN, nompC, localizes to

cilia tips and functions as a mechanoreceptor (Cheng et al., 2010; Liang et al., 2011); the TRPV

channels then amplify the induced current (Lee et al., 2010).

Calcium not only plays an indispensable role in general cilia biology, but may also play a large

role in InvC biology. Several of the aforementioned proteins, including Inversin/NPHP-2,

CNGA1/TAX-4, CNGB1/TAX-2, EFCAB7, and IQCE have calcium or calmodulin binding domains. In

the case of NPHP-2, the calcium binding EF-hand is required for ciliary targeting/retention

(Warburton-Pitt et al., 2014). Additionally, frog olfactory cilia have a proximal, post-TZ

enrichment of calcium channels (French et al., 2010). Pkd2, though a nonspecific cation channel,

also has an EF-hand, which may function in calcium-based squelching of Pkd2 response or create

a positive feedback loop, leading to further Pkd2 channel opening. Calcium signaling also plays a

role in nodal cilium-associated left-right pattern formation (Reviewed in Norris, 2012). Because

intraciliary calcium levels are very dynamic and are strongly tied to signal transduction and

amplification, it is likely that calcium modulates the binding affinities, localizations, and

activation status of InvC components. However, this has not been examined in detail in any

system.

1.5.2 – Ciliogenesis

InvC components function in ciliogenesis pathways in a very cell type specific manner. Early

work in *inv-/-* mice suggested that Inversin was not required for cilia formation in renal epithelial

cells (Morgan et al., 2002; Otto et al., 2003; Phillips et al., 2004); however, recent work has both

confirmed this earlier data in MEFs (Veland et al., 2013), and linked Inversin/*nphp-2* to ciliogenic

defects in MDCK and *C. elegans* amphid channel and phasmid cilia (Mergen et al., 2013;

Warburton-Pitt et al., 2012). Cell-specific roles for Inversin are not surprising given the range of

functions and localization patterns in different tissues (e.g., Nurnberger et al., 2002; Nurnberger

et al., 2004).

1.5.3 – Cilia Cycling

Cilia are dynamic organelles that are retracted and regrown in a cell-cycle dependent manner

(reviewed in Quarmby and Parker, 2005). The cell can send disassembly signals to the cilium,

and the cilium may also be able to send signals to the cell to divide. Many InvC-associated

proteins have been implicated in cilia cycling, including Nek8, Inversin, and Hdac6 (Morgan et

al., 2002; reviewed in Fry et al., 2012).

When cilia disassembly is triggered, the plasma membrane-associated Hef1 translocates to the

basal body and phosphorylates Aurora A (reviewed in Plotnikova et al., 2008). Aurora A then

phosphorylates Hdac6, which deacetylates the ciliary microtubules, destabilizing them, and

leading to their degeneration (Pugacheva et al., 2007). Inversin directly antagonizes this

pathway, binding both Aurora A and Hef1, inhibiting both, and reducing their phosphorylation,

leading to the stabilization of the ciliary axoneme (Mergen et al., 2013). Loss of Inversin allows

the disassembly pathways to become hyperactive, deciliating cells inappropriately; because

Inversin functions upstream of Hdac6, Hdac6 inhibitors can block Inversin related ciliation

phenotypes (Mergen et al., 2013). In *C. elegans*, the proximally-localized *hdac-6* also seems to

function to destabilize amphid channel and phasmid cilia (Li et al., 2010; Warburton-Pitt et al.,

2014). Defects in ciliary double mutants—including combinations of *nphp-2*, *unc-119*, and

arl-13—can be suppressed by *hdac-6* deletion, indicating this role of the proximal cilium may be

conserved (Warburton-Pitt et al., 2014).

Several organisms possess cilia only on terminally differentiated cells, including *C. elegans*. This

suggests that any protein or activity required exclusively for cycling would not be conserved in

C. elegans, allowing for genetic separation of cilia cycling and ciliogenesis. Interestingly, the

entire NPHP5/NPHP6 TZ module, which physically interacts with Inversin, is not conserved in

C. elegans (Sang et al., 2011), suggesting this module may play a role in cilia cycling. However,

no studies to date have used this approach to explore cilia cycling.

1.5.4 – Cilia Length Regulation

It has been long known that cilia length is strongly tied to proper function (Afzelius et al., 1985), and has been associated with disease (Follit et al., 2008; Mokrzan et al., 2007; Murcia et al., 2000; Sohara et al., 2008; Tammachote et al., 2009). To date, *Chlamydomonas* has long been the primary model used to explore length regulation (Barsel et al., 1988; Jarvik et al., 1984; Kuchka and Jarvik, 1987; Tuxhorn et al., 1998); however, *Chlamydomonas* has no described InvC and no conserved Inv complex components other than a possible Nek8 ortholog. Other data does suggest the presence of an InvC in Chlamydomonas. Lf5p, a serine/threonine kinase which regulates flagellar length, localizes to a 1µm proximal portion of the flagella, but distal to the TZ. Though many flagellar mutants were tested for Lf5p localization, none were found to be necessary (Tam et al., 2013). Lf5p homologs in other models are ambiguous because of the high conservation of the S/T kinase domain, making precise ortholog identifications difficult. No known proteins in any organism share homology with the other non-kinase half of L5fp. There are multiple, non-mutually exclusive, suggested mechanisms of length regulation, including diffusion of requisite components (Levy, 1974); free tubulin concentration (Sharma et al., 2011); IFT train size, particle frequency, quantity, and component localization (Engel et al., 2009; Iomini et al., 2001; Marshall and Rosenbaum, 2001; Tam et al., 2003); and alteration of microtubule polymerization kinetics (Marshall and Rosenbaum, 2001), among possibilities. Length regulation has also been tied to several signaling pathways (Abdul-Majeed et al., 2012), including positive control by Notch (Lopes et al., 2010) and non-canonical Wnt signaling (Oishi et al., 2006), and modulation by calcium/cAMP/PKA pathways (Besschetnova et al., 2010). Cilia length has been linked to several Inv complex components and proximally enriched proteins, including Inversin/*nphp-2*, Nphp3, Nek8, and Pkd1. Nphp3 (Bergmann et al., 2008; Zhou et al., 2010) and Nek8 (Smith et al., 2006) hypomorphs and knockouts exhibit elongated cilia. There is mixed data regarding Inversin/*nphp-2*, with reports suggesting (Mergen et al.,

2013; Warburton-Pitt et al., 2012) or discounting (Phillips et al., 2004; Zhao and Malicki, 2011) a role in length control. These differences are likely due to cell type specific roles of Inversin, similarly to the established tissue-specific elongation phenotypes reported in Pkd1 mice (Hopp et al., 2012). Basal body and TZ proteins also have an established role in length control; both Nde1 and Nphp4/*nphp-4* knockouts and mutants exhibit elongated cilia (Burckle et al., 2011; Kim et al., 2011; Warburton-Pitt et al., 2012).

It is more difficult to ascertain stunted cilia phenotypes. For instance, *C. elegans* requires multiple genes for the formation of a distal microtubule singlet segment (e.g., Hao et al., 2011; Ou et al., 2007; Snow et al., 2004); mutants of these genes have shorter overall cilia, but normal length microtubule doublet segments. Whether these count as "stunted" cilia is a matter of personal preference. In this vein, our recent work shows that multiple InvC-associated genes have elongated or stunted polyglutamylated tubulin compartments; whether this indicates a missized doublet segment, a missized cilium, or ectopic glutamylation is unknown (Warburton-Pitt et al., 2014).

How these different genes regulate cilia length is relatively unknown. *nphp-2* genetically interacts with the TZ-associated *nphp-4* to regulate IFT velocities (Warburton-Pitt et al., 2012), and both Inversin and Pkd2 interact with cytoskeletal components (Chen et al., 2008; Nurnberger et al., 2004; Rundle et al., 2004).

1.6 – Interactions between the InvC and other ciliary compartments

1.6.1 – Interaction with the Transition Zone and Basal Body

The InvC has long been associated with the TZ and BB; indeed, InvC components are sometimes even mistaken for being TZ/BB components. Many studies have probed the link between the

compartments and found that they are genetically and physically linked, and together have a hand influencing almost every ciliary feature discussed in the above sections.

Physical interactions have been detected between multiple InvC and TZ components. Inversin physically interacts with members of all three TZ genetic modules (the NPHP5/NPHP6/Atxn10 module, the NPHP1/4/8/Plk1 module, and the MKS1/MKS6/Tectonic2 module), interactions that are conserved in many models including mammalian cell lines (Otto et al., 2003; Sang et al., 2011), zebrafish (Zhao and Malicki, 2011), and *C. elegans* (Andrew Jauregui, PhD thesis). Inversin has also been demonstrated to form a physical complex with B9d2 and TTC30B/Fleer, which regulates IFT, ciliary cargo transport, and non-canonical Wnt PCP signaling (Zhao and Malicki, 2011). Because of these physical interactions, it has been suggested that the InvC may function as a bridge linking the TZ and the cilia shaft (Czarnecki and Shah, 2012). Nphp3, though not as well characterized, has also been shown to interact with TZ components, including Nphp1 and Nphp15/Cep164 (Chaki et al., 2012; Sang et al., 2011).

InvC- and TZ-associated genes have been shown to genetically interact in many, many contexts. Inversin and Nphp4 interact in kidney cyst formation in Zebrafish (Burckle et al., 2011), and the Inversin physical interactor Ahi1 interacts with Nphp1 in opsin localization (Louie et al., 2010). In *C. elegans*, *nphp-4* negatively regulates NPHP-2 expression/stability (Andre Jauregui, PhD thesis), and *nphp-2* interacts with *nphp-4* and *mks-6* to control dendrite and cilia length (Warburton-Pitt et al., 2012).

1.6.1.1 – Ciliogenesis. Interactions between the InvC and the TZ also modulate the two-step process of ciliogenesis, the initiation/docking step driven by TZ and BB components, and the second elongation step driven by IFT. *nphp-2* mutant worms have disordered—though not mislocalized—TZ Y-links, which are required for membrane attachment of the axoneme (Warburton-Pitt et al., 2014). Disruption of Y-link organization may be at the root of a cilia

misplacement phenotype seen in *nphp-2* mutants in which cilia cannot anchor in the correct location (Warburton-Pitt et al., 2014; Warburton-Pitt et al., 2012); this may also disrupt interactions between the cilium and surrounding glial cells, leading to cell non-autonomous defects of fasiculated cilia (Williams et al., 2010; **Error! Reference source not found.**). These -links are in part composed of TZ proteins—including the aforementioned NPHP-4, MKS-5, Cc2d2a, and Ahi1—which may lie at the heart of several observed TZ and InvC ciliogenic phenotypes (Chih et al., 2011; Williams et al., 2011). The elongation step of ciliogenesis has also been linked to Inversin; Nphp1 interacts in Hdac6-Aurora A mediated tubulin stabilization in a manner similar to Inversin (Mergen et al., 2013).

1.6.1.2 – Protein localization. The TZ and BB are also required for proper targeting of InvC-associated proteins. The BB/periciliary membrane associated *mks-3* is required to restrict NPHP-2 and ARL-13/Arl13b to the proximal cilium (Cevik et al., 2013; Warburton-Pitt et al., 2014). Multiple TZ-associated genes, are also required for the localization of NPHP-2, ARL-13, TAX-2, and TAX-4 in *C. elegans* (Cevik et al., 2013; Warburton-Pitt et al., 2014; Wojtyniak et al., 2013). In primary cilia, the TZ has been shown to act as an intermediate step in InvC protein localization, in a manner dependent on coiled-coil motifs (Shiba et al., 2010). The converse dependence does not seem to be true; Inversin is not required for Nphp1/4 TZ localization in primary cilia, and *nphp-2* is not required for MKS-3, B9 domain proteins, or NPHP-1/-4 TZ targeting (Shiba et al., 2010; Warburton-Pitt et al., 2012).

1.6.1.3 – Signaling pathways. InvC components modulate Wnt signaling pathways in conjunction with cilia base proteins. Both basal body (Gerdes et al., 2007; Kishimoto et al., 2008) and TZ proteins are required for PCP signaling. In addition to the PCP-modulating Inv complex described above, a possible separate PCP-modulating complex containing Inversin, Nphp4, Rpgrip1l, and disheveled also exists (Burckle et al., 2011; Mahuzier et al., 2012). This complex

may be the same as the Inversin-Fleer-B9d2 complex, which has independently been shown to

regulate several Wnt related pathways (Zhao and Malicki, 2011). Nphp4 represses canonical

signaling in a manner similar to Inversin, by binding disheveled and targeting it for proteasomal

degradation (Burckle et al., 2011). Interestingly, Rpgrip1l/Mks5 functions to antagonize

disheveled degradation, a function in direct competition with Inversin and Nphp4 (Mahuzier et

al., 2012). It is also very intriguing that the three known members of the

Inversin/Rpgrip1l/Nphp4 complex have an interesting genetic relationship in *C. elegans*:

knocking out any two of these genes results in synthetic ciliogenesis defect (Warburton-Pitt et

al., 2012; Williams et al., 2010). Wnt signaling has not been definitively established to function

in association with *C. elegans* cilia, though NPHP-2 appears to physically interact with the

disheveled DSH-2 (Andrew Jauregui, PhD thesis). Echoing data from mammalian studies,

deletion of Wnt components in *C. elegans* does not abrogate cilia formation (Oikonomou et al.,

2011).

The TZ also plays a role in other signaling pathways. Like Inversin and Nphp3, Nphp4 inhibits

Hippo signaling (Habbig et al., 2011). The Hedgehog regulating Evc compartment appears to

partially overlap both the TZ and the InvC, suggesting it requires interactions with both for

proper function (Pusapati et al., 2014). As described above, the InvC has also been linked to Ca^{2+}

signaling; a very large number of TZ components also have Ca^{2+} binding domains, including the

C2 domains of MKS-5, MKS-6 (Williams et al., 2011), Nphp4, Nphp8, Ahi1 (Sang et al., 2011), and

Cc2d2a (Gorden et al., 2008; Noor et al., 2008; Tallila et al., 2008), the related B9 domains of

MKS-1, MKSR-1, MKSR-2 (Bialas et al., 2009; Williams et al., 2008), and the calmodulin-binding

domain of Nphp5, which binds the same calmodulin as Inversin (Otto et al., 2005). C2 domains

also function in membrane interactions, an important aspect of TZ function in membrane

anchoring. Curiously, while TZ components primarily contain C2-family Ca^{2+} binding domains

(excepting IQ domain-containing Nphp5), InvC-associated components tend to possess EF-hand and calmodulin—an EF-hand protein—binding domains. This distinction suggests that the two compartments may have differing functions with respect to calcium. It is tempting to speculate that calcium acts to modulate InvC component function, whereas the TZ acts as a calcium sponge/barrier, preventing the extremely high intraciliary calcium concentration from leaking into the cytoplasm (reviewed in Hu and Nelson, 2011). Signals could then be transmitted out of the cilium by second messengers, and not by direct calcium diffusion, which has been demonstrated to be very slow (Delling et al., 2013).

1.6.1.4 – Other TZ and InvC interactions. IFT is an extraordinarily complex, multi-motor, cell-type specific, ciliary subcompartment regulated, transport system. *C. elegans nphp-2* has been demonstrated to interact with *nphp-4* in regulation of IFT particle velocities (Warburton-Pitt et al., 2012). The *nphp-2* interactor *arl-13* and the InvC-associated *hdac-6* and *arl-3* also all modulate IFT particle composition and velocity (Cevik et al., 2010; Li et al., 2010), and the *nphp-2* genetic interactor *klp-11* (Warburton-Pitt et al., 2014) is an IFT motor itself. The biology underlying these interactions is completely unknown, despite multiple attempts, as the GFP reporters used to characterize IFT sensitize the cilia to defects (Cevik et al., 2010; Jauregui et al., 2008; Li et al., 2010).

1.6.2 – The Inversin Compartment in Disease

Most of the genes discussed throughout this review are linked to a class of syndromes termed the "ciliopathies" because of the cilia dysfunction at their root. Two of the best studied of these ciliopathies are polycystic kidney disease and retinitis pigmentosa, the degeneration of photoreceptors. Mutations in Inversin/Nphp2, Nphp3, Nek8/Nphp9, and Anks6/Nphp16 all lead to nephronophthisis (Hoff et al., 2013; Olbrich et al., 2003; Otto et al., 2003; Otto et al., 2008;

Taskiran et al., 2014). This possibly occurs through dysregulation of Wnt signaling during kidney development when the onset of urine flow should be detected by renal tubule cilia (Simons et al., 2005). A large amount of animal model evidence supports this hypothesis, including work in the *inv* mouse Inversin model (Morgan et al., 1998), the *pcy* mouse Nphp3 model (Olbrich et al., 2003), the *jck* mouse Nek8 model (Liu et al., 2002), and in morpholino-injected Zebrafish (Hoff et al., 2013; Lienkamp et al., 2010; Liu et al., 2002; Simons et al., 2005; Zhou et al., 2010); more generally, overexpression of transgenic constitutively active β-catenin leads to PKD in mice (Saadi-Kheddouci et al., 2001). This research bears out in human NPHP2 patients, who exhibit increased disheveled and β-catenin expression (Bellavia et al., 2010). Mutations found in NPHP patients can prevent proper cilia targeting of the protein product (Smith et al., 2006; Sohara et al., 2008), can alter residues needed for function in Wnt signaling (Simons et al., 2005), or can lead to truncated and nonfunctional proteins that would theoretically prevent localization of downstream effectors (Hoff et al., 2013; Olbrich et al., 2003; Otto et al., 2003). A common disease pathway in the four known InvC nephronophthisis genes is supported by evidence showing that morpholinos against Nek8, Nphp3, and Anks6 yield identical pronephric tubule phenotypes in zebrafish (Hoff et al., 2013). However, it has been shown that the abnormal upregulation of canonical Wnt pathways is not responsible for the growth of kidney cysts, and that the PCP defects that characterize these diseases arise at an earlier stage in development (Sugiyama et al., 2011, reviewed in Wuebken and Schmidt-Ott, 2011).

1.6.3 – Conservation of the Inversin Compartment

Though the InvC has only been characterized in a handful of organisms, associated genes are conserved across broad clades. Inversin itself appears to be conserved within the clade Opisthokonta, but Nphp3 appears to be almost universal in eukaryotes, with homologs found

amongst both unikonts and bikonts. Nphp3 is not present in Ecdysozoans—a group containing arthopods and nematodes, among other organisms—suggesting it has been lost. Like Nphp3, Unc119b is also conserved throughout Eukarya, but has not been lost in Ecdysozoans. A significant weakness in the InvC literature is the lack of work examining the conservedness of subciliary localization of InvC components. The localization of both Inversin and Unc119b appears to be conserved, but the localizations of Nphp3, Nek8, TAX-2, and TAX-4 have only been reported in single models.

Not all cell types within organisms with InvC-bearing cilia have a conserved InvC. In *C. elegans*, NPHP-2 has markedly different localization in different cell types; NPHP-2 appears to be primarily cilia base localized in IL2 and male-specific cilia (**Error! Reference source not found.**). oreover, NPHP-2 does not require its EF-hand for localization in IL2 cilia, unlike in other cell types (Warburton-Pitt et al., 2014). Inversin also displays cell type-specific localization patterns; results in IMCD3 cells show that Inversin can localize to a variable length of the proximal cilium (Sang et al., 2011).

These localization differences raise a crucial question: is the InvC determined solely by the localization of Inversin, or can it exist separately of Inversin? Though TAX-2 and NPHP-2 were shown to co-localize in AWB cilia in *C. elegans* (Wojtyniak et al., 2013), is that enough to claim that TAX-2 is an inversin compartment component, especially since NPHP-2 appears to localize to the cilia base in that cell-type? No experiment has definitively examined the localization of known InvC components in cell types in which Inversin is not normally localized to a classic InvC.

1.7 – Supplemental Information/Material and Methods

This chapter focuses primarily on the compartmentalization of the mammalian renal tubule epithelium primary cilia and *C. elegans* amphid channel and phasmid cilia, the models in which a

majority of the research has been performed; data derived from other models, including the

flagella of *Chlamydomonas,* and the Zebrafish pronephros and Kupffer's Vesicle cilia, is

specifically identified as such.

1.7.1 – Abbreviations/Definitions

Inv	Inversin
InvC	Inversin Compartment
BB	Basal Body
pseudeo-BB	The basal body region of *C. elegans*, missing the characteristic centrioles
TZ	Transition Zone
Inv Complex	Physical complex comprising Inversin, Nphp3, Nek8, and Anks6
IFT	Intraflagellar Transport
PKD	Polycystic Kidney Disease
NPHP	Nephronophthisis
MKS	Meckel Syndrome
PCP	Planar Cell Polarity

1.8 – Figures and Tables

C. elegans
Archetypal Cilium

Mammalian
Archetypal Cilium

Tip

Singlet
Region

Doublet
Region

Transition
Zone

Pseudo
Basal Body

Periciliary
Membrane

Distal
Dendrite

Adherens
Junction

Tip

Doublet
Region

Ciliary
Pocket

Periciliary Membrane

Transition Zone

Basal Body

Mother
Centriole

Rootlet

Daughter Centriole
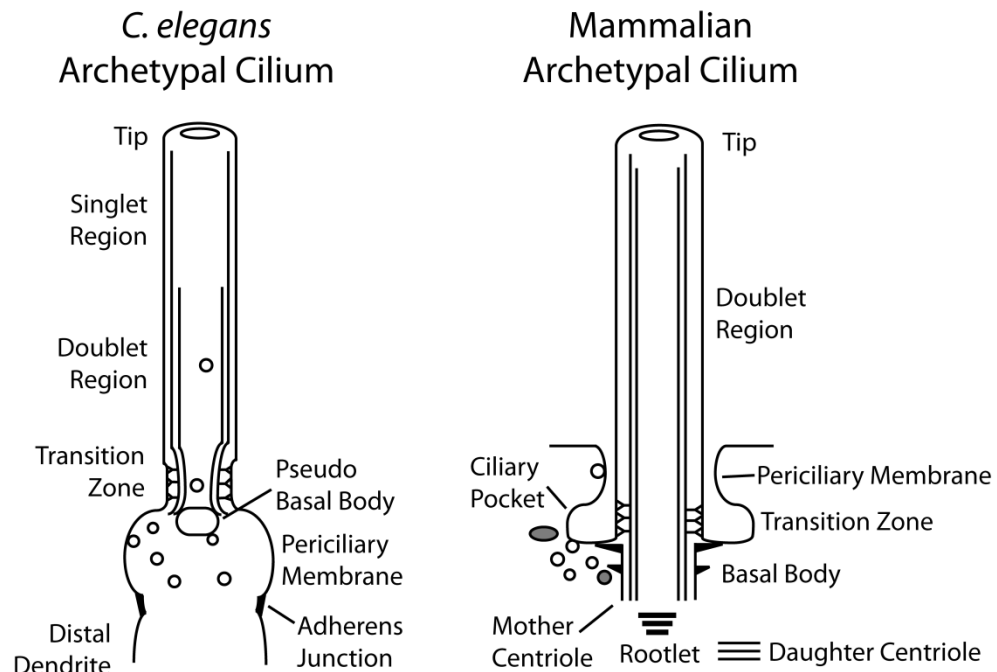
Figure 1. Structures of *C. elegans* and mammalian cilia

Cartoons of *C. elegans* and mammalian cilia highlighting regions mentioned in the text. Both

diagrams show the ciliary and cell membranes and the microtubules of the axoneme (a single

line indicates microtubule singlets, and a double line indicates microtubule doublets). The

C. elegans cilium cartoon illustrates the cilia tip complex, singlet region, the doublet region, the

transition zone, the pseudo-basal body, the periciliary membrane, the distal dendrite, and

adherens junctions (joining the distal dendrite to neighboring glial cells, not shown). The

pseudo-BB complex is represented by a rounded rectangle. Vesicles are shown residing in the

cilia base, and docking with the membrane and pseudo-BB. More speculatively, vesicles are also

shown in the TZ and the cilia shaft. The mammalian cilium cartoon illustrates the cilia tip

complex, the doublet region, the TZ, the basal body, the periciliary membrane, and the ciliary

pocket. Vesicles are shown residing near the cilia base and docking with the membrane of the

cilia pocket. The cilia necklace, not labelled, is the external leaflet of the TZ cilia membrane.

Figure designed based on (Blacque and Sanders, 2014) .
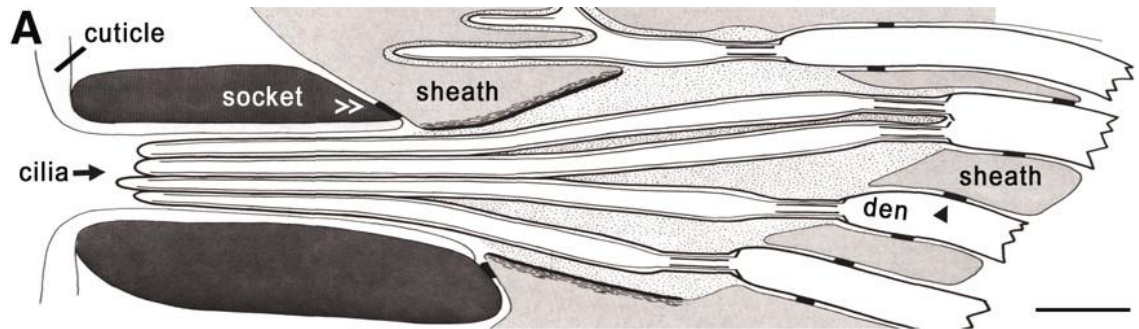
Figure 2. *C. elegans* **cilia lie in a pore**

Schematic of a longitudinal cross-section of amphid cilia in *C. elegans*. Cilia are located at the distal ends of dendrites, and extend into the ciliary pore. The pore is formed from two glial cells: the sheath cell surrounding the proximal cilium, and the socket cell surrounding the distal cilium. The socket cell encircles the cilia bundle tightly, whereas within the sheath cell there is an extracellular space filled with matrix material. Here are tight junctions between the socket and sheath cells, and the distal dendrite and sheath cell. Figure modified from (Perkins et al., 1986).
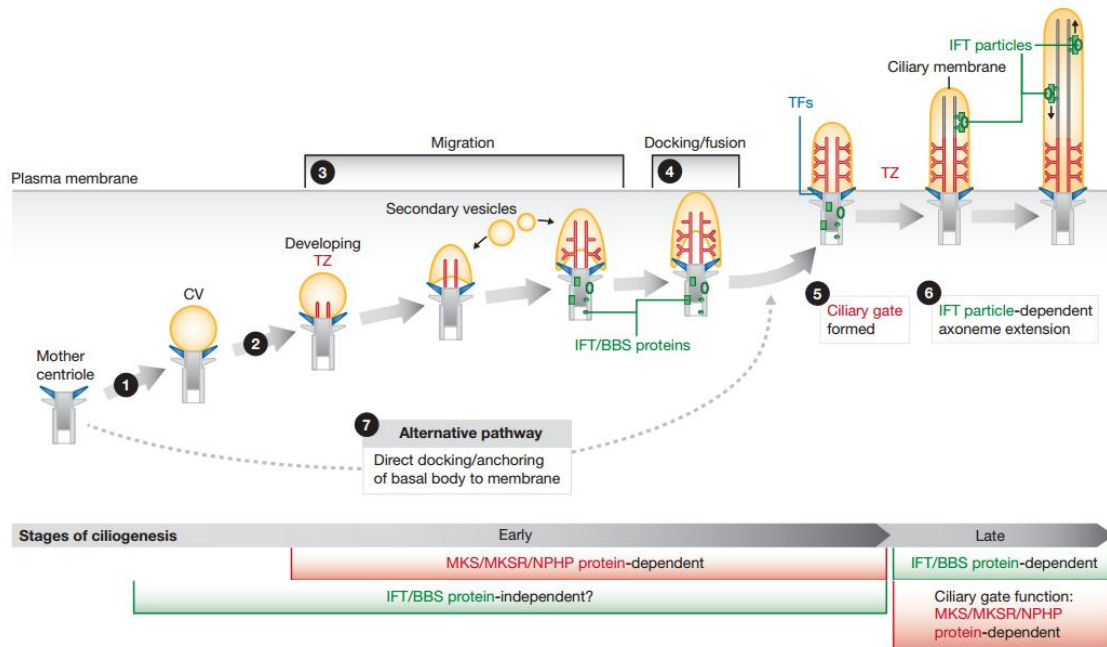
Figure 3. Ciliogenesis is a two stage process.

Ciliogenesis occurs in two stages: assembly of the centriolar complex, docking to the membrane, and biogenesis of the TZ, followed by extension of the axoneme by IFT. In some cell types, the first step includes docking of the centriolar complex to a ciliary vesicle, which then docks with the membrane; in other cell types, the centriolar complex docks to the plasma membrane directly. Reproduced from (Reiter et al., 2012).
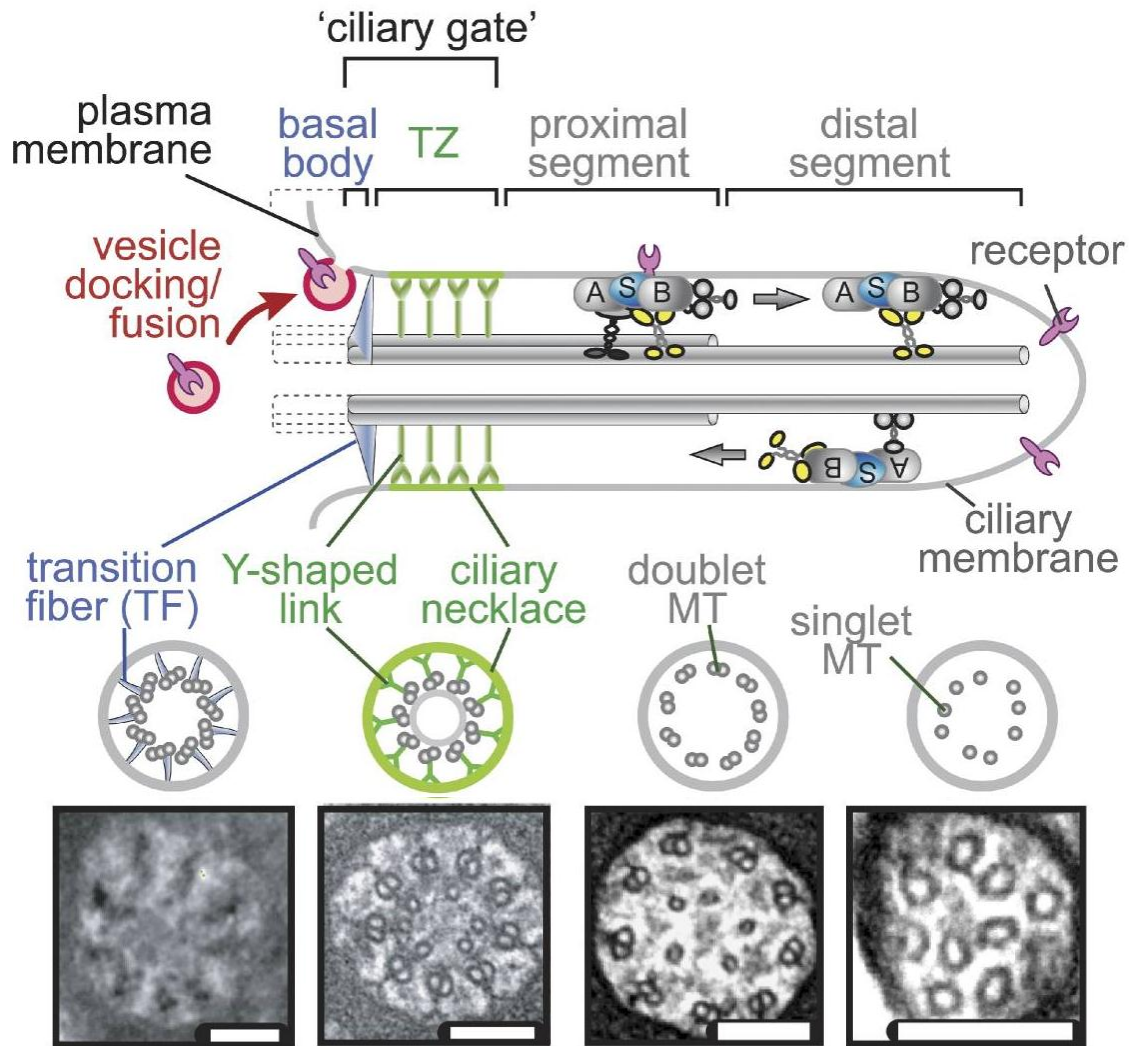
Figure 4. Schematic of cilia structure

A model of the cilium showing the relative structures of the individual ciliary compartments, and IFT motors functioning in them. Basal body is marked with dashed lines to indicate a lack of a centriole. Below are electron micrographs of ciliary cross sections through each of the compartments. Yellow motor is OSM-3, black motor is kinesin-II, and gray motor is dynein. Figure duplicated from (Williams et al., 2011).
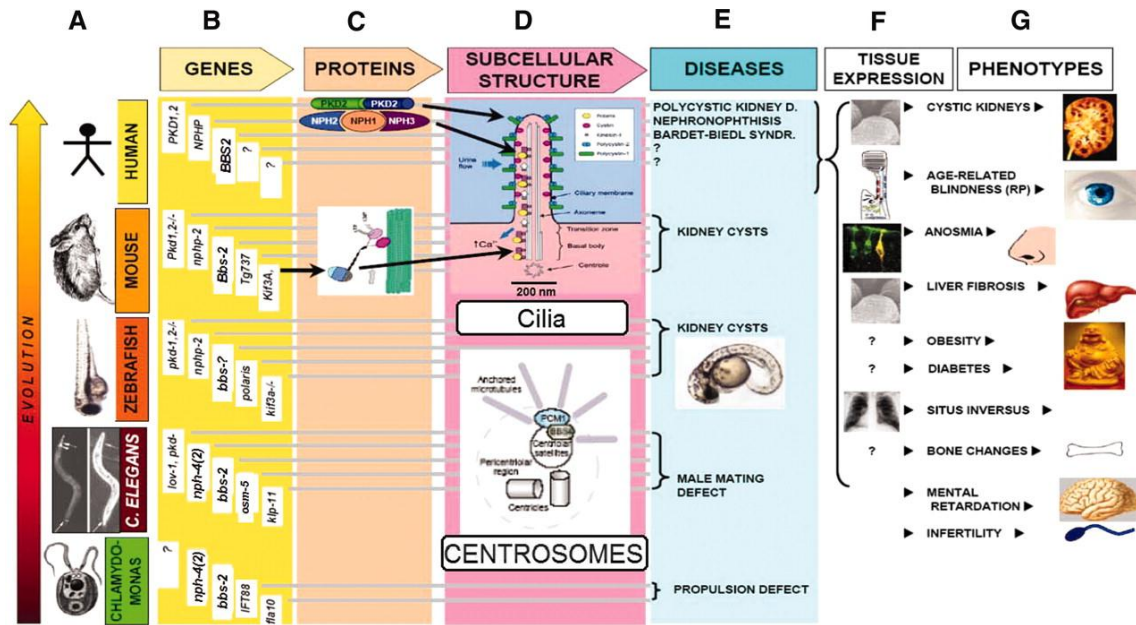
Figure 5. Cystic kidney diseases are ciliopathies

The cystic kidney hypothesis states that the genes mutated in most cystic kidney disease encode

proteins that localize to cilia. These genes are conserved across eukaryotes, and while they have

a diversity of functions in different organisms, they are still associated with cilia. In humans, a

variety of phenotypes are associated with dysfunctional cilia because of the wide

tissue-expression of ciliary genes. From (Hildebrandt and Zhou, 2007).
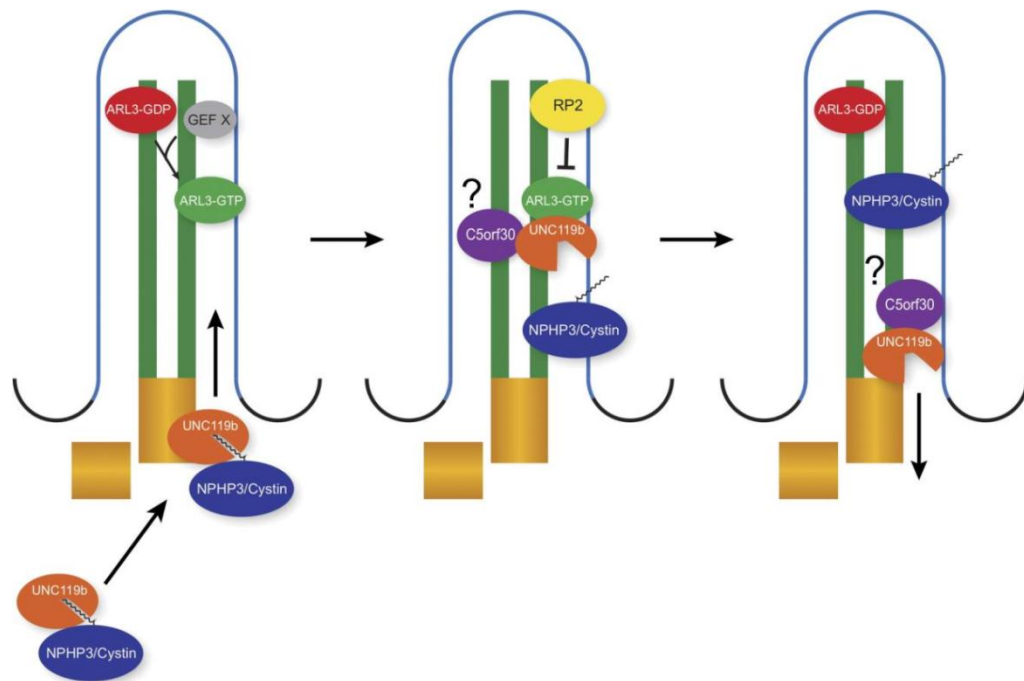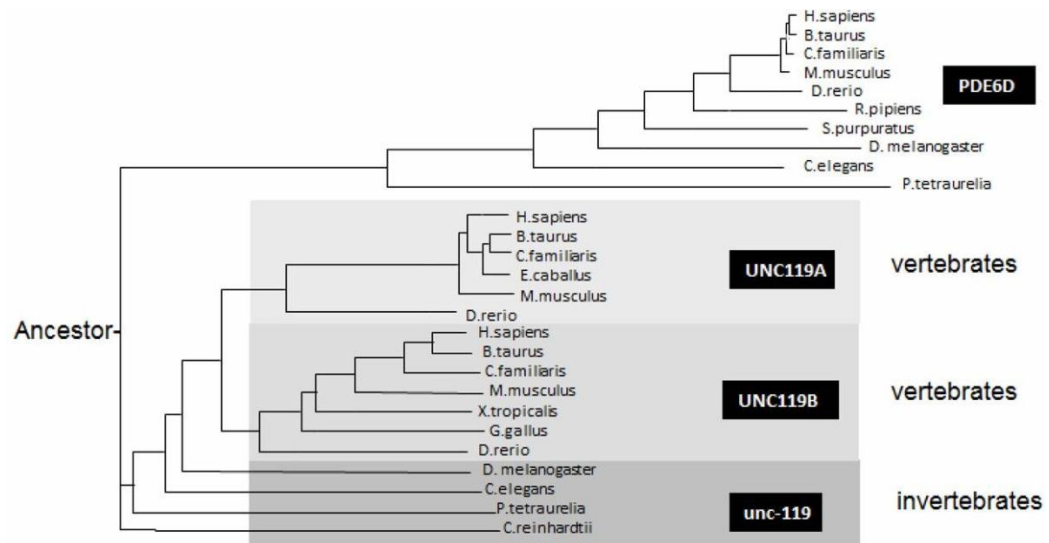
Figure 6. The UNC119B Shuttle

(A) Unc119b and PDE6d are related acyl-binding proteins. Reproduced from (Constantine 2013).

(B) Schematic of the Unc119b shuttle system. The mechanism is described in the text (1.4.4 –

Establishing the Inv Compartment). Figure reproduced from (Wright et al., 2011)

1.9 – References

Abdul-Majeed, S., Moloney, B. C. and Nauli, S. M. (2012). Mechanisms regulating cilia growth and cilia function in endothelial cells. *Cell Mol. Life Sci.* **69,** 165-173.

Afzelius, B. A., Gargani, G. and Romano, C. (1985). Abnormal length of cilia as a possible cause of defective mucociliary clearance. *Eur. J. Respir. Dis.* **66,** 173-180.

Akella, J. S., Wloga, D., Kim, J., Starostina, N. G., Lyons-Abbott, S., Morrissette, N. S., Dougan, S. T., Kipreos, E. T. and Gaertig, J. (2010). MEC-17 is an alpha-tubulin acetyltransferase. *Nature* **467,** 218-22.

Awata, J., Takada, S., Standley, C., Lechtreck, K. F., Bellve, K. D., Pazour, G. J., Fogarty, K. E. and Witman, G. B. (2014). Nephrocystin-4 controls ciliary trafficking of membrane and large soluble proteins at the transition zone. *J. Cell. Sci.*

Axelrod, J. D., Miller, J. R., Shulman, J. M., Moon, R. T. and Perrimon, N. (1998). Differential recruitment of dishevelled provides signaling specificity in the planar cell polarity and wingless signaling pathways. *Genes Dev.* **12,** 2610-2622.

Bae, Y. K., Kim, E., L'Hernault S, W. and Barr, M. M. (2009). The CIL-1 PI 5-phosphatase localizes TRP polycystins to cilia and activates sperm in C. elegans. *Curr Biol* **19,** 1599-607.

Bae, Y. K., Qin, H., Knobel, K. M., Hu, J., Rosenbaum, J. L. and Barr, M. M. (2006). General and cell-type specific mechanisms target TRPP2/PKD-2 to cilia. *Development* **133,** 3859-3870.

Baker, K. and Beales, P. L. (2009). Making sense of cilia in disease: The human ciliopathies. *Am. J. Med. Genet. C. Semin. Med. Genet.* **151C,** 281-295.

Barr, M. M. and Sternberg, P. W. (1999). A polycystic kidney-disease gene homologue required for male mating behaviour in C. elegans. *Nature* **401,** 386-389.

Barrios-Rodiles, M., Brown, K. R., Ozdamar, B., Bose, R., Liu, Z., Donovan, R. S., Shinjo, F., Liu, Y., Dembowy, J., Taylor, I. W. et al. (2005). High-throughput mapping of a dynamic signaling network in mammalian cells. *Science* **307,** 1621-1625.

Barsel, S. E., Wexler, D. E. and Lefebvre, P. A. (1988). Genetic analysis of long-flagella mutants of chlamydomonas reinhardtii. *Genetics* **118,** 637-648.

Bartolini, F., Bhamidipati, A., Thomas, S., Schwahn, U., Lewis, S. A. and Cowan, N. J. (2002). Functional overlap between retinitis pigmentosa 2 protein and the tubulin-specific chaperone cofactor C. *J. Biol. Chem.* **277,** 14629-14634.

Bellavia, S., Dahan, K., Terryn, S., Cosyns, J. P., Devuyst, O. and Pirson, Y. (2010). A homozygous mutation in INVS causing juvenile nephronophthisis with abnormal reactivity of the wnt/beta-catenin pathway. *Nephrol. Dial. Transplant.* **25,** 4097-4102.

Bergmann, C., Fliegauf, M., Bruchle, N. O., Frank, V., Olbrich, H., Kirschner, J., Schermer, B., Schmedding, I., Kispert, A., Kranzlin, B. et al. (2008). Loss of nephrocystin-3 function can cause embryonic lethality, meckel-gruber-like syndrome, situs inversus, and renal-hepatic-pancreatic dysplasia. *Am. J. Hum. Genet.* **82,** 959-970.

Besschetnova, T. Y., Kolpakova-Hart, E., Guan, Y., Zhou, J., Olsen, B. R. and Shah, J. V. (2010). Identification of signaling pathways regulating primary cilium length and flow-mediated adaptation. *Curr Biol* **20,** 182-7.

Bhogaraju, S., Cajanek, L., Fort, C., Blisnick, T., Weber, K., Taschner, M., Mizuno, N., Lamla, S., Bastin, P., Nigg, E. A. et al. (2013). Molecular basis of tubulin transport within the cilium by IFT74 and IFT81. *Science* **341,** 1009-1012.

Bhogaraju, S., Engel, B. D. and Lorentzen, E. (2013). Intraflagellar transport complex structure and cargo interactions. *Cilia* **2,** 10-2530-2-10.

Bialas, N. J., Inglis, P. N., Li, C., Robinson, J. F., Parker, J. D., Healey, M. P., Davis, E. E., Inglis, C. D., Toivonen, T., Cottell, D. C. et al. (2009). Functional interactions between the ciliopathy-associated meckel syndrome 1 (MKS1) protein and two novel MKS1-related (MKSR) proteins. *J. Cell. Sci.* **122,** 611-624.

Bielas, S. L., Silhavy, J. L., Brancati, F., Kisseleva, M. V., Al-Gazali, L., Sztriha, L., Bayoumi, R. A., Zaki, M. S., Abdel-Aleem, A., Rosti, R. O. et al. (2009). Mutations in INPP5E, encoding inositol polyphosphate-5-phosphatase E, link phosphatidyl inositol signaling to the ciliopathies. *Nat Genet*.

Bisgrove, B. W., Snarr, B. S., Emrazian, A. and Yost, H. J. (2005). Polaris and polycystin-2 in dorsal forerunner cells and kupffer's vesicle are required for specification of the zebrafish left-right axis. *Dev Biol* **287,** 274-88.

Blacque, O. E. and Sanders, A. A. (2014). Compartments within a compartment: What can tell us about ciliary subdomain composition, biogenesis, function, and disease. *Organogenesis* **10,**.

Blandin, G., Marchand, S., Charton, K., Daniele, N., Gicquel, E., Boucheteil, J. B., Bentaib, A., Barrault, L., Stockholm, D., Bartoli, M. et al. (2013). A human skeletal muscle interactome centered on proteins involved in muscular dystrophies: LGMD interactome. *Skelet Muscle* **3,** 3-5040-3-3.

Brady, J. D., Rich, T. C., Le, X., Stafford, K., Fowler, C. J., Lynch, L., Karpen, J. W., Brown, R. L. and Martens, J. R. (2004). Functional role of lipid raft microdomains in cyclic nucleotide-gated channel activation. *Mol. Pharmacol.* **65,** 503-511.

Burckle, C., Gaude, H. M., Vesque, C., Silbermann, F., Salomon, R., Jeanpierre, C., Antignac, C., Saunier, S. and Schneider-Maunoury, S. (2011). Control of the wnt pathways by nephrocystin-4 is required for morphogenesis of the zebrafish pronephros. *Hum. Mol. Genet.*

Bycroft, M., Bateman, A., Clarke, J., Hamill, S. J., Sandford, R., Thomas, R. L. and Chothia, C. (1999). The structure of a PKD domain from polycystin-1: Implications for polycystic kidney disease. *Embo J* **18,** 297-305.

Cantagrel, V., Silhavy, J. L., Bielas, S. L., Swistun, D., Marsh, S. E., Bertrand, J. Y., Audollent, S., Attie-Bitach, T., Holden, K. R., Dobyns, W. B. et al. (2008). Mutations in the cilia gene ARL13B lead to the classical form of joubert syndrome. *Am. J. Hum. Genet.* **83,** 170-179.

Caparros-Martin, J. A., Valencia, M., Reytor, E., Pacheco, M., Fernandez, M., Perez-Aytes, A., Gean, E., Lapunzina, P., Peters, H., Goodship, J. A. et al. (2013). The ciliary evc/Evc2 complex interacts with smo and controls hedgehog pathway activity in chondrocytes by regulating sufu/Gli3 dissociation and Gli3 trafficking in primary cilia. *Hum. Mol. Genet.* **22,** 124-139.

Caspary, T., Larkins, C. E. and Anderson, K. V. (2007). The graded response to sonic hedgehog depends on cilia architecture. *Dev. Cell.* **12,** 767-778.

Cavalier-Smith, T. (2002). The phagotrophic origin of eukaryotes and phylogenetic classification of protozoa. *Int. J. Syst. Evol. Microbiol.* **52,** 297-354.

Cevik, S., Hori, Y., Kaplan, O. I., Kida, K., Toivenon, T., Foley-Fisher, C., Cottell, D., Katada, T., Kontani, K. and Blacque, O. E. (2010). Joubert syndrome Arl13b functions at ciliary membranes and stabilizes protein transport in caenorhabditis elegans. *J. Cell Biol.* **188,** 953-969.

Cevik, S., Sanders, A. A., Van Wijk, E., Boldt, K., Clarke, L., van Reeuwijk, J., Hori, Y., Horn, N., Hetterschijt, L., Wdowicz, A. et al. (2013). Active transport and diffusion barriers restrict joubert syndrome-associated ARL13B/ARL-13 to an inv-like ciliary membrane subdomain. *PLoS Genet.* **9,** e1003977.

Chaki, M., Airik, R., Ghosh, A. K., Giles, R. H., Chen, R., Slaats, G. G., Wang, H., Hurd, T. W., Zhou, W., Cluckey, A. et al. (2012). Exome capture reveals ZNF423 and CEP164 mutations, linking renal ciliopathies to DNA damage response signaling. *Cell* **150,** 533-548.

Chapple, J. P., Hardcastle, A. J., Grayson, C., Spackman, L. A., Willison, K. R. and Cheetham, M. E. (2000). Mutations in the N-terminus of the X-linked retinitis pigmentosa protein RP2 interfere with the normal targeting of the protein to the plasma membrane. *Hum. Mol. Genet.* **9,** 1919-1926.

Chapple, J. P., Hardcastle, A. J., Grayson, C., Willison, K. R. and Cheetham, M. E. (2002). Delineation of the plasma membrane targeting domain of the X-linked retinitis pigmentosa protein RP2. *Invest. Ophthalmol. Vis. Sci.* **43,** 2015-2020.

Chen, X. Z., Li, Q., Wu, Y., Liang, G., Lara, C. J. and Cantiello, H. F. (2008). Submembraneous microtubule cytoskeleton: Interaction of TRPP2 with the cell cytoskeleton. *FEBS J.* **275,** 4675-4683.

Cheng, L. E., Song, W., Looger, L. L., Jan, L. Y. and Jan, Y. N. (2010). The role of the TRP channel NompC in drosophila larval and adult locomotion. *Neuron* **67,** 373-380.

Chih, B., Liu, P., Chinn, Y., Chalouni, C., Komuves, L. G., Hass, P. E., Sandoval, W. and Peterson, A. S. (2011). A ciliopathy complex at the transition zone protects the cilia as a privileged membrane domain. *Nat. Cell Biol.* **14,** 61-72.

Choudhary, C., Kumar, C., Gnad, F., Nielsen, M. L., Rehman, M., Walther, T. C., Olsen, J. V. and Mann, M. (2009). Lysine acetylation targets protein complexes and co-regulates major cellular functions. *Science* **325,** 834-840.

Chu, C. W., Hou, F., Zhang, J., Phu, L., Loktev, A. V., Kirkpatrick, D. S., Jackson, P. K., Zhao, Y. and Zou, H. (2011). A novel acetylation of beta-tubulin by san modulates microtubule polymerization via down-regulating tubulin incorporation. *Mol. Biol. Cell* **22,** 448-456.

Clare, D. K., Magescas, J., Piolot, T., Dumoux, M., Vesque, C., Pichard, E., Dang, T., Duvauchelle, B., Poirier, F. and Delacour, D. (2014). Basal foot MTOC organizes pillar MTs required for coordination of beating cilia. *Nat. Commun.* **5,** 4888.

Coene, K. L., Roepman, R., Doherty, D., Afroze, B., Kroes, H. Y., Letteboer, S. J., Ngu, L. H., Budny, B., van Wijk, E., Gorden, N. T. et al. (2009). OFD1 is mutated in X-linked joubert syndrome and interacts with LCA5-encoded lebercilin. *Am. J. Hum. Genet.* **85,** 465-481.

Corbit, K. C., Aanstad, P., Singla, V., Norman, A. R., Stainier, D. Y. and Reiter, J. F. (2005). Vertebrate smoothened functions at the primary cilium. *Nature* **437,** 1018-1021.

Corbit, K. C., Shyer, A. E., Dowdle, W. E., Gaulden, J., Singla, V., Chen, M. H., Chuang, P. T. and Reiter, J. F. (2008). Kif3a constrains beta-catenin-dependent wnt signalling through dual ciliary and non-ciliary mechanisms. *Nat. Cell Biol.* **10,** 70-76.

Czarnecki, P. G. and Shah, J. V. (2012). The ciliary transition zone: From morphology and molecules to medicine. *Trends Cell Biol.* **22,** 201-210.

Dammermann, A., Pemble, H., Mitchell, B. J., McLeod, I., Yates, J. R.,3rd, Kintner, C., Desai, A. B. and Oegema, K. (2009). The hydrolethalus syndrome protein HYLS-1 links core centriole structure to cilia formation. *Genes Dev.* **23,** 2046-2059.

Das, G., Jenny, A., Klein, T. J., Eaton, S. and Mlodzik, M. (2004). Diego interacts with prickle and strabismus/van gogh to localize planar cell polarity complexes. *Development* **131,** 4467-4476.

Delling, M., DeCaen, P. G., Doerner, J. F., Febvay, S. and Clapham, D. E. (2013). Primary cilia are specialized calcium signalling organelles. *Nature* **504,** 311-314.

Delmas, P., Nomura, H., Li, X., Lakkis, M., Luo, Y., Segal, Y., Fernandez-Fernandez, J. M., Harris, P., Frischauf, A. M., Brown, D. A. et al. (2002). Constitutive activation of G-proteins by polycystin-1 is antagonized by polycystin-2. *J Biol Chem* **277,** 11276-83.

den Hollander, A. I., Koenekoop, R. K., Mohamed, M. D., Arts, H. H., Boldt, K., Towns, K. V., Sedmak, T., Beer, M., Nagel-Wolfrum, K., McKibbin, M. et al. (2007). Mutations in LCA5, encoding the ciliary protein lebercilin, cause leber congenital amaurosis. *Nat. Genet.* **39,** 889-895.

Di Fulvio, S., Azakir, B. A., Therrien, C. and Sinnreich, M. (2011). Dysferlin interacts with histone deacetylase 6 and increases alpha-tubulin acetylation. *PLoS One* **6,** e28563.

Ding, X. Q., Fitzgerald, J. B., Matveev, A. V., McClellan, M. E. and Elliott, M. H. (2008). Functional activity of photoreceptor cyclic nucleotide-gated channels is dependent on the integrity of cholesterol- and sphingolipid-enriched membrane domains. *Biochemistry* **47,** 3677-3687.

Dishinger, J. F., Kee, H. L., Jenkins, P. M., Fan, S., Hurd, T. W., Hammond, J. W., Truong, Y. N., Margolis, B., Martens, J. R. and Verhey, K. J. (2010). Ciliary entry of the kinesin-2 motor KIF17 is regulated by importin-beta2 and RanGTP. *Nat Cell Biol* **12,** 703-10.

Dorn, K. V., Hughes, C. E. and Rohatgi, R. (2012). A smoothened-Evc2 complex transduces the hedgehog signal at primary cilia. *Dev. Cell.* **23,** 823-835.

Doroquez, D. B., Berciu, C., Anderson, J. R., Sengupta, P. and Nicastro, D. (2014). A high-resolution morphological and ultrastructural map of anterior sensory cilia and glia in caenorhabditis elegans. *Elife* **3,** e01948.

Dowdle, W. E., Robinson, J. F., Kneist, A., Sirerol-Piquer, M. S., Frints, S. G., Corbit, K. C., Zaghloul, N. A., van Lijnschoten, G., Mulders, L., Verver, D. E. et al. (2011). Disruption of a ciliary B9 protein complex causes meckel syndrome. *Am. J. Hum. Genet.* **89,** 94-110.

Engel, B. D., Ludington, W. B. and Marshall, W. F. (2009). Intraflagellar transport particle size scales inversely with flagellar length: Revisiting the balance-point length control model. *J. Cell Biol.* **187,** 81-89.

Evans, J. E., Snow, J. J., Gunnarson, A. L., Ou, G., Stahlberg, H., McDonald, K. L. and Scholey, J. M. (2006). Functional modulation of IFT kinesins extends the sensory repertoire of ciliated neurons in caenorhabditis elegans. *J Cell Biol* **172,** 663-9.

Fan, S., Hurd, T. W., Liu, C. J., Straight, S. W., Weimbs, T., Hurd, E. A., Domino, S. E. and Margolis, B. (2004). Polarity proteins control ciliogenesis via kinesin motor interactions. *Curr. Biol.* **14,** 1451-1461.

Fisch, C. and Dupuis-Williams, P. (2011). Ultrastructure of cilia and flagella – back to the future! *Biol. Cell.* **103,** 249-270.

Florio, S. K., Prusti, R. K. and Beavo, J. A. (1996). Solubilization of membrane-bound rod phosphodiesterase by the rod phosphodiesterase recombinant delta subunit. *J. Biol. Chem.* **271,** 24036-24047.

Fogelgren, B., Lin, S. Y., Zuo, X., Jaffe, K. M., Park, K. M., Reichert, R. J., Bell, P. D., Burdine, R. D. and Lipschutz, J. H. (2011). The exocyst protein Sec10 interacts with polycystin-2 and knockdown causes PKD-phenotypes. *PLoS Genet.* **7,** e1001361.

Follit, J. A., Li, L., Vucica, Y. and Pazour, G. J. (2010). The cytoplasmic tail of fibrocystin contains a ciliary targeting sequence. *J Cell Biol* **188,** 21-8.

Follit, J. A., San Agustin, J. T., Xu, F., Jonassen, J. A., Samtani, R., Lo, C. W. and Pazour, G. J. (2008). The golgin GMAP210/TRIP11 anchors IFT20 to the golgi complex. *PLoS Genet.* **4,** e1000315.

Follit, J. A., Xu, F., Keady, B. T. and Pazour, G. J. (2009). Characterization of mouse IFT complex B. *Cell Motil. Cytoskeleton* **66,** 457-468.

Fouquet, J. P., Prigent, Y. and Kann, M. L. (1996). Comparative immunogold analysis of tubulin isoforms in the mouse sperm flagellum: Unique distribution of glutamylated tubulin. *Mol. Reprod. Dev.* **43,** 358-365.

Frank, V., Habbig, S., Bartram, M. P., Eisenberger, T., Veenstra-Knol, H. E., Decker, C., Boorsma, R. A., Gobel, H., Nurnberg, G., Griessmann, A. et al. (2013). Mutations in NEK8 link multiple organ dysplasia with altered hippo signalling and increased c-MYC expression. *Hum. Mol. Genet.* **22,** 2177-2185.

French, D. A., Badamdorj, D. and Kleene, S. J. (2010). Spatial distribution of calcium-gated chloride channels in olfactory cilia. *PLoS One* **5,** e15676.

Fry, A. M., O'Regan, L., Sabir, S. R. and Bayliss, R. (2012). Cell cycle regulation by the NEK family of protein kinases. *J. Cell. Sci.* **125,** 4423-4433.

Fujiwara, T., Ritchie, K., Murakoshi, H., Jacobson, K. and Kusumi, A. (2002). Phospholipids undergo hop diffusion in compartmentalized cell membrane. *J. Cell Biol.* **157,** 1071-1081.

Fukui, H., Shiba, D., Asakawa, K., Kawakami, K. and Yokoyama, T. (2012). The ciliary protein Nek8/Nphp9 acts downstream of inv/Nphp2 during pronephros morphogenesis and left-right establishment in zebrafish. *FEBS Lett.* **586,** 2273-2279.

Fukushige, T., Siddiqui, Z. K., Chou, M., Culotti, J. G., Gogonea, C. B., Siddiqui, S. S. and Hamelin, M. (1999). MEC-12, an alpha-tubulin required for touch sensitivity in C. elegans. *J Cell Sci* **112,** 395-403.

Garcia-Gonzalo, F. R., Corbit, K. C., Sirerol-Piquer, M. S., Ramaswami, G., Otto, E. A., Noriega, T. R., Seol, A. D., Robinson, J. F., Bennett, C. L., Josifova, D. J. et al. (2011). A transition zone complex regulates mammalian ciliogenesis and ciliary membrane composition. *Nat. Genet.* **43,** 776-784.

Geng, L., Okuhara, D., Yu, Z., Tian, X., Cai, Y., Shibazaki, S. and Somlo, S. (2006). Polycystin-2 traffics to cilia independently of polycystin-1 by using an N-terminal RVxP motif. *J Cell Sci* **119,** 1383-95.

Gerdes, J. M., Liu, Y., Zaghloul, N. A., Leitch, C. C., Lawson, S. S., Kato, M., Beachy, P. A., Beales, P. L., DeMartino, G. N., Fisher, S. et al. (2007). Disruption of the basal body compromises proteasomal function and perturbs intracellular wnt response. *Nat. Genet.* **39,** 1350-1360.

Ghossoub, R., Molla-Herman, A., Bastin, P. and Benmerah, A. (2011). The ciliary pocket: A once-forgotten membrane domain at the base of cilia. *Biol. Cell.* **103,** 131-144.

Gibbons, I. R. and Grimstone, A. V. (1960). On flagellar structure in certain flagellates. *J. Biophys. Biochem. Cytol.* **7,** 697-716.

Gilula, N. B. and Satir, P. (1972). The ciliary necklace. A ciliary membrane specialization. *J. Cell Biol.* **53,** 494-509.

Godsel, L. M. and Engman, D. M. (1999). Flagellar protein localization mediated by a calcium-myristoyl/palmitoyl switch mechanism. *EMBO J.* **18,** 2057-2065.

Gong, Z., Son, W., Chung, Y. D., Kim, J., Shin, D. W., McClung, C. A., Lee, Y., Lee, H. W., Chang, D. J., Kaang, B. K. et al. (2004). Two interdependent TRPV channel subunits, inactive and nanchung, mediate hearing in drosophila. *J. Neurosci.* **24,** 9059-9066.

Gorden, N. T., Arts, H. H., Parisi, M. A., Coene, K. L., Letteboer, S. J., van Beersum, S. E., Mans, D. A., Hikida, A., Eckert, M., Knutzen, D. et al. (2008). CC2D2A is mutated in joubert syndrome and interacts with the ciliopathy-associated basal body protein CEP290. *Am. J. Hum. Genet.* **83,** 559-571.

Graser, S., Stierhof, Y. D., Lavoie, S. B., Gassner, O. S., Lamla, S., Le Clech, M. and Nigg, E. A. (2007). Cep164, a novel centriole appendage protein required for primary cilium formation. *J. Cell Biol.* **179,** 321-330.

Grayson, C., Bartolini, F., Chapple, J. P., Willison, K. R., Bhamidipati, A., Lewis, S. A., Luthert, P. J., Hardcastle, A. J., Cowan, N. J. and Cheetham, M. E. (2002). Localization in the human retina of the X-linked retinitis pigmentosa protein RP2, its homologue cofactor C and the RP2 interacting protein Arl3. *Hum. Mol. Genet.* **11,** 3065-3074.

Habbig, S., Bartram, M. P., Muller, R. U., Schwarz, R., Andriopoulos, N., Chen, S., Sagmuller, J. G., Hoehne, M., Burst, V., Liebau, M. C. et al. (2011). NPHP4, a cilia-associated protein, negatively regulates the hippo pathway. *J. Cell Biol.* **193,** 633-642.

Habbig, S., Bartram, M. P., Sagmuller, J. G., Griessmann, A., Franke, M., Muller, R. U., Schwarz, R., Hoehne, M., Bergmann, C., Tessmer, C. et al. (2012). The ciliopathy disease protein NPHP9 promotes nuclear delivery and activation of the oncogenic transcriptional regulator TAZ. *Hum. Mol. Genet.* **21,** 5528-5538.

Hao, L., Thein, M., Brust-Mascher, I., Civelekoglu-Scholey, G., Lu, Y., Acar, S., Prevo, B., Shaham, S. and Scholey, J. M. (2011). Intraflagellar transport delivers tubulin isotypes to sensory cilium middle and distal segments. *Nat. Cell Biol.* **13,** 790-798.

Haycraft, C. J., Banizs, B., Aydin-Son, Y., Zhang, Q., Michaud, E. J. and Yoder, B. K. (2005). Gli2 and Gli3 localize to cilia and require the intraflagellar transport protein polaris for processing and function. *PLoS Genet* **1,** e53.

He, X. (2008). Cilia put a brake on wnt signalling. *Nat. Cell Biol.* **10,** 11-13.

Heiman, M. G. and Shaham, S. (2009). DEX-1 and DYF-7 establish sensory dendrite length by anchoring dendritic tips during cell migration. *Cell* **137,** 344-355.

Higashide, T. and Inana, G. (1999). Characterization of the gene for HRG4 (UNC119), a novel photoreceptor synaptic protein homologous to unc-119. *Genomics* **57,** 446-50.

Hildebrandt, F. and Zhou, W. (2007). Nephronophthisis-associated ciliopathies. *J. Am. Soc. Nephrol.* **18,** 1855-1871.

Hoff, S., Halbritter, J., Epting, D., Frank, V., Nguyen, T. M., van Reeuwijk, J., Boehlke, C., Schell, C., Yasunaga, T., Helmstadter, M. et al. (2013). ANKS6 is a central component of a nephronophthisis module linking NEK8 to INVS and NPHP3. *Nat. Genet.* **45,** 951-956.

Hopp, K., Heyer, C. M., Hommerding, C. J., Henke, S. A., Sundsbak, J. L., Patel, S., Patel, P., Consugar, M. B., Czarnecki, P. G., Gliem, T. J. et al. (2011). B9D1 is revealed as a novel meckel syndrome (MKS) gene by targeted exon-enriched next-generation sequencing and deletion analysis. *Hum. Mol. Genet.* **20,** 2524-2534.

Hopp, K., Ward, C. J., Hommerding, C. J., Nasr, S. H., Tuan, H. F., Gainullin, V. G., Rossetti, S., Torres, V. E. and Harris, P. C. (2012). Functional polycystin-1 dosage governs autosomal dominant polycystic kidney disease severity. *J. Clin. Invest.* **122,** 4257-4273.

Hori, Y., Kobayashi, T., Kikko, Y., Kontani, K. and Katada, T. (2008). Domain architecture of the atypical arf-family GTPase Arl13b involved in cilia formation. *Biochem. Biophys. Res. Commun.* **373,** 119-124.

Hsiao, Y. C., Tong, Z. J., Westfall, J. E., Ault, J. G., Page-McCaw, P. S. and Ferland, R. J. (2009). Ahi1, whose human ortholog is mutated in joubert syndrome, is required for Rab8a localization, ciliogenesis and vesicle trafficking. *Hum. Mol. Genet.* **18,** 3926-3941.

Hu, Q., Milenkovic, L., Jin, H., Scott, M. P., Nachury, M. V., Spiliotis, E. T. and Nelson, W. J. (2010). A septin diffusion barrier at the base of the primary cilium maintains ciliary membrane protein distribution. *Science* **329,** 436-9.

Hu, Q. and Nelson, W. J. (2011). Ciliary diffusion barrier: The gatekeeper for the primary cilium compartment. *Cytoskeleton (Hoboken)* **68,** 313-324.

Huang, H. and He, X. (2008). Wnt/beta-catenin signaling: New (and old) players and new insights. *Curr. Opin. Cell Biol.* **20,** 119-125.

Huang, L., Szymanska, K., Jensen, V. L., Janecke, A. R., Innes, A. M., Davis, E. E., Frosk, P., Li, C., Willer, J. R., Chodirker, B. N. et al. (2011). TMEM237 is mutated in individuals with a joubert syndrome related disorder and expands the role of the TMEM family at the ciliary transition zone. *Am. J. Hum. Genet.* **89,** 713-730.

Huangfu, D., Liu, A., Rakeman, A. S., Murcia, N. S., Niswander, L. and Anderson, K. V. (2003). Hedgehog signalling in the mouse requires intraflagellar transport proteins. *Nature* **426,** 83-87.

Hubbert, C., Guardiola, A., Shao, R., Kawaguchi, Y., Ito, A., Nixon, A., Yoshida, M., Wang, X. F. and Yao, T. P. (2002). HDAC6 is a microtubule-associated deacetylase. *Nature* **417,** 455-458.

Hukema, R. K., Rademakers, S., Dekkers, M. P., Burghoorn, J. and Jansen, G. (2006). Antagonistic sensory cues generate gustatory plasticity in caenorhabditis elegans. *EMBO J.* **25,** 312-322.

Humbert, M. C., Weihbrecht, K., Searby, C. C., Li, Y., Pope, R. M., Sheffield, V. C. and Seo, S. (2012). ARL13B, PDE6D, and CEP164 form a functional network for INPP5E ciliary targeting. *Proc. Natl. Acad. Sci. U. S. A.* **109,** 19691-19696.

Humke, E. W., Dorn, K. V., Milenkovic, L., Scott, M. P. and Rohatgi, R. (2010). The output of hedgehog signaling is controlled by the dynamic association between suppressor of fused and the gli proteins. *Genes Dev* **24,** 670-82.

Hunnicutt, G. R., Kosfiszer, M. G. and Snell, W. J. (1990). Cell body and flagellar agglutinins in chlamydomonas reinhardtii: The cell body plasma membrane is a reservoir for agglutinins whose migration to the flagella is regulated by a functional barrier. *J. Cell Biol.* **111,** 1605-1616.

Hurd, T., Zhou, W., Jenkins, P., Liu, C. J., Swaroop, A., Khanna, H., Martens, J., Hildebrandt, F. and Margolis, B. (2010). The retinitis pigmentosa protein RP2 interacts with polycystin 2 and regulates cilia-mediated vertebrate development. *Hum Mol Genet* **19,** 4330-44.

Hurd, T. W., Fan, S. and Margolis, B. L. (2011). Localization of retinitis pigmentosa 2 to cilia is regulated by importin beta2. *J. Cell. Sci.* **124,** 718-726.

Iomini, C., Babaev-Khaimov, V., Sassaroli, M. and Piperno, G. (2001). Protein particles in chlamydomonas flagella undergo a transport cycle consisting of four phases. *J. Cell Biol.* **153,** 13-24.

Ishikawa, H., Kubo, A., Tsukita, S. and Tsukita, S. (2005). Odf2-deficient mother centrioles lack distal/subdistal appendages and the ability to generate primary cilia. *Nat. Cell Biol.* **7,** 517-524.

Ishikawa, H., Thompson, J., Yates, J. R.,3rd and Marshall, W. F. (2012). Proteomic analysis of mammalian primary cilia. *Curr. Biol.* **22,** 414-419.

Ismail, S. A., Chen, Y. X., Miertzschke, M., Vetter, I. R., Koerner, C. and Wittinghofer, A. (2012). Structural basis for Arl3-specific release of myristoylated ciliary cargo from UNC119. *EMBO J.* **31,** 4085-4094.

Ismail, S. A., Chen, Y. X., Rusinova, A., Chandra, A., Bierbaum, M., Gremer, L., Triola, G., Waldmann, H., Bastiaens, P. I. and Wittinghofer, A. (2011). Arl2-GTP and Arl3-GTP regulate a GDI-like transport system for farnesylated cargo. *Nat. Chem. Biol.* **7,** 942-949.

Jacoby, M., Cox, J. J., Gayral, S., Hampshire, D. J., Ayub, M., Blockmans, M., Pernot, E., Kisseleva, M. V., Compere, P., Schiffmann, S. N. et al. (2009). INPP5E mutations cause primary cilium signaling defects, ciliary instability and ciliopathies in human and mouse. *Nat Genet*.

Janke, C., Rogowski, K., Wloga, D., Regnard, C., Kajava, A. V., Strub, J. M., Temurak, N., van Dijk, J., Boucher, D., van Dorsselaer, A. et al. (2005). Tubulin polyglutamylase enzymes are members of the TTL domain protein family. *Science* **308,** 1758-1762.

Jarvik, J. W., Reinhart, F. D., Kuchka, M. R. And Adler, S. A. (1984). Altered flagellar size-control in shf-1 short-flagella mutants of chlamydomonas reinhardtii. *J. Protozool.* **31,** 199-204.

Jauregui, A. R. and Barr, M. M. (2005). Functional characterization of the C. elegans nephrocystins NPHP-1 and NPHP-4 and their role in cilia and male sensory behaviors. *Exp. Cell Res.* **305,** 333-342.

Jauregui, A. R., Nguyen, K. C., Hall, D. H. and Barr, M. M. (2008). The caenorhabditis elegans nephrocystins act as global modifiers of cilium structure. *J Cell Biol* **180,** 973-88.

Jensen, V. L., Bialas, N. J., Bishop-Hurley, S. L., Molday, L. L., Kida, K., Nguyen, P. A., Blacque, O. E., Molday, R. S., Leroux, M. R. and Riddle, D. L. (2010). Localization of a guanylyl cyclase to chemosensory cilia requires the novel ciliary MYND domain protein DAF-25. *PLoS Genet.* **6,** e1001199.

Kaplan, O. I., Molla-Herman, A., Cevik, S., Ghossoub, R., Kida, K., Kimura, Y., Jenkins, P., Martens, J. R., Setou, M., Benmerah, A. et al. (2010). The AP-1 clathrin adaptor facilitates cilium formation and functions with RAB-8 in C. elegans ciliary membrane transport. *J. Cell. Sci.* **123,** 3966-3977.

Kee, H. L., Dishinger, J. F., Blasius, T. L., Liu, C. J., Margolis, B. and Verhey, K. J. (2012). A size-exclusion permeability barrier and nucleoporins characterize a ciliary pore complex that regulates transport into cilia. *Nat. Cell Biol.* **14,** 431-437.

Kim, E., Arnould, T., Sellin, L. K., Benzing, T., Fan, M. J., Gruning, W., Sokol, S. Y., Drummond, I. and Walz, G. (1999). The polycystic kidney disease 1 gene product modulates wnt signaling. *J Biol Chem* **274,** 4947-53.

Kim, M., Kim, M., Lee, M. S., Kim, C. H. and Lim, D. S. (2014). The MST1/2-SAV1 complex of the hippo pathway promotes ciliogenesis. *Nat. Commun.* **5,** 5370.

Kim, S., Zaghloul, N. A., Bubenshchikova, E., Oh, E. C., Rankin, S., Katsanis, N., Obara, T. and Tsiokas, L. (2011). Nde1-mediated inhibition of ciliogenesis affects cell cycle re-entry. *Nat. Cell Biol.* **13,** 351-360.

Kishimoto, N., Cao, Y., Park, A. and Sun, Z. (2008). Cystic kidney gene seahorse regulates cilia-mediated processes and wnt pathways. *Dev. Cell.* **14,** 954-961.

Kubo, T., Yanagisawa, H. A., Yagi, T., Hirono, M. and Kamiya, R. (2010). Tubulin polyglutamylation regulates axonemal motility by modulating activities of inner-arm dyneins. *Curr Biol* **20,** 441-5.

Kuchka, M. R. and Jarvik, J. W. (1987). Short-flagella mutants of chlamydomonas reinhardtii. *Genetics* **115,** 685-691.

Kunitomo, H., Uesugi, H., Kohara, Y. and Iino, Y. (2005). Identification of ciliated sensory neuron-expressed genes in caenorhabditis elegans using targeted pull-down of poly(A) tails. *Genome Biol* **6,** R17.

Lancaster, M. A., Louie, C. M., Silhavy, J. L., Sintasath, L., Decambre, M., Nigam, S. K., Willert, K. and Gleeson, J. G. (2009). Impaired wnt-beta-catenin signaling disrupts adult renal homeostasis and leads to cystic kidney ciliopathy. *Nat. Med.* **15,** 1046-1054.

Lancaster, M. A., Schroth, J. and Gleeson, J. G. (2011). Subcellular spatial regulation of canonical wnt signalling at the primary cilium. *Nat. Cell Biol.* **13,** 700-707.

Lans, H., Rademakers, S. and Jansen, G. (2004). A network of stimulatory and inhibitory galpha-subunits regulates olfaction in caenorhabditis elegans. *Genetics* **167,** 1677-1687.

Larkins, C. E., Aviles, G. D., East, M. P., Kahn, R. A. and Caspary, T. (2011). Arl13b regulates ciliogenesis and the dynamic localization of shh signaling proteins. *Mol. Biol. Cell* **22,** 4694-4703.

Le, N. H., van der Bent, P., Huls, G., van de Wetering, M., Loghman-Adham, M., Ong, A. C., Calvet, J. P., Clevers, H., Breuning, M. H., van Dam, H. et al. (2004). Aberrant polycystin-1 expression results in modification of activator protein-1 activity, whereas wnt signaling remains unaffected. *J. Biol. Chem.* **279,** 27472-27481.

Lee, J., Moon, S., Cha, Y. and Chung, Y. D. (2010). Drosophila TRPN(=NOMPC) channel localizes to the distal end of mechanosensory cilia. *PLoS One* **5,** e11012.

Lee, J. E., Silhavy, J. L., Zaki, M. S., Schroth, J., Bielas, S. L., Marsh, S. E., Olvera, J., Brancati, F., Iannicelli, M., Ikegami, K. et al. (2012). CEP41 is mutated in joubert syndrome and is required for tubulin glutamylation at the cilium. *Nat. Genet.* **44,** 193-199.

Levy, E. M. (1974). Flagellar elongation as a moving boundary problem. *Bull. Math. Biol.* **36,** 265-273.

L'Hernault, S. W. and Rosenbaum, J. L. (1985). Chlamydomonas alpha-tubulin is posttranslationally modified by acetylation on the epsilon-amino group of a lysine. *Biochemistry* **24,** 473-8.

Li, J. B., Gerdes, J. M., Haycraft, C. J., Fan, Y., Teslovich, T. M., May-Simera, H., Li, H., Blacque, O. E., Li, L., Leitch, C. C. et al. (2004). Comparative genomics identifies a flagellar and basal body proteome that includes the BBS5 human disease gene. *Cell* **117,** 541-552.

Li, Y., Kelly, W. G., Logsdon, J. M.,Jr, Schurko, A. M., Harfe, B. D., Hill-Harfe, K. L. and Kahn, R. A. (2004). Functional genomic analysis of the ADP-ribosylation factor family of GTPases: Phylogeny among diverse eukaryotes and function in C. elegans. *FASEB J.* **18,** 1834-1850.

Li, Y., Wei, Q., Zhang, Y., Ling, K. and Hu, J. (2010). The small GTPases ARL-13 and ARL-3 coordinate intraflagellar transport and ciliogenesis. *J. Cell Biol.* **189,** 1039-1051.

Li, Y., Zhang, X., Polakiewicz, R. D., Yao, T. P. and Comb, M. J. (2008). HDAC6 is required for epidermal growth factor-induced beta-catenin nuclear localization. *J. Biol. Chem.* **283,** 12686-12690.

Liang, X., Madrid, J., Saleh, H. S. and Howard, J. (2011). NOMPC, a member of the TRP channel family, localizes to the tubular body and distal cilium of drosophila campaniform and chordotonal receptor cells. *Cytoskeleton (Hoboken)* **68,** 1-7.

Liem, K. F.,Jr, He, M., Ocbina, P. J. and Anderson, K. V. (2009). Mouse Kif7/Costal2 is a cilia-associated protein that regulates sonic hedgehog signaling. *Proc. Natl. Acad. Sci. U. S. A.* **106,** 13377-13382.

Lienkamp, S., Ganner, A., Boehlke, C., Schmidt, T., Arnold, S. J., Schafer, T., Romaker, D., Schuler, J., Hoff, S., Powelske, C. et al. (2010). Inversin relays frizzled-8 signals to promote proximal pronephros development. *Proc. Natl. Acad. Sci. U. S. A.* **107,** 20388-20393.

Liu, S., Lu, W., Obara, T., Kuida, S., Lehoczky, J., Dewar, K., Drummond, I. A. and Beier, D. R. (2002). A defect in a novel nek-family kinase causes cystic kidney disease in the mouse and in zebrafish. *Development* **129,** 5839-5846.

Loktev, A. V., Zhang, Q., Beck, J. S., Searby, C. C., Scheetz, T. E., Bazan, J. F., Slusarski, D. C., Sheffield, V. C., Jackson, P. K. and Nachury, M. V. (2008). A BBSome subunit links ciliogenesis, microtubule stability, and acetylation. *Dev. Cell.* **15,** 854-865.

Lopes, S. S., Lourenco, R., Pacheco, L., Moreno, N., Kreiling, J. and Saude, L. (2010). Notch signalling regulates left-right asymmetry through ciliary length control. *Development* **137,** 3625-32.

Louie, C. M., Caridi, G., Lopes, V. S., Brancati, F., Kispert, A., Lancaster, M. A., Schlossman, A. M., Otto, E. A., Leitges, M., Grone, H. J. et al. (2010). AHI1 is required for photoreceptor outer segment development and is a modifier for retinal degeneration in nephronophthisis. *Nat. Genet.* **42,** 175-180.

MacDonald, B. T., Tamai, K. and He, X. (2009). Wnt/beta-catenin signaling: Components, mechanisms, and diseases. *Dev. Cell.* **17,** 9-26.

Maerker, T., van Wijk, E., Overlack, N., Kersten, F. F., McGee, J., Goldmann, T., Sehn, E., Roepman, R., Walsh, E. J., Kremer, H. et al. (2008). A novel usher protein network at the periciliary reloading point between molecular transport machineries in vertebrate photoreceptor cells. *Hum. Mol. Genet.* **17,** 71-86.

Maguire, J. M., Silva, M., Wang, J., Nguyen, K., Hellen, E., Kern, A., Hall, D. and Barr, M. M. Myristoylated CIL-7 is required for polycystin-containing ECV release. *In preparation*.

Mahjoub, M. R., Trapp, M. L. and Quarmby, L. M. (2005). NIMA-related kinases defective in murine models of polycystic kidney diseases localize to primary cilia and centrosomes. *J. Am. Soc. Nephrol.* **16,** 3485-3489.

Mahuzier, A., Gaude, H. M., Grampa, V., Anselme, I., Silbermann, F., Leroux-Berger, M., Delacour, D., Ezan, J., Montcouquiol, M., Saunier, S. et al. (2012). Dishevelled stabilization by the ciliopathy protein Rpgrip1l is essential for planar cell polarity. *J. Cell Biol.* **198,** 927-940.

Marshall, W. F. and Rosenbaum, J. L. (2001). Intraflagellar transport balances continuous turnover of outer doublet microtubules: Implications for flagellar length control. *J. Cell Biol.* **155,** 405-414.

Marszalek, J. R., Ruiz-Lozano, P., Roberts, E., Chien, K. R. and Goldstein, L. S. (1999). Situs inversus and embryonic ciliary morphogenesis defects in mouse mutants lacking the KIF3A subunit of kinesin-II. *Proc Natl Acad Sci U S A* **96,** 5043-8.

McGrath, J., Brueckner, M., Afzelius, B. A., Bardaji, A., Martinez-Vea, A., Valero, A., Gutierrez, C., Garcia, C., Ridao, C., Oliver, J. A. et al. (2003). Cilia are at the heart of vertebrate left-right asymmetry. *Curr Opin Genet Dev* **13,** 385-92.

Mergen, M., Engel, C., Muller, B., Follo, M., Schafer, T., Jung, M. and Walz, G. (2013). The nephronophthisis gene product NPHP2/inversin interacts with aurora A and interferes with HDAC6-mediated cilia disassembly. *Nephrol. Dial. Transplant.* **28,** 2744-2753.

Miller, M. M., Iglesias, D. M., Zhang, Z., Corsini, R., Chu, L., Murawski, I., Gupta, I., Somlo, S., Germino, G. G. and Goodyer, P. R. (2011). T-cell factor/beta-catenin activity is suppressed in two different models of autosomal dominant polycystic kidney disease. *Kidney Int.* **80,** 146-153.

Mochizuki, T., Saijoh, Y., Tsuchiya, K., Shirayoshi, Y., Takai, S., Taya, C., Yonekawa, H., Yamada, K., Nihei, H., Nakatsuji, N. et al. (1998). Cloning of inv, a gene that controls left/right asymmetry and kidney development. *Nature* **395,** 177-81.

Mokrzan, E. M., Lewis, J. S. and Mykytyn, K. (2007). Differences in renal tubule primary cilia length in a mouse model of bardet-biedl syndrome. *Nephron Exp Nephrol* **106,** e88-e96.

Molla-Herman, A., Ghossoub, R., Blisnick, T., Meunier, A., Serres, C., Silbermann, F., Emmerson, C., Romeo, K., Bourdoncle, P., Schmitt, A. et al. (2010). The ciliary pocket: An endocytic membrane domain at the base of primary and motile cilia. *J Cell Sci* **123,** 1785-95.

Morgan, D., Eley, L., Sayer, J., Strachan, T., Yates, L. M., Craighead, A. S. and Goodship, J. A. (2002). Expression analyses and interaction with the anaphase promoting complex protein Apc2 suggest a role for inversin in primary cilia and involvement in the cell cycle. *Hum. Mol. Genet.* **11,** 3345-3350.

Morgan, D., Goodship, J., Essner, J. J., Vogan, K. J., Turnpenny, L., Yost, H. J., Tabin, C. J. and Strachan, T. (2002). The left-right determinant inversin has highly conserved ankyrin repeat and IQ domains and interacts with calmodulin. *Hum Genet* **110,** 377-84.

Morgan, D., Turnpenny, L., Goodship, J., Dai, W., Majumder, K., Matthews, L., Gardner, A., Schuster, G., Vien, L., Harrison, W. et al. (1998). Inversin, a novel gene in the vertebrate left-right axis pathway, is partially deleted in the inv mouse. *Nat Genet* **20,** 149-56.

Moritz, O. L., Tam, B. M., Hurd, L. L., Peranen, J., Deretic, D. and Papermaster, D. S. (2001). Mutant rab8 impairs docking and fusion of rhodopsin-bearing post-golgi membranes and causes cell death of transgenic xenopus rods. *Mol Biol Cell* **12,** 2341-51.

Morone, N., Fujiwara, T., Murase, K., Kasai, R. S., Ike, H., Yuasa, S., Usukura, J. and Kusumi, A. (2006). Three-dimensional reconstruction of the membrane skeleton at the plasma membrane interface by electron tomography. *J. Cell Biol.* **174,** 851-862.

Morsci, N. S. and Barr, M. M. (2011). Kinesin-3 KLP-6 regulates intraflagellar transport in male-specific cilia of caenorhabditis elegans. *Curr. Biol.* **21,** 1239-1244.

Moy, G. W., Mendoza, L. M., Schulz, J. R., Swanson, W. J., Glabe, C. G. and Vacquier, V. D. (1996). The sea urchin sperm receptor for egg jelly is a modular protein with extensive homology to the human polycystic kidney disease protein, PKD1. *J. Cell Biol.* **133,** 809-817.

Mukhopadhyay, S., Lu, Y., Qin, H., Lanjuin, A., Shaham, S. and Sengupta, P. (2007). Distinct IFT mechanisms contribute to the generation of ciliary structural diversity in C. elegans. *EMBO J* **26,** 2966-80.

Murcia, N. S., Richards, W. G., Yoder, B. K., Mucenski, M. L., Dunlap, J. R. and Woychik, R. P. (2000). The oak ridge polycystic kidney (orpk) disease gene is required for left-right axis determination. *Development* **127,** 2347-2355.

Nachury, M. V., Loktev, A. V., Zhang, Q., Westlake, C. J., Peranen, J., Merdes, A., Slusarski, D. C., Scheller, R. H., Bazan, J. F., Sheffield, V. C. et al. (2007). A core complex of BBS proteins cooperates with the GTPase Rab8 to promote ciliary membrane biogenesis. *Cell* **129,** 1201-13.

Nakada, C., Ritchie, K., Oba, Y., Nakamura, M., Hotta, Y., Iino, R., Kasai, R. S., Yamaguchi, K., Fujiwara, T. and Kusumi, A. (2003). Accumulation of anchored proteins forms membrane diffusion barriers during neuronal polarization. *Nat. Cell Biol.* **5,** 626-632.

Nakata, K., Shiba, D., Kobayashi, D. and Yokoyama, T. (2012). Targeting of Nphp3 to the primary cilia is controlled by an N-terminal myristoylation site and coiled-coil domains. *Cytoskeleton (Hoboken)* **69,** 221-234.

Newby, L. J., Streets, A. J., Zhao, Y., Harris, P. C., Ward, C. J. and Ong, A. C. (2002). Identification, characterization, and localization of a novel kidney polycystin-1-polycystin-2 complex. *J Biol Chem* **277,** 20763-73.

Noor, A., Windpassinger, C., Patel, M., Stachowiak, B., Mikhailov, A., Azam, M., Irfan, M., Siddiqui, Z. K., Naeem, F., Paterson, A. D. et al. (2008). CC2D2A, encoding a coiled-coil and C2 domain protein, causes autosomal-recessive mental retardation with retinitis pigmentosa. *Am. J. Hum. Genet.* **82,** 1011-1018.

Norris, D. P. (2012). Cilia, calcium and the basis of left-right asymmetry. *BMC Biol.* **10,** 102-7007-10-102.

North, B. J., Marshall, B. L., Borra, M. T., Denu, J. M. and Verdin, E. (2003). The human Sir2 ortholog, SIRT2, is an NAD+-dependent tubulin deacetylase. *Mol. Cell* **11,** 437-444.

Nurnberger, J., Bacallao, R. L. and Phillips, C. L. (2002). Inversin forms a complex with catenins and N-cadherin in polarized epithelial cells. *Mol Biol Cell* **13,** 3096-106.

Nurnberger, J., Kribben, A., Opazo Saez, A., Heusch, G., Philipp, T. and Phillips, C. L. (2004). The invs gene encodes a microtubule-associated protein. *J. Am. Soc. Nephrol.* **15,** 1700-1710.

O'Hagan, R., Piasecki, B. P., Silva, M., Phirke, P., Nguyen, K. C., Hall, D. H., Swoboda, P. and Barr, M. M. (2011). The tubulin deglutamylase CCPP-1 regulates the function and stability of sensory cilia in C. elegans. *Curr. Biol.* **21,** 1685-1694.

Oikonomou, G., Perens, E. A., Lu, Y., Watanabe, S., Jorgensen, E. M. and Shaham, S. (2011). Opposing activities of LIT-1/NLK and DAF-6/patched-related direct sensory compartment morphogenesis in C. elegans. *PLoS Biol.* **9,** e1001121.

Oishi, I., Kawakami, Y., Raya, A., Callol-Massot, C. and Izpisua Belmonte, J. C. (2006). Regulation of primary cilia formation and left-right patterning in zebrafish by a noncanonical wnt signaling mediator, duboraya. *Nat. Genet.* **38,** 1316-1322.

Olbrich, H., Fliegauf, M., Hoefele, J., Kispert, A., Otto, E., Volz, A., Wolf, M. T., Sasmaz, G., Trauer, U., Reinhardt, R. et al. (2003). Mutations in a novel gene, NPHP3, cause adolescent nephronophthisis, tapeto-retinal degeneration and hepatic fibrosis. *Nat. Genet.* **34,** 455-459.

Otto, E. A., Loeys, B., Khanna, H., Hellemans, J., Sudbrak, R., Fan, S., Muerb, U., O'Toole, J. F., Helou, J., Attanasio, M. et al. (2005). Nephrocystin-5, a ciliary IQ domain protein, is mutated in senior-loken syndrome and interacts with RPGR and calmodulin. *Nat. Genet.* **37,** 282-288.

Otto, E. A., Schermer, B., Obara, T., O'Toole, J. F., Hiller, K. S., Mueller, A. M., Ruf, R. G., Hoefele, J., Beekmann, F., Landau, D. et al. (2003). Mutations in INVS encoding inversin cause nephronophthisis type 2, linking renal cystic disease to the function of primary cilia and left-right axis determination. *Nat. Genet.* **34,** 413-420.

Otto, E. A., Trapp, M. L., Schultheiss, U. T., Helou, J., Quarmby, L. M. and Hildebrandt, F. (2008). NEK8 mutations affect ciliary and centrosomal localization and may cause nephronophthisis. *J. Am. Soc. Nephrol.* **19,** 587-592.

Ou, G., Blacque, O. E., Snow, J. J., Leroux, M. R. and Scholey, J. M. (2005). Functional coordination of intraflagellar transport motors. *Nature* **436,** 583-587.

Ou, G., Koga, M., Blacque, O. E., Murayama, T., Ohshima, Y., Schafer, J. C., Li, C., Yoder, B. K., Leroux, M. R. and Scholey, J. M. (2007). Sensory ciliogenesis in caenorhabditis elegans: Assignment of IFT components into distinct modules based on transport and phenotypic profiles. *Mol. Biol. Cell* **18,** 1554-1569.

Palazzo, A., Ackerman, B. and Gundersen, G. G. (2003). Cell biology: Tubulin acetylation and cell motility. *Nature* **421,** 230.

Pathak, N., Obara, T., Mangos, S., Liu, Y. and Drummond, I. A. (2007). The zebrafish fleer gene encodes an essential regulator of cilia tubulin polyglutamylation. *Mol. Biol. Cell* **18,** 4353-4364.

Pazour, G. J. and Bloodgood, R. A. (2008). Targeting proteins to the ciliary membrane. *Curr. Top. Dev. Biol.* **85,** 115-149.

Pennekamp, P., Karcher, C., Fischer, A., Schweickert, A., Skryabin, B., Horst, J., Blum, M. and Dworniczak, B. (2002). The ion channel polycystin-2 is required for left-right axis determination in mice. *Curr Biol* **12,** 938-43.

Perkins, L. A., Hedgecock, E. M., Thomson, J. N. and Culotti, J. G. (1986). Mutant sensory cilia in the nematode caenorhabditis elegans. *Dev Biol* **117,** 456-87.

Phillips, C. L., Miller, K. J., Filson, A. J., Nurnberger, J., Clendenon, J. L., Cook, G. W., Dunn, K. W., Overbeek, P. A., Gattone, V. H.,2nd and Bacallao, R. L. (2004). Renal cysts of inv/inv mice resemble early infantile nephronophthisis. *J. Am. Soc. Nephrol.* **15,** 1744-1755.

Pigino, G., Geimer, S., Lanzavecchia, S., Paccagnini, E., Cantele, F., Diener, D. R., Rosenbaum, J. L. and Lupetti, P. (2009). Electron-tomographic analysis of intraflagellar transport particle trains in situ. *J Cell Biol* **187,** 135-48.

Piperno, G., LeDizet, M. and Chang, X. J. (1987). Microtubules containing acetylated alpha-tubulin in mammalian cells in culture. *J. Cell Biol.* **104,** 289-302.

Piperno, G. and Ramanis, Z. (1991). The proximal portion of chlamydomonas flagella contains a distinct set of inner dynein arms. *J. Cell Biol.* **112,** 701-709.

Plotnikova, O. V., Golemis, E. A. and Pugacheva, E. N. (2008). Cell cycle-dependent ciliogenesis and cancer. *Cancer Res.* **68,** 2058-2061.

Pugacheva, E. N., Jablonski, S. A., Hartman, T. R., Henske, E. P. and Golemis, E. A. (2007). HEF1-dependent aurora A activation induces disassembly of the primary cilium. *Cell* **129,** 1351-63.

Pusapati, G. V., Hughes, C. E., Dorn, K. V., Zhang, D., Sugianto, P., Aravind, L. and Rohatgi, R. (2014). EFCAB7 and IQCE regulate hedgehog signaling by tethering the EVC-EVC2 complex to the base of primary cilia. *Dev. Cell.* **28,** 483-496.

Quarmby, L. M. and Parker, J. D. (2005). Cilia and the cell cycle? *J. Cell Biol.* **169,** 707-710.

Redeker, V. (2010). Mass spectrometry analysis of C-terminal posttranslational modifications of tubulins. *Methods Cell Biol* **95,** 77-103.

Reese, T. S. (1965). Olfactory cilia in the frog. *J. Cell Biol.* **25,** 209-230.

Reiter, J. F., Blacque, O. E. and Leroux, M. R. (2012). The base of the cilium: Roles for transition fibres and the transition zone in ciliary formation, maintenance and compartmentalization. *EMBO Rep.* **13,** 608-618.

Resh, M. D. (1999). Fatty acylation of proteins: New insights into membrane targeting of myristoylated and palmitoylated proteins. *Biochim. Biophys. Acta* **1451,** 1-16.

Ringo, D. L. (1967). Flagellar motion and fine structure of the flagellar apparatus in chlamydomonas. *J. Cell Biol.* **33,** 543-571.

Rosenberg, T., Schwahn, U., Feil, S. and Berger, W. (1999). Genotype-phenotype correlation in X-linked retinitis pigmentosa 2 (RP2). *Ophthalmic Genet.* **20,** 161-172.

Ross, A. J., May-Simera, H., Eichers, E. R., Kai, M., Hill, J., Jagger, D. J., Leitch, C. C., Chapple, J. P., Munro, P. M., Fisher, S. et al. (2005). Disruption of bardet-biedl syndrome ciliary proteins perturbs planar cell polarity in vertebrates. *Nat. Genet.* **37,** 1135-1140.

Rual, J. F., Venkatesan, K., Hao, T., Hirozane-Kishikawa, T., Dricot, A., Li, N., Berriz, G. F., Gibbons, F. D., Dreze, M., Ayivi-Guedehoussou, N. et al. (2005). Towards a proteome-scale map of the human protein-protein interaction network. *Nature* **437,** 1173-1178.

Rundle, D. R., Gorbsky, G. and Tsiokas, L. (2004). PKD2 interacts and co-localizes with mDia1 to mitotic spindles of dividing cells: Role of mDia1 IN PKD2 localization to mitotic spindles. *J Biol Chem* **279,** 29728-39.

Saadi-Kheddouci, S., Berrebi, D., Romagnolo, B., Cluzeaud, F., Peuchmaur, M., Kahn, A., Vandewalle, A. and Perret, C. (2001). Early development of polycystic kidney disease in transgenic mice expressing an activated mutant of the beta-catenin gene. *Oncogene* **20,** 5972-5981.

Sanchez de Diego, A., Alonso Guerrero, A., Martinez-A, C. and van Wely, K. H. (2014). Dido3-dependent HDAC6 targeting controls cilium size. *Nat. Commun.* **5,** 3500.

Sang, L., Miller, J. J., Corbit, K. C., Giles, R. H., Brauer, M. J., Otto, E. A., Baye, L. M., Wen, X., Scales, S. J., Kwong, M. et al. (2011). Mapping the NPHP-JBTS-MKS protein network reveals ciliopathy disease genes and pathways. *Cell* **145,** 513-528.

Satish Tammana, T. V., Tammana, D., Diener, D. R. and Rosenbaum, J. (2013). Centrosomal protein CEP104 (chlamydomonas FAP256) moves to the ciliary tip during ciliary assembly. *J. Cell. Sci.* **126,** 5018-5029.

Sengupta, P. and Barr, M. M. (2014). New insights into an old organelle: Meeting report on biology of cilia and flagella. *Traffic* **15,** 717-726.

Sharma, N., Kosan, Z. A., Stallworth, J. E., Berbari, N. F. and Yoder, B. K. (2011). Soluble levels of cytosolic tubulin regulate ciliary length control. *Mol. Biol. Cell* **22,** 806-816.

Shiba, D., Manning, D. K., Koga, H., Beier, D. R. and Yokoyama, T. (2010). Inv acts as a molecular anchor for Nphp3 and Nek8 in the proximal segment of primary cilia. *Cytoskeleton (Hoboken)* **67,** 112-119.

Shiba, D., Yamaoka, Y., Hagiwara, H., Takamatsu, T., Hamada, H. and Yokoyama, T. (2009). Localization of inv in a distinctive intraciliary compartment requires the C-terminal ninein-homolog-containing region. *J. Cell. Sci.* **122,** 44-54.

Simons, M., Gloy, J., Ganner, A., Bullerkotte, A., Bashkurov, M., Kronig, C., Schermer, B., Benzing, T., Cabello, O. A., Jenny, A. et al. (2005). Inversin, the gene product mutated in nephronophthisis type II, functions as a molecular switch between wnt signaling pathways. *Nat Genet* **37,** 537-43.

Simons, M. and Walz, G. (2006). Polycystic kidney disease: Cell division without a c(l)ue? *Kidney Int.* **70,** 854-864.

Singla, V., Romaguera-Ros, M., Garcia-Verdugo, J. M. and Reiter, J. F. (2010). Ofd1, a human disease gene, regulates the length and distal structure of centrioles. *Dev. Cell.* **18,** 410-424.

Smith, L. A., Bukanov, N. O., Husson, H., Russo, R. J., Barry, T. C., Taylor, A. L., Beier, D. R. and Ibraghimov-Beskrovnaya, O. (2006). Development of polycystic kidney disease in juvenile cystic kidney mice: Insights into pathogenesis, ciliary abnormalities, and common features with human disease. *J. Am. Soc. Nephrol.* **17,** 2821-2831.

Snow, J. J., Ou, G., Gunnarson, A. L., Walker, M. R., Zhou, H. M., Brust-Mascher, I. and Scholey, J. M. (2004). Two anterograde intraflagellar transport motors cooperate to build sensory cilia on C. elegans neurons. *Nat. Cell Biol.* **6,** 1109-1113.

Sohara, E., Luo, Y., Zhang, J., Manning, D. K., Beier, D. R. and Zhou, J. (2008). Nek8 regulates the expression and localization of polycystin-1 and polycystin-2. *J. Am. Soc. Nephrol.* **19,** 469-476.

Soppina, V., Herbstman, J. F., Skiniotis, G. and Verhey, K. J. (2012). Luminal localization of alpha-tubulin K40 acetylation by cryo-EM analysis of fab-labeled microtubules. *PLoS One* **7,** e48204.

Sorokin, S. (1962). Centrioles and the formation of rudimentary cilia by fibroblasts and smooth muscle cells. *J. Cell Biol.* **15,** 363-377.

Sorokin, S. P. (1968). Centriole formation and ciliogenesis. *Aspen Emphysema Conf.* **11,** 213-216.

Sugiyama, N., Tsukiyama, T., Yamaguchi, T. P. and Yokoyama, T. (2011). The canonical wnt signaling pathway is not involved in renal cyst development in the kidneys of inv mutant mice. *Kidney Int.* **79,** 957-965.

Sugiyama, N. and Yokoyama, T. (2006). Sustained cell proliferation of renal epithelial cells in mice with inv mutation. *Genes Cells* **11,** 1213-1224.

Suryavanshi, S., Edde, B., Fox, L. A., Guerrero, S., Hard, R., Hennessey, T., Kabi, A., Malison, D., Pennock, D., Sale, W. S. et al. (2010). Tubulin glutamylation regulates ciliary motility by altering inner dynein arm activity. *Curr Biol* **20,** 435-40.

Szymanska, K. and Johnson, C. A. (2012). The transition zone: An essential functional compartment of cilia. *Cilia* **1,** 10-2530-1-10.

Tallila, J., Jakkula, E., Peltonen, L., Salonen, R. and Kestila, M. (2008). Identification of CC2D2A as a meckel syndrome gene adds an important piece to the ciliopathy puzzle. *Am. J. Hum. Genet.* **82,** 1361-1367.

Tam, L. W., Dentler, W. L. and Lefebvre, P. A. (2003). Defective flagellar assembly and length regulation in LF3 null mutants in chlamydomonas. *J. Cell Biol.* **163,** 597-607.

Tam, L. W., Ranum, P. T. and Lefebvre, P. A. (2013). CDKL5 regulates flagellar length and localizes to the base of the flagella in chlamydomonas. *Mol. Biol. Cell* **24,** 588-600.

Tammachote, R., Hommerding, C. J., Sinders, R. M., Miller, C. A., Czarnecki, P. G., Leightner, A. C., Salisbury, J. L., Ward, C. J., Torres, V. E., Gattone, V. H.,2nd et al. (2009). Ciliary and centrosomal defects associated with mutation and depletion of the meckel syndrome genes MKS1 and MKS3. *Hum. Mol. Genet.* **18,** 3311-3323.

Tao, B., Bu, S., Yang, Z., Siroky, B., Kappes, J. C., Kispert, A. and Guay-Woodford, L. M. (2009). Cystin localizes to primary cilia via membrane microdomains and a targeting motif. *J. Am. Soc. Nephrol.* **20,** 2570-2580.

Taskiran, E. Z., Korkmaz, E., Gucer, S., Kosukcu, C., Kaymaz, F., Koyunlar, C., Bryda, E. C., Chaki, M., Lu, D., Vadnagara, K. et al. (2014). Mutations in ANKS6 cause a nephronophthisis-like phenotype with ESRD. *J. Am. Soc. Nephrol.*

Thomas, S., Wright, K. J., Le Corre, S., Micalizzi, A., Romani, M., Abhyankar, A., Saada, J., Perrault, I., Amiel, J., Litzler, J. et al. (2014). A homozygous PDE6D mutation in joubert syndrome impairs targeting of farnesylated INPP5E protein to the primary cilium. *Hum. Mutat.* **35,** 137-146.

Tukachinsky, H., Lopez, L. V. and Salic, A. (2010). A mechanism for vertebrate hedgehog signaling: Recruitment to cilia and dissociation of SuFu-gli protein complexes. *J Cell Biol* **191,** 415-28.

Tuxhorn, J., Daise, T. and Dentler, W. L. (1998). Regulation of flagellar length in chlamydomonas. *Cell Motil. Cytoskeleton* **40,** 133-146.

Varelas, X., Miller, B. W., Sopko, R., Song, S., Gregorieff, A., Fellouse, F. A., Sakuma, R., Pawson, T., Hunziker, W., McNeill, H. et al. (2010). The hippo pathway regulates wnt/beta-catenin signaling. *Dev. Cell.* **18,** 579-591.

Veland, I. R., Montjean, R., Eley, L., Pedersen, L. B., Schwab, A., Goodship, J., Kristiansen, K., Pedersen, S. F., Saunier, S. and Christensen, S. T. (2013). Inversin/nephrocystin-2 is required for fibroblast polarity and directional cell migration. *PLoS One* **8,** e60193.

Veltel, S., Gasper, R., Eisenacher, E. and Wittinghofer, A. (2008). The retinitis pigmentosa 2 gene product is a GTPase-activating protein for arf-like 3. *Nat. Struct. Mol. Biol.* **15,** 373-380.

Verhey, K. J. and Gaertig, J. (2007). The tubulin code. *Cell Cycle* **6,** 2152-60.

Vieira, O. V., Gaus, K., Verkade, P., Fullekrug, J., Vaz, W. L. and Simons, K. (2006). FAPP2, cilium formation, and compartmentalization of the apical membrane in polarized madin-darby canine kidney (MDCK) cells. *Proc Natl Acad Sci U S A* **103,** 18556-61.

Vierkotten, J., Dildrop, R., Peters, T., Wang, B. and Ruther, U. (2007). Ftm is a novel basal body protein of cilia involved in shh signalling. *Development* **134,** 2569-2577.

Vladar, E. K. and Axelrod, J. D. (2008). Dishevelled links basal body docking and orientation in ciliated epithelial cells. *Trends Cell Biol.* **18,** 517-520.

Wang, J., Silva, M., Haas, L. A., Morsci, N. S., Nguyen, K. C., Hall, D. H. and Barr, M. M. (2014). C. elegans ciliated sensory neurons release extracellular vesicles that function in animal communication. *Curr. Biol.* **24,** 519-525.

Warburton-Pitt, S.R.F., Silva, M., Nguyen, K.C.Q., Hall, D.H., Barr, M.M. "The *nphp-2* and *arl-13* genetic modules interact to regulate ciliogenesis and ciliary microtubule patterning in *C. elegans*" (Accepted, PLOS Genetics)

Warburton-Pitt, S. R., Jauregui, A. R., Li, C., Wang, J., Leroux, M. R. and Barr, M. M. (2012). Ciliogenesis in caenorhabditis elegans requires genetic interactions between ciliary middle segment localized NPHP-2 (inversin) and transition zone-associated proteins. *J. Cell. Sci.* **125,** 2592-2603.

Ward, C. J., Yuan, D., Masyuk, T. V., Wang, X., Punyashthiti, R., Whelan, S., Bacallao, R., Torra, R., LaRusso, N. F., Torres, V. E. et al. (2003). Cellular and subcellular localization of the ARPKD protein; fibrocystin is expressed on primary cilia. *Hum Mol Genet*.

Wei, Q., Xu, Q., Zhang, Y., Li, Y., Zhang, Q., Hu, Z., Harris, P. C., Torres, V. E., Ling, K. and Hu, J. (2013). Transition fibre protein FBF1 is required for the ciliary entry of assembled intraflagellar transport complexes. *Nat. Commun.* **4,** 2750.

Werner, M. E., Ward, H. H., Phillips, C. L., Miller, C., Gattone, V. H. and Bacallao, R. L. (2013). Inversin modulates the cortical actin network during mitosis. *Am. J. Physiol. Cell. Physiol.* **305,** C36-47.

Wiens, C. J., Tong, Y., Esmail, M. A., Oh, E., Gerdes, J. M., Wang, J., Tempel, W., Rattner, J. B., Katsanis, N., Park, H. W. et al. (2010). Bardet-biedl syndrome-associated small GTPase ARL6 (BBS3) functions at or near the ciliary gate and modulates wnt signaling. *J Biol Chem* **285,** 16218-30.

Williams, C. L., Li, C., Kida, K., Inglis, P. N., Mohan, S., Semenec, L., Bialas, N. J., Stupay, R. M., Chen, N., Blacque, O. E. et al. (2011). MKS and NPHP modules cooperate to establish basal body/transition zone membrane associations and ciliary gate function during ciliogenesis. *J. Cell Biol.* **192,** 1023-1041.

Williams, C. L., Masyukova, S. V. and Yoder, B. K. (2010). Normal ciliogenesis requires synergy between the cystic kidney disease genes MKS-3 and NPHP-4. *J Am Soc Nephrol* **21,** 782-93.

Williams, C. L., Winkelbauer, M. E., Schafer, J. C., Michaud, E. J. and Yoder, B. K. (2008). Functional redundancy of the B9 proteins and nephrocystins in caenorhabditis elegans ciliogenesis. *Mol. Biol. Cell* **19,** 2154-2168.

Winkelbauer, M. E., Schafer, J. C., Haycraft, C. J., Swoboda, P. and Yoder, B. K. (2005). The C. elegans homologs of nephrocystin-1 and nephrocystin-4 are cilia transition zone proteins involved in chemosensory perception. *J Cell Sci* **118,** 5575-87.

Wloga, D., Dave, D., Meagley, J., Rogowski, K., Jerka-Dziadosz, M. and Gaertig, J. (2010). Hyperglutamylation of tubulin can either stabilize or destabilize microtubules in the same cell. *Eukaryot. Cell.* **9,** 184-193.

Wojtyniak, M., Brear, A. G., O'Halloran, D. M. and Sengupta, P. (2013). Cell- and subunit-specific mechanisms of CNG channel ciliary trafficking and localization in C. elegans. *J. Cell. Sci.* **126,** 4381-4395.

Wright, K. J., Baye, L. M., Olivier-Mason, A., Mukhopadhyay, S., Sang, L., Kwong, M., Wang, W., Pretorius, P. R., Sheffield, V. C., Sengupta, P. et al. (2011). An ARL3-UNC119-RP2 GTPase cycle targets myristoylated NPHP3 to the primary cilium. *Genes Dev.* **25,** 2347-2360.

Wu, Y., Dai, X. Q., Li, Q., Chen, C. X., Mai, W., Hussain, Z., Long, W., Montalbetti, N., Li, G., Glynne, R. et al. (2006). Kinesin-2 mediates physical and functional interactions between polycystin-2 and fibrocystin. *Hum Mol Genet* **15,** 3280-92.

Wuebken, A. and Schmidt-Ott, K. M. (2011). WNT/beta-catenin signaling in polycystic kidney disease. *Kidney Int.* **80,** 135-138.

Xu, G. M., Gonzalez-Perrett, S., Essafi, M., Timpanaro, G. A., Montalbetti, N., Arnaout, M. A. and Cantiello, H. F. (2003). Polycystin-1 activates and stabilizes the polycystin-2 channel. *J Biol Chem* **278,** 1457-62.

Yasuhiko, Y., Imai, F., Ookubo, K., Takakuwa, Y., Shiokawa, K. and Yokoyama, T. (2001). Calmodulin binds to inv protein: Implication for the regulation of inv function. *Dev. Growth Differ.* **43,** 671-681.

Yin, Y., Bangs, F., Paton, I. R., Prescott, A., James, J., Davey, M. G., Whitley, P., Genikhovich, G., Technau, U., Burt, D. W. et al. (2009). The Talpid3 gene (KIAA0586) encodes a centrosomal protein that is essential for primary cilia formation. *Development* **136,** 655-664.

Yoder, B. K., Hou, X. and Guay-Woodford, L. M. (2002). The polycystic kidney disease proteins, polycystin-1, polycystin-2, polaris, and cystin, are co-localized in renal cilia. *J Am Soc Nephrol* **13,** 2508-16.

Zalli, D., Bayliss, R. and Fry, A. M. (2012). The Nek8 protein kinase, mutated in the human cystic kidney disease nephronophthisis, is both activated and degraded during ciliogenesis. *Hum. Mol. Genet.* **21,** 1155-1171.

Zhang, H., Constantine, R., Vorobiev, S., Chen, Y., Seetharaman, J., Huang, Y. J., Xiao, R., Montelione, G. T., Gerstner, C. D., Davis, M. W. et al. (2011). UNC119 is required for G protein trafficking in sensory neurons. *Nat. Neurosci.* **14,** 874-880.

Zhang, H., Li, S., Doan, T., Rieke, F., Detwiler, P. B., Frederick, J. M. and Baehr, W. (2007). Deletion of PrBP/delta impedes transport of GRK1 and PDE6 catalytic subunits to photoreceptor outer segments. *Proc. Natl. Acad. Sci. U. S. A.* **104,** 8857-8862.

Zhang, H., Liu, X. H., Zhang, K., Chen, C. K., Frederick, J. M., Prestwich, G. D. and Baehr, W. (2004). Photoreceptor cGMP phosphodiesterase delta subunit (PDEdelta) functions as a prenyl-binding protein. *J. Biol. Chem.* **279,** 407-413.

Zhao, C. and Malicki, J. (2011). Nephrocystins and MKS proteins interact with IFT particle and facilitate transport of selected ciliary cargos. *EMBO J.*

Zhou, C., Cunningham, L., Marcus, A. I., Li, Y. and Kahn, R. A. (2006). Arl2 and Arl3 regulate different microtubule-dependent processes. *Mol. Biol. Cell* **17,** 2476-2487.

Zhou, W., Dai, J., Attanasio, M. and Hildebrandt, F. (2010). Nephrocystin-3 is required for ciliary function in zebrafish embryos. *Am J Physiol Renal Physiol* **299,** F55-62.

Zuo, X., Guo, W. and Lipschutz, J. H. (2009). The exocyst protein Sec10 is necessary for primary ciliogenesis and cystogenesis in vitro. *Mol. Biol. Cell* **20,** 2522-2529.

Chapter 2: *nphp-2* interacts with two transition zone modules to regulate ciliogenesis and cilia placement

Note: This chapter is modified from the following publication:

Warburton-Pitt, S.R.F, Jauregui, A.R., Li, C., Wang, J., Leroux, M.R., Barr, M.M. "Ciliogenesis in *Caenorhabditis elegans* requires genetic interactions between ciliary middle segment localized NPHP-2 (inversin) and transition zone-associated proteins" J Cell Sci. 2012 Jun 1;125 (Pt 11):2592-603.

2.1 – Abstract

The cystic kidney diseases Nephronophthisis (NPHP), Meckel Gruber Syndrome (MKS), and Joubert Syndrome (JBTS) share an underlying etiology of dysfunctional cilia. Patients diagnosed with NPHP type II have mutations in the gene INVS/NPHP2, which encodes inversin, a cilia localizing protein. Here, we show that the *C. elegans* inversin ortholog, NPHP-2, localizes to the middle segment[7] of sensory cilia, and is partially redundant with *nphp-1* and *nphp-4* (orthologs of human nephrocystin-1 and nephrocystin-4, respectively) for cilia placement within the head and tail sensilla. *nphp-2* also genetically interacts with MKS ciliopathy gene orthologs, including *mks-1*, *mks-3*, *mks-6*, *mksr-1*, and *mksr-2*, in a sensilla-dependent manner to control cilia formation and placement. However, *nphp-2* is not required for correct localization of the NPHP and MKS encoded ciliary transition zone proteins or for intraflagellar transport (IFT). We conclude that INVS/NPHP2 is conserved in *C. elegans*, and that *nphp-2* plays an important role in *C. elegans* cilia acting as a modifier of the previously described NPHP and MKS pathways to control cilia formation and development.

---

[7] During the time-frame this manuscript was written, the doublet region was known as the "middle segment (MS)", and the singlet region was known as the "distal region (DR)". These older terms were not originally defined rigorously and were thus used to signify subtly different concepts by different authors.

2.2 – Introduction

2.2.1 – Ciliopathies

Human ciliopathies, including nephronophthisis (NPHP), Meckel Syndrome (MKS), and Joubert

Syndrome (JBTS), are a class of genetic disorders defined by defective cilia and cystic kidneys

(Badano et al., 2006). The primary nephropathy is often comorbid with retinal degeneration,

deafness, polydactyly, obesity and situs inversus (Hildebrandt and Zhou, 2007; Pazour and

Rosenbaum, 2002; Wheatley, 1995). Many syndromic ciliopathies share loci; in particular, NPHP,

MKS and JBTS have thirteen, ten, and thirteen genetic loci identified, respectively, and exhibit

considerable overlap (e.g., NPHP6/MKS4/JBTS5 and NPHP11/MKS3/JBTS6) such that there are

currently twenty-five distinct loci in sum (Table 3). Disease class overlap may be due partially to

the underlying oligogenic nature of the disorders (Hoefele et al., 2007). Ciliopathy associated

genes encode cystoproteins; a majority of these gene products localize to the cilium; the wide

array of symptoms associated with ciliopathies is due to the near-ubiquitous presence of cilia on

mammalian cells.

2.2.2 – *C. elegans* as a model to study cilia

Cilia are hair-like microtubule (MT)-based organelles that protrude from cell surfaces. Sensory

cilia act to receive and transmit information from the extracellular environment and are integral

to many signal transduction pathways (Goetz and Anderson, 2010). Eukaryotic cilia and

structurally related eukaryotic flagella are constructed by intraflagellar transport (IFT), a MT

motor based transport system. The nematode *Caenorhabditis elegans* is a powerful system to

study fundamental questions in cilia biology and to model human ciliopathies. The primary

sensory organs of *C. elegans* are the amphid and phasmid sensilla in the head and tail (Perkins et

al., 1986). The cilia within these sensilla have a wide range of morphologies and functions,

allowing for investigation of ciliary specializations and function (Bae and Barr, 2008; Jauregui et

al., 2008). The MKS1-related genes B9D1 and B9D2, first characterized as ciliary proteins in

C. elegans, are ciliopathic in humans, highlighting the power of this model (Bialas et al., 2009;

Dowdle et al., 2011; Williams et al., 2008).

C. elegans cilia are located on the distal dendritic endings of sensory neurons, where a

centriole-derived complex consisting principally of transition fibers (TF) precedes the

microtubule-based axoneme (Dammermann et al., 2009; Perkins et al., 1986). The first segment

of the axoneme is the transition zone (TZ), a region where many ciliary proteins congregate,

either regulating ciliary traffic, being imported/exported into the cilium, or playing

structural/functional roles essential for ciliogenesis and formation of the so-called 'ciliary gate'

(Rosenbaum and Whitman, 2002). The axoneme extends from the TZ. In *C. elegans* amphid

channel cilia, the axoneme comprises a MT doublet middle segment and a MT singlet distal

segment (Perkins et al., 1986).

2.2.3 – The transition zone ciliary protein complex

In *C. elegans* cilia, most ciliopathy-related proteins are either directly implicated in IFT function

(e.g., BBS-1, BBS-7, BBS-8), or localize to the TZ/basal body complex (e.g., NPHP-1, NPHP-4,

MKS-1, MKS-3, MKS-6) (Bialas et al., 2009; Blacque et al., 2004; Garcia-Gonzalo et al., 2011;

Jauregui and Barr, 2005; Qin et al., 2001; Williams et al., 2008; Winkelbauer et al., 2005). This TZ

complex is necessary for early ciliogenesis and the TZ is a region associated with traffic into and

out of the cilium (Williams et al., 2011). Single mutations in genes encoding TZ complex

members yield mild or nonobservable ciliogenic defects. However in certain pairwise

combinations, these mutations cause ciliogenesis defects result that are attributable to

anomalies in centriole/TZ membrane anchoring (Williams et al., 2008; Williams et al., 2010;

Williams et al., 2011). Mammalian NPHP1/JBTS4 and NPHP4 physically interact to form a

complex (Mollet et al., 2002). In *C. elegans*, *nphp-1* and *nphp-4* single and double mutants have

superficially normal cilia, though transmission electron microscopy reveals subtle ultrastructural

defects (Jauregui and Barr, 2005; Jauregui et al., 2008; Winkelbauer et al., 2005). Neither is

required for localization of the ciliary receptors OSM-9 and PKD-2; however, mutations in

nphp-4 indirectly affect the velocity of several IFT subcomponents (Jauregui et al., 2008). *mks-1*

(orthologous to MKS1/BBS13) encodes a B9 domain (a C2-like lipid/calcium binding domain

[Zhang and Aravind, 2010]) containing protein in the same family and pathway as *mksr-1* and

mksr-2 (orthologous to B9D1 and B9D2, respectively); mutations in any or all three of these

three genes produce no significant cilia defects (Bialas et al., 2009; Kyttala et al., 2006; Williams

et al., 2008). MKS-1, MKSR-1, and MKSR-2 are interdependent for proper localization, and

function together with NPHP-1 and NPHP-4 to regulate ciliogenesis (Bialas et al., 2009; Williams

et al., 2008). *mks-3* (orthologous to MKS3/TMEM67/NPHP11/Meckelin) plays a minor role in

sensation mediated behaviors, and genetically interacts with *nphp-4* to yield dysfunctional cilia

in the double mutant (Williams et al., 2010). Recently, MKS-6 (a C2 domain encoding orthologs

of JBTS9/CC2D2A) was shown to function together with NPHP-1 or NPHP-4 to control

centriole/TZ anchoring to the membrane, the initial step of ciliogenesis (Williams et al., 2011).

These genetic interactions have provided evidence for two functional pathways, or modules: an

"MKS pathway" involving MKS-1, MKSR-1, MKSR-2, MKS-3 and MKS-6, and an "NPHP pathway"

comprising NPHP-1 and NPHP-4.

Further work in both *C. elegans* and mammalian systems has reinforced these findings and

extended these modules. The Jackson group identified a NPHP5/NPHP6 module in addition to

the MKS and NPHP1/NPHP4 modules. These modules are physically linked through mutual

interactions with NPHP2 (Sang et al., 2011). In mice, the MKS module (comprising MKS1, TMEM216, TMEM67, CEP290, B9D1, and CCD2A) is essential for ciliogenesis in some tissues, and is necessary for localization of several membrane-associated ciliary proteins, including Arl13b, Smoothened, and Pkd2 (Garcia-Gonzalo et al., 2011). The MKS module also contains Tectonic1/TCTN1, a hedgehog signaling component, linking ciliogenesis, membrane composition, and signaling (Garcia-Gonzalo et al., 2011). Several of these genetic and functional interactions between TZ-associated genes are conserved in *C. elegans*, providing a powerful tool to define genetic pathways.

2.2.4 – Inversin in mammalian models

Mutations in INVS/NPHP2 are responsible for NPHP type II, an infantile autosomal recessive disease. The gene product inversin is named for the inversion of visceral asymmetry in the *inv* mouse, which is normally mediated by nodal monocilia (Morgan et al., 1998; Watanabe et al., 2003). Renal cysts of *inv* mice resemble those in infantile NPHP2 patients (Phillips et al., 2004). Interestingly, the N-terminal ankyrin repeat containing region of inversin can localize to node cilia and rescue left-right defects, but not renal cysts, indicating that inversin is a multifunctional protein that acts in a cell-type specific manner (Watanabe et al., 2003). In *Xenopus* and zebrafish, inversin acts as a molecular switch between canonical and noncanonical Wnt signaling by binding cytoplasmic disheveled (Dvl) and targeting it for degradation; disruption of this pathway interchange is concordant with disease expression (Bellavia et al., 2010; Benzing et al., 2007; Simons et al., 2005). In mammals, several isoforms of inversin localize to the proximal segment of sensory cilia, a region termed the "Inv compartment." The zebrafish ortholog of *mksr-2*, B9d2, physically interacts with and modulates ciliary localization of inversin, which in turn is necessary for anchoring the NPHP3 and NPHP9 gene products to the same compartment

(Shiba et al., 2009; Shiba et al., 2010; Zhao and Malicki, 2011).

2.2.5 – Summary of this study

In this study, we show that the *C. elegans* ortholog of INVS/NPHP2, *nphp-2*, is expressed in ciliated sensory neurons and encodes two protein isoforms that localize to the ciliary middle segment or "Inv compartment". We also demonstrate that *nphp-2* is partially redundant with *nphp-1* and *nphp-4* in regulation of TZ placement, TZ orientation, and IFT particle velocity but not for localization of other TZ proteins. Cilia in the *nphp-2 nphp-4* double mutant are severely compromised, although neither *nphp-2* nor *nphp-4* is necessary for localization of B9 domain proteins, MKS-1, MKSR-1, and MKSR-2 (Williams et al., 2008). Genetic experiments between *nphp-2* and MKS genes encoding TZ-localizing proteins demonstrate a complex interaction network, which varies in a sensillum-dependent manner. We conclude that *nphp-2* plays an important role in *C. elegans* cilia, and that *nphp-2* acts as a sensillum-specific modifier of the previously described NPHP and MKS pathways.

2.3 – Results

2.3.1 – Y32G9A.6 is the *C. elegans* ortholog of INVS/NPHP2

Inversin possess several domains, including protein interacting ankyrin repeats, two nuclear localization signals (NLS), two calmodulin binding IQ domains, a basic residue enriched region, and a C-terminal ninein homology region (Figure 7A) (Morgan et al., 2002). At least two of these regions, the ankyrin repeat and the ninein homology regions, are independently sufficient for ciliary localization of inversin (Shiba et al., 2009; Watanabe et al., 2003). Protein BLAST homology searches against the *C. elegans* genome yielded several candidates, including Y32G9A.6 (See 2.5.3 – *C. elegans* INVS homology search). The Y32G9A.6 promoter contains an X-box motif, found in many ciliary genes, and has been identified in at least two ciliary genomic screens, one of which demonstrated expression in ciliated neurons, and predicted Y32G9A.6 as "inversin-like" (Blacque et al., 2005; Efimenko et al., 2005). Protein primary sequence analysis of Y32G9A.6 predicts a D-box ubiquitination site, a bipartite nuclear localization signal, and an EF-hand (Figure 7A). All domains present in Y32G9A.6, with the exception of the EF hand, are conserved in inversin orthologs across several species (Figure 7A) (Morgan et al., 2002). Rather than having a direct calcium binding EF hand, inversin possesses an IQ domain, which binds the calcium sensor calmodulin. Amino acid sequence comparison of Y32G9A.6 and inversin shows 19.1% identity, and 35.2% similarity, and only marginally less – 16.9% identity and 32.6% similarity – when ankyrin repeats are omitted. This is less than other ciliary proteins, but is still significant (Table 4). Based on BLAST results, presence of an X-box promoter motif, conserved protein motifs, and domain organization similar to inversin, we characterized and showed that Y32G9A.6 is the *C. elegans* ortholog of inversin. This gene was coexpressed and genetically

interacted with the other NPHP genes (see below). We hereafter refer to the sequence Y32G9A.6 as *nphp-2*.

2.3.2 – *nphp-2* is expressed in ciliated neurons and encodes two cilium-localized isoforms

The expression pattern of *nphp-2* was determined through use of native promoter driven GFP expression. P$_{nphp-2}$::GFP was expressed in the ciliated sensory nervous system throughout development. In the adult, expression was evident in both hermaphrodite and male ciliated sensory neurons, including amphid, phasmid, and IL2 neurons. *nphp-2* was also expressed in male specific ciliated sensory nervous system, including the CEM, RnB, and HOB neurons (Figure 7B). Expression in the internal oxygen sensor neuron PQR was visible in the hermaphrodite, but could not be distinguished from the tail sensilla in the male.

RT-PCR with subsequent sequencing was used to confirm the predicted splicing pattern and cDNA sequence, and revealed two distinct isoforms. In addition to the predicted full length transcript (long isoform, NPHP-2L), a more abundant (approx. 10-fold) shorter isoform (NPHP-2S) was detectable. This latter isoform, spliced from within exon 10 to the start of exon 11, lacks a region encoding a twenty-two residue fragment (VLIARKNARALFRNYYHPGTEQ), which does not contain or lie within any identified domain. To ascertain the subcellular localization of each isoform, we used native promoter driven expression of GFP tagged splice form cDNA, *e.g.*, the short form P$_{nphp-2}$::NPHP-2S::GFP and the long form P$_{nphp-2}$::NPHP-2L::GFP. Cilia in transgenic NPHP-2S::GFP and NPHP-2L::GFP animals form properly in a wild-type background as determined by dye filling (Figure 13). Both NPHP-2S and NPHP-2L transgenes are functional and rescue dye filling defects in the *nphp-2 nphp-4* double mutant (Figure 14). To determine subciliary localization, NPHP-2S::GFP and NPHP-2L::GFP were coexpressed with

P$_{nphp-1}$::NPHP-1::CFP, a transition zone (TZ) marker. NPHP-2S::GFP localized cytoplasmically throughout neurons, including dendrites, cell bodies and axons, and to the middle segment of amphid channel and phasmid cilia (Figure 7C, Figure 15). NPHP-2S::GFP was excluded from the TZ and the nucleus (Figure 7C,D; Figure 15). NPHP-2L::GFP also primarily localized to the middle segments of amphid channel and phasmid cilia; dim signals were observable in cell bodies and dendrites, though not in axons. In addition, several bright NPHP-2L::GFP puncta were observable within the cell body (Figure 7C,D). Both NPHP-2S and NPHP-2L localized to the middle segment at all stages of development, from larval L1 to young adult (Figure 36). The middle segment localization of NPHP-2S and NPHP-2L differs markedly from the TZ localization of most other cystoproteins, including NPHP-1, NPHP-4, MKS-1, and MKS-6 (Bialas et al., 2009; Jauregui and Barr, 2005; Williams et al., 2008; Williams et al., 2011; Winkelbauer et al., 2005). To confirm middle segment localization, the length of the NPHP-2S and NPHP-2L localizations was measured (2.5±0.59 µm) and was found to be similar to the length of the MS as measured in EM micrographs (2-3µm) (David Hall, personal communication). GFP-tagged NPHP-2S and NPHP-2L ciliary motility was undetectable, indicating that NPHP-2 is—like the TZ proteins—unlikely to be a component of the IFT machinery (Figure 36).

2.3.3 – *nphp-2* is necessary for proper TZ/cilia placement

The available *nphp-2* mutant *gk653* contains a deletion from upstream of the start codon to within the first intron, removing the start ATG. A hidden Markov model splice site predictor correctly predicts the wild-type splice pattern, but predicts an alternate start site in *gk653*, which yields a transcript with a dysfunctional first exon followed by a continuation of the correct transcript (data not shown). RT-PCR of *nphp-2* cDNA confirms the presence of a transcript in *gk653* mutants (data not shown). We therefore generated (by Mos1 transposon mutagenesis)

and examined two additional *nphp-2* alleles, *nx101* and *nx102*, which contain in-frame deletions

over ankyrin repeats 5-11 and 5-8, respectively (Figure 7A, Figure 16).

To characterize mutant ciliary phenotypes associated with these deletion alleles, we incubated

animals with the lipophilic fluorescent dye DiI, which allows readout of gross cilium structure

and dendrite extension (Perkins et al., 1986). The dye is taken up by a subset of amphid and

phasmid ciliated neurons that are either directly exposed to the environment (e.g., ASK, PHA) or

are embedded in the cuticle (e.g., AWB). Failure of a neuron to take up DiI may be indicative of

cilia structural or dendritic extension defects. *nphp-2(gk653)* mutants had a moderate dye filling

defect (Dyf) in phasmid neurons, while amphid neurons appeared normal (Figure 8A).

nphp-2(*nx101)* and *nphp-2*(*nx102)* mutants exhibited phasmid Dyf phenotypes that were

weaker than those observed in *gk653* animals (0.59 in *gk653* vs. 0.83 and 0.85 in *nx101* and

nx102, respectively)*.* For this reason, we used *nphp-2*(*gk653)* for the remainder of experiments.

While no loss of function or null alleles of *nphp-2* exist, we predict that these would have

stronger Dyf phenotypes than the moderate severity observed in *gk653* animals.

To determine if cilia displacement defects are phasmid sensilla-specific, as dye filling suggests,

or general to core ciliated neurons, we directly examined cilia placement in both amphid and

phasmid sensilla. To label amphid and phasmid cilia, we coexpressed NPHP-1::CFP, a TZ marker,

and CHE-13::YFP, a TF/cilia axonemal marker. In wild-type amphid sensilla, TZs clustered closely

together and cilia were tightly grouped (Figure 8C, left). While both NPHP-1::CFP and

CHE-13::YFP localized properly in *nphp-2* animals, amphid TZs were dispersed over a larger area

and their associated cilia were no longer tightly bundled (Figure 8C, right). We quantified TZ

spread by measuring the distance between the anterior-most and posterior-most TZs (Williams

et al., 2011). We found that *nphp*-2 TZs in the amphid sensilla were dispersed over a distance

three times longer than WT (data not shown). In WT phasmid sensilla, PHA and PHB cilia and TZs

align (Figure 8C, left). In *nphp-2* phasmid sensilla, cilia and TZs were no longer aligned (Figure 8C, right). Use of another TZ marker, NPHP-4::YFP, yielded similar results: correct subcellular localization of the markers, but disorganized TZ regions in *nphp-2(gk653)* animals (Figure 17). In general, amphid sensilla TZ/cilia displacement was less severe than in phasmid sensilla (approx. 1-2 μm vs. 9 μm , respectively), which may explain the lack of an apparent amphid Dyf phenotype.

Next, we explored the possible correlation between the Dyf phenotype and ciliary displacement. *nphp-2* mutants expressing CHE-11::GFP, which marks the ciliary TZ and axoneme (Williams et al., 2011), were incubated with DiI. Displaced cilia that fail to make contact with the phasmid pore are Dyf, whereas properly positioned cilia dye fill. This implies that the phasmid Dyf phenotype likely stems from an anterior shift in phasmid TZ/cilia placement (Figure 8B). As we could not use TZ spread as a measure of cilia displacement in the phasmid sensilla as we did in the amphid cilia, we instead quantified the displacement by measuring the distance from the TZ to the cell body. In *nphp-2* mutants the distance between the cell body and the TZ was significantly shorter than WT (Figure 10), indicating that cilia were displaced towards the cell body. However, *nphp-2* displaced phasmid cilia had a concomitant increase in length, allowing for contact with the phasmid pore. We conclude that *nphp-2* affects TZ/cilia placement in both amphid and phasmid sensilla.

2.3.4 – Genetic analysis reveals a complex interaction network between

C. elegans ciliopathic orthologs

Given the oligogenic nature of nephronophthisis (Guay-Woodford et al., 2000; Kuida and Beier, 2000; Wolf and Hildebrandt, 2011), we explored genetic interactions of *nphp-2* with ciliopathy disease gene orthologs with TZ-localized products. First, we measured amphid and phasmid dye

filling. Sensilla of the single mutants *nphp-1(ok500), nphp-4(tm1925), mks-1(tm2705), mksr-1(ok2092), mksr-2(tm2452), mks-3(tm2547)*, and *mks-6(gk674)* are non-Dyf with the exception of the *nphp-2* phasmid Dyf phenotype (Figure 8A) (Williams et al., 2011). However, many double mutant combinations showed a synthetic dye filling defect (SynDyf), exhibiting a wide range of dye filling phenotypes (Table 1 and Figure 18). Double mutants between an MKS gene (*mks-1*, *mks-3*, *mks-6*) and *nphp-1* or *nphp-4* are severely Dyf in both amphids and phasmids, indicating that two parallel redundant pathways, an MKS pathway and a NPHP pathway, that act similarly in amphid and phasmid sensilla (Williams et al., 2008; Williams et al., 2011).

Examination of *nphp-2* double mutants reveals differences between ciliogenic roles in amphid and sensilla. In phasmid sensilla, *nphp-2* was SynDyf with *nphp-1*, *nphp-4*, *mks-3*, and *mks-6*, indicating that *nphp-2* acts as a modifier of both the MKS and NPHP pathways (Table 1, bottom). In the context of amphid sensilla, *nphp-2* was SynDyf with *nphp-1*, *nphp-4*, *mksr-1*, and *mksr-2* and was nonDyf in double mutant combinations with the MKS family members *mks-1*, *mks-3* and *mks-6* (Table 1, top)*.

nphp-2 single mutants showed an increase in amphid TZ spread, a shortening of phasmid dendrite length, and an increase in phasmid cilia length. Therefore, we measured these features, in addition to amphid cilia length, in several SynDyf double mutants, including *nphp-2 nphp-4*, *mks-6; nphp-2*, and *mks-6; nphp-4*, and in the single mutants *nphp-4* and *mks-6*. Dendrites, cilia, and TZs were visualized using the IFT-A marker CHE-11::GFP. In the amphid sensilla, single mutants *nphp-4* and *mks-6* did not exhibit a significant increase in TZ spread. In the double mutants, TZ spread was increased compared to their respective single mutants, indicative of errors in cilia placement (Figure 9A). Phasmid dendritic length, an indicator of TZ displacement in phasmid sensilla, was significantly decreased in single mutants (73% of the

average length of WT), implying mild TZ displacement. Double mutants had dendritic lengths

significantly shorter than any of the single mutants, implying severe TZ displacement (Figure 9B).

The dye filling results suggest that *nphp-2* has a sensillum-specific role, though *nphp-2* interacts

with *nphp-1* and *nphp-4* in both amphid and phasmid sensilla. By contrast, *nphp-2* genetically

interacts with different members of the MKS family in a sensillum specific manner. The

synergistic defects seen in both amphid TZ spread and phasmid dendritic length suggest genetic

redundancy between *nphp-2* and the NPHP-1/-4 and MKS pathways. Cilia length measurements

in both amphid and phasmid neurons also showed synthetic defects: double mutants had

significantly shorter cilia than single mutants, with the single exception of the phasmid cilia

length comparison between *nphp-4* and *nphp-2 nphp-4* mutants (Figure 9C). Curiously, the

mks-6; nphp-2 double mutant has synthetic defects in both amphid TZ spread and cilia length,

whereas mutants are not amphid SynDyf. This may indicate either that the pathway governing

dye filling is separate from the pathway governing cilia formation and placement, or that cilia

morphology and dye uptake do not always correlate as previously reported, e.g., a retracted

cilium may still contact the now elongated amphid pore and DiI solution. Taken with previous

work, these data support two primary TZ genetic pathways, an NPHP-1/-4 pathway and an MKS

pathway, with a role for *nphp-2* as a sensilla-specific modifier.

2.3.5 – *nphp-2* and *nphp-4* act redundantly to regulate cilia placement and IFT

The genetic interactions between *nphp-2* and TZ-associated genes imply redundant roles and

functions. We began exploring these by focusing on the association between *nphp-2* and

nphp-4. In contrast to either single mutant, and unlike most other double mutants, the *nphp-2*

nphp-4 double mutant was completely Dyf in both amphid and phasmid sensilla (Table 2). We

used IFT-B polypeptide OSM-5::GFP and IFT-A polypeptide CHE-11::GFP to visualize ciliary

TF-axonemal structures. In amphid sensilla, wild-type animals exhibit a pyramidal amphid channel ciliary bundle, with all TFs within 5 µm of each other (Snow et al., 2004) (Figure 10a,b). In *nphp-2 nphp-4* double mutants, no cohesive bundle was evident, cilia orientation within the bundle was disrupted, and a portion of the amphid channel cilia appeared to be elongated, curly, or stunted (Figure 10e,f). In the amphid sensilla, it was not possible to identify and associate defects with specific cilia. However, in phasmid sensilla, PHA and PHB exhibit both elongated and stunted phenotypes.

Defects in dye filling, cilia length, and cilia placement may be associated with defects in IFT. In amphid channel and phasmid cilia, the IFT machinery is composed of two complexes, IFT-A and IFT-B, which are transported by two anterograde Kinesin-2 motors, slow Kinesin-II and fast OSM-3, towards the cilia tip (Snow et al., 2004). In wild-type amphid channel cilia, the IFT-A associated Kinesin-II heterotrimeric motor traverses only the middle segment, whereas the IFT-B associated OSM-3 homodimeric motor travels along the entire length of the axoneme. As the IFT particles are linked by the BBS protein complex, when a particle is on the middle segment, both motors are engaged and move along at a speed of 0.7-0.8 µm/sec, whereas while on the distal segment, only OSM-3 is engaged, and the particle travels at the speed of 1.0-1.2 µm/sec (Ou et al., 2005; Snow et al., 2004). To probe IFT function, we measured the velocities of IFT-B polypeptide OSM-5::GFP, IFT-A polypeptide CHE-11::GFP, and homodimeric Kinesin-2 OSM-3::GFP. In *nphp-2* mutants, GFP-tagged OSM-5, CHE-11, and OSM-3 velocities in middle and distal segments were similar to wild type (Table 2). No abnormal accumulation of IFT reporters was seen at the ciliary base, indicating particles were being loaded onto the axoneme correctly (Figure 10c,d).

Amphid cilia disorganization in the *nphp-2 nphp-4* double mutant made it difficult to define the middle and distal ciliary segments. In *nphp-2 nphp-4* double mutants, both IFT-A component

CHE-11::GFP (1.02 ± 0.20 μm/s) and IFT-B component OSM-5::GFP (1.03 ± 0.17 μm/s) moved at

speeds comparable to the velocity of the IFT particle in the wild-type distal segment (1.13 ± 0.15

μm/s and 1.06 ± 0.16 μm/s, respectively) (Table 2). We also observed that the IFT-B associated

motor OSM-3::GFP travelled along the entire cilium at a velocity of 1.12 ± 0.24 μm/s, similar to

the distal segment velocity of OSM-3 in WT. The velocities of the IFT particle observed in *nphp-2*

nphp-4 mutants are similar to IFT-A and IFT-B velocities in Kinesin-II mutants, in which OSM-3 is

the only motor associated with the IFT particle (Pan et al., 2006). Previously, it was reported that

OSM-3 overexpression in *nphp-4* mutants results dendritic accumulation of OSM-3 (Jauregui et

al., 2008); we also observe this in *nphp-2 nphp-4* animals overexpressing OSM-3. Surprisingly,

OSM-3 overexpression suppressed the truncated cilia phenotype in the phasmid sensillum of

nphp-2 nphp-4 double mutants (average length 7.40 ± 0.62 μm). This rescue was not concordant

with a rescue of the Dyf phenotype (data not shown). We conclude that within amphid cilia,

nphp-2 does not modify IFT complex localization, velocity, or loading onto the axoneme.

However, in *nphp-2 nphp-4* double mutants, OSM-3 is the primary motor driving IFT, perhaps

due to the uncoupling of the heterotrimeric Kinesin-II motor from the IFT complex.

2.3.6 – *nphp-2* is not required for proper localization of NPHP-1, NPHP-4 or B9 proteins

To explore whether NPHP-2 might influence the localization of TZ proteins, we first tested and

observed that *nphp-2* is not essential for NPHP-1 or NPHP-4 TZ localization (Figure 8 and Figure

17). To determine whether NPHP-2 is required for the localization of proteins belonging to the

second TZ-associated gene pathway, we examined B9 protein localization in *nphp-2* mutants.

MKS-1::GFP and MKSR-2::GFP localized to the TZ in wild type animals (Figure 11a,g), *nphp-2*

single mutants (Figure 11b,h), and *nphp-2 nphp-4* double mutants (Figure 11c,i), although

several TZs were improperly positioned within the amphid sensillum. In wild-type animals,

MKSR-1::GFP localized to both the dendritic tip and the TZ (Bialas et al., 2009; Williams et al.,

2008), and is likewise unaffected in *nphp-2* single and *nphp-2 nphp-4* double mutants (Figure

11d-f). We conclude that *nphp-2* is not required for the proper TZ localization of NPHP

(NPHP-1/NPHP-4) pathway proteins or B9 proteins of the MKS pathway.

2.4 – Discussion

INVS/NPHP2, mutated in infantile NPHP type II, localizes to the ciliary proximal segment or "Inv compartment" and is a genetic modifier of polycystic kidney disease. Here we show that the *C. elegans* ortholog of INVS, NPHP-2, localizes to the *C. elegans* ciliary middle segment, similar to the "Inv compartment" of mammalian cilia, and plays a role in TZ placement. We also find the genetic interactions between *nphp-2* and the NPHP1/4 and MKS pathways in *C. elegans* reflects the physical interaction between NPHP and MKS modules in mammalian systems (Sang et al., 2011).

2.4.1 – The conservation of Inversin and the two *C. elegans* NPHP-2 isoforms

Use of multiple bioinformatic analyses and examination of expression and localization patterns establishes Y32G9A.6 as the ortholog of INVS (Blacque et al., 2005). INVS encodes an IQ domain, which interacts with calmodulin in a Ca^{2+}-dependent manner (Morgan et al., 2002). In contrast to INVS, *NPHP-2* is predicted to contain a Ca^{2+} binding EF hand, which may function in a similar manner as the IQ domain. INVS encodes multiple isoforms (Nurnberger et al., 2002; Ward et al., 2004); likewise, we find that *C. elegans nphp-2* encodes two isoforms. Both NPHP-2S::GFP and NPHP-2L::GFP localize to the middle segment, are excluded from the TZ, and rescue the *nphp-2 nphp-4* SynDyf defect, indicating that both isoforms function in TZ placement. The additional twenty-two amino acid residues in NPHP-2L appear to play a role in restricting NPHP-2L localization to cell-body puncta and the ciliary middle segment, but the functional difference between NPHP-2S and NPHP-2L remains unknown.

2.4.2 – Cause of ciliary defects in *nphp-2* animals

The defects present in *nphp-2(gk653)* animals may stem from one of several possibilities, including impingement on dendritic length, TZ placement, or TZ protein localization. First, an alteration of dendritic length could lead to the observed TZ displacement. *nphp-2* mutants have significantly shorter phasmid dendrites than WT animals, as do several TZ mutants. Double mutants have even shorter dendrites, further evidence of synergistic interactions between the genes. Though phasmid ciliogenesis is currently uncharacterized, these ciliary proteins seem to be necessary for phasmid dendritic extension, which may be mediated through ciliary attachment to the sheath and socket cells near the phasmid pore, as suggested by Williams et al (Williams et al., 2010). Second, *nphp-2* may affect TZ placement at the end of the dendrite. This placement may be mediated by the planar cell polarity (PCP) pathway, which, in zebrafish, is upregulated by inversin (Simons et al., 2005). The role of the PCP in the ciliated nervous system of *C. elegans* is unexplored, and is an exciting avenue for future research. Lastly, *nphp-2* mutation may interfere with correct localization of TZ proteins. This does not seem to be the case for localization of NPHP-1, the B9 proteins, the IFT-A polypeptide CHE-11, and the IFT-B polypeptides CHE-13, OSM-3, and OSM-5. However, in mammalian cells inversin is important for localizing NPHP3 and NPHP9. Likewise, NPHP-2 may have a role in the localization of other ciliary proteins in *C. elegans* (Otto et al., 2003; Shiba et al., 2010).

2.4.3 – Interactions between middle segment *nphp-2* and the TZ

A crucial question is raised by the middle segment localization of both isoforms of NPHP-2: how does a protein enriched in the middle segment and excluded from the TZ affect TZ placement? The middle segment forms after the TZ is placed at the tip of the dendrite during the first phase of ciliogenesis (Williams et al., 2011). Two distinct possibilities may account for this apparent paradox: first, that NPHP-2 may have a non-middle segment function, and second, that cilia

placement may follow formation of the middle segment. In adult animals, NPHP-2S has a high

non-middle segment concentration and is observed in the cell body, dendrite, and dendritic tip;

this population of NPHP-2S may modulate cilia placement. Alternatively, NPHP-2 localization

could be dynamically regulated during ciliogenesis, with a transient non-middle segment

population modulating cilia placement. The genetic interactions between NPHP-2 and TZ

proteins in *C. elegans* and physical interactions between NPHP-2 and NPHP and MKS proteins in

mammalian systems support this non-middle segment role for NPHP-2. If cilia begin forming

before the dendrite has fully extended, the cilium could guide its own placement through

interactions with the surrounding cellular matrix. This possibility is supported by evidence that

TZ placement defects are linked to defects in attachment of the cilium to the sheath cell

(Williams et al., 2010). In addition, SynDyf double mutants had ectopic dye filling of the amphid

and phasmid sheath cells, which has previously been linked to malformed cilia (Ohkura and

Burglin, 2011).

2.4.4 – The Inversin Compartment

A handful of other proteins share an "Inv compartment" middle segment localization pattern

with NPHP-2 in *C. elegans*: the membrane associated GTPase ARL-13 (which modulates

IFT-A/IFT-B association), the histone/tubulin deacetylase HDAC-6, and the IFT-A associated

Kinesin-II motor (Otto et al., 2003; Li et al., 2010; Cevik et al., 2010; Shiba et al., 2010). In

zebrafish, inversin ciliary localization is mediated by Fleer (orthologous to *C. elegans dyf-1*)

(Zhao and Malicki, 2011), an IFT-B polypeptide and a regulator of tubulin glutamylation (Ou et

al., 2005; Pathak et al., 2007). ARL-13, HDAC-6, and Fleer may play a role in IFT regulation via

possible tubulin post-translational modifications (Li et al., 2010). In addition, the mutations of

the tubulin deglutamylase *ccpp-1* cause ciliary degeneration, as mirrored by a progressive Dyf

phenotype (O'Hagan et al., 2011); OSM-3 appears to be the primary IFT motor functioning in *ccpp-1* mutants. The signaling and tubulin modifying roles of these components suggests that the Inv compartment may link cell signaling, tubulin modifications, and regulation of IFT. Combined, these observations lead to a quandary: does middle segment localization of these components regulate tubulin modification, or vice versa?

2.4.5 – Cell-type specificity of genetic networks

We found that amphid and phasmid cilia use modified gene networks (Figure 12) (Perkins et al., 1986). While the evolutionarily conserved IFT machinery is required for cilia formation, ciliary specialization can be shaped by sensillum or tissue specific modifications. Mammalian Tctn1 has tissue specific roles: it is essential for axonemal extension in nodal and neural tube cilia but is only necessary for Arl13b localization in the cilia of the notochord and early gut epithelia (Garcia-Gonzalo et al., 2011). Mammalian Mks1 also acts in a tissue specific manner, essential for formation of nodal and neural tube cilia, but not bile duct and lung cilia (Weatherbee et al., 2009). Sensillum/cell-type specificity is also evident in *C. elegans*: IFT in the cilia of AWB neurons is modified such that the kinesin motor OSM-3 moves independently of Kinesin-II and is not needed to build distal segments (Mukhopadhyay et al., 2007). Additionally, specifically in the cilia of male CEM neurons, the kinesin-3 motor *klp-6* regulates Kinesin-2 driven IFT (Morsci and Barr, 2011). Here, we show that *nphp-2* SynDyf phenotypes vary in a sensillum-specific manner. *nphp-2* interacts with *nphp-1* and *nphp-4* in both amphid and phasmid neurons, but interacts with MKS family members in a sensillum specific manner. We interpret this as evidence for a role for *nphp-2* as a modifier of NPHP-1/-4 and MKS pathways in these sensilla.

2.4.6 – The TZ physical and genetic modules in *C. elegans* and mammalian models

Much recent work has been done to elucidate the physical and genetic interactions between ciliopathy related genes. A mammalian proteomics screen for physical interactors of cystoproteins revealed three distinct physically interacting modules: a NPHP1-4-8 module, a MKS-1-6-TCTN2 module, and a NPHP5-6-ATXN10 module (Sang et al., 2011). The former two modules correspond to the *C. elegans* genetic interaction based NPHP-1/-4 and MKS pathways, though the latter NPHP5-6-ATXN10 module does not appear to be conserved. NPHP-2 acts as a physical nexus between these three modules, which agrees with our findings that *nphp-2* may act as a modifier of both the NPHP-1/-4 and MKS pathways (Sang et al., 2011). In addition to the genes examined here, Williams et al. showed that *mks-5*, a C2 domain encoding gene orthologous to mammalian RPGRIP1L, was SynDyf with *nphp-4*, *mks-6*, and *mksr-2* in both amphids and phasmids. This led them to link *mks-5* to both NPHP-1/-4 and MKS pathways, similarly to the treatment of *nphp-2* here (Williams et al., 2011).

In summary, we find that *nphp-2* acts as a genetic modifier of the NPHP and MKS pathways in *C. elegans*, and modulates sensillum-specific regulation of ciliary positioning. These results complement and extend our knowledge of the roles of ciliopathy genes in ciliogenesis and cilia placement, and integrate a wide range of ciliopathic genes into a single model.

2.5 – Materials and Methods

2.5.1 – General Molecular Biology Methods

Standard protocols were used for all molecular biology procedures. PCR amplification was used for genotyping and building transgenic constructs using the following templates: *C. elegans* genomic DNA, cDNA, or prebuilt constructs. High fidelity LA Taq (TaKaRa Bio Inc., Otsu, Shiga, Japan) or Phusion High Fidelity DNA Polymerase (Thermo Fisher Scientific, Vantaa, Finland) were used for amplification of DNA for constructs. Sequencing reactions were performed on site, and analyzed by SEBS DNA Sequencing Facility (Rutgers University, Piscataway, NJ, USA). PCR primer and construct sequences are available upon request.

2.5.2 – DNA and Protein Sequence Analysis

BLAST (Altschul et al., 1997) was used for identification of gene orthologs in *C. elegans*. Human protein sequence information was provided by NCBI, and *C. elegans* gene and protein sequence information was provided by Wormbase. SAGE data provided by Wormbase (Release WS221). Structural and domain predictions of gene products are by MotifScan (Hau et al., 2007). Percent identity and percent similarity were computed by MatGat 2.02 software (Campanella et al., 2003). Splice predictions in *gk653* deletion mutants were computed using Genemark.hmm (Lomsadze et al., 2005). ApE 1.17 was used for sequence manipulation.

2.5.3 – *C. elegans* INVS homology search

Basic Local Alignment Search Tool (BLAST) homology searches of inversin/nephrocystin-2 led to the identification of five possible orthologs, *unc-44*, *mlt-4*, T28D6.4, F36H1.2, and Y32G9A.6 (in order of decreasing similarity) (Altschul et al., 1997). The *unc-44* promoter does not contain a

palindromic X-box sequence, which is common to many ciliary genes, and the UNC-44 protein

contains a DEATH domain and a zona pellucida UNC-5 domain, neither of which are present in

Inversin (Blacque et al., 2005; Efimenko et al., 2005). SAGE tagging data also indicates that

unc-44 transcripts are not enriched in ciliated neurons (Wormbase Release WS221, Blacque et

al., 2005). Likewise, the *mlt-4* promoter does not contain an X-box, and the entire length of the

MLT-4 peptide encodes only ankyrin repeats. T28D6.4 promoter does contain an X-box, but the

gene product is predicted to contain only ankyrin repeats and an SH3 domain, not present in

Inversin. F36H1.2 has no X-box, and the predicted gene product has no similarities to Inversin

beyond the common ankyrin repeat motif and a possible weak nuclear localization signal. As

described in the results, Y32G9A.6 has an X-box, and shares many predicted domains with

Inversin, including a bipartite nuclear localization signal and a D-box ubiquitination site, with

similar overall domain organization. Performing a reverse protein BLAST homology search on

MLT-4 and Y32G9A.6 yielded a match for Inversin, while UNC-44, T28D6.4, or F36H1.2 did not.

A similar in depth search was performed for orthologs of NPHP3/MKS7. Only *C. elegans klc-2*

(kinesin light chain 2) had meaningful homology to NPHP3. *klc-2* has a C-terminal domain with

medium homology to NPHP-3, has a transcript enriched in ciliated neurons(Blacque et al., 2005),

but does not possess an X-box(Efimenko et al., 2005). In addition, NPHP3 does not appear in the

top results in a reciprocal BLAST search for KLC-2.

2.5.4 – RT-PCR and transcript sequencing

Total RNA from animals was isolated using Trizol Reagent (Invitrogen, Carlsbad, CA, USA).

Reverse Transcriptase with oligo-dT was used to isolate stable mature mRNA. Transcripts were

ligated into pGEM-T-Easy plasmid (Promega, Fitchburg, WI, USA) and transformed into DH10-β

competent cells. DNA from transformed colonies was amplified with Phusion, as above, using

the following primer sets: 5'-ATG TCC CAC ACG CTG ATC GAA GCA TTA GAC GAT GAG -3'with

5'-GTC GAC GGT CTT CTT TGT TTC TTC TGT TCA GCT TTT AAC TC-3' to amplify the first half of the

transcript, and 5'-GTC GAC TAG CGA CGG AAT TGT GGA AAC CGA GA-3' with 5'- AAG GAA CAG

GTG CCT ATG CGT GTC AAG GCA ATC-3' to amplify the second half of the transcript. These

amplicons were then sequenced.

2.5.5 – qRT-PCR

Total RNA from animals was isolated using Trizol Reagent. A 7900HT Sequence Detection

system (Applied Biosystems, Foster City, CA, USA) was used. Levels of *nphp-2* mRNA were

normalized to either actin or to the RNA polymerase large subunit. *nphp-2* mRNA was detected

using the following primer sets: 5'-TCG ACT AGC GAC GGA ATT GTG-3' with 5'-GTT TTG GAG

CGT TTG AAT CGG-3' and 5'-AAA AAG GAG CTG GAG GCA CTG-3' with 5'-CAA ATC GGA GAT

TGG CGG TA-3'. The actin gene, *act-1*, was used as a control, and was detected using the

following primer sets: 5'-CCA TTG TCG GAA GAC CAC GTC-3' with 5'-AGT TGG TGA CGA TAC CGT

GCT C-3'. The DNA polymerase gene *ama-1* was also used as a control, and was detected using

the following primer sets: 5'-GGA TGG AAT GTG GGT TGA GA-3' with 5'-CCG AGT AGT TTT TGC

GAA GG-3'.

2.5.6 – Strains and Maintenance

All strains were cultured at 20°C, unless otherwise noted, under standard conditions (Brenner,

1974). Deletion alleles such as *gk653* were outcrossed to *him-5(e1490)* at least four times.

nphp-2(nx101) and *nphp-2(nx102)* alleles are deletions of ankyrin repeats 5-11 and 5-8,

respectively, generated by imprecise Mos1 excision, and outcrossed once to *him-5(e1490)*. The

mks-6 allele used, *gk674*, deletes portions of a second gene, *xpa-1*, but has no discernible

effects on the function of XPA-1 (Williams et al., 2011). Strains used in this study appear in Table 6, organized by the figure in which they first appear.

2.5.7 – Imaging

Animals were imaged using standard *C. elegans* slide mounts and either a Zeiss Axio Plan-APOCHROMA 63X 1.4 oil DIC or 100X 1.4 oil DIC objectives on a Zeiss Axioplan 2 microscope (Zeiss, Oberkochen, Germany) with a Cascade 512B (Photometrics, Tucson, AZ, USA) digital camera, or on a Zeiss Imager.D1M with a Retiga-SRV Fast 1394 digital camera (Q-Imaging, Surrey, BC, Canada). Fluorochromes were either eGFP, VenusYFP, tdTomato, or CFP. IFT motility was recorded and kymographs and particle movement rate were measured using Metamorph (Version 7.6.1.0, MDS Analytical technologies, Sunnyvale, CA, USA) software. Strains were synchronized by picking L4 worms, culturing at 15°C overnight, and imaging within 24 hours. Worms were anesthetized in a drop of M9 containing 50mM muscimol, transferred to an agarose mount slide, and imaged immediately. AutoDeblur (Version 1.4.1, Media Cybernetics, Bethesda, MD, USA) software was used for 3D Blind deconvolution of image stacks. The amphid channel middle segment is the region of the cilium between the transition zone and the point where amphid cilia align; the distal segment is the region of the cilium past this point (Snow et al., 2004). Figures and diagrams were created with Adobe Photoshop CS3 (Version 10.0, Adobe Systems, San Jose, CA, USA) and Adobe Illustrator CS3 (Version 13.0.0, Adobe Systems). Cilia length, dendrite length, and TZ spread measurements were analyzed using ANOVA, followed by Tukey's post hoc test.

2.5.8 – Dye Filling Assays

For staining of cell bodies and cilia for evaluation of NPHP-2 localization, animals were incubated

with 2.5µg/mL DiO (2.5mg/mL dimethyl formamide stock, diluted 1:1000 in M9) (Invitrogen,

Carlsbad, CA, USA) for 30 minutes, rinsed three times, and then allowed to recover on a seeded

plate for one hour before imaging.

For scoring dye uptake as an indicator of amphid and phasmid ciliary structural defects, we used

a dye filling protocol modified from Tong and Bürglin (2010). Staged one day old, young adult

hermaphrodites are washed off plates in M9, and rinsed twice. Worms were then incubated in

40µg/mL DiI (2.5mg/mL dimethyl formamide stock, diluted 1:1000 in M9) (Invitrogen) for one

hour in the dark, rinsed twice in M9, and allowed to recover on a seeded plate for one hour in

the dark. Animals were anesthetized using 10mM levamisole and mounted on a slide. Worms

were scored as fraction of amphid or phasmid cell bodies stained by identifying and scoring

individual neurons, and averaging together the twelve amphid neurons (ASK, ADL, ASI, AWB,

ASH, and ASJ neurons on both left and right sides) or the four phasmid neurons (PHA and PHB,

left and right). These were compared using the non-parametric Kruskal-Wallis test, followed by

Dunn's multiple comparison test. GraphPad Prism (Version 5.01, GraphPad Software, La Jolla,

CA, USA) was used for all statistical analysis and bar graph creation.

2.6 – Acknowledgments

We thank the Barr Laboratory for constructive criticism on the manuscript. Some strains were provided by Dr. Bradley Yoder, the *C. elegans* Genetics Center (funded by the National Institutes of Health), the Japanese National BioResources Project, and the *C. elegans* Gene Knockout Consortium.

2.7 – Figures and Legends
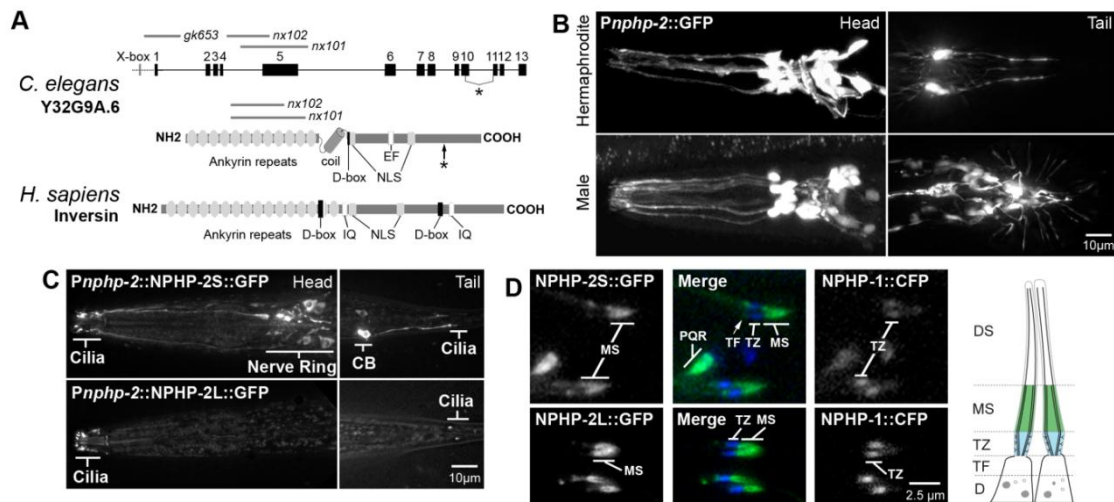
Figure 7. *nphp-2* is the ortholog of mammalian inversin, is expressed in ciliated neurons, and encodes two isoforms with slightly different ciliary localization patterns.

(A) The *C. elegans* ortholog of human inversin, NPHP-2, has similar domain structure to human inversin, containing conserved ankyrin repeats, nuclear localization sequences, and destruction box (D-Box). Novel features include a coil and an EF hand. *nphp-2* encodes a full length isoform (NPHP-2L)and a shorter isoform (NPHP-2S) lacking the twenty-two amino acid region indicated by the asterisk (*). *nphp-2(gk653)* removes the start codon but not the upstream X-box RFX transcription factor binding site. *nphp-2(nx101)* and *nphp-2(nx102)* are deletions of ankyrin repeats 5-11 and 5-8, respectively. (B) *nphp-2 is* expressed in the ciliated sensory nervous system of both the hermaphrodite and male. (C) The *nphp-2* gene encodes at least two splice forms, one short (NPHP-2S) and one long (NPHP-2L). NPHP-2S::GFP localizes throughout the sensory neuron, in the cell body, axon, dendrite, and cilium, but is excluded from the nucleus and TZ. NPHP-2L::GFP is predominantly localized to middle segments of cilia in the amphid and phasmid sensilla. (D) Co-expression of NPHP-1::CFP and either NPHP-2S::GFP or NPHP-2L::GFP

was used to visualize ciliary TZs in phasmid sensilla. NPHP-2S::GFP localizes to dendrite and

middle segments. NPHP-2L::GFP also localizes to the middle segment. The length of NPHP-2S

and NPHP-2L middle segment localization is consistent with the length of the total middle

segment (Dr. David Hall, personal communication). Arrows indicate a cilia base, the dividing

point between the cilium and dendritic tip, and bars indicate the middle segment (MS),

transition zone (TZ), or cilium. To the right, subcellular localization of NPHP-2S::GFP and

NPHP-2L::CFP (colored in green) and NPHP-1::CFP (colored in blue) are diagrammed. DS, distal

segment; TF, transition fibers; D, dendrite. Inversin primary structure in (A) adapted from Otto

et al., 2003.
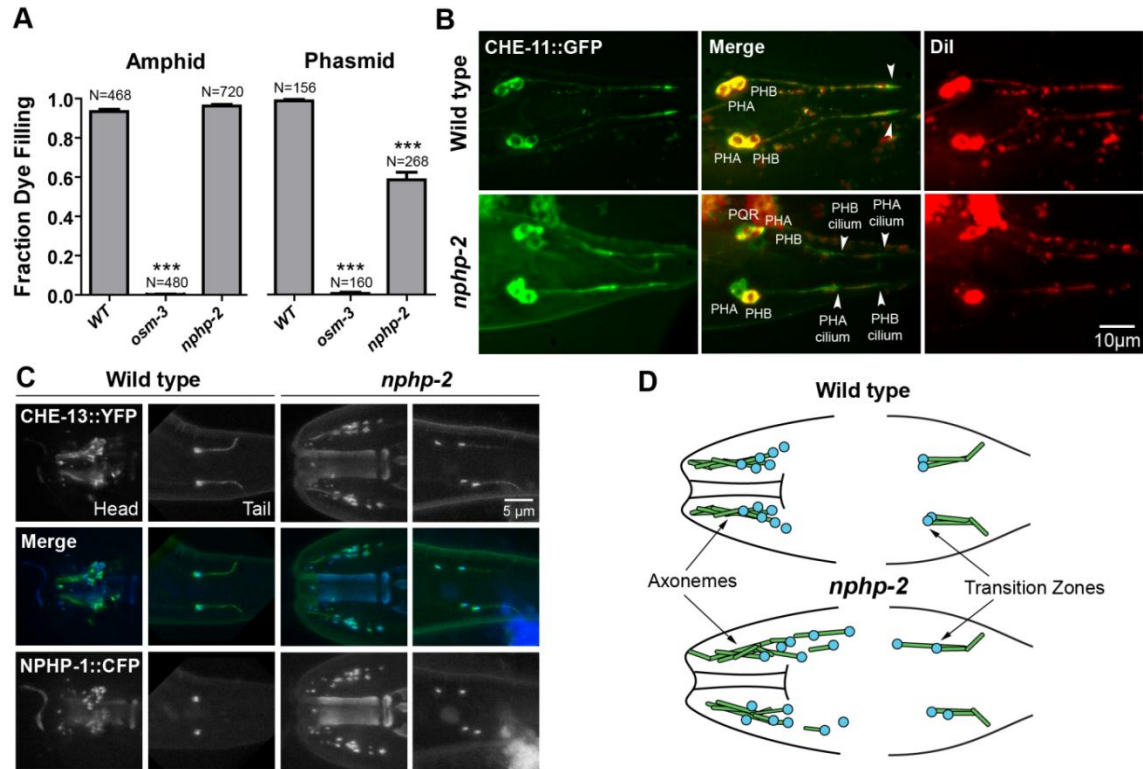
Figure 8. *nphp-2* mutants are moderately dye filling defective and have defects in transition zone positioning.

(A) *nphp-2(gk653)* mutants incubated with DiI show a phasmid but not amphid dye filling defect. ***, p<0.0001, Kruskal-Wallis test with Dunn's post hoc test. Sample size n is the number of cell bodies scored, and is listed above each experimental group. (B) Phasmid ciliary bases and axonemes were labeled with the IFT-A polypeptide marker CHE-11::GFP (a,d) and incubated with DiI (c,f). Cilia that are improperly placed within the animal do not reach the amphid or phasmid channel pore, are not exposed to the environment, and likely lead to dye filling defects (b,e). Arrowheads indicate the base of cilia (transition fibers), corresponding to increased CHE-11::GFP fluorescence. In panel (e), only PHB fills with DiI, presumably because its cilium is correctly positioned. In contrast, the PHA cilium is displaced anteriorly and the PHA neuron does not dye fill. (C) Axonemes of cilia in amphid and phasmid sensilla were labeled with IFT-B

polypeptide CHE-13::CFP (c,f), and amphid and phasmid TZs were labeled with NPHP-1::CFP (a,d). NPHP-1 localized properly in *nphp-2(gk653)* mutants (d-f), but de-clustering of channel cilia TZs and a separation of phasmid cilia TZ pairs is observed (diagramed, D).
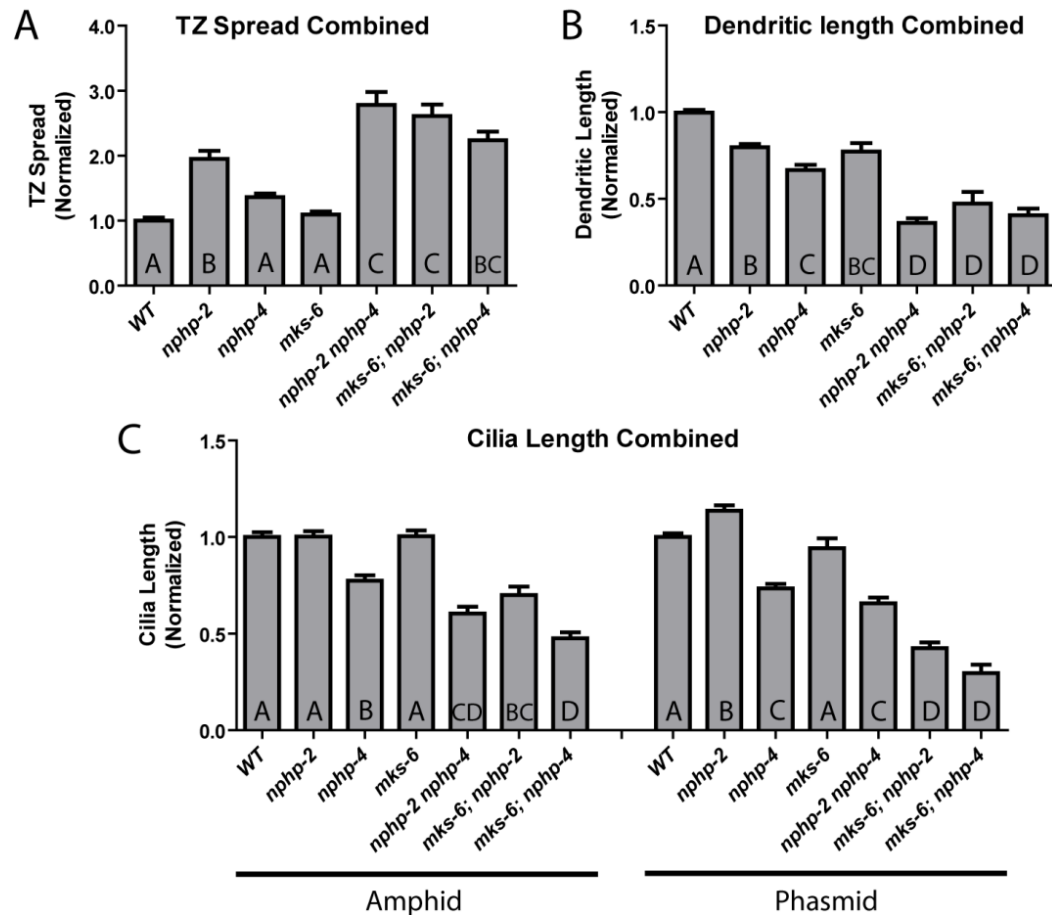
Figure 9. Ciliary single and double mutants exhibit defects in amphid and phasmid cilia length, amphid TZ spread, and phasmid dendritic length.

Cilia, TZs, and phasmid dendrites were labeled using CHE-11::GFP. Data was normalized to N2 WT. Statistical analysis performed was ANOVA followed by Tukey's post hoc test. Groups of mutants are labeled on the bar graph; two mutants in the same group are not statistically different from one another. Bars represent SEM. (A) TZ spread was measured as the distance from the posteriormost TZ to the anteriormost TZ. *nphp-2* was the only single mutant significantly different from WT. All double mutants were significantly different from WT and the single mutants that comprised them. (B) Phasmid dendrite length was measured from the base of the TZ to the cell body. All single mutants had significantly shorter dendrites that WT. All

double mutants had significantly shorter dendrites than the single mutants that comprised

them. (C) Cilia length was measured from the base of the TZ to the observable tip of the cilia. In

amphid neurons, *nphp-4* was the only single mutant significantly different than WT, and all

double mutants had significantly shorter cilia than the single mutants that comprised them. In

phasmid neurons, *nphp-2* had significantly longer cilia than WT and *nphp-4* had significantly

shorter cilia than WT. *mks-6; nphp-2* and *mks-6; nphp-4* had significantly shorter cilia than their

respective single mutants, whereas *nphp-2 nphp-4* did not significantly differ from *nphp-4*.
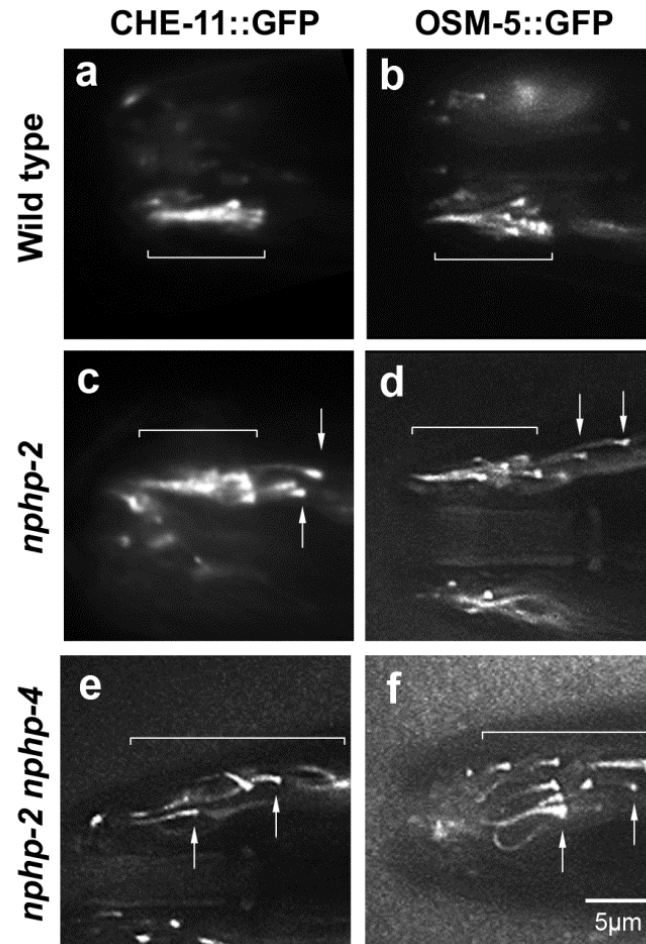
Figure 10. *nphp-2* and *nphp-4* are involved in regulating TZ/cilia placement and orientation.

Amphid channel TFs/axonemes were labeled with either IFT-A complex polypeptide CHE-11::GFP (a,c,e) or IFT-B complex polypeptide OSM-5::GFP (b,d,f). Wild-type amphid channel cilia form a tight bundle (a-b); moderate cilia placement defects are seen in *nphp-2* single mutants (c-d). These defects are exacerbated in *nphp-2 nphp-4* double mutants, which also exhibit defects in length and orientation (e-f). Brackets indicate amphid cilia regions, arrows in (c-d) point to the base of cilia placed outside the amphid bundle.
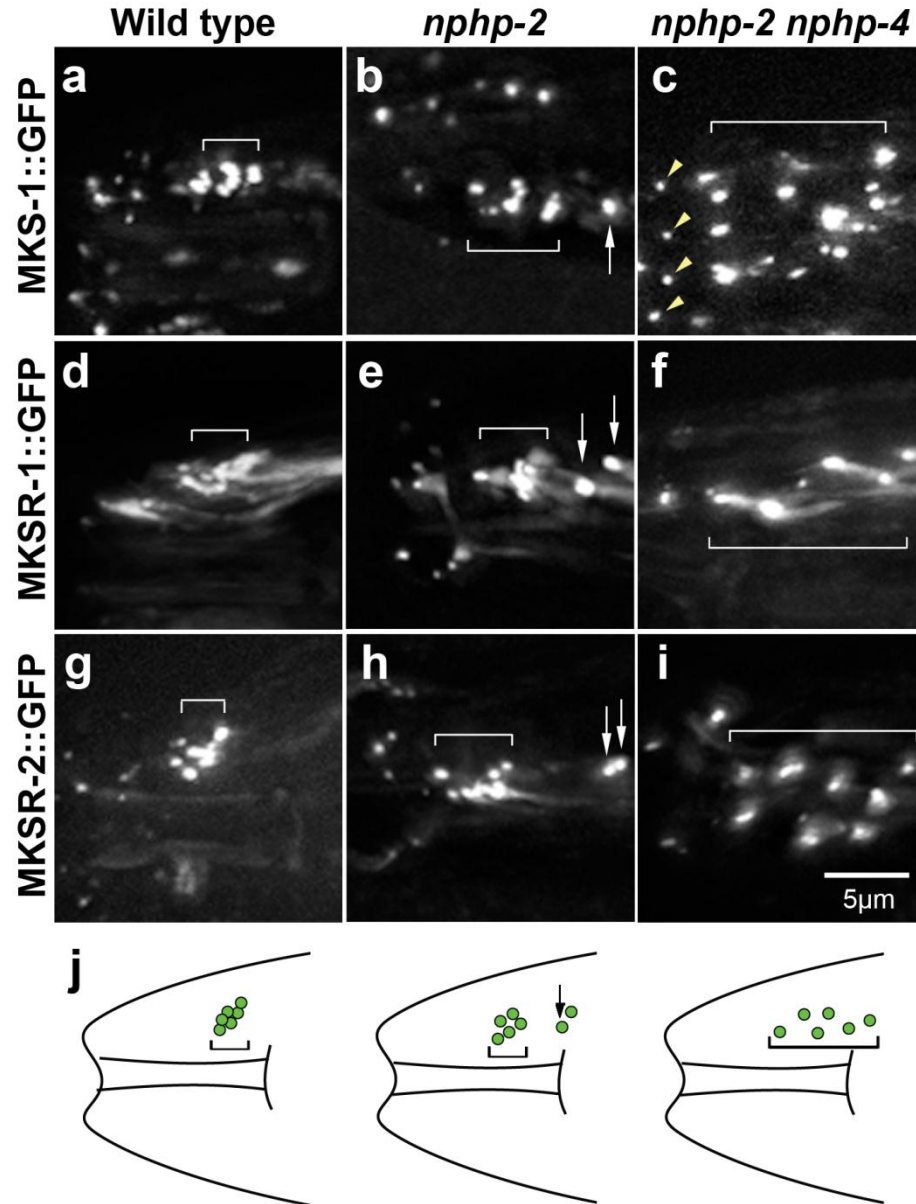
Figure 11. B9 proteins are not mislocalized in *nphp-2* single or *nphp-2 nphp-4* double mutants.

MKS-1::GFP (a-c), MKSR-1::GFP (d-f) and MKSR-2::GFP (g-i) localize to the TZ of amphid channel

cilia in both wild-type animals and *nphp-2 nphp-4* mutants (Williams et al., 2008). Additional

puncta present using MKS-1::GFP reporter were due to localization of MKS-1::GFP in labial cilia

(yellow arrowhead). Brackets indicate spread of amphid channel transition zones, which is

greatly expanded in *nphp-2 nphp-4* double mutants. Arrows indicate improperly placed TZs in

the *nphp-2* single mutant (b,e,h). Phenotypes are summarized in the cartoon (j).

Amphid

mks-1   mks-3
nphp-2   mks-6
nphp-1   nphp-4

Phasmid

mks-1   mks-3
nphp-2   mks-6
nphp-1   nphp-4

nphp-1/NPHP1/JBTS4   mks-1/MKS1/BBS13
nphp-2/INVS   mks-3/TMEM67/NPHP11
nphp-4/NPHP4   mks-6/CC2D2A/JBTS9
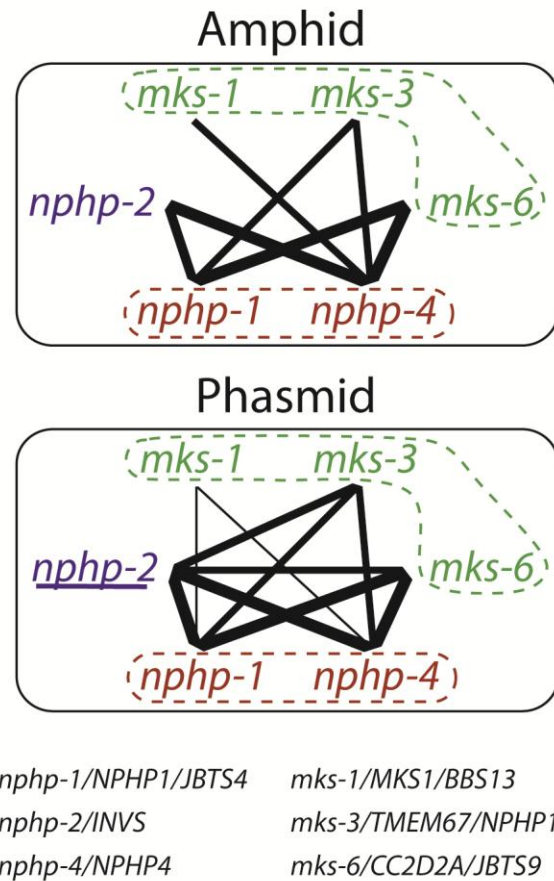
Figure 12. Schematic of SynDyf genetic interactions between *nphp-2* and TZ associated genes.

Using double mutant analysis, we constructed genetic interaction networks between ciliopathy genes within each sensilla based on their dye filling phenotypes. Genes within a common pathway are not SynDyf. Line weights indicate severity of defects among double mutants, and all shown interactions are significantly different from wild type. Underline indicates single mutant Dyf defect.

Fraction Dye Filling in Amphids

	Single	n	mks-6	n	mks-3	n	mks-1	n	nphp-4	n	nphp-2	n
WT	0.93±0.07	468										
osm-3	0.00±0.00**	480										
nphp-1	WT¹	-	0.00±0.00**	432	0.29±0.14**	348	0.85±0.13	432	0.87±0.11	768	0.14±0.18§§	516
nphp-2	0.96±0.01	720	0.90±0.14	424	0.92±0.09	456	0.93±0.07	444	0.00±0.00§§	480		
nphp-4	0.88±0.13	384	0.02±0.04**	480	0.29±0.14**	480	0.18±0.11**	384				
mks-1	0.95±0.08	408	0.98±0.05	420	0.97±0.05	432						
mks-3	0.95±0.06	480	0.95±0.06	522								
mks-6	0.95±0.08	538										

Fraction Dye Filling in Phasmids

	Single	n	mks-6	n	mks-3	n	mks-1	n	nphp-4	n	nphp-2	n
WT	0.99±0.01	156										
osm-3	0.00±0.01**	160										
nphp-1	WT¹	-	0.00±0.00**	120	0.37±0.04**	232	0.70±0.05**	164	0.94±0.02	304	0.00±0.00§§	220
nphp-2	0.59±0.04**	268	0.39±0.05§	196	0.28±0.05§§	156	0.49±0.06	156	0.01±0.01§§	160		
nphp-4	0.96±0.02	160	0.00±0.00**	160	0.35±0.04**	224	0.78±0.04**	128				
mks-1	1.00±0.00	148	0.97±0.02	156	0.99±0.01	152						
mks-3	0.98±0.01	160	0.98±0.01	212								
mks-6	1.00±0.00	216										

Table 1. Quantification of dye filling defects in double mutant amphid and phasmid neurons.

Amphid and phasmid neurons were scored individually, and then averaged with other neurons within the same animal. N is the number of individual neurons scored. The statistical analysis performed was Kruskal-Wallis test followed by Dunn's post hoc test. * indicates p value < 0.05 versus WT, ** indicates p value < 0.001. In double mutants in *nphp-2* background, § indicates p value < 0.05 versus *nphp-2* single mutant, §§ indicates p value < 0.001. Scores are plus/minus the standard error of the mean. [1](From Jauregui et al., 2008). Double mutants that differ significantly are presented in Figure 7.

	IFT Particle Velocity (µm/sec)			
IFT-A CHE-11::GFP	**Middle segment**	**N**	**Distal segment**	**N**
WT	0.72 ± 0.09	119	1.13 ± 0.15	117
nphp-2	0.71 ± 0.08	151	1.06 ± 0.14	109
nphp-4	0.74 ± 0.14	252	1.11 ± 0.16	144
nphp-2 nphp-4	1.02 ± 0.20, N = 155			

	IFT Particle Velocity (µm/sec)			
IFT-B OSM-5::GFP	**Middle segment**	**N**	**Distal segment**	**N**
WT	0.72 ± 0.06	125	1.06 ± 0.16	132
nphp-2	0.69 ± 0.10	304	1.04 ± 0.16	180
nphp-4	0.75 ± 0.13	336	1.03 ± 0.14	132
nphp-2 nphp-4	1.03 ± 0.17, N = 123			

	IFT Particle Velocity (µm/sec)			
IFT-B OSM-3::GFP	**Middle segment**	**N**	**Distal segment**	**N**
WT	0.73 ± 0.12	98	1.09 ± 0.15	111
nphp-2	0.75 ± 0.08	87	1.20 ± 0.18	116
nphp-4[1]	0.83 ± 0.15	101	1.16 ± 0.14	55
nphp-2 nphp-4	1.12 ± 0.24, N = 141			

Table 2. *nphp-2* does not affect IFT velocities in amphid channel cilia.

IFT speed of complex A and B polypeptides in *nphp-2* single and *nphp-2 nphp-4* double mutants was measured by tracing particles on kymographs. The middle segment is the region of the cilium between the TZ and the point where amphid cilia converge (See Fig. 4b). Velocity of IFT-A component CHE-11::GFP, IFT-B component OSM-5::GFP, and Kinesin-2 motor OSM-3::GFP was not significantly altered in middle or distal segments in the *nphp-2* single mutant compared to wild type. OSM-3::GFP velocity was slightly increased in the *nphp-4* single mutant. IFT velocities of all reporters in *nphp-2 nphp-4* double mutants resembled that of IFT velocities in wild-type distal segments, although it was not possible to distinguish between middle and distal segments because of the severe TZ placement and ciliary defects. [1]Data for OSM-3::GFP velocities in *nphp-4* mutants is from Jauregui et al., 2008.
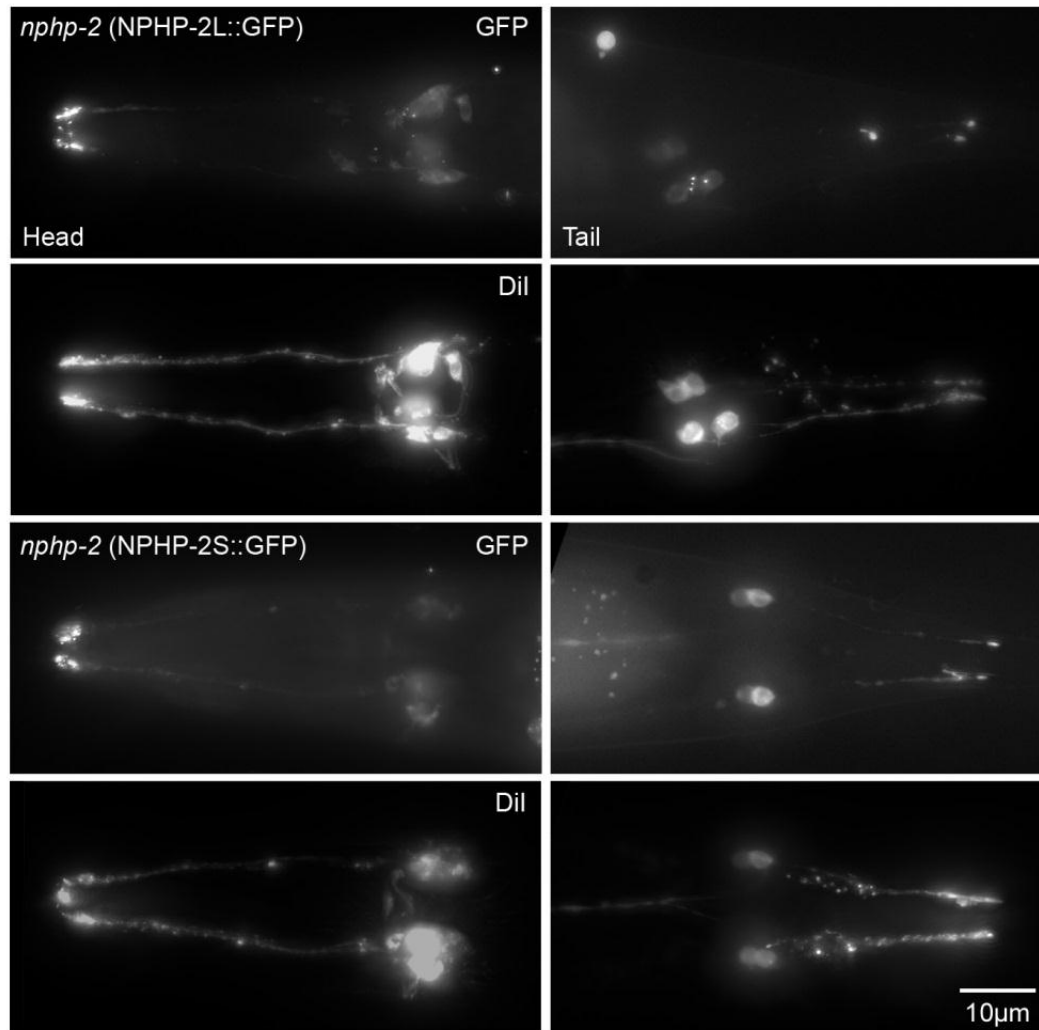
Figure 13. GFP-tagged NPHP-2S and NPHP-2L do not interfere with ciliogenesis.

Wild-type animals expressing native promoter driven NPHP-2S::GFP or NPHP-2L::GFP were incubated with DiI to assess gross cilia morphology. Neurons in both NPHP-2S and NPHP-2L animals dye-filled properly, indicating that overexpression of either NPHP-2 isoform does not lead to ciliogenic defects. The small puncta visible in the panels showing tail dye filling are due to dye filling of the ciliary sheath cells.
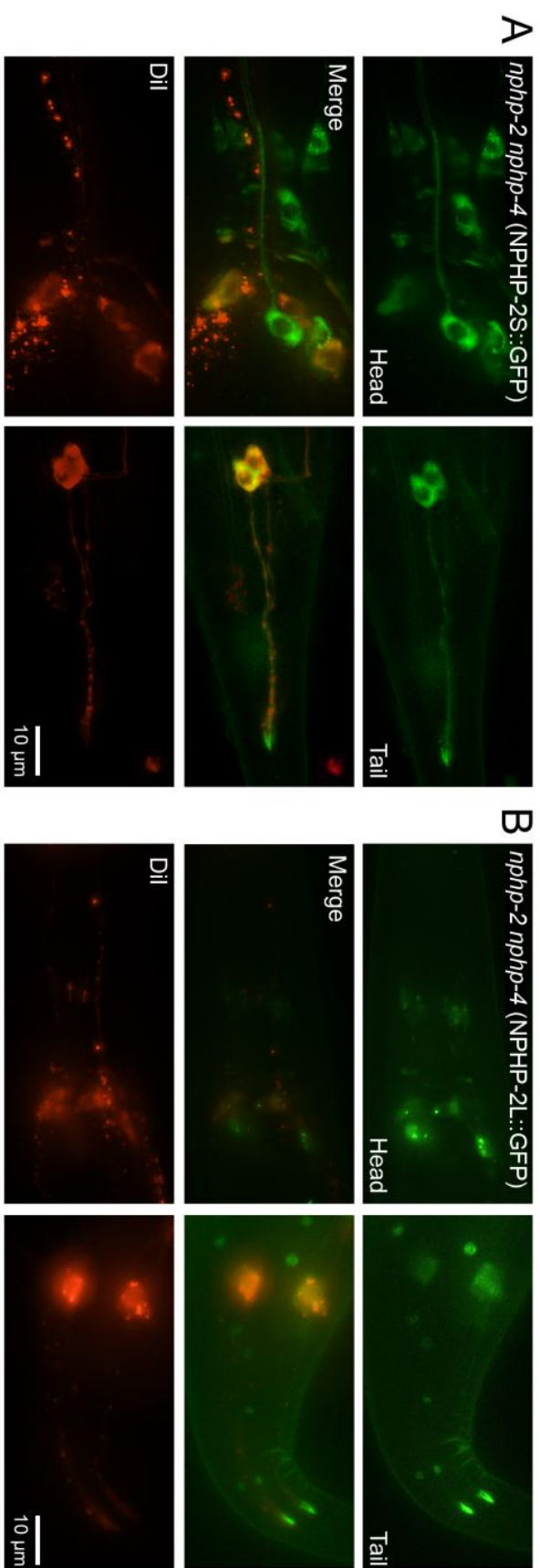
Figure 14. GFP-tagged NPHP-2S and NPHP-2L rescue *nphp-2 nphp-4* dye filling defect.

nphp-2 nphp-4 double mutants expressing native promoter driven (A) NPHP-2S or (B) NPHP-2L were incubated with DiI to assess gross cilia morphology. Both short and long NPHP-2 isoforms rescued the severe *nphp-2 nphp-4* mutant Dyf defect.
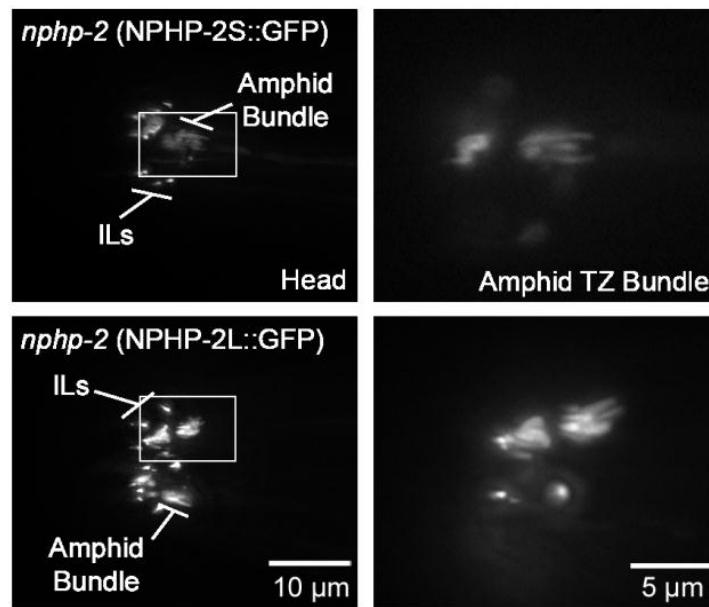
Figure 15. NPHP-2 short and long isoforms localize to the middle segment of amphid cilia

Localization of GFP-tagged NPHP-2S and NPHP-2L in the amphid sensillum. Similarly to in the

phasmid sensillum, both isoforms of NPHP-2 localize to the middle segment. Panels on the left

show both amphid sensilla, and panels on the right show a magnified view of a single amphid

channel cilia bundle.

Structure of NPHP-2(nx101) - splices in frame from exon 4 to exon 6.

Structure of NPHP-2(nx102) - in frame deletion from exon 4 to exon 5
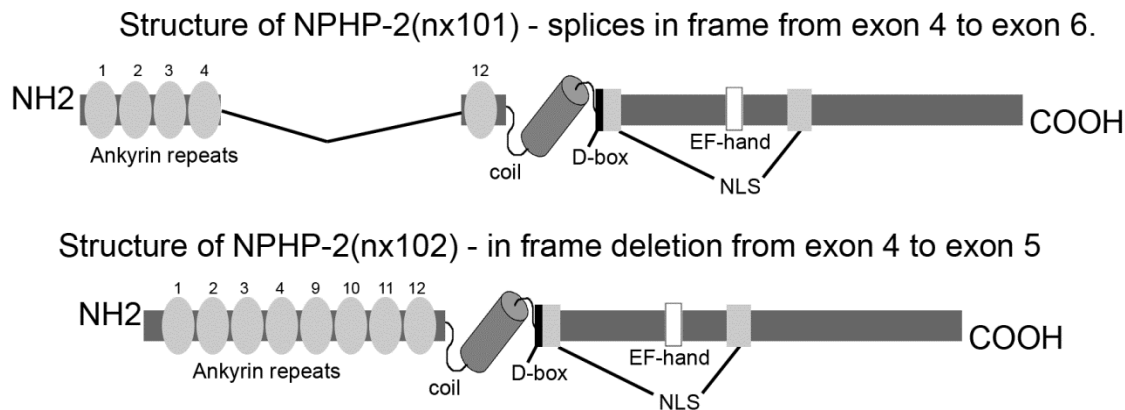
Figure 16. Predicted protein domains encoded by *nphp-2(nx101)* and *nphp-2(nx102).*

Both *nphp-2(nx101)* and *nphp-2(nx102)* are in-frame deletions, and are predicted to encode

truncated NPHP-2 protein. Both are missing a series of ankyrin repeats, *nx101* missing repeats

5-11, and *nx102* missing repeats 5-8.
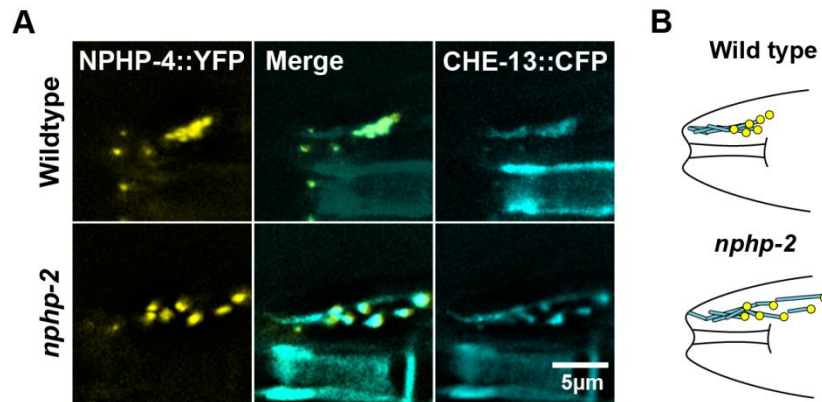
Figure 17. *nphp-2* exhibits disorganized amphid bundles

Amphid cilia were labeled with CHE-13 fluorescent reporter (c,f), and amphid TZ were labeled with NPHP-4::YFP (a,d). As with the NPHP-1 TZ marker, NPHP-4 localized properly in

nphp-2(gk653) mutants (d-f), and mutants exhibit the same disorganization of TZ (diagrammed).
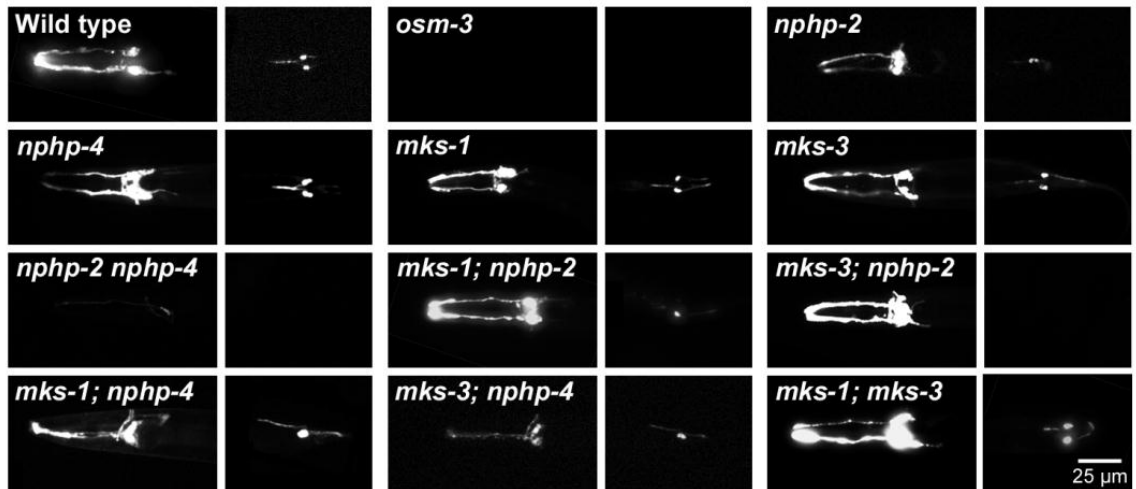
Figure 18. Double mutants exhibit dye filling defects that can vary between amphid and phasmid sensilla.

Animals were incubated with DiI to assess gross cilia morphology. In wild-type animals, neurons within two amphid bundles and two phasmid pairs were filled with dye. All single mutants except *nphp-2* dye filled normally. Double mutants exhibited varying expressivity of the Dyf phenotype, and were either defective for phasmid dye filling (*mks-1*; *nphp-2*, *mks-3*; *nphp-2*, *mks-6*; *nphp-2*), both amphid and phasmid dye filling (*nphp-2 nphp-4*, *mks-1*; *nphp-4*, *mks-3*; *nphp-4*, *mks-6*; *nphp-4*, *nphp-1*; *nphp-2*, *nphp-1*; *mks-1*, *mks-3 nphp-1*) or were non-Dyf (*mks-1*; *mks-3*, *mks-6*; *mks-1*, *mks-6*; *mks-3*, *nphp-1*; *nphp-4*). Worms with phasmid Dyf defects were typically missing one or both pairs of phasmid neurons; more rarely, only one neuron of a pair was missing.

NPHP	MKS	JBTS	Other Names	Reference	*C. elegans* ortholog	Reference
1		4	SLSN1	(Hildebrandt et al., 1997; Parisi et al., 2004)	*nphp-1*	(Otto et al., 2000)
2			INVS	(Otto et al., 2003)	*nphp-2*	(Warburton-Pitt et al, 2012)
3	7		RHPD1	(Bergmann et al., 2008; Olbrich et al., 2003)	-	(Warburton-Pitt et al, 2012)
4			SLSN4	(Mollet et al., 2002)	*nphp-4*	(Otto et al., 2005; Winkelbauer et al., 2005)
5			IQCB1/ SLSN5	(Chang et al., 2006)	-	
6	4	5	CEP290/ BBS14/ SLSN6	(Attanasio et al., 2007; Baala et al., 2007; Valente et al., 2006)	?	
7			GLIS2	(Arts et al., 2007)	*tra-1*(?)	BLAST
8	5	7	CORS3/ RPGRIP1L	(Delous et al., 2007; Otto et al., 2008)	*nphp-8/ mks-5*	(Otto et al., 2010)
9			NEK8	(Liu et al., 2011)	*nekl-1, nekl-2*	BLAST
10			BBS16/ SLSN7	(Smith et al., 2006)	-	
11	3	6	TMEM67	(Baala et al., 2007; Bae and Barr, 2008; Otto et al., 2009)	*mks-3*	(Davis et al., 2011)
12		11	TTC21B	(Bredrup et al., 2011)	ZK328.7	BLAST
13			WDR19	(Efimenko et al., 2006)	*dyf-2*	(Kyttala et al., 2006)
14		19	ZNF423	(Chaki et al, 2012)	*che-1*	BLAST
15			CEP164	(Chaki et al, 2012)	-	
16			ANKS6	(Hoff et al, 2013)	C01H6.2	BLAST
	1		BBS13	(Bae and Barr, 2008; Williams et al., 2008)	*mks-1/ xbx-7*	(Williams et al., 2008)
	2	2	CORS2/ TMEM216	(Tallila et al., 2008; Valente et al., 2010)	*mks-2/ C30B5.9*	(Huang et al, 2011)
	6	9		(Noor et al., 2008; Williams et al., 2011)	*mks-6*	(Shaheen et al., 2011)
	8		TCTN2	(Hopp et al., 2011)	*tctn-1?*	
	9		MKSR1/ B9D1	(Bae and Barr, 2008; Williams et al., 2008)	*mksr-1*	(Williams et al., 2008)
	10		MKSR2/ B9D2	(Bae and Barr, 2008; Williams et al., 2008)	*mksr-2*	(Williams et al., 2008)
	11	20	TMEM231	(Shaheen et al, 2013; Srour et al, 2012)	*T26A8.2*	BLAST
		1	CORS1/ INPP5E	(Bae et al., 2009)	*cil-1*	(Ferland et al., 2004)
		3		(Cantagrel et al., 2008)		
		8	ARL13B	(Cevik et al., 2010)	*arl-13*	(Cevik et al., 2010)

		10	OFD1	(Dafinger et al., 2011)	-	
		12	KIF7/HLS2	(Garcia-Gonzalo et al., 2011)	*klp-12*(?)	BLAST
		13	TCTN1	(Garcia-Gonzalo et al., 2011)	*tctn-1?*	
		14	TMEM237	(Huang et al, 2011)	jbts-14	(Huang et al, 2011)
		15	CEP41	(Lee et al, 2012)	-	
		16	TMEM138	(Lee et al, 2012)	F10B5.9	BLAST
		17		(Srour et al, 2012)	-	
		18	TCTN3/ OFD4	(Thomas et al, 2012)	*tctn-1?*	

Table 3. Nephronophthisis (NPHP), Meckel Syndrome (MKS), and Joubert Syndrome (JBTS) share multiple loci.

Classes of multiple ciliopathies, which are indicated by type number, often share loci. Senior-Løken Syndrome (SLSN) exhibits extensive overlap with NPHP due to its disease classification criteria, nephronophthisis comorbid with retinitis pigmentosa. Loci are also shared with other ciliopathies, including Bardet-Beidel Syndrome (BBS), Renal–Hepatic–Pancreatic Dysplasia (RHPD), Cerebello Oculo Renal Syndrome (CORS) – a subtype of Joubert Syndrome, Oral-Facial-Digital Syndrome (OFD), and hydrolethalus syndrome (HLS). Known *C. elegans* homologs are listed to the right; synonymous names are separated by commas. There are two *C. elegans* orthologs of NEK8, the paralogs *nekl-1* and *nekl-2*, which are separated by an ampersand. References pertain to identification of NPHP, MKS, and JBTS loci, and earliest identification of *C. elegans* homologs. Orthologs found by BLAST are reported only if the highest scoring match has an E value less than 10^{-20}, and exhibits homology beyond common domains. A question mark (?) indicates that BLAST searching the *C. elegans* protein sequence does not yield the mammalian ortholog as the closest match.

C. elegans	Human	% Identity	% Similarity
NPHP-2 (full)	INVS/NPHP2 (full)	19.1	35.2
NPHP-2 (no ank)	INVS/NPHP2 (no ank)	16.9	32.6
NPHP-4	NPHP4	23.7	43.5
MKS-3	MKS3/TMEM67/Meckelin	28.8	50.7

Table 4. *nphp-2* has similar conservation as other *C. elegans* ciliopathic gene orthologs.

Percent identity and percent similarity between full length *NPHP-2* ("full"), NPHP-2 without ankyrin repeats ("no ank"), NPHP-4 and MKS-3 and their mammalian orthologs. Due to slightly lower evolutionary conservation than other ciliary genes, the INVS/NPHP2 ortholog was not immediately identified in *C. elegans*, though percent identity and percent similarity are near those of other genes investigated.

	Fraction Amphid Dyf	N	Fraction Phasmid Dyf	N
mks-1	0.95±0.08	408	1.00±0.00	148
mks-1; nphp-2	0.93±0.07	444	0.49±0.06	156
mksr-1	0.95±0.01	660	0.98±0.01	236
mksr-1; nphp-2	0.81±0.02§§§	552	0.61±0.03	236
mksr-2	0.95±0.01	516	0.97±0.02	176
mksr-2; nphp-2	0.76±0.03§§§	142	0.68±0.05	216

Table 5. *mksr-1; nphp-2* and *mksr-2; nphp-2* mutants are not SynDyf

B9 gene single and double mutants were incubated with DiI to assess cilia morphology. Amphid

and phasmid neurons were scored individually, and then averaged with other neurons within

the animal. The statistical analysis performed was Kruskal-Wallis test followed by Dunn's post

hoc test. No single mutants were Dyf in either amphids or phasmids. Double mutant phasmid

Dyf defects were not significantly different from *nphp-2* single mutant Dyf defects, but double

mutant amphid defects were SynDyf in *nphp-2* background. §§§ indicates p < 0.0001 versus

nphp-2 single mutant. Scores are plus/minus the standard error of the mean.

Figure 7	PT1995: *pha-1(e2123); him-5(e1490); myEx684[P$_{nphp-2}$::NPHP-2S::GFP + pBX]*
	PT1994: *pha-1(e2123); him-5(e1490); myEx683[P$_{nphp-2}$::NPHP-2L::GFP + pBX]*
	PT2354: *nphp-2(gk653)*; *myEx743[P$_{nphp-2}$::NPHP-2L::GFP, ccRFP];* *yhEx149[NPHP-1::CFP, CHE-13::YFP, pRF4]*
	PT2355: *nphp-2(gk653)*; *myEx744[P$_{nphp-2}$::NPHP-2S::GFP, ccRFP];* *yhEx149[NPHP-1::CFP, CHE-13::YFP, pRF4]*
	PT1055: *dpy-5(e907); him-5(e1490); myEx[dpy-5(+); Pnphp-2::GFP]*
Figure 8	CB1490: *him-5(e1490)*
	PR802: *osm-3(p802); him-5(e1490)*
	PT2145: *nphp-2(gk653) him-5(e1490)*
	PT50: *che-11(e1810); myEx10[P$_{che-11}$::CHE-11::GFP + pRF4]*
	PT1958: *nphp-2(gk653) him-5(e1490); myEx10[P$_{che-11}$::CHE-11::GFP + pRF4]*
	YH237: *yhEx149[P$_{nphp-1}$::NPHP-1::CFP; P$_{che-13}$::CHE-13::YFP + pRF4]*
	PT1960: *nphp-2(gk653); yhEx149[P$_{nphp-1}$::NPHP-1::CFP; P$_{che-13}$::CHE-13::YFP + pRF4]*
Figure 9	PT1334: *nph-4(tm925) him-5(e1490) V; Ex[CHE-11::GFP + pRF4]*
	MX712: *mks-6(gk674); nxEx[CHE-11::GFP + ROL-6(su1006)]*
	PT2029: *nphp-2(gk653) nphp-4(tm925) him-5(e1490);* *Ex[P$_{che-11:}$:CHE-11::GFP + pRF4]*
	MX: *mks-6(gk674); nphp-2(gk653); nxEx[CHE-11::GFP + ROL-6(su1006)]*
	MX716: *mks-6(gk674); nphp-4(tm925); nxEx[CHE-11::GFP + ROL-6(su1006)]*
Figure 10	PT40: *him-5(e1490); osm-5(sa126); myEx1[P$_{osm-5}$::OSM-5::GFP + pRF4]*
	PT1956: *nphp-2(gk653); myEx1[P$_{osm-5}$::OSM-5::GFP + pRF4]*
	PT1411: *nph-4(tm925) him-5(e1490) V; myEx1 [OSM-5::GFP + pRF4]*
	PT2027: *nphp-2(gk653) nphp-4(tm925) him-5(e1490);* *Ex[P$_{osm-5}$::OSM-5::GFP + pRF4]*
Figure 11	MX549: *dpy-5(e907); nxEx[P$_{mks-1b}$::MKS-1b::GFP + dpy-5(+)]*
	PT2006: *dpy-5(e907); nphp-2(gk653) him-5(e1490); Ex[P$_{mks-1}$::MKS-1::GFP*

	+ dpy-5(+)]
	PT2026: *dpy-5(e907); nphp-2(gk653) nphp-4(tm925) him-5(e1490);*
	Ex[P$_{mks-1}$::MKS-1::GFP + dpy-5(+)]
	MX349: *dpy-5(e907); nxEx[P$_{mksr-1}$::MKSR-1::GFP + dpy-5 (+)]*
	PT2004: *dpy-5(e907); nphp-2(gk653) him-5(e1490);*
	Ex[P$_{mksr-1}$::MKSR-1::GFP + dpy-5(+)]
	PT2024: *dpy-5(e907); nphp-2(gk653) nphp-4(tm925) him-5(e1490);*
	Ex[P$_{mksr-1}$::MKSR-1::GFP + dpy-5(+)]
	MX342: *dpy-5(e907); nxEx[P$_{mksr-2}$::MKSR-2::GFP + dpy-5 (+)]*
	PT2002: *dpy-5(e907); nphp-2(gk653) him-5(e1490);*
	Ex[P$_{mksr-2}$::MKSR-2::GFP + dpy-5(+)]
	PT2022: *dpy-5(e907); nphp-2(gk653) nphp-4(tm925) him-5(e1490);*
	Ex[P$_{mksr-2}$::MKSR-2::GFP + dpy-5(+)]
Table 1	PT1817: *mks-1(tm2705); him-5(e1490)*
	PT1818: *mks-3(tm2547); him-5(e1490)*
	PT1983: *nphp-2(gk653) nphp-4(tm1925) him-5(e1490)*
	PT2162: *mks-1(tm2705); nphp-2(gk653) him-5(e1490)*
	PT2154: *mks-3(tm2547); nphp-2(gk653) him-5(e1490)*
	PT2164: *mks-1(tm2705); nphp-4(tm1925) him-5(e1490)*
	PT2165: *mks-3(tm2547); nphp-4(tm1925) him-5(e1490)*
	PT1891: *mks-3(tm2547); mks-1(tm2705); him-5(e1490)*
	PT1036: *nphp-1(ok500); him-5(e1490)*
	VC1466: *xpa-1&mks-6(gk674); him-5(e1490)*
	PT2154: *mks-3(tm2547); nphp-2(gk653) him-5(e1490)*
	PT1891: *mks-3(tm2547); mks-1(tm2705); him-5(e1490)*
	PT1981: *nphp-1(ok500); nphp-2(gk653) him-5(e1490)*
	PT1040: *nphp-1(ok500); nphp-4(tm1925) him-5(e1490)*
	PT2163: *nphp-1(ok500); mks-1(tm2705); him-5(e1490)*
	PT2155: *mks-3(tm2547) nphp-1(ok500); him-5(e1490)*
	PT2191: *xpa-1&mks-6(gk674); nphp-2(gk653) him-5(e1490)*
	PT2143: *xpa-1&mks-6(gk674); nphp-4(tm1925) him-5(e1490)*
	PT2120: *xpa-1&mks-6(gk674); mks-1(tm2705); him-5(e1490)*
	PT2142: *xpa-1&mks-6(gk674); mks-3(tm2547); him-5(e1490)*

	TM3083: *mksr-1(tm3083)*
	TM2452: *mksr-2(tm2452)*
	PT1999: *nphp-2(gk653)*; *mksr-1(tm3083)*
	PT1997: *mksr-2(tm2452)*; *nphp-2(gk653)*
Table 2	OSM-3::GFP: *Ex [OSM-3::GFP; pRF4]*
	PT2483: *nphp-2(gk653); Ex[OSM-3::GFP; pRF4]*
	PT2484: *nphp-2(gk653) nphp-4(tm1925); Ex[OSM-3::GFP; pRF4]*
Figure 13	PT2485: *nphp-2(gk653); myEx743(P$_{nphp-2}$::NPHP-2S::GFP)*
	PT2486: *nphp-2(gk653); myEx744(P$_{nphp-2}$::NPHP-2L::GFP)*
Figure 14	PT: *nphp-2(gk653) nphp-4(tm1925); myEx743(P$_{nphp-2}$::NPHP-2S::GFP)*
	PT: *nphp-2(gk653) nphp-4(tm1925); myEx744(P$_{nphp-2}$::NPHP-2L::GFP)*
Figure 17	YH224: *yhEx142[P$_{nphp-4}$::NPHP-4::YFP; CHE-13::CFP + pRF4]*
	PT1962: *nphp-2(gk653); yhEx142[P$_{nphp-4}$::NPHP-4::YFP; CHE-13::CFP + pRF4]*

Table 6. List of strains used in this work.

A list of strains used in this work, organized by the figure in which they first appear.

2.8 – References

Note: These references are formatted to the standards of the Journal of Cell Biology.

Altschul, S. F., Madden, T. L., Schaffer, A. A., Zhang, J., Zhang, Z., Miller, W. and Lipman, D. J. (1997). Gapped BLAST and PSI-BLAST: A new generation of protein database search programs. *Nucleic Acids Res.* **25,** 3389-3402.

Badano, J. L., Mitsuma, N., Beales, P. L. and Katsanis, N. (2006). The ciliopathies: An emerging class of human genetic disorders. *Annu. Rev. Genomics Hum. Genet.* **7,** 125-148.

Bae, Y. K. and Barr, M. M. (2008). Sensory roles of neuronal cilia: Cilia development, morphogenesis, and function in *C. elegans*. *Front. Biosci.* **13,** 5959-5974.

Bellavia, S., Dahan, K., Terryn, S., Cosyns, J. P., Devuyst, O. and Pirson, Y. (2010). A homozygous mutation in INVS causing juvenile nephronophthisis with abnormal reactivity of the Wnt/beta-catenin pathway. *Nephrol. Dial. Transplant.* **25,** 4097-4102.

Benzing, T., Simons, M. and Walz, G. (2007). Wnt signaling in polycystic kidney disease. *J. Am. Soc. Nephrol.* **18,** 1389-1398.

Bialas, N. J., Inglis, P. N., Li, C., Robinson, J. F., Parker, J. D., Healey, M. P., Davis, E. E., Inglis, C. D., Toivonen, T., Cottell, D. C. et al. (2009). Functional interactions between the ciliopathy-associated Meckel Syndrome 1 (MKS1) protein and two novel MKS1-related (MKSR) proteins. *J. Cell. Sci.* **122,** 611-624.

Blacque, O. E., Perens, E. A., Boroevich, K. A., Inglis, P. N., Li, C., Warner, A., Khattra, J., Holt, R. A., Ou, G., Mah, A. K. et al. (2005). Functional genomics of the cilium, a sensory organelle. *Curr. Biol.* **15,** 935-941.

Blacque, O. E., Reardon, M. J., Li, C., McCarthy, J., Mahjoub, M. R., Ansley, S. J., Badano, J. L., Mah, A. K., Beales, P. L., Davidson, W. S. et al. (2004). Loss of *C. elegans* BBS-7 and BBS-8 protein function results in cilia defects and compromised intraflagellar transport. *Genes Dev.* **18,** 1630-1642.

Brenner, S. (1974). The genetics of *Caenorhabditis elegans*. *Genetics* **77,** 71-94.

Campanella, J. J., Bitincka, L. and Smalley, J. (2003). MatGAT: An application that generates similarity/identity matrices using protein or DNA sequences. *BMC Bioinformatics* **4,** 29.

Dammermann, A., Pemble, H., Mitchell, B. J., McLeod, I., Yates, J. R.,3rd, Kintner, C., Desai, A. B. and Oegema, K. (2009). The hydrolethalus syndrome protein HYLS-1 links core centriole structure to cilia formation. *Genes Dev.* **23,** 2046-2059.

Dowdle, W. E., Robinson, J. F., Kneist, A., Sirerol-Piquer, M. S., Frints, S. G., Corbit, K. C., Zaghloul, N. A., van Lijnschoten, G., Mulders, L., Verver, D. E. et al. (2011). Disruption of a ciliary B9 protein complex causes Meckel Syndrome. *Am. J. Hum. Genet.* **89,** 94-110.

Efimenko, E., Bubb, K., Mak, H. Y., Holzman, T., Leroux, M. R., Ruvkun, G., Thomas, J. H. and Swoboda, P. (2005). Analysis of xbx genes in *C. elegans*. *Development* **132,** 1923-1934.

Ferrante, M. I., Giorgio, G., Feather, S. A., Bulfone, A., Wright, V., Ghiani, M., Selicorni, A., Gammaro, L., Scolari, F., Woolf, A. S. et al. (2001). Identification of the gene for Oral-Facial-Digital type I syndrome. *Am. J. Hum. Genet.* **68,** 569-576.

Garcia-Gonzalo, F. R., Corbit, K. C., Sirerol-Piquer, M. S., Ramaswami, G., Otto, E. A., Noriega, T. R., Seol, A. D., Robinson, J. F., Bennett, C. L., Josifova, D. J. et al. (2011). A transition zone complex regulates mammalian ciliogenesis and ciliary membrane composition. *Nat. Genet.* **43,** 776-784.

Goetz, S. C. and Anderson, K. V. (2010). The primary cilium: A signalling centre during vertebrate development. *Nat. Rev. Genet.* **11,** 331-344.

Guay-Woodford, L. M., Wright, C. J., Walz, G. and Churchill, G. A. (2000). Quantitative trait loci modulate renal cystic disease severity in the mouse bpk model. *J. Am. Soc. Nephrol.* **11,** 1253-1260.

Hau, J., Muller, M. and Pagni, M. (2007). HitKeeper, a generic software package for hit list management. *Source Code Biol. Med.* **2,** 2.

Hildebrandt, F. and Zhou, W. (2007). Nephronophthisis-associated ciliopathies. *J. Am. Soc. Nephrol.* **18,** 1855-1871.

Hoefele, J., Wolf, M. T., O'Toole, J. F., Otto, E. A., Schultheiss, U., Deschenes, G., Attanasio, M., Utsch, B., Antignac, C. and Hildebrandt, F. (2007). Evidence of oligogenic inheritance in nephronophthisis. *J. Am. Soc. Nephrol.* **18,** 2789-2795.

Jauregui, A. R. and Barr, M. M. (2005). Functional characterization of the *C. elegans* nephrocystins NPHP-1 and NPHP-4 and their role in cilia and male sensory behaviors. *Exp. Cell Res.* **305,** 333-342.

Jauregui, A. R., Nguyen, K. C., Hall, D. H. and Barr, M. M. (2008). The *Caenorhabditis elegans* nephrocystins act as global modifiers of cilium structure. *J. Cell Biol.* **180,** 973-988.

Kuida, S. and Beier, D. R. (2000). Genetic localization of interacting modifiers affecting severity in a murine model of polycystic kidney disease. *Genome Res.* **10,** 49-54.

Kyttala, M., Tallila, J., Salonen, R., Kopra, O., Kohlschmidt, N., Paavola-Sakki, P., Peltonen, L. and Kestila, M. (2006). MKS1, encoding a component of the flagellar apparatus basal body proteome, is mutated in Meckel Syndrome. *Nat. Genet.* **38,** 155-157.

Li, Y., Wei, Q., Zhang, Y., Ling, K. and Hu, J. (2010). The small GTPases ARL-13 and ARL-3 coordinate intraflagellar transport and ciliogenesis. *J. Cell Biol.* **189,** 1039-1051.

Lomsadze, A., Ter-Hovhannisyan, V., Chernoff, Y. O. and Borodovsky, M. (2005). Gene identification in novel eukaryotic genomes by self-training algorithm. *Nucleic Acids Res.* **33,** 6494-6506.

Mollet, G., Salomon, R., Gribouval, O., Silbermann, F., Bacq, D., Landthaler, G., Milford, D., Nayir, A., Rizzoni, G., Antignac, C. et al. (2002). The gene mutated in juvenile nephronophthisis type 4 encodes a novel protein that interacts with nephrocystin. *Nat. Genet.* **32,** 300-305.

Morgan, D., Goodship, J., Essner, J. J., Vogan, K. J., Turnpenny, L., Yost, H. J., Tabin, C. J. and Strachan, T. (2002). The left-right determinant inversin has highly conserved ankyrin repeat and IQ domains and interacts with calmodulin. *Hum. Genet.* **110,** 377-384.

Morgan, D., Turnpenny, L., Goodship, J., Dai, W., Majumder, K., Matthews, L., Gardner, A., Schuster, G., Vien, L., Harrison, W. et al. (1998). Inversin, a novel gene in the vertebrate left-right axis pathway, is partially deleted in the inv mouse. *Nat. Genet.* **20,** 149-156.

Morsci, N. S. and Barr, M. M. (2011). Kinesin-3 KLP-6 regulates intraflagellar transport in male-specific cilia of *Caenorhabditis elegans*. *Curr. Biol.* **21,** 1239-1244.

Mukhopadhyay, S., Lu, Y., Qin, H., Lanjuin, A., Shaham, S. and Sengupta, P. (2007). Distinct IFT mechanisms contribute to the generation of ciliary structural diversity in *C. elegans*. *EMBO J.* **26,** 2966-2980.

Nurnberger, J., Bacallao, R. L. and Phillips, C. L. (2002). Inversin forms a complex with catenins and N-cadherin in polarized epithelial cells. *Mol. Biol. Cell* **13,** 3096-3106.

O'Hagan, R., Piasecki, B. P., Silva, M., Phirke, P., Nguyen, K. C., Hall, D. H., Swoboda, P. and Barr, M. M. (2011). The tubulin deglutamylase CCPP-1 regulates the function and stability of sensory cilia in *C. elegans*. *Curr. Biol.* **21,** 1685-1694.

Ohkura, K. and Burglin, T. R. (2011). Dye-filling of the amphid sheath glia: Implications for the functional relationship between sensory neurons and glia in *Caenorhabditis elegans*. *Biochem. Biophys. Res. Commun.* **406,** 188-193.

Otto, E. A., Schermer, B., Obara, T., O'Toole, J. F., Hiller, K. S., Mueller, A. M., Ruf, R. G., Hoefele, J., Beekmann, F., Landau, D. et al. (2003). Mutations in INVS encoding inversin cause nephronophthisis type 2, linking renal cystic disease to the function of primary cilia and left-right axis determination. *Nat. Genet.* **34,** 413-420.

Ou, G., Blacque, O. E., Snow, J. J., Leroux, M. R. and Scholey, J. M. (2005). Functional coordination of intraflagellar transport motors. *Nature* **436,** 583-587.

Pan, X., Ou, G., Civelekoglu-Scholey, G., Blacque, O. E., Endres, N. F., Tao, L., Mogilner, A., Leroux, M. R., Vale, R. D. and Scholey, J. M. (2006). Mechanism of transport of IFT particles in *C. elegans* cilia by the concerted action of kinesin-II and OSM-3 motors. *J. Cell Biol.* **174,** 1035-1045.

Pathak, N., Obara, T., Mangos, S., Liu, Y. and Drummond, I. A. (2007). The zebrafish fleer gene encodes an essential regulator of cilia tubulin polyglutamylation. *Mol. Biol. Cell* **18,** 4353-4364.

Pazour, G. J. and Rosenbaum, J. L. (2002). Intraflagellar transport and cilia-dependent diseases. *Trends Cell Biol.* **12,** 551-555.

Perkins, L. A., Hedgecock, E. M., Thomson, J. N. and Culotti, J. G. (1986). Mutant sensory cilia in the nematode *Caenorhabditis elegans*. *Dev. Biol.* **117,** 456-487.

Phillips, C. L., Miller, K. J., Filson, A. J., Nurnberger, J., Clendenon, J. L., Cook, G. W., Dunn, K. W., Overbeek, P. A., Gattone, V. H.,2nd and Bacallao, R. L. (2004). Renal cysts of inv/inv mice resemble early infantile nephronophthisis. *J. Am. Soc. Nephrol.* **15,** 1744-1755.

Qin, H., Rosenbaum, J. L. and Barr, M. M. (2001). An autosomal recessive polycystic kidney disease gene homolog is involved in intraflagellar transport in *C. elegans* ciliated sensory neurons. *Curr. Biol.* **11,** 457-461.

Rosenbaum, J. L. and Witman, G. B. (2002). Intraflagellar transport. *Nat. Rev. Mol. Cell Biol.* **3,** 813-825.

Sang, L., Miller, J. J., Corbit, K. C., Giles, R. H., Brauer, M. J., Otto, E. A., Baye, L. M., Wen, X., Scales, S. J., Kwong, M. et al. (2011). Mapping the NPHP-JBTS-MKS protein network reveals ciliopathy disease genes and pathways. *Cell* **145,** 513-528.

Shiba, D., Manning, D. K., Koga, H., Beier, D. R. and Yokoyama, T. (2010). Inv acts as a molecular anchor for Nphp3 and Nek8 in the proximal segment of primary cilia. *Cytoskeleton (Hoboken)* **67,** 112-119.

Shiba, D., Yamaoka, Y., Hagiwara, H., Takamatsu, T., Hamada, H. and Yokoyama, T. (2009). Localization of inv in a distinctive intraciliary compartment requires the C-terminal ninein-homolog-containing region. *J. Cell. Sci.* **122,** 44-54.

Simons, M., Gloy, J., Ganner, A., Bullerkotte, A., Bashkurov, M., Kronig, C., Schermer, B., Benzing, T., Cabello, O. A., Jenny, A. et al. (2005). Inversin, the gene product mutated in nephronophthisis type II, functions as a molecular switch between wnt signaling pathways. *Nat. Genet.* **37,** 537-543.

Snow, J. J., Ou, G., Gunnarson, A. L., Walker, M. R., Zhou, H. M., Brust-Mascher, I. and Scholey, J. M. (2004). Two anterograde intraflagellar transport motors cooperate to build sensory cilia on *C. elegans* neurons. *Nat Cell Biol* **6,** 1109-13.

Tong, Y. G. and Burglin, T. R. (2010). Conditions for dye-filling of sensory neurons in *Caenorhabditis elegans*. *J. Neurosci. Methods* **188,** 58-61.

Ward, H. H., Wang, J. and Phillips, C. (2004). Analysis of multiple invs transcripts in mouse and MDCK cells. *Genomics* **84,** 991-1001.

Watanabe, D., Saijoh, Y., Nonaka, S., Sasaki, G., Ikawa, Y., Yokoyama, T. and Hamada, H. (2003). The left-right determinant inversin is a component of node monocilia and other 9+0 cilia. *Development* **130,** 1725-1734.

Weatherbee, S. D., Niswander, L. A. and Anderson, K. V. (2009). A mouse model for Meckel Syndrome reveals Mks1 is required for ciliogenesis and hedgehog signaling. *Hum. Mol. Genet.* **18,** 4565-4575.

Wheatley, D. N. (1995). Primary cilia in normal and pathological tissues. *Pathobiology* **63,** 222-238.

Williams, C. L., Li, C., Kida, K., Inglis, P. N., Mohan, S., Semenec, L., Bialas, N. J., Stupay, R. M., Chen, N., Blacque, O. E. et al. (2011). MKS and NPHP modules cooperate to establish basal body/transition zone membrane associations and ciliary gate function during ciliogenesis. *J. Cell Biol.* **192,** 1023-1041.

Williams, C. L., Masyukova, S. V. and Yoder, B. K. (2010). Normal ciliogenesis requires synergy between the cystic kidney disease genes MKS-3 and NPHP-4. *J. Am. Soc. Nephrol.* **21,** 782-793.

Williams, C. L., Winkelbauer, M. E., Schafer, J. C., Michaud, E. J. and Yoder, B. K. (2008). Functional redundancy of the B9 proteins and nephrocystins in *Caenorhabditis elegans* ciliogenesis. *Mol. Biol. Cell* **19,** 2154-2168.

Winkelbauer, M. E., Schafer, J. C., Haycraft, C. J., Swoboda, P. and Yoder, B. K. (2005). The *C. elegans* homologs of nephrocystin-1 and nephrocystin-4 are cilia transition zone proteins involved in chemosensory perception. *J. Cell. Sci.* **118,** 5575-5587.

Wolf, M. T. and Hildebrandt, F. (2011). Nephronophthisis. *Pediatr. Nephrol.* **26,** 181-194.

Zhang, D. and Aravind, L. (2010). Identification of novel families and classification of the C2 domain superfamily elucidate the origin and evolution of membrane targeting activities in eukaryotes. *Gene* **469,** 18-30.

Zhao, C. and Malicki, J. (2011). Nephrocystins and MKS proteins interact with IFT particle and facilitate transport of selected ciliary cargos. *EMBO J.*

Chapter 3: The *nphp-2* and *arl-13* genetic modules interact to regulate ciliogenesis and ciliary microtubule patterning in *C. elegans*

Note: This chapter is modified from the following publication:

Warburton-Pitt, S.R.F., Silva, M., Nguyen, K.C.Q., Hall, D.H., Barr, M.M. "The *nphp-2* and *arl-13* genetic modules interact to regulate ciliogenesis and ciliary microtubule patterning in *C. elegans*" (Accepted, PLOS Genetics)

References in this chapter are formatted in accordance with PLoS Genetics standards.

3.1 – Abstract

Cilia are microtubule-based cellular organelles that mediate signal transduction. Cilia are organized into several structurally and functionally distinct compartments: the basal body, the transition zone (TZ), and the cilia shaft. In vertebrates, the cystoprotein Inversin localizes to a portion of the cilia shaft adjacent to the TZ, a region termed the "Inversin compartment" (InvC). The mechanisms that establish and maintain the InvC are unknown. In the roundworm *C. elegans,* the cilia shafts of amphid channel and phasmid sensory cilia are subdivided into two regions defined by different microtubule ultrastructure: a proximal doublet-based region adjacent to the TZ, and a distal singlet-based region. It has been suggested that *C. elegans* cilia also possess an InvC, similarly to mammalian primary cilia.

Here we explored the biogenesis, structure, and composition of the *C. elegans* ciliary doublet region and InvC. We show that the InvC is conserved and distinct from the doublet region. *nphp-2* (the *C. elegans* Inversin homolog) and the doublet region genes *arl-13*, *klp-11,* and *unc-119* are redundantly required for ciliogenesis. InvC and doublet region genes can be sorted into two modules—*nphp-2*+*klp-11* and *arl-13*+*unc-119*—which are both antagonized by the

hdac-6 deacetylase. The genes of this network modulate the sizes of the NPHP-2 InvC and ARL-13 doublet region. Glutamylation, a tubulin post-translational modification, is not required for ciliary targeting of InvC and doublet region components; rather, glutamylation is modulated by *nphp-2*, *arl-13*, and *unc-119*. The ciliary targeting and restricted localization of NPHP-2, ARL-13, and UNC-119 does not require TZ-, doublet region, and InvC-associated genes. NPHP-2 does require its calcium binding EF hand domain for targeting to the InvC. We conclude that the *C. elegans* InvC is distinct from the doublet region, and that components in these two regions interact to regulate ciliogenesis via cilia placement, ciliary microtubule ultrastructure, and protein localization.

3.2 – Author Summary

Cilia are sensory organelles that are found on most types of human cells and play essential roles in diverse processes ranging from vision and olfaction to embryonic symmetry breaking and kidney development. Individual cilia are divided into multiple functionally and compositionally distinct compartments, including a proximal "Inversin" compartment, which is located near the base of cilia. We used the nematode *C. elegans*, a well-defined animal model of cilia biology, to characterize the genetics, components, and defining properties of the proximal cilium. The Inversin compartment is conserved in *C. elegans*, and is established independent of another proximal ciliary region, the microtubule doublet-based region. We showed how components of both the doublet region and the Inversin compartment genetically interact to regulate many pathways linked to core aspects of cilia biology, including ciliogenesis, cilia placement, cilia ultrastructure, microtubule stability, and the protein composition of ciliary compartments. In addition to expanding and clarifying our knowledge of basic cilia biology, these results also have

direct implications for human health research because several of the genes and pathways

explored in our work are linked to ciliopathies, a group of diseases caused by dysfunctional cilia.

3.3 – Introduction

Cilia are cellular "antennae" that mediate the transduction of environmental signals into intracellular pathways. Cilia play an integral role in many cellular functions, including developmental signaling, symmetry breaking, cell-cell adhesion, cell-cycle control, stress response, and DNA damage response (e.g., [1-6]). The vast majority of cilia share a set of evolutionarily conserved features: cilia are supported by a microtubule-based backbone, the axoneme; are built by intraflagellar transport (IFT), a microtubule motor driven cargo transport system [7]; and can be divided into structurally and functionally distinct compartments. These compartments include the microtubule triplet basal body which roots the cilium to the cell, the microtubule doublet transition zone (TZ) which anchors the cilium to the membrane, and the microtubule doublet cilia shaft where IFT occurs. The basal body and TZ also act as selective filters for inbound and outbound ciliary cargo, functioning through physical occlusion and cargo-specific recognition mechanisms [7-9]. The cilia shaft has traditionally been treated as an undifferentiated whole [10], though recent evidence has shed light on subdivisions of the cilia shaft [11].

Inversin/Nephrocystin-2 specifically localizes to the Inversin compartment (InvC), a proximal portion of the cilia shaft adjacent to the TZ [12]. This region has been suggested to play a role in signal transduction and amplification [13-15], cilia placement, and ciliogenesis [16, 17]. Products of several genes—including *INVS/NPHP2*, *NPHP3*, *NEK8/NPHP9*, and *ANKS6/NPHP16*—localize to the InvC. Interactions between InvC genes and other cilia genes have only recently begun to be explored and have not been well-generalized across animal and cell culture models.

The mechanisms that initially establish the InvC are currently unknown, though recruitment pathways for several InvC components are known. Work in vertebrate models has shed light on an InvC-specific physical interaction complex composed of Inversin, Nek8, Nphp3, and Anks6 [18-20]. Nek8, Nphp3, and Anks6 localize to the InvC in an Inversin-dependent manner, but Inversin itself localizes independently of the other proteins [18, 19]. Unc119b—a possible, though not proven, InvC component—may mediate an InvC-targeting pathway. In mammalian cells, Unc119b binds myristoylated cargo, including Nphp3, and shuttles it into the cilium. Once the Unc119b-Nphp3 complex has translocated into the cilium, the small GTPase Arl3 triggers Unc119b to release bound cargo [21]. InvC components other than Nphp3 are not known to be myristoylated and shuttled via Unc119b, suggesting additional InvC targeting pathways must exist. Whether Unc119b is required for the localization of Inversin and how Unc119b itself is targeted to the proximal cilium is unknown.

The nematode *Caenorhabditis elegans* is a well-studied model of cilia biology [22]. *C. elegans* possesses a ciliated nervous system [23-26] which is primarily used by the roundworm to detect internal and external cues and signals. Amphid channel cilia in the head and phasmid cilia in the tail are exposed to and sense the external environment through cuticular pores [27, 28]. Unlike most mammalian primary cilia, the cilia shafts of *C. elegans* amphid channel and phasmid cilia are divided into two regions: a proximal microtubule doublet-based region attached to the TZ, and a distal microtubule singlet-based region that extends from the doublet region [27, 28]. As both the doublet region of *C. elegans* cilia and the InvC of mammalian primary cilia lie at the proximal end of the cilium, directly adjacent to the TZ at the cilia base, and constitute only a portion of the length of the cilia shaft, previous work has viewed them as compositionally and functionally similar [13, 17, 29]. The relationship between the mammalian InvC and the

C. elegans doublet region of cilia has not been well characterized; Here we present evidence that the InvC and the doublet region are distinct, but overlapping, ciliary regions.

The *C. elegans* genome encodes orthologs for several of the mammalian InvC-associated proteins, including Inversin itself (NPHP-2), Unc119b (UNC-119), Arl3 (ARL-3), and possibly Nek8 (the uncharacterized paralogous pair NEKL-1 and NEKL-2), but likely not Nphp3 or Anks6. Of these, NPHP-2 and ARL-3 have previously been shown to be doublet region-localizing in *C. elegans* [17, 30]. *C. elegans* also possess several doublet region-enriched proteins, which are not InvC restricted in mammalian primary cilia; these include the kinesin-II IFT motor KLP-11 and the membrane-associated small GTPase ARL-13 [30]. The IFT motors Kinesin-II and OSM-3 work cooperatively to carry the IFT assemblies IFT-A and IFT-B and to build the doublet region— OSM-3 alone is sufficient to build the singlet region [31]. ARL-13 likely stabilizes the interaction between IFT-A and IFT-B particles and is required for ultrastructural integrity of the doublet region [30, 32]. *arl-13* mutants exhibit multiple ciliary defects, some of which can be suppressed by deletion of histone deacetylase *hdac-6*, through an unknown mechanism [30]. Mammalian *HDAC6* also antagonizes ciliogenesis in mammalian primary cilia: *HDAC6* knockouts can suppress ciliogenesis defects arising from *INVS/NPHP2* RNAi in MDCK cells [16].

In this work, we aimed to molecularly dissect the proximal cilium of *C. elegans* and to gain insight into the nature of the InvC and doublet region. We examined interactions between genes associated with the doublet region, determined the territories and localization dependencies of the protein products of these genes, and performed ultrastructural analysis of deletion mutants of these genes. We find that the InvC is conserved in *C. elegans*, is established early in development, and is distinct from the doublet region. *nphp-2* interacts with doublet region genes to regulate cilia placement, microtubule ultrastructural patterning, tubulin glutamylation,

and territory sizes of NPHP-2 and ARL-13. Finally, we show that *nphp-2*, *arl-13*, *klp-11*, and *unc-119* fall into two parallel redundant genetic modules, and that interactions between the two modules are modulated by *hdac-6* and *arl-3*. Together, the InvC and the doublet region function in concert to regulate many critical aspects of ciliogenesis and cilia biology.

3.4 – Results

3.4.1 – Genetic interactions between *nphp-2* and *arl-13* are modulated specifically by *hdac-6*

nphp-2 and *arl-13* single mutants have statistically similar, moderate ciliogenic defects (Figure 19). As *hdac-6* and *arl-3* modulate several *arl-13* phenotypes [30], we sought to determine if *nphp-2* and *arl-13* genetically interact and if *hdac-6* and *arl-3* modulate *nphp-2* phenotypes. We examined double, triple, and quadruple mutant combinations using "dye filling" of ciliated neurons as a gross indicator of ciliogenesis and cilia integrity [27]. Properly formed and placed cilia are environmentally exposed and take up fluorescent DiI dye, whereas stunted or misplaced cilia are not exposed and cannot take up DiI. Unlike the mild dye-filling defects (Dyf) of *nphp-2* and *arl-13* single mutants, *arl-13; nphp-2* double mutants were severely synthetic dye-filling defective (SynDyf) in both the amphids and phasmids (Figure 19). *hdac-6* deletion did not suppress *nphp-2* or *arl-13* Dyf; this is contrary to previously published data indicating that *hdac-6* can partially suppress the weak *arl-13* single mutant Dyf, and may be due to a difference in dye filling or scoring method (*cf.* [30] and 3.6.7 – Dye-Filling Assays). However, *hdac-6* suppressed the *arl-13; nphp-2* severe SynDyf phenotype to the mild Dyf severity of the single mutants in both amphids and phasmids (Figure 19). *hdac-6* may function by suppressing defects arising from one of the pathways or at a point where the two pathways converge. Combined,

this data indicates that *arl-13* and *nphp-2* act in partially redundant parallel pathways antagonized by *hdac-6*.

arl-3 has also been implicated as a modulator of the *arl-13* pathway [30]. We found that, unlike the interactions with *hdac-6*, interactions with *arl-3* are cell-type specific (Figure 28). Both *arl-3* single mutants and *arl-3; hdac-6* double mutants were nonDyf in both amphids and phasmids. In amphids, *arl-13; arl-3* was mildly SynDyf, whereas *arl-3; nphp-2* is nonDyf (cf. Figure 19 and Figure 28A). *hdac-6* deletion suppressed the *arl-13; arl-3* phenotype to a severity similar to that of the *arl-13* single mutants. In phasmids, both *arl-13; arl-3* and *arl-3; nphp-2* double mutants exhibited a moderate SynDyf phenotype. *hdac-6* suppressed *arl-13; arl-3* defects, but not *arl-3; nphp-2* defects. Strikingly, in both amphids and phasmids, *arl-3* deletion prevented the *hdac-6* Dyf suppression in the *arl-13; hdac-6; nphp-2* triple mutant described above. The SynDyf phenotype of *arl-13; arl-3* is qualitatively different from the suppression of *arl-13* Dyf defects by *arl-3* found previously [30]. Similarly to the difference in *hdac-6* suppression of *arl-13* defects discussed above, this may be due to different scoring methods or assay conditions. We conclude that *arl-3* functions parallel to both *nphp-2* and *arl-13* pathways, and likely lies in the same regulatory pathway as, but acts antagonistically to, *hdac-6*.

3.4.2 – *nphp-2* and *arl-13* genetically interact to regulate amphid cilia ultrastructure

To gain a better understanding of the defects present in *nphp-2* single and *arl-13; nphp-2* double mutants, and to examine the effects of *hdac-6* mediated suppression of the double mutant defects, we used serial-section transmission electron microscopy (TEM) to examine the ultrastructure of amphid channel cilia. Wild-type amphid cilia are divided into three segments based on microtubule ultrastructure: the TZ, the doublet region, and the singlet region (Figure

20A). One of the two microtubules within a doublet, the A-tubule, extends to form the

microtubule singlet seen in the distal cilium (Figure 20A1); the second tubule of the doublet, the

B-tubule, terminates at the distal end of the doublet region. The doublet microtubules of the TZ

and doublet region are arranged in a circular pattern in close proximity to the ciliary membrane

(Figure 20A2, A3). Within a particular cilium, microtubule ultrastructural characteristics—the

location in the lumen, membrane association, and singlet/doublet architecture—are similar

across all nine outer microtubule doublets.

In *nphp-2* single mutants, in a given amphid cross-section at a single level, we observe singlet

regions of some cilia, doublet regions of other cilia, and TZs of the remaining cilia. This is

consistent with amphid cilia that were shifted lengthwise with respect to each other, indicating

a potential anchoring defect (Figure 20B3). Additionally, within a given cilium, doublet and

singlet microtubule spans were no longer aligned. In sections across the proximal axoneme, this

appeared as singlets amongst the expected doublets, and in sections across the distal axoneme,

this appeared as doublets interspersed between the expected singlets (Figure 20B1-3). These

defects indicate that *nphp-2* is required both for microtubule patterning and for cilia anchoring.

While the chemical fixation method utilized here does not preserve Y-link ultrastructure well,

nphp-2 mutants exhibited significantly greater Y-link disorder than observed in wild-type

animals. The TZ defects seen in *nphp-2* animals may be related to both the lengthwise cilia shift

and the TZ-placement defect previously reported in *nphp-2* mutants [17]. This set of defects has

not been reported in any other *C. elegans* cilia mutant, suggesting that *nphp-2* functions in a

novel capacity.

arl-13 single mutants also exhibit a range of ultrastructural defects [30, 32]. Doublets are

observed in the central lumen of the cilium, which may originate from either displaced outer

doublets or mispatterned inner singlets. In both *C. elegans arl-13* and *hennin/ARL13B* mouse

mutants, there is also an increased frequency of early B-tubule detachment from the A-tubule, indicative of microtubule stability or patterning defects [33]. Similar to *nphp-2* mutants, ectopic microtubule singlets were sometimes visible in the doublet region of *arl-13* worms [30, 32]. *arl-13; nphp-2* double mutants exhibited extreme ultrastructural defects, likely causative of the severe Dyf phenotype (Figure 20C1-3). Cilia were almost completely absent from the amphid channel pore. No other cilia were visible even at the distal dendritic level. In one instance, a single cilium was visible in TEM sections. At the TZ level, an incomplete set of doublets was visible within the single cilium (Figure 20C3). Closer to the socket cell/sheath cell transition, a set of singlets was visible (Figure 20C2). At the distal pore, we were unable to resolve any internal structure due to electron dense material filling the cilium (Figure 20C1).

Remarkably, in *arl-13; hdac-6; nphp-2* triple mutants almost all defects observed in the double mutant were suppressed (Figure 20D1-3). The only defects remaining were misplaced TZs (Figure 20D3), ectopic singlets in the doublet region (Figure 20D2), and ectopic doublets in the singlet region Figure 20D1), similar to those present in the *nphp-2* single mutant. We did not observe inner doublets as reported in *arl-13* single mutants [30, 32]. These results are consistent with the observed *hdac-6* suppression of *arl-13; nphp-2* Dyf defects.

Because *nphp-2* and *arl-13* both exhibit ectopic microtubule singlets, *nphp-2* mutants exhibit ectopic microtubule doublets, and *nphp-2; arl-13* double mutants exhibit severe defects in ciliogenesis, we conclude that *nphp-2* and *arl-13* function together redundantly in regulation of microtubule patterning and ciliogenesis. Because ciliogenic defects are suppressed by *hdac-6*, but ectopic doublets and singlets are not, ciliogenesis and microtubule patterning may be independently regulated.

3.4.3 – NPHP-2 and ARL-13 do not require TZ- and doublet region-associated genes for ciliary targeting

Localization of InvC and doublet region components can be broken down into three steps: first the protein is targeted to the cilia base, second, the protein is imported into the cilium, and third, the protein is restricted to a subdomain of the cilium [18]. The factors required for the initial establishment of the InvC and doublet region cilia targeting and localization restriction are unknown. The TZ functions as a regulator of ciliary protein import (Reviewed in [34]), and has been implicated in the import of InvC and doublet region components in mammalian cilia [35, 36]. As both *nphp-2* and *arl-13* genetically interact with TZ-associated genes [17, 32], we wanted to determine if NPHP-2 and ARL-13 ciliary targeting and import requires TZ components. In *C. elegans*, TZ genes are organized into two genetic and physical modules—the *mks* module and the *nphp-1+nphp-4* module [8, 17, 20, 37]. We examined the localization of NPHP-2 and ARL-13 in mutants missing a component of each module (Figure 21A,C). In both *nphp-4* and *mks-3* single mutants, NPHP-2::GFP was properly targeted to and imported into the cilium. Mislocalized NPHP-2::GFP puncta in the periciliary region were sometimes visible (Figure 21A). In *mks-3; nphp-4* double mutants, there were severe ciliogenic and dendritic extension errors, as previously reported [17, 37]; in phasmid cilia that were visible and placed properly, NPHP-2::GFP localization appeared as in *mks-3* and *nphp-4* single mutants (Figure 29A). In a wild-type background, ARL-13::GFP localized exclusively to the doublet region in amphid channel and phasmid neurons (Figure 21C). Like NPHP-2::GFP, ARL-13::GFP was targeted to and imported into the cilium properly in *mks-3* and *nphp-4* mutants. Similar to published reports, we also observed ARL-13::GFP mislocalization to the periciliary membrane, as judged by a fluorescent "fringe" surrounding the periciliary region where the membrane lies (Figure 21C, enhanced contrast in Figure 29B), which has been suggested to be due to a failure of the TZ diffusion

barrier [29]. In amphid cilia, like in phasmid cilia, both NPHP-2 and ARL-13 were targeted to the

cilium and imported properly, and both infrequently exhibited mild mislocalization (Figure 30).

We investigated whether doublet region-associated genes were required for doublet region

restriction of NPHP-2::GFP and ARL-13::GFP. *hdac-6* had no obvious effect on the localization of

NPHP-2::GFP (Figure 29A). NPHP-2::GFP was targeted and restricted to the proximal cilium in

both *klp-11* and *arl-13* mutants. In both mutants, periciliary puncta similar to those seen in

TZ-associated mutants were visible (Figure 21B). *unc-119* mutants also exhibited proper

NPHP-2::GFP ciliary targeting. In *unc-119* mutants, NPHP-2::GFP exhibited a unique distal

dendrite mislocalization pattern, distinct from the periciliary puncta seen in other TZ and

doublet region mutants (Figure 21B).

In *klp-11* and *nphp-2* mutants, ARL-13::GFP was restricted to a proximal portion of the cilium as

in wild type, but with a periciliary membrane mislocalization pattern similar to TZ mutants.

ARL-13::GFP also did not require *unc-119* for ciliary localization. In *unc-119* mutants,

ARL-13::GFP and NPHP-2::GFP localized along the distal dendrite in a similar manner (Figure

21D).

In all TZ, doublet region, and InvC mutants examined, NPHP-2::GFP and ARL-13::GFP still

localized to the cilium, suggesting that either unknown factors or redundant pathways are

required for establishing ciliary territories. Periciliary mislocalization was observed for both

reporters across all mutant backgrounds. This suggests either that a delicate, easily perturbed

interaction network is required for NPHP-2 and ARL-13 ciliary import/export, or that the

overexpressed reporter constructs are "leaking" out of the cilium in sensitized mutant

backgrounds, or a combination of both possibilities.

3.4.4 – NPHP-2 requires its EF-hand for proper localization and function

We next looked to determine which domains of NPHP-2 were required for InvC localization. In mammalian models, several domains in Inversin are required for ciliary targeting and InvC restriction: the ankyrin repeat region, IQ2 domain, and ninein-homologous region (Figure 22A) [12, 38]. The IQ and ninein homology domains are not conserved in *C. elegans* NPHP-2; only the ankyrin repeat region, hydroxylation motif (Figure 35A), and two nuclear localization signals (NLSs) are conserved (Figure 22A) [17]. NLS motifs are hypothesized to play a role in ciliary protein import, and are required for ciliary import of the IFT motor KIF17 [9]. NPHP-2 also contains a predicted calcium binding EF-hand which may function in the same calcium detection capacity as the IQ domain of Inversin [17].

We built NPHP-2::GFP constructs missing the EF-hand (NPHP-2-EFΔ::GFP, residues 520-533), NLS1 (NPHP-2-NLS1Δ::GFP, residues 441-446), or NLS2 (NPHP-2-NLS2Δ::GFP, residues 598-603) (Figure 22A). Full-length NPHP-2::GFP localized to a short proximal region of amphid channel and phasmid cilia as well as IL, CEP, OLQ, amphid channel and phasmid cilia, and the AWC wing cilia (Figure 22B). Native promoter driven NPHP-2::GFP was not visible in AWB cilia, as reported previously for AWB-specific promoter driven NPHP-2 [13]. NPHP-2-EFΔ::GFP was generally faint or absent in amphid channel, AWC, and phasmid cilia, indicating that the EF-hand is strictly required for normal localization of NPHP-2 in these cell types. NPHP-2-EFΔ::GFP properly localized in IL cilia, indicating that the fluorescent reporter was being synthesized and folded correctly. NPHP-2-EFΔ::GFP was additionally present in either CEP or OLQ cilia, though specific identification was difficult due to their close proximity. Deletion of either NLS1 or NLS2 did not perturb NPHP-2 localization (Figure 22B).

We next tested whether these domain deletion constructs were functional by attempting to rescue the severe Dyf phenotype of *nphp-2 nphp-4* mutants; *nphp-4* single mutants are nonDyf,

allowing for easy determination of rescue [17]. Rescue of the *nphp-2 nphp-4* SynDyf phenotype

by NPHP-2-NLS1Δ::GFP and NPHP-2-NLS2Δ::GFP was comparable to rescue by full length

NPHP-2::GFP. NPHP-2-EFΔ::GFP only weakly rescued the SynDyf phenotype, indicating that the

EF-hand is critical for both normal function and localization of NPHP-2 (Figure 22C). These

results indicate that the calcium-binding EF-hand plays a significant role in both localization and

function of NPHP-2 in amphid channel and phasmid cilia, but is dispensable for localization in

cilia of CEP, OLQ, and inner labial neurons.

3.4.5 – UNC-119 is associated with the doublet region

Mammalian Unc119b localizes to the proximal cilium and is required for the targeting of several

proteins to the InvC [21], and *C. elegans unc-119* is required for singlet region biogenesis in

amphid cilia [39], suggesting a compartment-specific role. We therefore examined the

localization of p*osm-6*::GFP::UNC-119. In phasmid cilia, GFP::UNC-119 localization was similar to

NPHP-2::GFP and ARL-13::GFP: its localization was restricted only to a small proximal portion of

the cilium and was excluded from the TZ. Similar to localization in phasmid cilia, GFP::UNC-119

likely localized to the doublet region and not the entire cilium of amphid cilia (Figure 23A).

GFP::UNC-119 was not motile in cilia.

We also examined the dependence of UNC-119 localization on doublet region-associated genes.

Specific amphid mislocalization was difficult to determine, and we therefore focused on

phasmid cilia (Figure 31). In phasmid cilia, GFP::UNC-119 did not require *nphp-2*, *arl-13*, *hdac-6*,

or *klp-11* for ciliary targeting or restriction to the proximal cilium (Figure 23B).

3.4.6 – IFT motors and *unc-119* genetically interact with doublet

region-associated genes

We examined the genetic interactions between the doublet region-associated genes *nphp-2*, *arl-13*, and their modulators *hdac-6* and *arl-3* with the two IFT motors, *osm-3* and *klp-11*. In both amphids and phasmids, *arl-13; klp-11* was SynDyf [32]. *arl-13; klp-11* dye-filling defects were slightly suppressed by deletion of *hdac-6* (Figure 24A, Figure 32A). *klp-11; arl-3* double mutants yielded a very mild SynDyf phenotype (Figure 28B). *osm-3* single mutants are missing a singlet region and are completely Dyf, which precludes searching for synthetic interactors of *osm-3*. Instead, we assayed *osm-3* double mutants for suppression of the severe dye-filling defect; in no mutant background examined was the defect suppressed (Figure 24B, Figure 32B).

We next examined genetic interactions between *unc-119* and other doublet region-associated genes. *unc-119* single mutants were severely Dyf, with the phasmid phenotype being less severe than the amphids (Figure 24B, Figure 32A) [39]. In phasmids, both *nphp-2* and *klp-11* were SynDyf with *unc-119*. Surprisingly, we found that *hdac-6* suppressed Dyf defects in the *unc-119; nphp-2* double mutant to the level of the *nphp-2* single mutant (Figure 24B). *arl-3* deletion was also able to significantly suppress the *unc-119* Dyf phenotype in both amphids and phasmids (Figure 28B).

Genetic interactions between *nphp-2*, *arl-13*, *klp-11*, *unc-119*, *hdac-6,* and *arl-3* are summarized in Figure 24C. Doublet region-associated genes fall into two redundant pathways or modules: *nphp-2+klp-11* and *arl-13+unc-119*. Deletion of two genes within a module does not result in an increase in Dyf severity over that present in single mutants, but deletion of any two genes from different modules yields a SynDyf phenotype. Interactions between these modules are regulated by *hdac-6* and *arl-3*.

Double mutants with a deletion in a single TZ gene and a single doublet region gene are SynDyf.

To determine whether *hdac-6* mediated suppression of SynDyf defects extended to these cross-compartmental genetic interactions, we assayed for suppression of SynDyf defects in *nphp-2 nphp-4* mutants by *hdac-6* and *arl-3*. We found that neither *hdac-6* nor *arl-3* suppressed the severe *nphp-2 nphp-4* SynDyf defect (Figure 32D). This suggests that *hdac-6* functions specifically in doublet region pathways.

3.4.7 – Axonemal glutamylation is downstream of the action of *nphp-2*, *arl-13*, *unc-119*, and *hdac-6*

Post-translational glutamylation predominantly occurs on the C-terminal tails of α- and β-tubulin of axonemal B-tubules [40-44], and regulates microtubule stability and IFT motor function [45]. Glutamylation is specifically associated with the doublet region, as B-tubules define and are only present in the doublet region. Additionally, in *Chlamydomonas* and *Paramecium*, TZ microtubules are not glutamylated [40, 46]. In *C. elegans* and vertebrates, mutants with defects in tubulin glutamylation or *arl-13* exhibit B-tubule degeneration [33, 45, 47]. We therefore determined whether doublet region associated genes regulated tubulin glutamylation, or whether tubulin glutamylation specified the localization of doublet region proteins.

In wild-type animals, the anti-glutamylated tubulin antibody GT335 labeled the doublet region of amphid channel and phasmid cilia (Figure 25A) [47]. *nphp-2* mutants exhibited characteristic cilia displacement in the amphids, but no qualitative changes in head cilia glutamylation. The glutamylation signal in *nphp-2* phasmid cilia ranged from wild-type-like to extremely elongated, which is consistent with the TEM observation of B-tubules extending into the distal axoneme (Figure 20B). *arl-13* mutants exhibited elongated staining in amphid channel cilia. Amphid staining in *unc-119* mutants was extremely shortened and cilia were angled inwards. *hdac-6* mutants appeared to have shortened GT335 staining of amphid channel cilia. We also observed

significant differences in the length of the phasmid GT335 ciliary signal. Both *arl-13*

(3.95±0.25μm) and *nphp-2* (4.30±0.32μm) mutants had phasmid staining significantly longer

than in wild type (2.79±0.07μm), while *unc-119* (2.40±0.05μm) mutants had staining significantly

shorter (Figure 34E). The length of GT335 staining in amphid cilia was not quantified due to the

difficulty of unbiased measurement of a single cilium within the amphid bundle.

To determine if doublet region-associated protein localization was dependent on tubulin

glutamylation status, we examined the localization of NPHP-2::GFP and GFP::UNC-119 in *ccpp-1*

and *ttll-4* mutants. Mutants of *ccpp-1*, which encodes a tubulin deglutamylase, display

degenerating amphid channel and phasmid cilia with a concomitant dye-filling defect; this is

suppressed by deletion of the opposing glutamylase, encoded by the tubulin tyrosine ligase-like

gene *ttll-4* [45]. In each mutant, NPHP-2::GFP and GFP::UNC-119 reporters were targeted to cilia

and were restricted to the proximal cilium similarly to wild-type (Figure 25B,C). This was

surprising in the case of *ccpp-1* mutants, as cilia degenerate as the worm ages (Figure 25B,C).

These reporters were still doublet region-associated in earlier larval stages of *ccpp-1* mutants

when ciliary degeneration was not as severe (Figure 36C,D). Combined, these results indicate

that *nphp-2*, *arl-13*, *unc-119*, and *hdac-6* lie upstream in regulation of tubulin glutamylation

pathways, and the localization patterns of their protein products are not defined by tubulin

glutamylation.

3.4.8 – Doublet region protein territories are genetically regulated

To allow for a more direct comparison of subciliary localization, we stained transgenic

NPHP-2::GFP, ARL-13::GFP, and GFP::UNC-119 strains with GT335 (Figure 26). NPHP-2::GFP did

not fully overlap with GT335, only colabelling the proximal portion of the doublet region of

amphid and phasmid cilia. However, ARL-13::GFP colabelled with a greater portion of the GT335

doublet region signal in amphid cilia than did NPHP-2::GFP, and completely colabelled with

GT335 in phasmid cilia (Figure 26, Figure 33A); this suggests that ARL-13 is associated with the

microtubule doublets that define the doublet region. GFP::UNC-119 colabelled with either a

significant fraction of the length of the GT335 signal. Additionally, GFP::UNC-119 did not extend

beyond the GT335 labelled doublet region, indicating that GFP::UNC-119 is excluded from the

TZ, which is not labelled by GT335.

We also examined the territory length of each of the fluorescent reporters as a fraction of the

total cilia length. Transgenic animals were incubated with DiI to label the length of the cilium.

NPHP-2::GFP marked a significantly shorter fraction of the length of the cilium than did

ARL-13::GFP or GFP::UNC-119 (Figure 33C).

To understand how the localization of doublet region-associated proteins is genetically

regulated, we measured the length of the cilium marked by NPHP-2::GFP, ARL-13::GFP,

GFP::UNC-119, and KAP-1::GFP—a component of Kinesin-II—in different mutant backgrounds

(Figure 34). ARL-13::GFP and NPHP-2::GFP have interdependent localizations: in *arl-13* mutants,

the NPHP-2::GFP territory was extended along the cilium, and in *nphp-2* mutants, the

ARL-13::GFP territory was extended. *unc-119* mutants exhibited shortened ARL-13::GFP and

NPHP-2::GFP territories (Figure 34A,B). Additionally, *klp-11* mutants had a shorter NPHP-2::GFP,

but not ARL-13::GFP, localization signal (Figure 34A). No significant differences were found in

the territory lengths of GFP::UNC-119 and KAP-1::GFP in any of the mutant backgrounds (Figure

34C,D). The length of the tubulin glutamylation signal is also genetically controlled; the GT335

signal is shortened in *unc-119* mutants, and elongated in *nphp-2* and *arl-13* mutants (Figure

34E).

In sum, the NPHP-2::GFP territory size is shorter than the territories of doublet region

components ARL-13 and Kinesin-II, marks a shorter length of the cilium than ARL-13 and

UNC-119, is shorter than the doublet region-linked glutamylated tubulin signal, and colabels only a portion of both amphid channel and phasmid GT335 staining. We conclude that NPHP-2 marks a region of the cilium distinct from the doublet region, and propose that this region is analogous to the InvC of mammalian cilia.

3.5 – Discussion

In this study, we present evidence that (1) *C. elegans* possesses a conserved InvC compartment, (2) interactions between *nphp-2* and *arl-13* regulate microtubule ultrastructural patterning, (3) InvC and doublet region sizes are distinct and genetically regulated, (4) *hdac-6* and *arl-3* modulate interactions between *nphp-2*, *arl-13*, *klp-11*, and *unc-119*, (5) and that microtubule glutamylation is downstream of the action of InvC and doublet region genes. Additionally, we found that genes associated with the proximal cilium (TZ, InvC, and doublet region) can be grouped into parallel genetic modules, which interact to drive ciliary anchoring and proper ciliogenesis. Finally, we addressed several possible mechanisms for the ciliary targeting and InvC restriction of NPHP-2.

3.5.2 – The nature of the doublet region

There has been confusion regarding the relationship between the mammalian InvC and the *C. elegans* doublet region. Because amphid channel and phasmid cilia have elongated microtubule singlets, doublet region proteins appear to be proximally restricted. This was also taken in reverse: proteins localized to the proximal cilium were considered de facto doublet region components. As the mammalian InvC is similarly characterized by proximally restricted proteins, and both the mammalian InvC and *C. elegans* doublet region had an underlying ultrastructure of microtubule doublets, the *C. elegans* doublet region and the mammalian

proximal InvC were considered analogous [19, 20, 35, 235, 236]. In *C. elegans*, a number of factors have been associated with the doublet region, including NPHP-2, ARL-13, UNC-119, ARL-3, HDAC-6, the Kinesin-II components KAP-1/KLP-11/KLP-20 [9, 235, 237], and glutamylated tubulin [18].

However, mammalian orthologs of many *C. elegans* doublet region proteins localize along the entire cilium [22-32]; this casts doubt on the equivalence between the *C. elegans* doublet region and the mammalian InvC. In mammalian primary cilia, the majority of the axoneme is composed of microtubule doublets; it is likely that the *C. elegans* ciliary doublet region is analogous to the entire mammalian ciliary doublet-based cilia shaft. To better clarify the associations between protein localizations and ciliary anatomy, in this work we refer to regions of the cilium by referencing the underlying ultrastructure. This clarifies localization confusion between systems: "ARL-13/Arl13b localizes to the doublet region of cilia" is true in both *C. elegans* amphid channel cilia and mammalian primary cilia.

However, several factors associated with the *C. elegans* doublet region do have proximally restricted localization in mammalian primary cilia, including NPHP-2 and UNC-119. Additionally, each doublet region-associated protein likely has different localization requirements: Kinesin-II is known to be doublet associated and is not influenced by glutamylation [9, 18], NPHP-2 localizes to a restricted subregion of the doublet region, and ARL-13 is membrane associated and its localization has been proposed to be regulated by membrane composition [33]. Because of this, we conclude that in *C. elegans,* what has been known as the proximal cilium (or "middle segment") is not a distinct region of the cilium patterned by underlying microtubule doublets, but is rather a set of overlapping but distinct protein territories (modelled in Figure 27).

3.5.3 – NPHP-2 localization requires an EF-hand

Calcium signaling plays a crucial role in signal transduction and ciliary function [58, 59]; cilia have high intraciliary calcium concentrations, and many TZ proteins possess calcium binding domains [60]. The NPHP-2 vertebrate homolog, Inversin, has two identified calmodulin-binding IQ domains [61, 62], one of which is required for proper localization [12]. Calmodulin detects intracellular calcium concentrations through a calcium-binding EF-hand. Though *C. elegans* NPHP-2 does not encode a predicted IQ domain, it does possess an EF-hand. This EF-hand is required for the localization and function of NPHP-2 in amphid and phasmid cilia, similarly to the IQ2 domain of Inversin. A significant difference exists between the EF-hand of NPHP-2 and the IQ2 domain of Inversin: deletion of the EF-hand of NPHP-2 results in a complete lack of ciliary localization, whereas deletion of the IQ2 domain of Inversin results in a mislocalization of Inversin along the entire cilium. In both systems, Inversin/NPHP-2 no longer localizes to the InvC. This suggests that Ca^{2+} detection/binding by and the subsequent hypothetical modulation of the activity of Inversin/NPHP-2 is a critical, conserved feature of the protein. Two possibilities arise for the function of these domains: Ca^{2+} specifies the localization of NPHP-2, modulates the activity of the protein, or both. In the first case, intraciliary calcium might bind to NPHP-2, and change binding affinities and physical properties of the protein. This may prevent NPHP-2 from exiting the cilium, and possibly restricting it to the InvC. In the second case, intraciliary calcium concentrations can be modulated by the opening and closing of ciliary calcium channels in response to stimuli; NPHP-2 would then act as a component in signal transduction pathways linking calcium flux to downstream effects (e.g., modulation of glutamylation, localization of other proteins, Wnt signaling pathways, ciliary maintenance pathways). If calcium does specify InvC restriction, then in *C. elegans*, non-InvC targeted NPHP-2 may be cleared actively or passively out of the cilium through a nonconserved means. It is also possible that the

calcium-dependency of Inversin and NPHP-2 has diverged.

3.5.4 – UNC-119 is a proximal ciliary protein

We found that UNC-119 localizes to the proximal cilium and is excluded from the distal region.

GFP::UNC-119 and GT335 colabel, indicating that GFP::UNC-119 is excluded from the TZ, as TZ

microtubules are not glutamylated (See Figure 26, in which GT335 colabels with TZ-excluded

ARL-13::GFP and NPHP-2::GFP). In *C. elegans*, UNC-119 labels a shorter portion of the cilium

than ARL-13 or GT335, markers associated with the doublet region. Additionally, mammalian

Unc119b physically interacts with the InvC component Nphp3 and is proximally restricted in cilia

of RPE cells, suggesting that Unc119b is associated with the InvC [21]. However, GFP::UNC-119

marked a larger portion of the cilium than did NPHP-2::GFP.

The *C. elegans* genome encodes homologs of many of many Unc119b shuttle proteins, including

Unc119b, Arl3, and RP2, and two myristoylated ciliary proteins which require *unc-119* for ciliary

localization [63]. *arl-3* genetically interacts with *unc-119* and *nphp-2*, suggesting that in

C. elegans the components of the shuttle are in place. These shuttle components do not appear

to be required for the localization of NPHP-2, as NPHP-2 is imported into the cilium in *unc-119*

and *arl-3* mutants. In *unc-119* mutants, NPHP-2 exhibited a unique distal dendritic localization

pattern that cannot be attributable to TZ leakage; it is unknown whether this population

represents NPHP-2 that has not been properly imported into the cilium or is mistargeted

NPHP-2.

3.5.5 – The function of *hdac-6*

In both mammalian systems and *C. elegans*, Hdac6/*hdac-6* functions as an antagonist of

ciliogenesis and cilia stability [16, 48]. In mammalian primary cilia, Hdac6 functions as an

α-tubulin K40 deacetylase regulates microtubule function and stability [48, 64-67]. The

C. elegans genome encodes a single α-tubulin with the acetylatable residue K40, MEC-12.

However, there is no direct evidence for *mec-12* expression in amphid and phasmid neurons,

and the anti-α-tubulin-K40 antibody 6-11b-1 does not label amphid and phasmid cilia in WT

animals or *hdac-6* mutants (Figure 37) [68]. Alternative tubulin acetylation sites may exist,

including on β-tubulin [69]; *hdac-6* could deacetylate these secondary sites. NPHP-2 contains a

predicted N-terminal acetylation site (at 2S) which may be deacetylated by HDAC-6; this may

modulate binding between NPHP-2 and its targets [70]. Additionally, HDAC-6 may have other

unidentified ciliary targets [30]. Determining the mechanism by which HDAC-6 acts as a genetic

modifier of InvC and doublet region gene defects is an important future direction.

3.5.6 – Doublet region and InvC components modulate tubulin

post-translational modification

Tubulin glutamylation is associated with the proximal portions of microtubule B-tubules in

C. elegans cilia, mouse spermatozoa flagella, and *Chlamydomonas* flagella [42, 45, 71]. In

C. elegans, microtubule glutamylation is linked to microtubule ultrastructure, stability, and

maintenance [45, 72]. Multiple doublet region genes regulate microtubule glutamylation, and

we observed a correlation between ectopic glutamylation and ectopic microtubule doublets.

Additionally, ciliary targeting of doublet region proteins is not dependent on glutamylation

status. Therefore, *nphp-2*, *arl-13*, *hdac-6*, and *unc-119* function upstream of microtubule

glutamylation, which may enable them to exert an influence on microtubule patterning, IFT,

ciliogenesis, and, in the case of *unc-119*, singlet region biogenesis. These pathways may be

conserved: in Arl13b/*hennin* mutant mice, ciliary microtubule glutamylation intensity is reduced,

and microtubule B-tubules have ultrastructural defects [33, 50].

3.5.7 – Doublet region- and InvC-associated genes form genetic modules

In *C. elegans*, TZ-associated genes can be grouped into two distinct, partially redundant genetic and physical modules [8, 17, 37]. Doublet region- and InvC-associated genes may be grouped in a similar manner into a *nphp-2+klp-11* module and an *arl-13+unc-119* module. *hdac-6* appears to function outside the two modules, negatively regulating both: deletion of *hdac-6* in SynDyf double mutants suppresses the SynDyf phenotype. In mammalian primary cilia, Hdac6 also plays an antagonistic role, destabilizing cilia through deacetylation of tubulin, a pathway suppressed by Inversin [16]. *arl-3* may function outside of the two modules in a cell-type specific manner; in phasmids it genetically interacts with components from both modules, but in amphids *arl-3* only genetically interacts with only the *arl-13+unc-119* module and not the *nphp-2+klp-11* module. In amphid cilia, *nphp-2* also does not interact with the TZ SynDyf network.

Curiously, a further two genetic module organization exists between TZ genes and the InvC/doublet region genes. *nphp-2 nphp-4, mks-3; nphp-2,* and *arl-13; nphp-4* double mutants exhibit severe ciliogenic defects [17]. Deletion of one TZ gene from either TZ module and one doublet region gene from either doublet region module yields a SynDyf phenotype, though not all combinations have been tested. The TZ SynDyf network and the doublet region SynDyf network can be thought of as two genetically interacting "super-modules", each consisting of two to three sub-modules described in this and previous work [8, 17, 20, 37].

3.5.8 – Origin of the Inversin Compartment

The localization requirements for multiple InvC localizing components have been previously determined, but how the InvC is initially established is not known (See 5.2.1 – InvC Biogenesis).

In *C. elegans*, the InvC is likely established early in cilia development, as NPHP-2 is proximally restricted in phasmid cilia as early as the first larval L1 stage immediately following hatching (Figure 36A), and is not motile (Figure 36B), unlike the larval stage-dependent dynamic localization of ARL-13 [29]. We have eliminated several mechanisms for the establishment of the InvC. Ciliary ultrastructure does not seem to play a role, as in both mammals and *C. elegans*, the localization of Inversin/NPHP-2 is associated with only a sub-portion of the doublet region where there are no identifiable ultrastructural features [12]. Tubulin post-translational modifications also do not appear to specify the InvC, as *nphp-2* (and genetically interacting doublet region components) lies upstream of glutamylation pathways. The TZ does not appear to play a major role in specifying the InvC. NPHP-2 still localizes and is restricted to the proximal cilium in TZ single and double mutants. IFT is another candidate mechanism, but we found that although IFT components genetically interact with InvC and doublet region associated genes, Kinesin-II is not required for NPHP-2 localization. In mammalian cilia, the Unc119b shuttle is required for the ciliary import of Nphp3; this activity is upstream of the action of Inversin in Nphp3 localization. In *C. elegans* phasmid cilia, NPHP-2 does not require either *unc-119* or its effector *arl-3* for ciliary import or InvC restriction (Figure 29A).

Several mechanisms for establishing the InvC remain. First, calcium may play a role. Both Inversin and NPHP-2 require a calcium binding domain for InvC localization [12]; the origin and nature of the calcium signal these domains detect is unknown. Second, the InvC may also be initially established by a diffusion of factors from the cilia base. A third possibility is that cilia membrane composition may help define the InvC. The cilium has a distinct membrane composition from the plasma membrane, and the different ciliary subregions may also have differential membrane composition.

3.5.9 – Final Summary

We propose that the logic underlying the establishment of the NPHP-2/Inversin compartment

may be similar in *C. elegans* and mammals, in a manner independent of microtubule

ultrastructure. We have shown that doublet region- and InvC-associated genes interact to guide

ciliogenesis, cilia placement, cilia ultrastructure, protein composition, and tubulin

post-translational modification. The next challenge is to determine what initially patterns the

doublet region and InvC, and to understand the function of these cilia regions.

3.6 – Methods and Materials

3.6.1 – General Molecular Biology

Standard protocols were followed for all molecular biological procedures. PCR amplification

using Taq polymerase (New England BioLabs, Ipswich, MA, USA) was used for genotyping

deletion alleles, and was followed by restriction digest for SNP diagnosis. PCR amplification for

construction of transgenic constructs was performed with Phusion High fidelity DNA polymerase

(New England BioLabs), templated off *C. elegans* genomic DNA. Sequencing was performed

offsite (GeneWiz, South Plainfield, NJ, USA). PCR primer and construct sequences are available

upon request.

3.6.2 – Bioinformatics and Computer Tools

Protein BLAST was used to find sequence orthologs [78]. All protein sequence information other

than that of *C. elegans* was provided by NCBI, and all *C. elegans* nucleotide and protein

sequences were provided by WormBase (Releases WS229 and WS234). Structural motif and

domain predictions were generated by MotifScan [79]. Acetylation motifs were identified using

NetAcet 1.0 [70]. Coiled-coil regions were identified with COILS [80]. ApE 2.0.36 was used for

sequence manipulation, annotation, and restriction site identification.

3.6.3 – Strains and Maintenance

All strains were cultured at room temperature, unless otherwise noted, under standard

conditions [81]. Transgenic strains using *pha-1* selection were grown at 25°C, and *pha-1(e2123)*

mutants were grown at 15°C. Deletion alleles were outcrossed to *him-5* at least four times.

Strains used in this study are listed in Table 8A. Alleles used were as follows: *nphp-2(gk653),*

nphp-4(tm925), mks-3(tm2547), arl-13(gk513), unc-119(ed3), hdac-6(ok3203), arl-3(tm1703), him-5(e1490), osm-3(p802), klp-11(tm324), ccpp-1(ok1821), and ttll-4(tm3310). Primers used for diagnosis are listed in Table 8B. All transgenic strains used in Figure 19 to Figure 26 were tested using dye-filling for dominant negative defects in ciliogenesis. We observed no adverse effects in NPHP-2::GFP and GFP::UNC-119 transgenic strains but did find dominant negative defects in ARL-13::GFP transgenic strains (Table 7).

The full length isoform of NPHP-2 was used in all NPHP-2 reporter constructs. The full length isoform, NPHP-2L, differs from the shorter isoform, NPHP-2S, in that the shorter isoform is missing 22 non-conserved amino acids of unknown function. Both isoforms have similar subciliary localization.

3.6.4 – Electron Microscopy

nphp-2 and *arl-13; hdac-6; nphp-2* young adult animals were fixed using 3.5% glutaraldehyde + 1% PFA in 0.1M HEPES and then in 1% OsO4 + 1.25% K4Fe(CN)4 in 0.1M HEPES. Samples were infiltrated and embedded in Embed-812 plastic resin. *arl-13; nphp-2* young adult animals were fixed using high-pressure freeze fixation and freeze substitution in 2% OsO4 + 2% water in acetone as the primary fixative [82]. Samples were slowly freeze substituted in an RMC freeze substitution device, before infiltration with Embed-812 plastic resin. Images for wild-type animals fixed by a comparable immersion fixation method (cf. [27]) are now curated by the Hall lab at Einstein courtesy of E. Hedgecock. These wild type images are also available online at www.wormimage.org.

For TEM, serial sections (70 nm thickness) of fixed animals were collected on copper slot grids coated with formvar and evaporated carbon and stained with 4% uranyl acetate in 70% methanol, followed by washing and incubating with aqueous lead citrate. Images were captured

on a Philips CM10 transmission electron microscope at 80kV with a Morada 11 megapixel TEM

CCD camera driven by iTEM software (Olympus Soft Imaging Solutions).

For each strain, we imaged three individuals that were fixed chemically. Additionally, we were

concerned that the severe defects seen in the *arl-13; nphp-2* double mutant were partially due

to the harsh chemical fixation method. We fixed a fourth double mutant using high pressure

freeze (HPF) fixation, which introduced fewer artifacts to confirm the validity of the chemical

fixation data. We used the same strain in the construction of the double *arl-13; nphp-2* and

triple *arl-13; hdac-6; nphp-2* mutants as was used in the previously published EM of the *arl-13*

single mutant.

3.6.5 – Imaging

Animals were mounted on 5% Noble agar pads on standard microscope slides, and immobilized

with a five minute incubation in 10mM sodium azide. Worms were imaged using a Zeiss

Plan-AXIOCHROMA 100X 1.4NA oil objective on a Zeiss Axio Imager.D1M (Zeiss, Oberkochen,

Germany) with a Retiga-SRV Fast 1394 digital camera (Q-Imaging, Surrey, BC, Canada). Exposure

time for antibodies was 100ms, and exposure time for GFP fluorophores was 250ms. Images

were captured and manipulated using Metamorph software (Version 7.6.1.0, MDS Analytical

technologies, Sunnyvale, CA, USA). Image stacks were 3D deconvolved using Auto Deblur

software (Version 1.4.1, Media Cybernetics, Bethesda, MD, USA). Figures and diagrams were

created with Adobe Photoshop CS3 (Version 10.0, Adobe Systems, San Jose, CA, USA) and Adobe

Illustrator (Version 13.0.0, Adobe Systems). Image brightness and contrast were modified

uniformly across an image, but gamma was not adjusted from 1.00. Brightness manipulations

are similar, but not identical, across panels and figures. Significant variations in absolute

intensity are noted where appropriate. For all strains, unless noted, worms were picked at L4

stage 24 hours before imaging.

3.6.6 – Statistical Analysis

All statistical analysis was performed with a combination of GraphPad Prism (Version 5.01, GraphPad Software, La Jolla, CA, USA) and Microsoft Excel (Version 14.0.7106, 32-Bit, Microsoft Corporation, Seattle, WA, USA). Sample size (n) for all figures is listed in Table 9. Minimum p value for significance was set at 0.01 for all analyses unless otherwise specified. All parametric and continuous data types were analyzed using unpaired t-tests with Welch's correction to avoid assumption of equal variance. When multiple t-tests were performed on related data sets presented together, the Holm-Bonferroni multiple comparison adjustment was used to ensure the total alpha for the analysis did not exceed 0.01. All nonparametric and discontinuous data types were analyzed using Mann-Whitney U-test. Similar to the analysis of continuous data types, the Holm-Bonferroni multiple comparison adjustment was employed to ensure total alpha for all related comparisons did not exceed 0.01. Specific pairwise comparisons made are described in figure legends. Letters on graphs indicate statistically distinct groups, e.g., all groups marked 'A' are significantly different from all groups marked 'B'.

3.6.7 – Dye-Filling Assays

Staged young adult hermaphrodites were washed of plates with M9, and then rinsed three further times in M9, using gentle centrifugation to pellet the worms between rinses. Worms were then incubated in 40µg/mL DiI (2.5mg/mL dimethyl formamide stock, diluted 1:1000 in M9) (Invitrogen) for 30 minutes in the dark. Worms were then rinsed three times in M9 as before, and were then placed on a seeded plate for a further 30-60 minutes to recover and flush dye from the digestive tract. Animals were anesthetized with 10mM sodium azide and then

immediately scored on a compound microscope (see Imaging section) using for dye-filling by manual counting of filled cell bodies. Cell body counts within the amphid or phasmid organs were averaged together to yield the average number of cells filling per organ per worm, and subjected to statistical analysis. Ectopically dye-filled neurons (e.g., IL2s) were not included in the total count.

3.6.8 – Antibody Staining

Antibody staining was performed under the standard Ruvkun-Finney protocol (Anatomical Methods, [83]) using GT335, an antibody against branch point single and polyglutamylated tubulin. Both primary (GT335, mouse, 1:100, Enzo Life Sciences) and secondary antibody (Alexa Flour 568 goat anti-mouse, 1:2000 dilution, Life Technologies) washes were performed at 4°C overnight. Young adult hermaphrodites were selected for imaging using the number of eggs in the animal—between one and ten—as a proxy for age.

3.7 – Acknowledgements

3.8 – Abbreviations List

Dyf   Dye Filling defective

GT335   Anti-glutamylated tubulin antibody

IFT   Intraflagellar Transport

InvC   Inversin Compartment

MDCK   Madin-Darby Canine Kidney cells

NLS   Nuclear Localization Signal

RPE   Retinal Pigment Epithelial cells

SynDyf   Synthetically Dye filling defective

TEM   Transmission Electron Microscopy

TZ   Transition Zone

WT   Wild-Type

3.9 – Figures and Legends
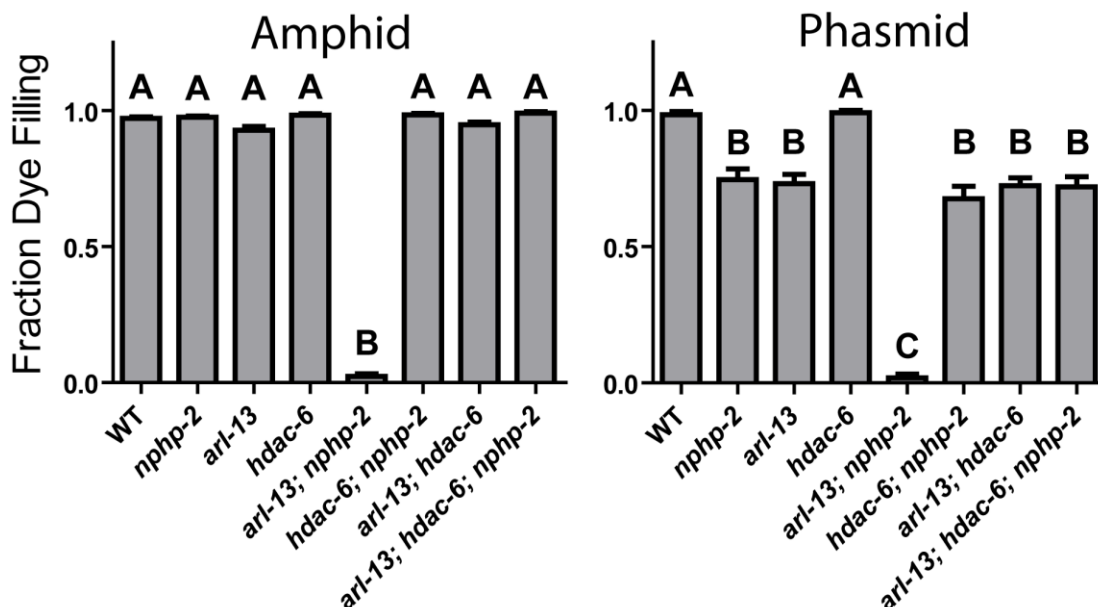
Figure 19. The synthetic dye-filling defective phenotype of *arl-13; nphp-2* mutants is modulated by *hdac-6*

hdac-6 deletion suppresses *arl-13; nphp-2* double mutant phenotypes. In phasmids, *nphp-2* and *arl-13* single mutants are mildly Dyf, which is not suppressed by *hdac-6* deletion. In both amphids and phasmids, *arl-13; nphp-2* is severely SynDyf and was suppressed by *hdac-6*. Data in both panels was analyzed with pairwise Mann-Whitney U-test between all groups, followed by the Holm-Bonferroni multiple comparison adjustment with a total alpha of 0.01. Groups from either panel sharing a capital letter are not significantly different, whereas groups from either panel with different capital letters do differ significantly.
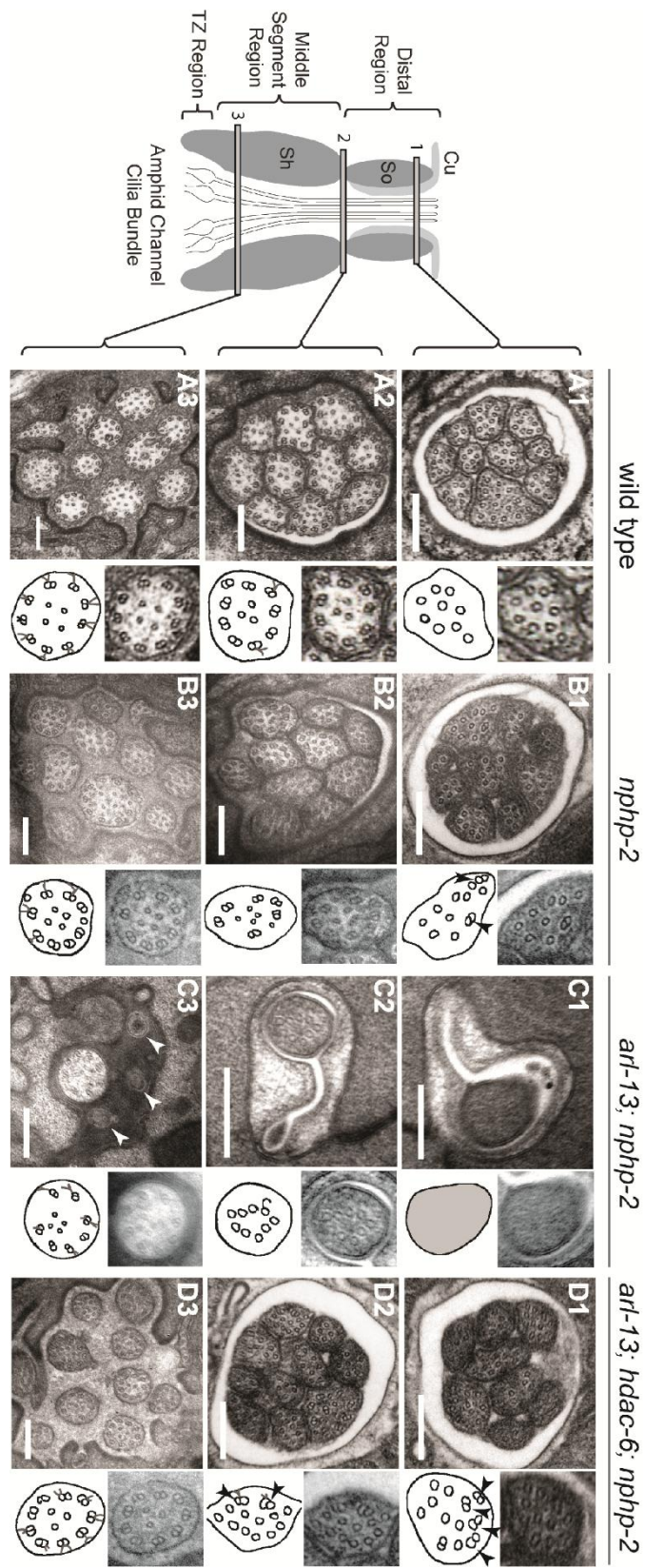
Figure 20. *nphp-2* single, *arl-13; nphp-2* double, and *arl-13; hdac-6; nphp-2* triple mutants exhibit defects in ciliary ultrastructure

Horizontal panels indicated by 1, 2, and 3 correspond to singlet region, doublet region-to-singlet region transition, and TZ levels, respectively, and are comparable across the genotypes. The insets show an enlarged view of the region within the white box, and are diagrammed in the accompanying cartoon. All scale bars are 250nm. (A1-3) In wild-type amphids, all doublet B-tubules within a cilium have similar spans. (A1) Distal microtubule singlets are devoid of B-tubules. B-tubule containing microtubule doublets are present in (A2) the doublet region and (A3) the TZ. (B1-3) In *nphp-2* animals, amphid channel cilia are shifted lengthwise with respect to each other (cf. Figure 6A). Within a cilium, spans of microtubule doublet B-tubules are asynchronous; arrows in insets indicate these microtubules. TZ Y-links are disorganized (C1-3) In *arl-13; nphp-2* animals, most amphid channel cilia are absent. (C1) The distal end is filled with electron dense material with unresolvable microtubules. (C2) A single, stub-like cilium is visible, consisting of only microtubule singlets. (C3) TZ microtubules are abnormal with some missing microtubule doublets. We also observe vesicle-like structures at this level that are indicated by arrows. (D1-3) In *arl-13; hdac-6; nphp-2* animals, most amphid cilia are visible. Ectopic singlets and doublets are still present. Cilia are shifted posteriorly towards the tail. (D1-2) insets show asynchronous microtubules within cilia.
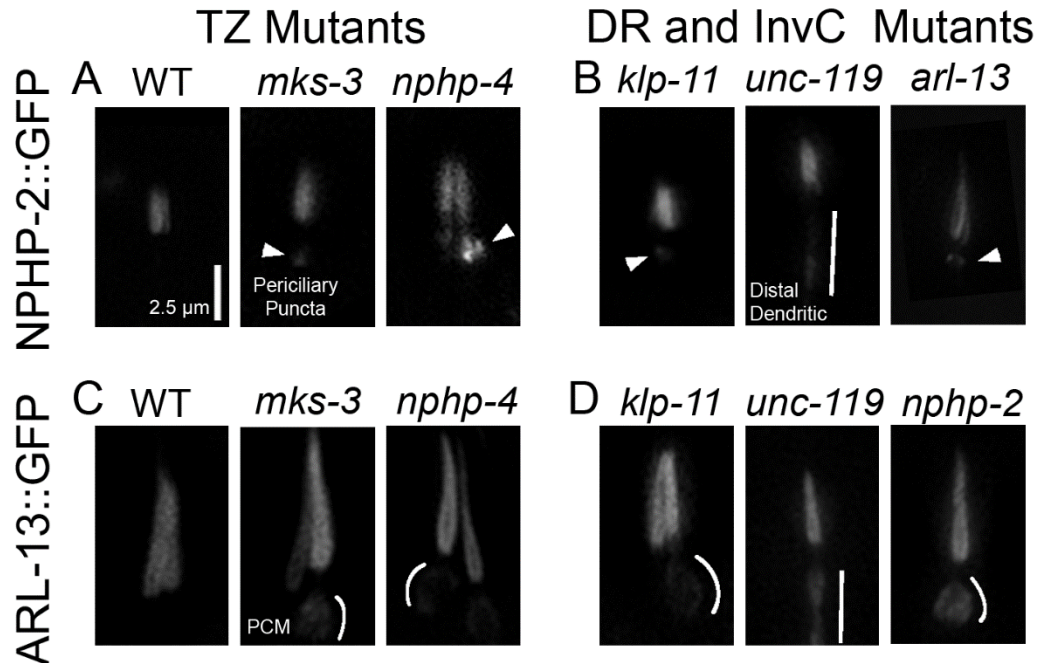
Figure 21. NPHP-2 and ARL-13 do not require TZ-, doublet region-, and InvC-associated genes for ciliary targeting

(A) In WT, NPHP-2 is restricted to the proximal cilium. In both *nphp-4* and *mks-3* mutants NPHP-2::GFP was targeted to the cilium and restricted to the post-TZ proximal cilium. Several NPHP-2::GFP puncta were visible in the periciliary compartment. (B) In doublet region and InvC mutants, NPHP-2::GFP was targeted to the cilium and restricted to the post-TZ proximal cilium in *klp-11*, *arl-13*, and *unc-119* mutants. *arl-13* and *klp-11* mutants exhibited periciliary NPHP-2::GFP puncta, and *unc-119* mutants exhibited distal dendritic accumulation of NPHP-2::GFP. (C) In WT, ARL-13::GFP localizes to the proximal cilium. In both *nphp-4* and *mks-3* mutants, ARL-13::GFP was targeted to the cilium and restricted to the post-TZ proximal cilium. ARL-13::GFP also mislocalized to the periciliary membrane compartment in TZ mutants. (D) In *nphp-2* and *klp-11* mutants, ARL-13::GFP was targeted to the cilium and restricted to the post-TZ proximal cilium. In these mutants, ARL-13::GFP also mislocalized to the periciliary membrane compartment, and in *unc-119* mutants, ARL-13::GFP mislocalized to the distal dendrite.

Periciliary puncta – arrowheads, periciliary membrane – white arc, distal dendrite/periciliary accumulation – white bar. Periciliary membrane localization was judged by a visible enrichment of ARL-13::GFP on the edges of the periciliary compartment without a concomitant enrichment in the interior lumen of the periciliary region.

A Full Length NPHP-2, NPHP-2-EFΔ, NPHP-2-NLS1Δ, NPHP-2-NLS2Δ domain diagrams showing Ankyrin repeats, coil, D-box, NLS1, EF-hand, NLS2, and GFP.

B Head and Tail fluorescence images of Full Length, EFΔ, NLS1Δ, and NLS2Δ. Head images label IL2, CEP, AWC, OLQ, and Amphid Bundle. Tail images label Phasmid Bundle. Scale bar 5 μm.

C Fraction Dye Filling Amphids (left) and Phasmids (right) bar graphs for WT, *nphp-2 nphp-4*, Full Length, EFΔ, NLS1Δ, NLS2Δ with significance letters.

Figure 22. The EF hand is necessary for proper NPHP-2 localization and function

(A) Diagram of the domains present in Inversin, NPHP-2, and each of the NPHP-2 domain deletion constructs. (B) Localization of GFP-tagged NPHP-2 domain deletion constructs. In the head, full length NPHP-2::GFP localizes to the InvC of amphid channel cilia, to the base of IL2 cilia, and to the base of either OLQ or CEP cilia. In the tail (outlined by dashes), NPHP-2::GFP localizes to the InvC of phasmid cilia. Localization of both NPHP-2-NLS1Δ::GFP and NPHP-2-NLS2Δ::GFP appeared roughly wild-type in all cell types, though both constructs appeared enriched in AWC wing cilia. NPHP-2-EFΔ::GFP is present in IL2 and CEP cilia but fails to localize to amphid channel and phasmid cilia. (C) NPHP-2-NLS1Δ::GFP, NPHP-2-NLS2Δ::GFP, and NPHP-2-EFΔ::GFP can rescue *nphp-2 nphp-4* amphid and phasmid dye-filling defects, but NPHP-2-EFΔ::GFP rescue is significantly worse than full length NPHP-2::GFP in both amphid and phasmid neurons. Yellow arrowheads – IL2 cilia, red arrowheads – OLQ, blue arrowheads – CEP cilia, white bar – amphid/phasmid bundle. Letters indicate statistically distinct groups. Data was analyzed with pairwise Mann-Whitney U-test against both positive and negative controls, followed by the Holm-Bonferroni multiple comparison adjustment with a total alpha of 0.01. Non-transgene expressing siblings were used as negative controls in rescue experiments.
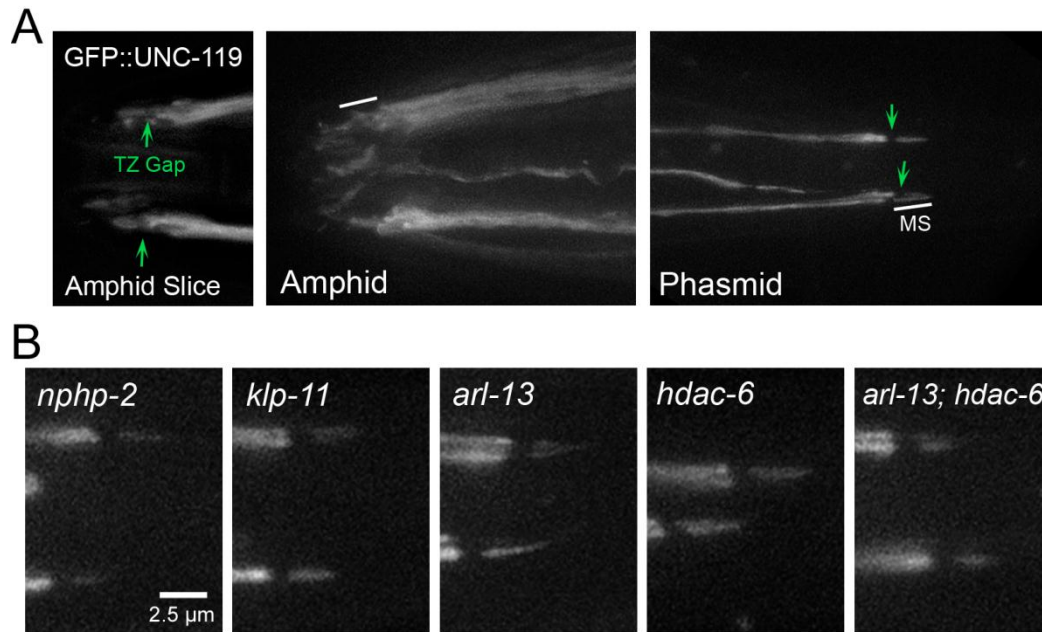
Figure 23. UNC-119 localizes to the proximal cilium in phasmids and does not require DR and InvC genes to target the cilium

(A) N-terminal GFP tagged UNC-119 localizes to dendrites and cilia of amphid channel and phasmid neurons. The TZ gap (arrow) can be discerned in the cilia of amphid channel neurons. In cilia of the CEP and OLQ neurons, GFP::UNC-119 fluorescence was faint and infrequently visible. In phasmid cilia, GFP::UNC-119 localizes to the doublet region, and is excluded from the TZ (arrow) and singlet region. (B) GFP::UNC-119 localization in doublet region- and InvC-associated mutants. GFP::UNC-119 localizes to the proximal cilium in all mutant backgrounds examined.
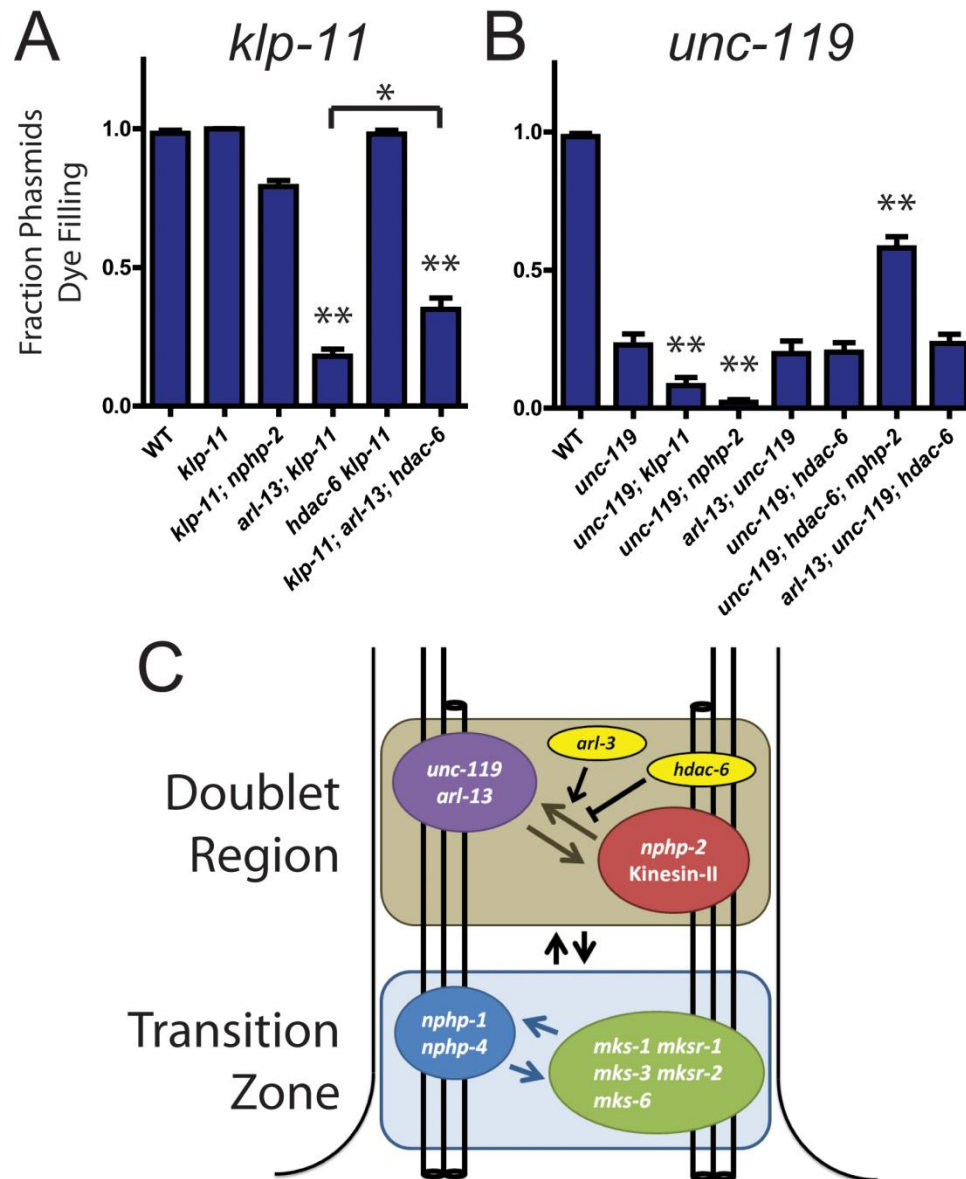
Figure 24. *klp-11* and *unc-119* genetically interact with *arl-13* and *nphp-2* in an *hdac-6* dependent manner

(A) *klp-11* single mutants are not Dyf. *klp-11* is SynDyf with *arl-13*, which is partially suppressed by deletion of *hdac-6*. (B) *unc-119* single mutants are moderately Dyf. *unc-119* is SynDyf with both *klp-11* and *nphp-2*. *unc-119; hdac-6; nphp-2* triple mutants exhibit suppression of the *unc-119* Dyf phenotype. (C) Diagram of interactions between *klp-11*, *arl-13*, *nphp-2*, *unc-119*, and *hdac-6*, and between DR and TZ genes, based on SynDyf phenotypes presented in panels A

and B and in Figures 1 and S5. The T-bar indicates *hdac-6* mediated suppression of SynDyf

phenotypes. Data was analyzed with pairwise Mann-Whitney U-test between wild type, double

mutants, and their respective single mutants, followed by the Holm-Bonferroni multiple

comparison adjustment. *, significant versus single mutants at a total alpha of 0.05. **,

significant versus single mutants at a total alpha of 0.01. *nphp-2*, *arl-13*, *hdac-6*, and *arl-13;*

hdac-6 Dyf data is presented in Figure 1.
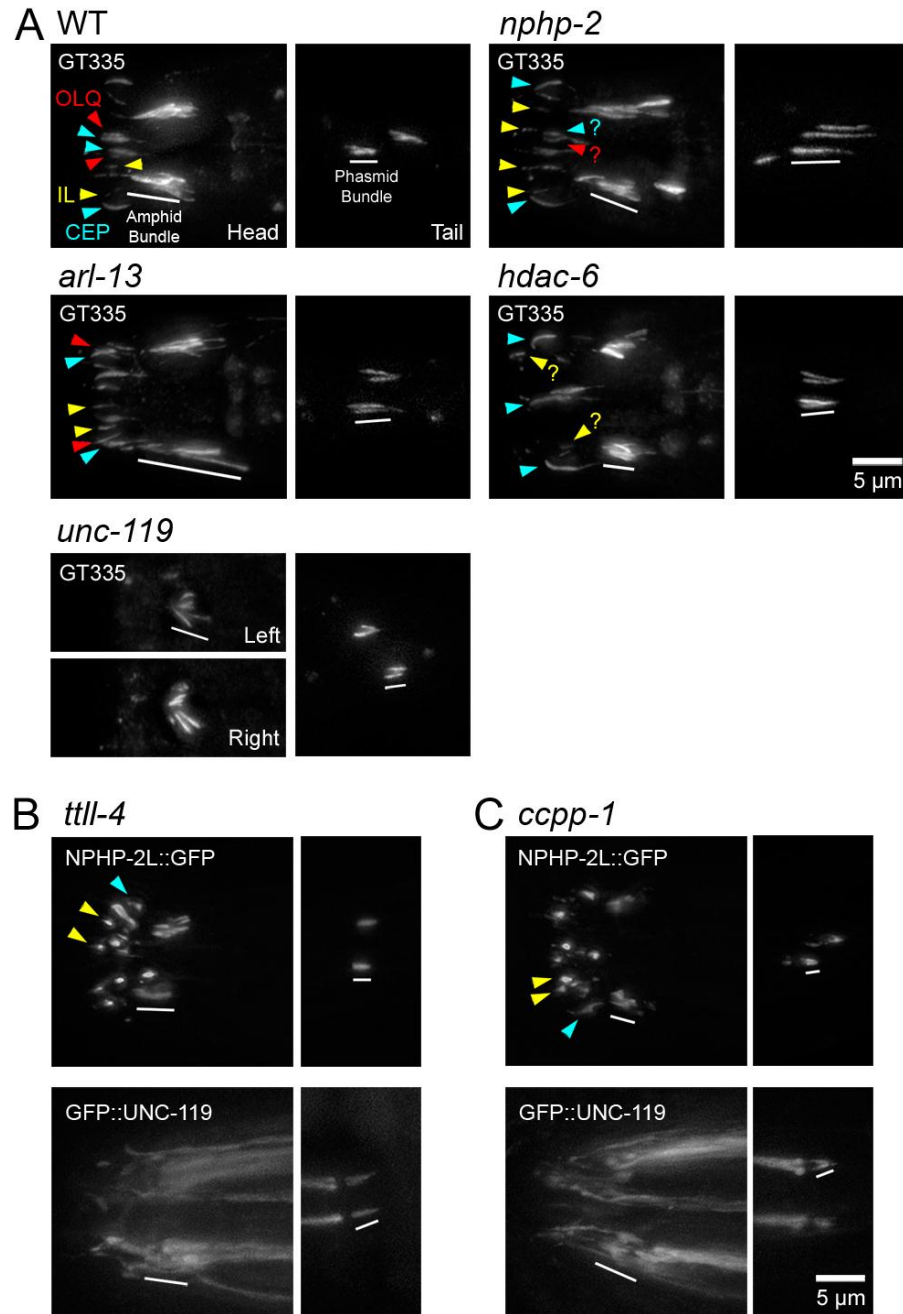
Figure 25. *nphp-2, arl-13*, and *hdac-6* regulate glutamylation in head and tail cilia

(A) Worms stained with GT335 anti-glutamylated tubulin antibody. In WT background, GT335

labels amphid and phasmid doublet region microtubules, and CEP doublet region and singlet

region microtubules consistently, and OLQ cilia inconsistently. CEP distal microtubule singlets

were also labelled by GT335. Inner labial cilia were also glutamylated, but specific IL1 and IL2

identification was not possible. *nphp-2* mutants showed characteristic posterior shifted cilia, and glutamylation in the head looked similar to WT, with infrequent weak inner labial cilia staining. Phasmids exhibited an elongated glutamylation signal. *arl-13* mutants exhibited elongated staining of amphid bundle, CEP, and OLQ cilia. Amphid staining in *unc-119* mutants was extremely shortened and cilia were angled inwards. *unc-119* mutants exhibited almost no staining of CEP, IL, and OLQ cilia. *hdac-6* mutants displayed shorter amphid bundle staining, and reduced IL and OLQ staining. (B) In *ttll-4* mutants, NPHP-2::GFP and GFP::UNC-119 localize similarly to WT. (C) In *ccpp-1* mutants, both NPHP-2::GFP and GFP::UNC-119 localize similarly to in WT, and GFP::UNC-119 is present in the TZ and accumulates at the distal dendrite. Yellow arrowheads – IL2 cilia, red arrowheads – OLQ cilia, blue arrowheads – CEP cilia, white bar – amphid/phasmid bundle.
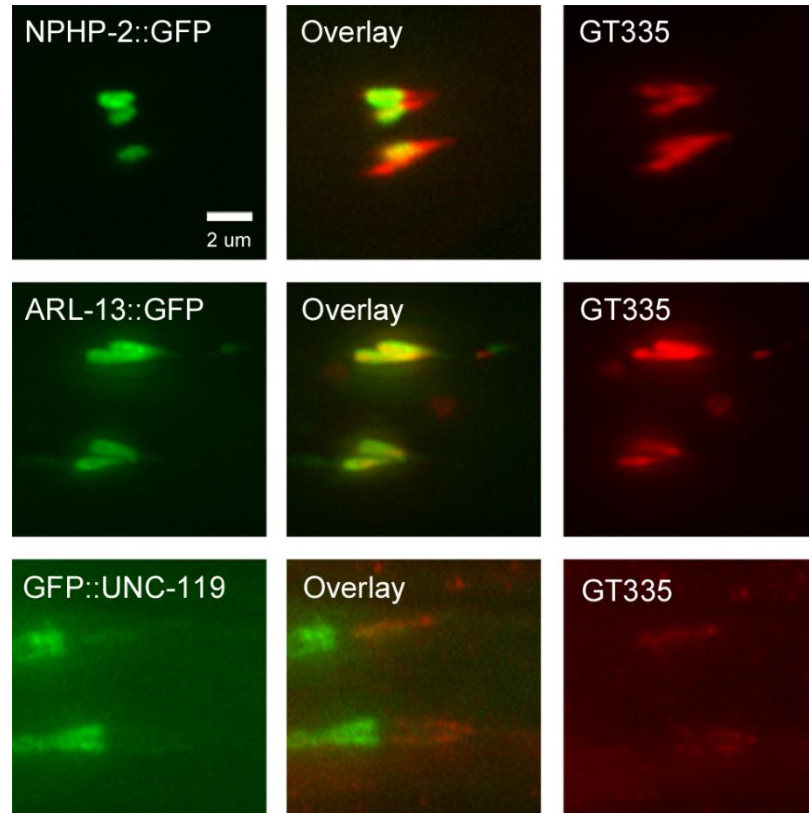
Figure 26. NPHP-2::GFP, ARL-13::GFP, and GFP::UNC-119 colabel with GT335 staining

In amphid channel and phasmid cilia, NPHP-2::GFP, ARL-13::GFP, and GFP::UNC-119 signals

overlap with GT335 staining. ARL-13::GFP and GT335 staining overlap completely. NPHP-2::GFP

does not overlap completely with GT335. TZ staining by GT335 is frequently visible, as in the

NPHP-2::GFP overlay. Though the signal of GFP::UNC-119 is dim due to the staining procedure,

GFP::UNC-119 appears not to overlap completely with GT335. Data is quantified in Figure S6A.
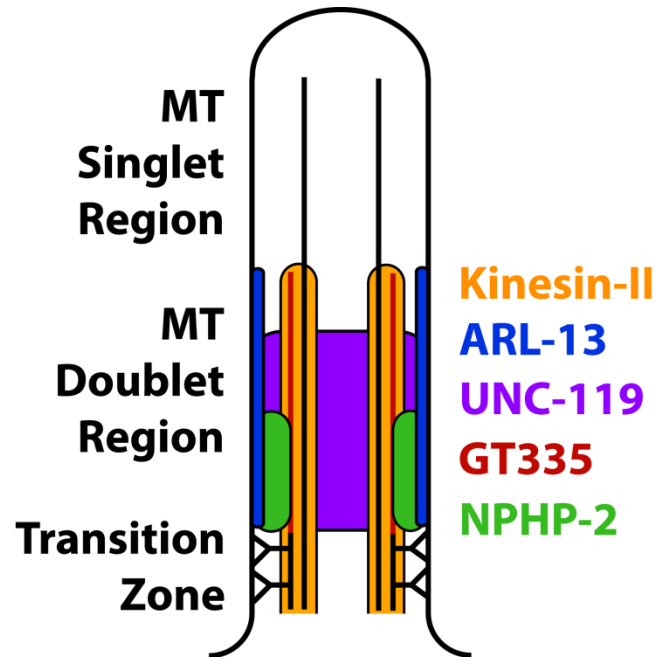
Figure 27. Model of the composition of the proximal cilium

ARL-13 is depicted as membrane associated based on published characterizations [32]. NPHP-2

is depicted as membrane associated based on the membrane association of Inversin in

mammalian primary cilia, and because in *C. elegans* NPHP-2 reporters appear membrane

associated by casual observation [12, 17]. Kinesin-II is microtubule associated, and UNC-119 is

depicted nonspecifically because of the diffuse localization of GFP::UNC-119. Poly-glutamylated

tubulin is depicted as a modification of the B-tubule, as reported [40].
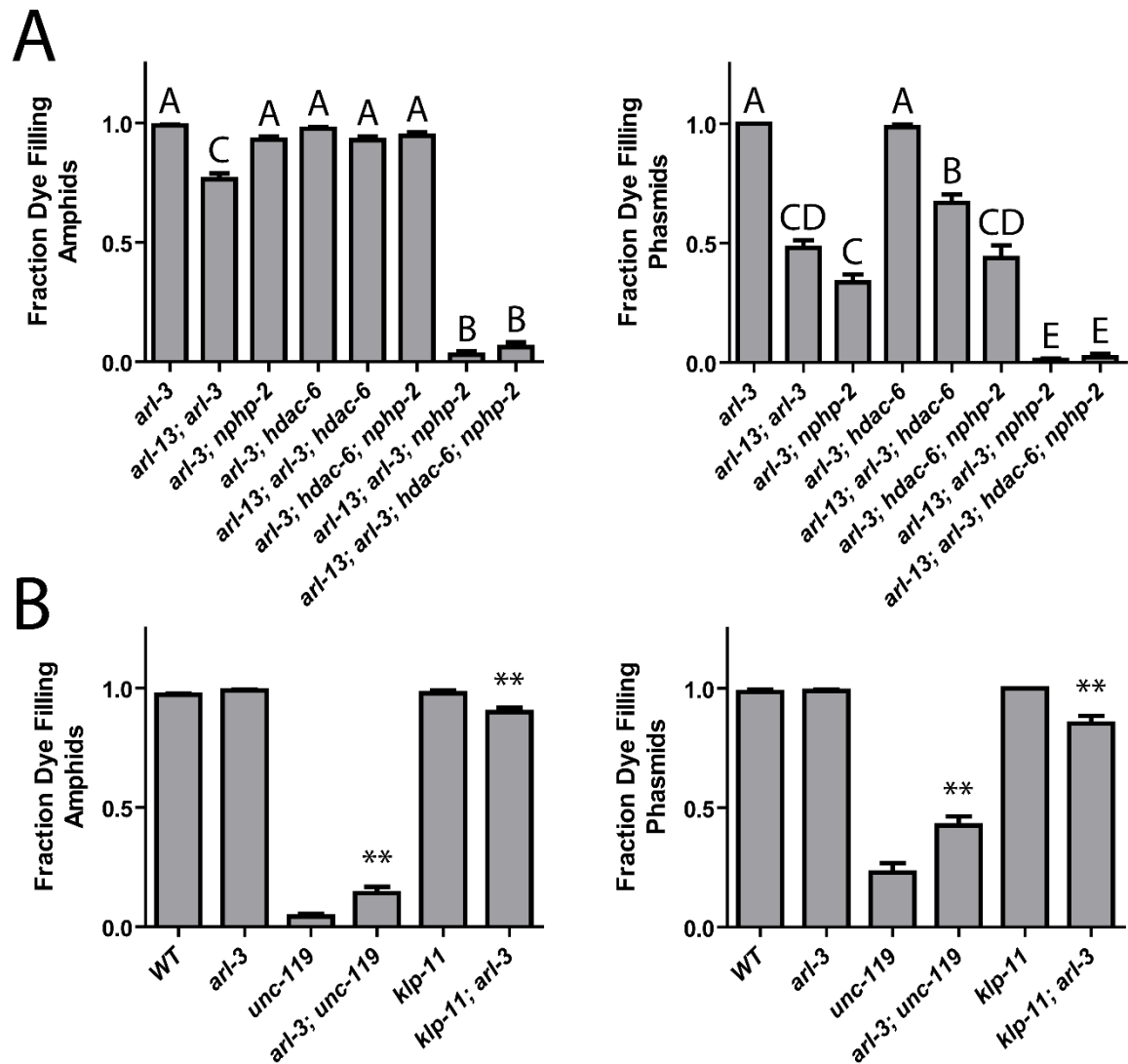
Figure 28. *arl-3* genetically interacts with InvC and doublet region associated genes

Dye filling was used to test for synthetic interactions between InvC and doublet region genes.

(A) *arl-3* interacts with *nphp-2* and *arl-13* in a sensillum-specific manner. *arl-3* single mutants

and *arl-3; hdac-6* double mutants are nonDyf in amphids and phasmids. In both amphids and

phasmids, *arl-13; arl-3* double mutants are mildly SynDyf, which is suppressed by *hdac-6*

deletion. *arl-3* deletion did not suppress *arl-13; nphp-2* defects. *hdac-6* mediated suppression of

arl-13; nphp-2 defects requires *arl-3*. In phasmids, but not amphids, *nphp-2* genetically

interacted with *arl-3*, but this was not suppressed by *hdac-6* deletion. (B) *arl-3* genetically

interacts with *unc-119* and *klp-11* in amphids and phasmids. *arl-3* deletion moderately

suppressed *unc-119* single mutant Dyf. *klp-11; arl-3* was slightly SynDyf. Data in panel A was

statistically analyzed in conjunction with data from Figure 1 because of the overlap in genotypes

examined. Both panel A and Figure 1 were analyzed with pairwise Mann-Whitney U-test

between all groups, followed by the Holm-Bonferroni multiple comparison adjustment with a

total alpha of 0.01. Genotypes from either panel A of this figure or Figure 1 sharing a capital

letter are not significantly different, whereas groups from either panel with different capital

letters do differ significantly. Data panel B was analyzed using pairwise Mann-Whitney U-test

between double mutants, their respective single mutants, and wild type followed by the

Holm-Bonferroni multiple comparison adjustment with a total alpha of 0.01. **, double mutant

phenotype is significantly different from both respective single mutants.
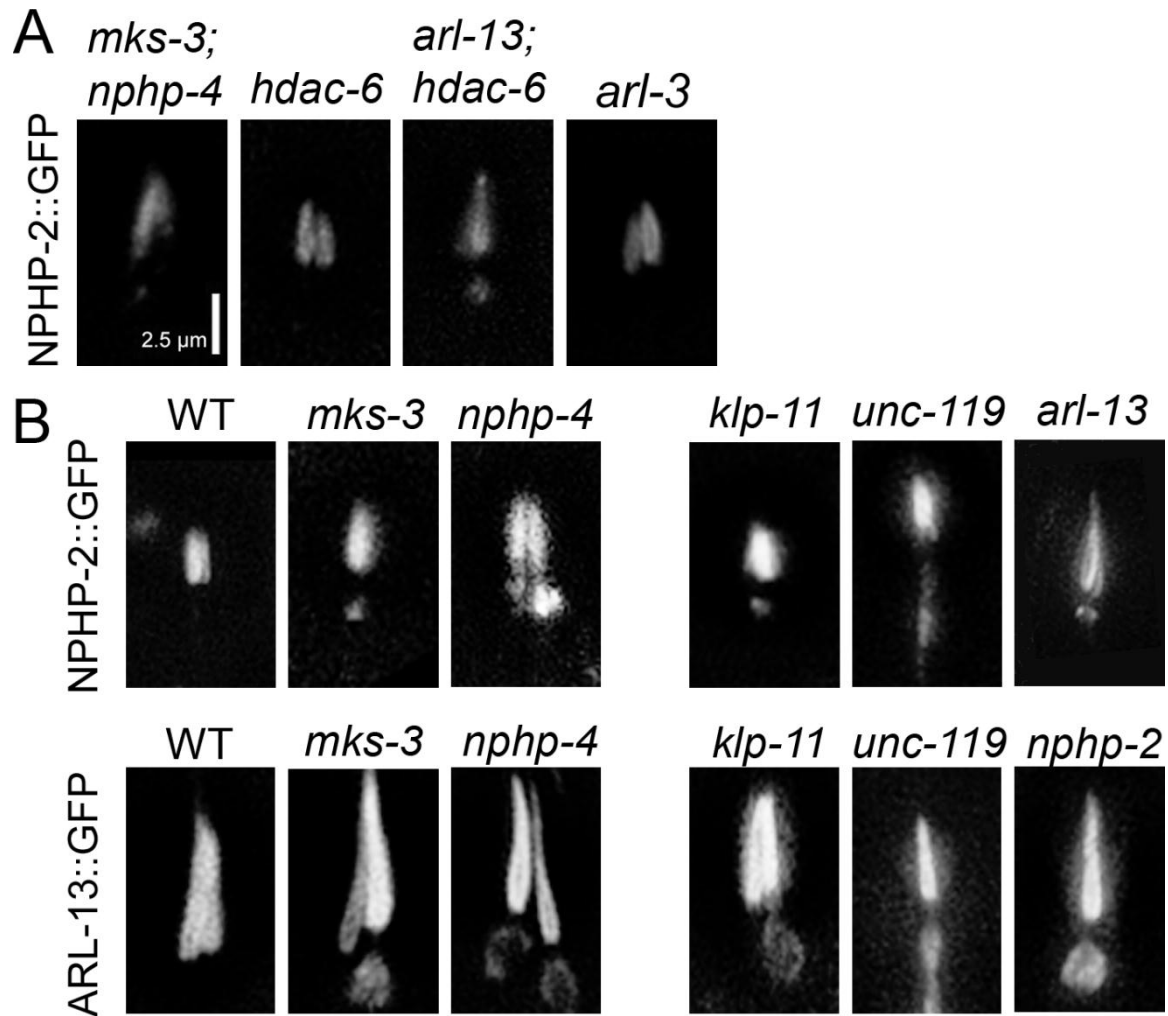
Figure 29. Localization requirements of NPHP-2::GFP and ARL-13::GFP in phasmid cilia

(A) NPHP-2::GFP does not require *mks-3; nphp-4*, *hdac-6*, or *arl-13; hdac-6* for ciliary targeting or restriction to the proximal cilium. (B) Contrast enhanced version of Figure 3C,D. ARL-13::GFP mislocalizes to the periciliary compartment in TZ and doublet region mutants.
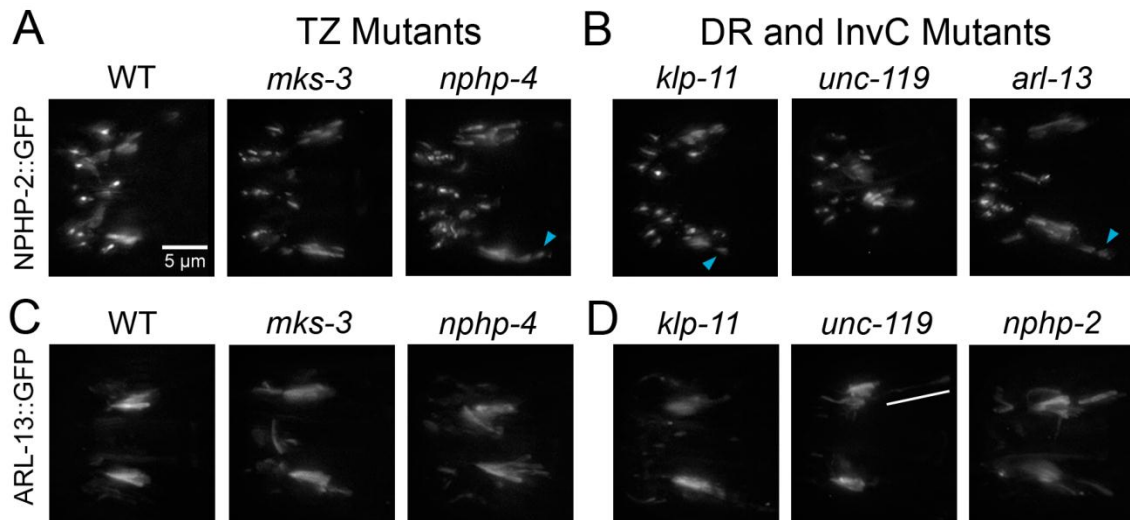
Figure 30. NPHP-2 and ARL-13 do not require TZ-, doublet region-, and InvC-associated genes for ciliary targeting in amphids

(A) Localization of NPHP-2::GFP is subtly disrupted in *mks-3*, *nphp-4* and *mks-3; nphp-4* mutants. Periciliary puncta in amphid channel cilia and altered staining in IL2, CEP, and OLQ cilia are visible. (B) The NPHP-2::GFP amphid bundle is shortened in *klp-11* and *unc-119* mutants, and elongated in *arl-13* mutants. Periciliary puncta are visible in *klp-11* and *arl-13* mutants. *hdac-6* deletion does not suppress the *arl-13* phenotype. (C) ARL-13::GFP localizes primarily to the doublet region of amphid channel cilia, and to a nonspecific proximal region of IL2 cilia. In *mks-3* and *nphp-4* mutants, ARL-13::GFP localization in amphid channel cilia looks grossly wild-type. CEP and OLQ cilia show increased ARL-13::GFP localization. (D) *unc-119* mutants exhibit distal dendritic accumulation of ARL-13::GFP. *klp-11* and *nphp-2* mutants exhibit increased CEP and OLQ ARL-13::GFP localization. Arrowheads indicate periciliary puncta. Bar indicates distal dendritic localization.
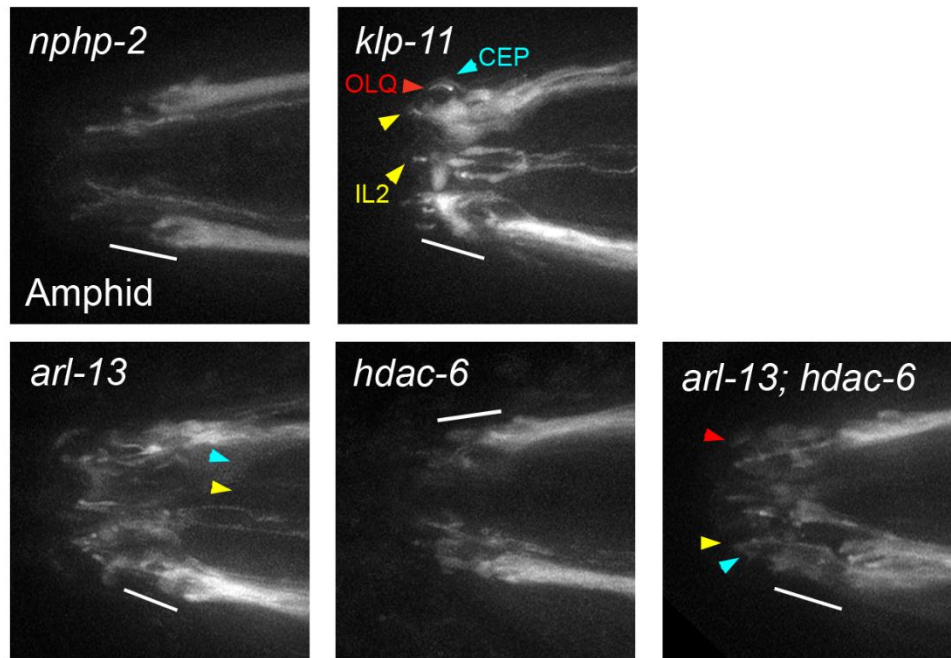
Figure 31. Amphid UNC-119 localization in InvC and doublet region mutants

GFP::UNC-119 appears similar in wild-type (Figure 5A), *nphp-2,* and *hdac-6* amphid channel cilia.

klp-11 and *arl-13* exhibit an accumulation of GFP::UNC-119 in amphid channel, OLQ, CEP, and

inner labial cilia. *hdac-6* deletion does not suppress GFP::UNC-119 mislocalization in *arl-13*

mutants. Green arrow – TZ gap, yellow arrowheads – IL2 cilia, red arrowheads – OLQ cilia, blue

arrowheads – CEP cilia, white bar – amphid bundle.
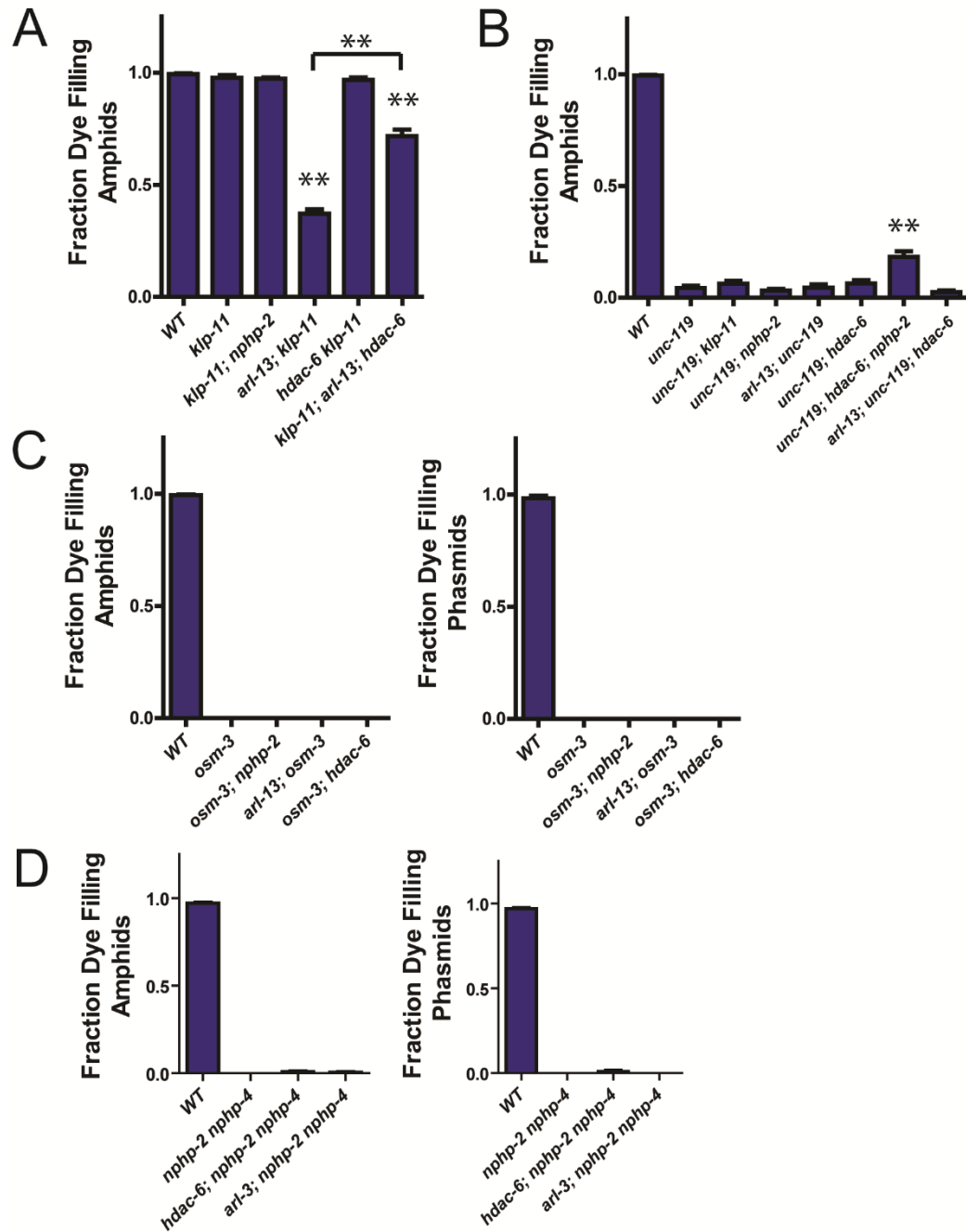
Figure 32. Amphid dye-filling of IFT and *unc-119* mutants

(A) *klp-11* single mutants are not Dyf. *klp-11* is SynDyf with *arl-13*, which is suppressed by

deletion of *hdac-6*. (B) *unc-119* single mutants are severely Dyf. *hdac-6; nphp-2* suppresses the

unc-119 Dyf phenotype to a small degree. (C) *osm-3* single mutants are both severely amphid

and phasmid Dyf. In no double mutant was this suppressed. (D) *hdac-6; nphp-2 nphp-4* and

arl-3; nphp-2 nphp-4 worms were assayed for suppression of SynDyf defects. Neither strain

exhibited significant suppression as compared to the *nphp-2 nphp-4* double mutant. Data was

analyzed with pairwise Mann-Whitney U-test between wild type, double mutants, triple

mutants and their respective single mutants, followed by the Holm-Bonferroni multiple

comparison adjustment. **, significant versus single mutants at a total alpha of 0.01.
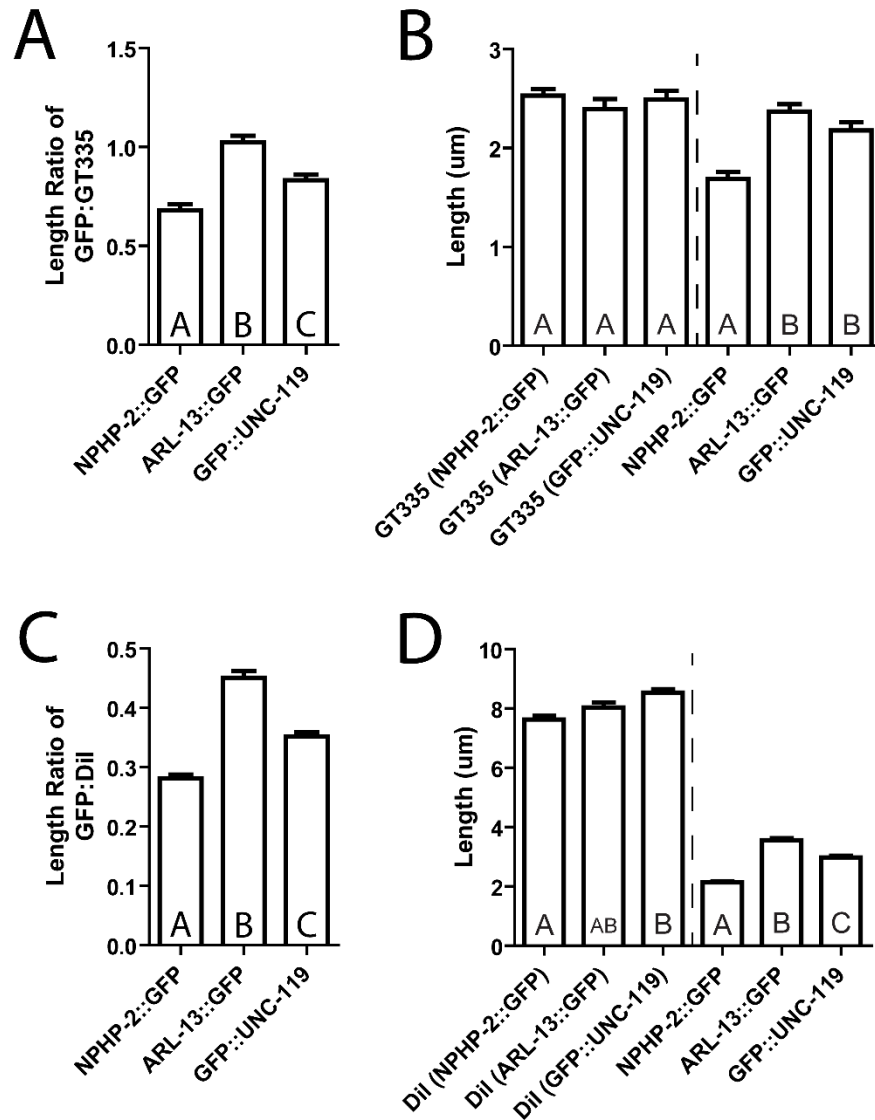
Figure 33. NPHP-2::GFP marks a significantly smaller region of the cilium than ARL-13::GFP and GFP::UNC-119

(A) Worms expressing NPHP-2::GFP, ARL-13::GFP, and GFP::UNC-119 reporters were stained with GT335. The ratio of the length of each reporter localization pattern to the length of the entire cilium, minus the TZ was computed per-cilium. NPHP-2::GFP marks a significantly shorter proportion of the cilium than either ARL-13::GFP or GFP::UNC-119. (B) Absolute lengths of data presented in panel A. (C) Worms expressing NPHP-2::GFP, ARL-13::GFP, and GFP::UNC-119

reporters were incubated with DiI to label cilia. The ratio of the length of each reporter

localization pattern to the length of the entire cilium, minus the TZ was computed per-cilium.

NPHP-2::GFP marks a significantly shorter proportion of the cilium than either ARL-13::GFP or

GFP::UNC-119. (D) Absolute lengths of data presented in panel C. Phasmid cilia lengths in

transgenic strains as measured using DiI staining, and reporter localization size. Data in each

panel was analyzed with pairwise t-tests with Welch's Correction, followed by the

Holm-Bonferroni multiple comparison adjustment for a total alpha of 0.01.

A
NPHP-2 Localization Length (μm)

B
ARL-13 Localization Length (μm)

C
UNC-119 Localization Length (μm)

D
KAP-1 Localization Length (μm)

E
GT335 Signal Length (μm)

F
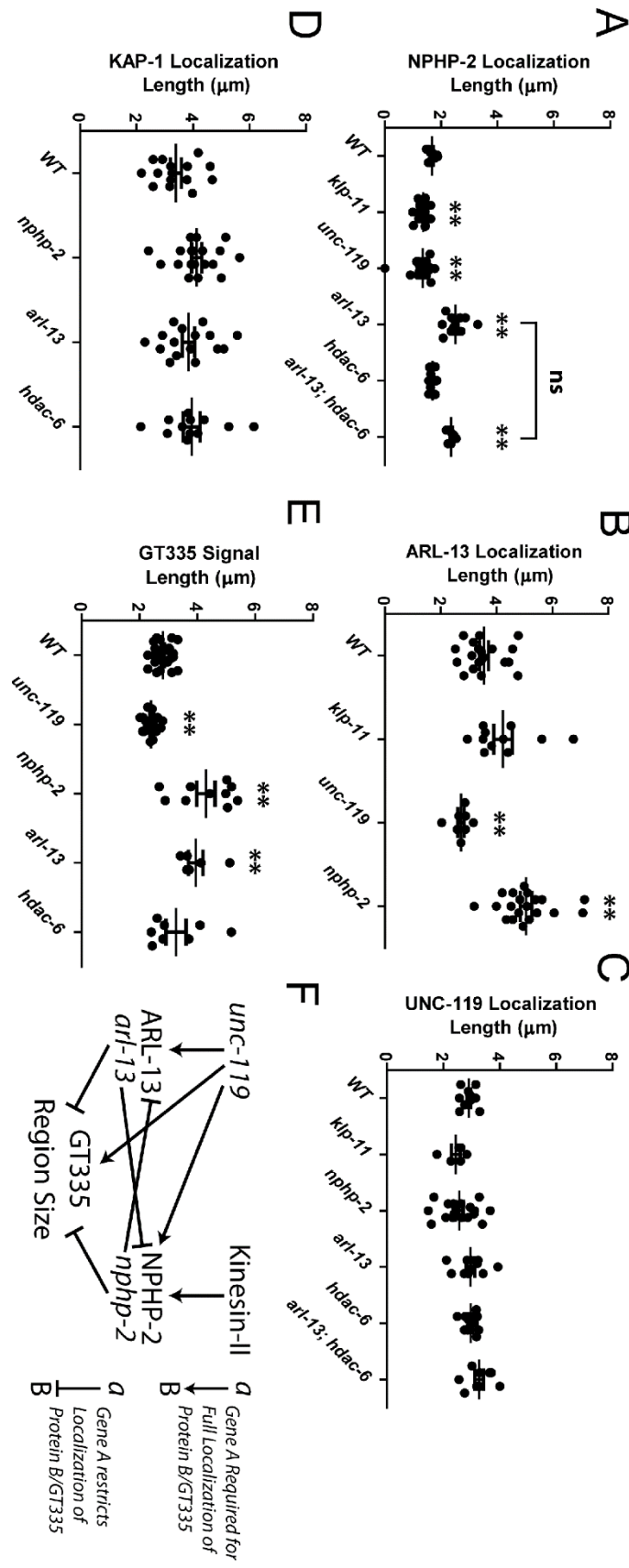
Figure 34. Doublet region- and InvC-associated genes regulate the localization patterns of doublet region and InvC components

Each data point represents the averaged lengths of the GFP signal or immunofluorescence in all visible and distinct phasmid cilia within a single animal. (A) NPHP-2::GFP localization length is significantly decreased in *klp-11* and *unc-119* mutants, and significantly increased in *arl-13* mutants. *hdac-6* deletion partially suppresses the *arl-13* phenotype. (B) ARL-13::GFP localization length is increased in *nphp-2* and decreased in *unc-119* mutants. (C) GFP::UNC-119 localization length does not change significantly in any strain. (D) KAP-1 localization length measurements were more variable that the other reporters due to a faint KAP-1::GFP signal, but were not significantly different from wild type in any strain. Localization length was significantly altered in *nphp-2* mutants. (E) *nphp-2* and *arl-13* had significantly longer GT335 signals than in wild type. *nphp-2* mutants have increased variability in GT335 signal lengths compared to WT. (F) Diagram representing genetic control of doublet region protein localization in phasmid cilia. An arrow between a gene and a protein/GT335 indicates that the gene is required for the protein/GT335 to label its entire territory. A T-bar between a gene and a protein/GT335 indicates that the gene restricts the size of the protein territory/GT335 signal length. Data was analyzed with an unpaired t-test with Welch's Correction against wild type, followed by the Holm-Bonferroni multiple comparison adjustment for all comparisons in a given panel. **$p < 0.01$.

A Hydroxylation Motif

```
ILITLLKHGADPNAIDADDR    177    C. elegans NPHP-2
CADALLKAGADVNKTDHSQR     82    Human INVS
CADALLKAGADVNKTDHSRR     82    Mouse Invs
CAEALLKHGAQVNRSDRSGR     59    X.trop Invs

VAHLLLDHGADVNAQNRLGA    136    Mouse Anks6
VAHLLLDHGADVNAQNRLGA    136    Rat Anks6
VAHLLLDHGADVNAQNRLGA    145    Human ANKS6
VAMILLENGADVNAQNRLGA    147    X.trop Anks6

VVRLLMEWGADPNHTARTVG    216    Rat Anks6
VVRLLMEWGADPNHAARTVG    225    Human ANKS6
VVRLLMEWGADPNHTARTVG    216    Mouse Anks6
VVRLLLDWGADVNYRVKTTG    246    X.trop Anks6
```

B Acetylation Motif   SUMOylation Motif

MSHTL...   ...NELKAEQ...   ...SIPKKEL...

NH2 — Ankyrin repeats — coil — D-box — EF-hand — NLS — COOH

Hydroxylation Motif

Figure 35. NPHP-2 contains a strongly conserved hydroxylation motif and a predicted acetylation site

(A) Hydroxylation motif is highlighted in green. Hydroxylated asparagine is highlighted in blue. ANKS6 and INVS alignment are from [19]. (B) NPHP-2 domain model. NPHP-2 contains a predicted acetylation site at 2S, and two predicted SUMOylation sites. Green letters indicate modified residues. Acetylation and SUMOylation motifs do not appear to be conserved.
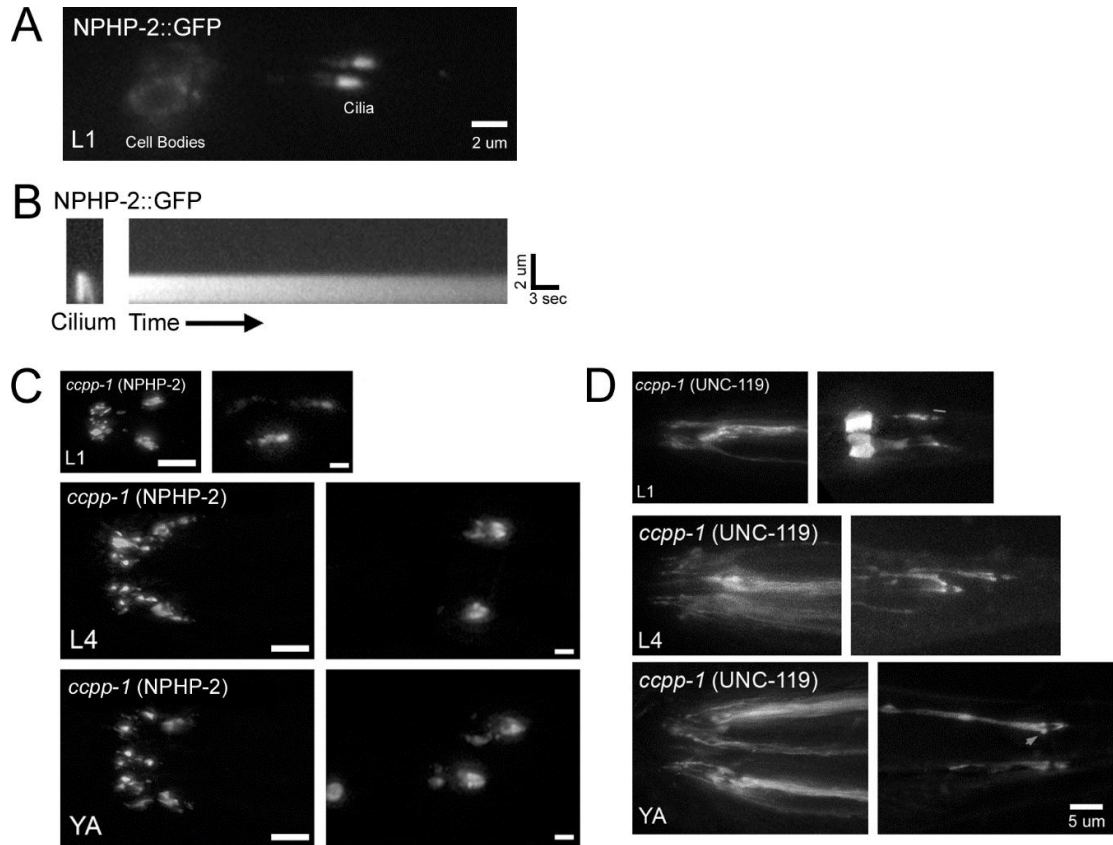
Figure 36. Localization of NPHP-2 and UNC-119 in L1 stage worms

(A) NPHP-2::GFP localizes to the proximal portion of the cilium in L1 animals. (B) Kymograph of NPHP-2::GFP in L1 phasmid cilia. No movement of NPHP-2::GFP was detectable. Total duration of recording was 40 seconds. (C) NPHP-2::GFP localizes to amphid and phasmid cilia in L1 and L4 stage *ccpp-1* mutants. (D) GFP::UNC-119 localizes to amphid and phasmid cilia in L1 and L4 stage *ccpp-1* mutants. White bars indicate ciliary GFP::UNC-119 localization. White arrow indicates abnormal cilia base accumulation of GFP::UNC-119.
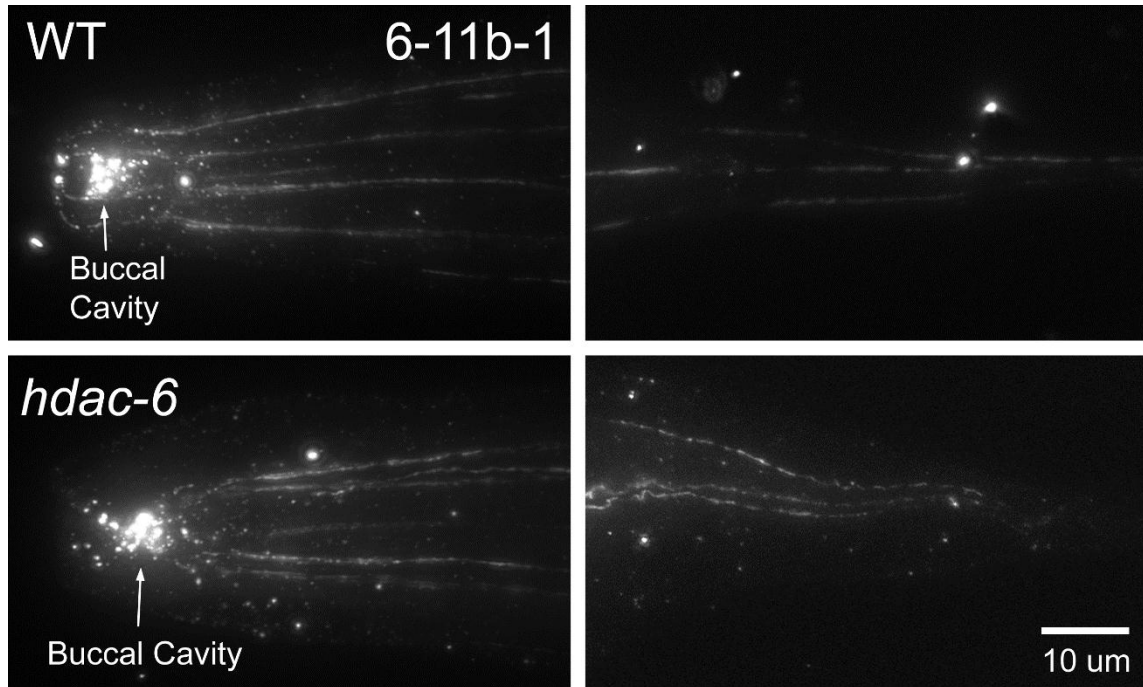
Figure 37. The anti-acetylated tubulin antibody 6-11b-1 does not label amphid channel and phasmid cilia in either WT animals or *hdac-6* mutants

6-11b-1 antibody labels only dendrites of the touch neurons. *hdac-6* deletion does not increase the amount of acetylation detected in touch neurons. Non-specific labelling is seen in the buccal cavity, and not in amphid cilia, as determined by analysis of 3D image stacks.

Strain	Amphid Dye Filling	Phasmid Dye Filling
PT2789: *him-5(e1490)* V; *myEx743*(p*nphp-2*::NPHP-2L::GFP + ccRFP)	1.00 ± 0.00	1.00 ± 0.00
PT2791: *him-5(e1490)* V; *myEx849*(p*nphp-2*::NPHP-2L-EFdel::GFP + ccRFP)	1.00 ± 0.00	1.00 ± 0.00
PT2793: *him-5(e1490)* V; *myEx850*(p*nphp-2*::NPHP-2L-NLS1del::GFP + ccRFP)	0.99 ± 0.00	0.98 ± 0.02
PT2795: *him-5(e1490)* V; *myEx851*(p*nphp-2*::NPHP-2L-NLS2del::GFP + ccRFP)	0.98 ± 0.01	1.00 ± 0.00
PT2797: *mks-3(tm2547)* II; *myEx743*(p*nphp-2*::NPHP-2L::GFP + ccRFP::GFP)	1.00 ± 0.00	1.00 ± 0.00
PT2798: *nphp-4(tm925) him-5(e1490)* V; *myEx743*(p*nphp-2*::NPHP-2L::GFP + ccRFP::GFP)	0.88 ± 0.07	1.00 ± 0.00
PT2800: *klp-11(tm324)* IV; *him-5(e1490)* V; *myEx743*(p*nphp-2*::NPHP-2L::GFP + ccRFP::GFP)	0.99 ± 0.01	1.00 ± 0.00
PT2802: *arl-13(gk513)* I; *him-5(e1490)* V; *myEx743*(p*nphp-2*::NPHP-2L::GFP + ccRFP::GFP)	0.73 ± 0.06	0.61 ± 0.07
PT2556: *hdac-6(ok3203)* IV; *him-5(e1490)* V; *myEx743*(p*nphp-2*::NPHP-2L::GFP + ccRFP::GFP)	0.97 ± 0.01	1.00 ± 0.00
PT2803: *arl-13(gk513)* I; *hdac-6(ok3203)* IV; *him-5(e1490)* V; *myEx743*(p*nphp-2*::NPHP-2L::GFP + ccRFP::GFP)	0.96 ± 0.03	0.77 ± 0.10
PT2847: *ttll-4(tm3310)* III; *him-5(e1490)* V; *myEx743*(p*nphp-2*::NPHP-2L::GFP + ccRFP::GFP)	0.97 ± 0.01	0.94 ± 0.06
ZP354: *him-5(e1490)* V; *jhuEx352*(p*arl-13*::ARL-13::GFP + pBx)	0.95 ± 0.01	0.88 ± 0.04
PT2804: *nphp-4(tm925) him-5(e1490)* V; *jhuEx352*(p*arl-13*::ARL-13::GFP + pBx)	0.63 ± 0.05	0.77 ± 0.03
PT2805: *mks-3(tm2547)* II; *him-5(e1490)* V; *jhuEx352*(p*arl-13*::ARL-13::GFP + pBx)	0.92 ± 0.05	0.88 ± 0.07
PT2806: *nphp-2(gk653) him-5(e1490)* V; *jhuEx352*(p*arl-13*::ARL-13::GFP + pBx)	0.92 ± 0.02	0.25 ± 0.03
PT2807: *klp-11(tm324)* IV; *him-5(e1490)* V; *jhuEx352*(p*arl-13*::ARL-13::GFP + pBx)	0.87 ± 0.02	0.57 ± 0.06
PT2809: *him-5(e1490)* V; *myEx848*(p*osm-6*::GFP::UNC-119 + ccRFP)	0.98 ± 0.01	0.99 ± 0.01
PT2641: *nphp-2(gk653) him-5(e1490)* V; *myEx848*(p*osm-6*::GFP::UNC-119 + ccRFP)	0.98 ± 0.01	0.70 ± 0.07
PT2640: *arl-13(gk513)* I; *him-5(e1490)* V; *myEx848*(p*osm-6*::GFP::UNC-119 + ccRFP)	0.93 ± 0.02	0.75 ± 0.05
PT2642: *klp-11(tm324)* IV; *him-5(e1490)* V; *myEx848*(p*osm-6*::GFP::UNC-119 + ccRFP)	0.98 ± 0.01	0.98 ± 0.03

PT2638: *hdac-6(ok3203)* IV; *him-5(e1490)* V; *myEx848*(p*osm-6*::GFP::UNC-119 + ccRFP)	1.00 ± 0.00	1.00 ± 0.00
PT2639: *arl-13(gk513)* I; *hdac-6(ok3203)* IV; *him-5(e1490)* V; *myEx848*(p*osm-6*::GFP::UNC-119 + ccRFP)	0.96 ± 0.01	0.75 ± 0.05
PT2852: *ttll-4(tm3310)* III; *him-5(e1490)* V; *myEx848*(p*osm-6*::GFP::UNC-119 + ccRFP)	1.00 ± 0.00	1.00 ± 0.00

Table 7. Transgenic strains used in this study have mild to no ciliogenic defects

Worms from each transgenic strain imaged or otherwise quantified in Figures 1-9—other than strains with a Dyf or SynDyf background—were assayed for dye-filling defects to determine if there were any gross defects in ciliogenesis or cilia placement. Scores reported are average fraction of cell bodies taking up dye, plus/minus std. err. Yellow cells mark possible dominant negative defects. Transgenic strains expressing NPHP-2::GFP and GFP::UNC-119 did not exhibit defects, but strains expressing ARL-13::GFP all exhibited mild defects .

Strain List   **Figures strain used in**

Non-transgenic Strains	1	2	3	4	5	6	7	8	9	S1	S2	S3	S4	S5	S6	S7	S8	S9	S10
CB1490: *him-5(e1490)* V	X	X		X		X	X	X		X				X		X			X
PT2145: *nphp-2(gk653) him-5(e1490)* V	X	X				X										X			
PT2815: *arl-13(gk513)* I; *him-5(e1490)* V	X					X										X			
PT2816: *hdac-6(ok3203)* IV; *him-5(e1490)* V	X					X										X			X
PT2758: *arl-13(gk513)* I; *nphp-2(gk653) him-5(e1490)* V	X	X																	
PT2817: *hdac-6(ok3203)* IV; *nphp-2(gk653) him-5(e1490)* V	X	X																	
ZP391: *arl-13(gk513)* I; *hdac-6(ok3203)* IV; *him-5(e1490)* V	X																		
PT2759: *arl-13(gk513)* I; *hdac-6(ok3203)* IV; *nphp-2(gk653) him-5(e1490)* V	X																		
PT871: *klp-11(tm324)* IV; *him-5(e1490)* V						X				X				X					
PT2818: *klp-11(tm324)* IV; *nphp-2(gk653) him-5(e1490)* V						X								X					
PT2819: *arl-13(gk513)* I; *klp-11(tm324)* IV; *him-5(e1490)* V						X								X					
PT2820: *klp-11(tm324) hdac-6(ok3203)* IV; *him-5(e1490)* V						X								X					
PT2821: *arl-13(gk513)* I; *klp-11(tm324) hdac-6(ok3203)* IV; *him-5(e1490)* V						X								X					
PT1974: *osm-3(p802)* IV; *him-5(e1490)* V														X					
PT2823: *osm-3(p802)* IV; *nphp-2(gk653) him-5(e1490)* V														X					
PT2824: *arl-13(gk513)* I; *osm-3(p802)* IV; *him-5(e1490)* V														X					
PT2825: *osm-3(p802) hdac-6(ok3203)* IV; *him-5(e1490)* V														X					
PT277: *unc-119(ed3)* III; *him-5(e1490)* V						X	X			X				X		X			
PT2827: *unc-119(ed3)* III; *klp-11(tm324)* IV; *him-5(e1490)* V						X								X					
PT2829: *unc-119(ed3)* III; *nphp-2(gk653) him-5(e1490)* V						X								X					
PT2830: *arl-13(gk513)* I; *unc-119(ed3)* III; *him-5(e1490)* V						X								X					
PT2831: *unc-119(ed3)* III; *hdac-6(ok3203)* IV; *him-5(e1490)* V						X								X					
PT2832: *unc-119(ed3)* III; *hdac-6(ok3203)* IV; *nphp-2(gk653) him-5(e1490)* V						X								X					

Strains	1	2	3	4	5	6	7	8	9	S1	S2	S3	S4	S5	S6	S7	S8	S9	S10
PT2833: *arl-13(gk513)* I; *unc-119(ed3)* III; *hdac-6(ok3203)* IV; *him-5(e1490)* V						X							X						
PT2842: *arl-13(gk513)* I; *hdac-6(ok3203)* IV; *nphp-2(gk653) him-5(e1490)* V	X																		
PT2835: *arl-3(tm1703); him-5(e1490)* V									X										
PT2837: *arl-13(gk513)* I; *arl-3(tm1703)* II; *him-5(e1490)* V									X										
PT2836: *arl-3(tm1703)* II; *nphp-2(gk653) him-5(e1490)* V									X										
PT2838: *arl-3(tm1703)* II; *hdac-6(ok3203)* IV; *him-5(e1490)* V									X										
PT2840: *arl-13(gk513)* I; *arl-3(tm1703)* II; *hdac-6(ok3203)* IV; *him-5(e1490)* V									X										
PT2841: *arl-3(tm1703)* II; *hdac-6(ok3203)* IV; *nphp-2(gk653) him-5(e1490)* V									X										
PT2839: *arl-13(gk513)* I; *arl-3(tm1703)* II; *nphp-2(gk653) him-5(e1490)* V									X										
PT2842: *arl-13(gk513)* I; *arl-3(tm1703)* II; *hdac-6(ok3203)* IV; *nphp-2(gk653) him-5* V									X										
PT2834: *arl-3(tm1703)* II; *unc-119(ed3)* III; *him-5(e1490)* V									X										
PT2822: *arl-3(tm1703)* II; *klp-11(tm324)* IV; *him-5(e1490)* V									X										
hdac-6(ok3203) IV; *nphp-2(gk653) nphp-4(tm925) him-5(e1490)* V									X				X						
arl-3(tm1703) II; *nphp-2(gk653) nphp-4(tm925) him-5(e1490)* V									X				X						
PT1983: *nphp-2(gk653) nphp-4(tm925) him-5(e1490)* V				X					X				X						

Transgenic Strains	1	2	3	4	5	6	7	8	9	S1	S2	S3	S4	S5	S6	S7	S8	S9	S10
PT2789: *him-5(e1490)* V; *myEx743*(p*nphp-2*::NPHP-2L::GFP + ccRFP)			X	X			X			X	X				X	X		X	
PT2790: *nphp-2(gk653) nphp-4(tm925) him-5(e1490)* V; *myEx743*(p*nphp-2*::NPHP-2L::GFP + ccRFP)			X																
PT2791: *him-5(e1490)* V; *myEx849*(p*nphp-2*::NPHP-2L-EFdel::GFP + ccRFP)			X																

Strain							
PT2792: *nphp-2(gk653) nphp-4(tm925) him-5(e1490)* V; *myEx849*(p*nphp-2*::NPHP-2L-EFdel::GFP + ccRFP)		X					
PT2793: *him-5(e1490)* V; *myEx850*(p*nphp-2*::NPHP-2L-NLS1del::GFP + ccRFP)		X					
PT2794: *nphp-2(gk653) nphp-4(tm925) him-5(e1490)* V; *myEx850*(p*nphp-2*::NPHP-2L-NLS1del::GFP + ccRFP)		X					
PT2795: *him-5(e1490)* V; *myEx851*(p*nphp-2*::NPHP-2L-NLS2del::GFP + ccRFP)		X					
PT2796: *nphp-2(gk653) nphp-4(tm925) him-5(e1490)* V; *myEx851*(p*nphp-2*::NPHP-2L-NLS2del::GFP + ccRFP)		X					
PT2797: *mks-3(tm2547)* II; *myEx743*(p*nphp-2*::NPHP-2L::GFP + ccRFP::GFP)	X			X	X		
PT2798: *nphp-4(tm925) him-5(e1490)* V; *myEx743*(p*nphp-2*::NPHP-2L::GFP + ccRFP::GFP)	X			X	X		
PT2799: *mks-3(tm2547)* II; *nphp-4(tm925) him-5(e1490)* V; *myEx743*(p*nphp-2*::NPHP-2L::GFP + ccRFP::GFP)				X			
PT2800: *klp-11(tm324)* IV; *him-5(e1490)* V; *myEx743*(p*nphp-2*::NPHP-2L::GFP + ccRFP::GFP)	X			X	X		X
PT2560: *unc-119(ed3)* III; *him-5(e1490)* V; *myEx743*(p*nphp-2*::NPHP-2L::GFP + ccRFP::GFP)	X			X	X		X
PT2802: *arl-13(gk513)* I; *him-5(e1490)* V; *myEx743*(p*nphp-2*::NPHP-2L::GFP + ccRFP::GFP)	X			X	X		X
PT2556: *hdac-6(ok3203)* IV; *him-5(e1490)* V; *myEx743*(p*nphp-2*::NPHP-2L::GFP + ccRFP::GFP)				X			X
PT2803: *arl-13(gk513)* I; *hdac-6(ok3203)* IV; *him-5(e1490)* V; *myEx743*(p*nphp-2*::NPHP-2L::GFP + ccRFP::GFP)				X			X
ZP354: *him-5(e1490)* V; *jhuEx352*(p*arl-13*::ARL-13::GFP + pBx)	X		X	X	X	X	X

Strain	1	2	3	4	5	6	7	8	9
PT2804: *nphp-4(tm925) him-5(e1490)* V; *jhuEx352*(p*arl-13*::ARL-13::GFP + pBx)	X			X	X				
PT2805: *mks-3(tm2547)* II; *him-5(e1490)* V; *jhuEx352*(p*arl-13*::ARL-13::GFP + pBx)	X			X	X				
PT2806: *nphp-2(gk653) him-5(e1490)* V; *jhuEx352*(p*arl-13*::ARL-13::GFP + pBx)	X			X	X			X	
PT2807: *klp-11(tm324)* IV; *him-5(e1490)* V; *jhuEx352(*p*arl-13*::ARL-13::GFP + pBx)	X			X	X			X	
PT2808: *unc-119(ed3)* III; *him-5(e1490)* V; *jhuEx352*(p*arl-13*::ARL-13::GFP + pBx)	X			X	X			X	
PT2809: *him-5(e1490)* V; *myEx848*(p*osm-6*::GFP::UNC-119 + ccRFP)		X	X			X	X	X	
PT2641: *nphp-2(gk653) him-5(e1490)* V; *myEx848*(p*osm-6*::GFP::UNC-119 + ccRFP)		X				X		X	
PT2640: *arl-13(gk513)* I; *him-5(e1490)* V; *myEx848*(p*osm-6*::GFP::UNC-119 + ccRFP)		X				X		X	
PT2642: *klp-11(tm324)* IV; *him-5(e1490)* V; *myEx848*(p*osm-6*::GFP::UNC-119 + ccRFP)		X				X		X	
PT2638: *hdac-6(ok3203)* IV; *him-5(e1490)* V; *myEx848*(p*osm-6*::GFP::UNC-119 + ccRFP)		X				X		X	
PT2639: *arl-13(gk513)* I; *hdac-6(ok3203)* IV; *him-5(e1490)* V; *myEx848*(p*osm-6*::GFP::UNC-119 + ccRFP)		X				X		X	
PT2847: *ttll-4(tm3310)* III; *him-5(e1490)* V; *myEx743*(p*nphp-2*::NPHP-2L::GFP + ccRFP::GFP)			X						
PT2848: *ccpp-1(ok1821)* I; *him-5(e1490)* V; *myEx743*(p*nphp-2*::NPHP-2L::GFP + ccRFP::GFP)			X						X
PT2852: *ttll-4(tm3310)* III; *him-5(e1490)* V; *myEx848*(p*osm-6*::GFP::UNC-119 + ccRFP)			X						

PT2853: *ccpp-1(ok1821)* I; *him-5(e1490)* V; *myEx84*8(p*osm-6*::GFP::UNC-119 + ccRFP)	X	X
KAP-1::GFP: *Ex*(P*panciliary*::KAP-1::GFP + pRF4)	X	
PT2854: *nphp-2(gk653)*; *Ex*(P*panciliary*::KAP-1::GFP + pRF4)	X	
PT2855: *arl-13(gk513)* I; *Ex*(P*panciliary*::KAP-1::GFP + pRF4)	X	
PT2857: *hdac-6(ok3203)* IV; *Ex*(P*panciliary*::KAP-1::GFP + pRF4)	X	

Table 8. List of strains and PCR deletion diagnosis primers used in this work

Strains are organized by the figures in which they appear.

	N – Worms – Amphid Data	N – Worms – Phasmid Data
Figure 1		
WT	99	60
nphp-2	121	60
arl-13	81	92
hdac-6	59	60
arl-13; nphp-2	40	40
hdac-6; nphp-2	40	40
arl-13; hdac-6	109	113
arl-13; hdac-6; nphp-2	40	40

	N – Worms – Amphid Data	N – Worms – Phasmid Data
Figure 4C		
WT	99	60
nphp-2 nphp-4	88	88
myEx743(p*nphp-2*::NPHP-2L::GFP + ccRFP)	11	10
nphp-2 nphp-4; myEx849(p*nphp-2*::NPHP-2L-EFdel::GFP + ccRFP)	47	47
nphp-2 nphp-4; myEx850(p*nphp-2*::NPHP-2L-NLS1del::GFP + ccRFP)	27	26
nphp-2 nphp-4; myEx851(p*nphp-2*::NPHP-2L-NLS2del::GFP + ccRFP)	20	21

	N – Worms – Phasmid Data
Figure 6A	
WT	60
klp-11	40
klp-11; nphp-2	120
arl-13; klp-11	100
hdac-6 klp-11	40
klp-11; arl-13; hdac-6	53
Figure 6B	
unc-119	59
unc-119; klp-11	40
unc-119; nphp-2	82
arl-13; unc-119	38
unc-119; hdac-6	42
unc-119; hdac-6; nphp-2	50

arl-13; unc-119; hdac-6	62

Figure 8C	N – Cilia
Ratio of fluorescent reporter length to GT335 length	
NPHP-2::GFP and GT335 colabel	13
ARL-13::GFP and GT335 colabel	35
GFP::UNC-119 and GT335 colabel	30
Length fluorescent reporter length	
GFP::UNC-119	58
ARL-13::GFP	35
NPHP-2::GFP	13
Length of GT335	
GT335 (GFP::UNC-119)	63
GT335 (ARL-13::GFP)	35
GT335 (NPHP-2::GFP)	18
*In some animals, GFP was too dim to measure, leading to a difference between GFP and GT335 Ns. These unmatched lengths have no effect on ratio data, as all ratios were computed per-cilium.	

Supplemental Figure 1	N – Worms – Amphid Data	N – Worms – Phasmid Data
arl-3	38	38
arl-13; arl-3	87	99
arl-3; nphp-2	104	105
arl-3; hdac-6	51	50
arl-13; arl-3; hdac-6	52	52
arl-3; hdac-6; nphp-2	40	40
arl-13; arl-3; nphp-2	52	52
arl-13; arl-3; hdac-6; nphp-2	45	45
unc-119	58	59
arl-3; unc-119	48	47
klp-11	40	40
klp-11; arl-3	56	56

	N – Worms – Amphid Data	N – Worms – Phasmid Data
Supplemental Figure 5A		
WT	99	60
klp-11	40	40
klp-11; nphp-2	119	120
arl-13; klp-11	100	100
hdac-6 klp-11	39	40
klp-11; arl-13; hdac-6	53	53
Supplemental Figure 5B		
unc-119	58	59
unc-119; klp-11	40	40
unc-119; nphp-2	83	82
arl-13; unc-119	38	38
unc-119; hdac-6	42	42
unc-119; hdac-6; nphp-2	48	50
arl-13; unc-119; hdac-6	62	62
Supplemental Figure 5C		
osm-3	18	18
osm-3; nphp-2	20	20
arl-13; osm-3	11	11
osm-3; hdac-6	20	20
Supplemental Figure 5D		
nphp-2 nphp-4	40	40
hdac-6; nphp-2 nphp-4	31	31
arl-3; nphp-2 nphp-4	40	40

Supplemental Figure S6	N – Cilia
Ratio	
GFP::UNC-119	39
NPHP-2::GFP	35
ARL-13::GFP	61
Cilia Length by DiI	
GFP::UNC-119	39
NPHP-2::GFP	35
ARL-13::GFP	61

GFP length	
GFP::UNC-119	39
NPHP-2::GFP	35
ARL-13::GFP	67
*In some ARL-13::GFP animals, DiI was too dim to measure, leading to a difference between GFP and DiI Ns. These unmatched lengths have no effect on ratio data, as all ratios were computed per-cilium.	

Supplemental Figure 7A	N – Worms
myEx743(p*nphp-2*::NPHP-2L::GFP + ccRFP)	10
klp-11; myEx743	21
unc-119; myEx743	25
arl-13; myEx743	12
hdac-6; myEx743	19
arl-13; hdac-6; myEx743	8
Supplemental Figure 7B	
jhuEx352(p*arl-13*::ARL-13::GFP + pBx)	7
klp-11; jhuEx352	11
unc-119; jhuEx352	8
nphp-2; jhuEx352	20
Supplemental Figure 7C	
myEx848(p*osm-6*::GFP::UNC-119 + ccRFP)	12
klp-11; myEx848	6
nphp-2; myEx848	19
arl-13; myEx848	11
hdac-6; myEx848	11
arl-13; hdac-6; myEx848	9
Supplemental Figure 7D	
Ex(P*panciliary*::KAP-1::GFP + pRF4)	15
nphp-2; Ex(KAP-1::GFP)	19

arl-13; Ex(KAP-1::GFP)	16
hdac-6; Ex(KAP-1::GFP)	12
Supplemental Figure 7E	
WT	10
unc-119	20
nphp-2	10
arl-13	6
hdac-6	8
*Each worm score is the average of 2-4 cilia	

Table 9. Experimental sample sizes for figures with statistical analysis.

3.9 – References

Note: These references are formatted to the standards of PLOS Genetics.

1. Ke YN, Yang WX. (2014) Primary cilium: An elaborate structure that blocks cell division? Gene 547(2): 175-185.

2. Fry AM, Leaper MJ, Bayliss R. (2014) The primary cilium: Guardian of organ development and homeostasis. Organogenesis 10(1): 62-68.

3. Goggolidou P. (2014) Wnt and planar cell polarity signaling in cystic renal disease. Organogenesis 10(1): 86-95.

4. Yoshiba S, Hamada H. (2014) Roles of cilia, fluid flow, and Ca^{2+} signaling in breaking of left-right symmetry. Trends Genet 30(1): 10-17.

5. Yuan S, Sun Z. (2013) Expanding horizons: Ciliary proteins reach beyond cilia. Annu Rev Genet 47: 353-376.

6. Jackson PK. (2013) Nek8 couples renal ciliopathies to DNA damage and checkpoint control. Mol Cell 51(4): 407-408.

7. Rosenbaum JL, Witman GB. (2002) Intraflagellar transport. Nat Rev Mol Cell Biol. 3(11): 813-825.

8. Williams CL, Li C, Kida K, Inglis PN, Mohan S, et al. (2011) MKS and NPHP modules cooperate to establish basal body/transition zone membrane associations and ciliary gate function during ciliogenesis. J Cell Biol 192(6): 1023-1041.

9. Dishinger JF, Kee HL, Jenkins PM, Fan S, Hurd TW, et al. (2010) Ciliary entry of the kinesin-2 motor KIF17 is regulated by importin-beta2 and RanGTP. Nat Cell Biol 12(7): 703-710.

10. Satir P, Pedersen LB, Christensen ST. (2010) The primary cilium at a glance. J Cell Sci 123(Pt 4): 499-503.

11. Blacque OE, Sanders AA. (2014) Compartments within a compartment: What can tell us about ciliary subdomain composition, biogenesis, function, and disease. Organogenesis 10(1).

12. Shiba D, Yamaoka Y, Hagiwara H, Takamatsu T, Hamada H, et al. (2009) Localization of Inv in a distinctive intraciliary compartment requires the C-terminal ninein-homolog-containing region. J Cell Sci 122(Pt 1): 44-54.

13. Wojtyniak M, Brear AG, O'Halloran DM, Sengupta P. (2013) Cell- and subunit-specific mechanisms of CNG channel ciliary trafficking and localization in *C. elegans*. J Cell Sci 126(Pt 19): 4381-4395.

14. Gong Z, Son W, Chung YD, Kim J, Shin DW, et al. (2004) Two interdependent TRPV channel subunits, inactive and nanchung, mediate hearing in drosophila. J Neurosci 24(41): 9059-9066.

15. French DA, Badamdorj D, Kleene SJ. (2010) Spatial distribution of calcium-gated chloride channels in olfactory cilia. PLoS One 5(12): e15676.

16.   Mergen M, Engel C, Muller B, Follo M, Schafer T, et al. (2013) The nephronophthisis gene product NPHP2/Inversin interacts with aurora A and interferes with HDAC6-mediated cilia disassembly. Nephrol Dial Transplant 28(11): 2744-2753.

17.   Warburton-Pitt SR, Jauregui AR, Li C, Wang J, Leroux MR, et al. (2012) Ciliogenesis in *Caenorhabditis elegans* requires genetic interactions between ciliary middle segment localized NPHP-2 (Inversin) and transition zone-associated proteins. J Cell Sci 125(Pt 11): 2592-2603.

18.   Shiba D, Manning DK, Koga H, Beier DR, Yokoyama T. (2010) Inv acts as a molecular anchor for Nphp3 and Nek8 in the proximal segment of primary cilia. Cytoskeleton (Hoboken) 67(2): 112-119.

19.   Hoff S, Halbritter J, Epting D, Frank V, Nguyen TM, et al. (2013) ANKS6 is a central component of a nephronophthisis module linking NEK8 to INVS and NPHP3. Nat Genet 45(8): 951-956.

20.   Sang L, Miller JJ, Corbit KC, Giles RH, Brauer MJ, et al. (2011) Mapping the NPHP-JBTS-MKS protein network reveals ciliopathy disease genes and pathways. Cell 145(4): 513-528.

21.   Wright KJ, Baye LM, Olivier-Mason A, Mukhopadhyay S, Sang L, et al. (2011) An ARL3-UNC119-RP2 GTPase cycle targets myristoylated NPHP3 to the primary cilium. Genes Dev 25(22): 2347-2360.

22.   Inglis PN, Ou G, Leroux MR, Scholey JM. (2007) The sensory cilia of *Caenorhabditis elegans*. WormBook : 1-22.

23.   Barr MM, Sternberg PW. (1999) A polycystic kidney-disease gene homologue required for male mating behaviour in *C. elegans*. Nature 401(6751): 386-389.

24.   Morsci NS, Barr MM. (2011) Kinesin-3 KLP-6 regulates intraflagellar transport in male-specific cilia of *Caenorhabditis elegans*. Curr Biol 21(14): 1239-1244.

25.   Wang J, Schwartz HT, Barr MM. (2010) Functional specialization of sensory cilia by an RFX transcription factor isoform. Genetics 186(4): 1295-1307.

26.   Bae YK, Kim E, L'Hernault S W, Barr MM. (2009) The CIL-1 PI 5-phosphatase localizes TRP polycystins to cilia and activates sperm in *C. elegans*. Curr Biol 19(19): 1599-607.

27.   Perkins LA, Hedgecock EM, Thomson JN, Culotti JG. (1986) Mutant sensory cilia in the nematode *Caenorhabditis elegans*. Dev Biol 117(2): 456-487.

28.   Doroquez DB, Berciu C, Anderson JR, Sengupta P, Nicastro D. (2014) A high-resolution morphological and ultrastructural map of anterior sensory cilia and glia in *Caenorhabditis elegans*. Elife 3: e01948.

29.   Cevik S, Sanders AA, Van Wijk E, Boldt K, Clarke L, et al. (2013) Active transport and diffusion barriers restrict joubert syndrome-associated ARL13B/ARL-13 to an Inv-like ciliary membrane subdomain. PLoS Genet 9(12): e1003977.

30.   Li Y, Wei Q, Zhang Y, Ling K, Hu J. (2010) The small GTPases ARL-13 and ARL-3 coordinate intraflagellar transport and ciliogenesis. J Cell Biol 189(6): 1039-51.

31.   Snow JJ, Ou G, Gunnarson AL, Walker MR, Zhou HM, et al. (2004) Two anterograde intraflagellar transport motors cooperate to build sensory cilia on *C. elegans* neurons. Nat Cell Biol 6(11): 1109-13.

32.   Cevik S, Hori Y, Kaplan OI, Kida K, Toivenon T, et al. (2010) Joubert syndrome Arl13b functions at ciliary membranes and stabilizes protein transport in *Caenorhabditis elegans*. J Cell Biol 188(6): 953-969.

33.   Caspary T, Larkins CE, Anderson KV. (2007) The graded response to sonic hedgehog depends on cilia architecture. Dev Cell 12(5): 767-778.

34.   Reiter JF, Blacque OE, Leroux MR. (2012) The base of the cilium: Roles for transition fibres and the transition zone in ciliary formation, maintenance and compartmentalization. EMBO Rep 13(7): 608-618.

35.   Nakata K, Shiba D, Kobayashi D, Yokoyama T. (2012) Targeting of Nphp3 to the primary cilia is controlled by an N-terminal myristoylation site and coiled-coil domains. Cytoskeleton (Hoboken) 69(4): 221-234.

36.   Humbert MC, Weihbrecht K, Searby CC, Li Y, Pope RM, et al. (2012) ARL13B, PDE6D, and CEP164 form a functional network for INPP5E ciliary targeting. Proc Natl Acad Sci U S A 109(48): 19691-19696.

37.   Williams CL, Masyukova SV, Yoder BK. (2010) Normal ciliogenesis requires synergy between the cystic kidney disease genes MKS-3 and NPHP-4. J Am Soc Nephrol 21(5): 782-93.

38.   Watanabe D, Saijoh Y, Nonaka S, Sasaki G, Ikawa Y, et al. (2003) The left-right determinant Inversin is a component of node monocilia and other 9+0 cilia. Development 130(9): 1725-1734.

39.   Ou G, Koga M, Blacque OE, Murayama T, Ohshima Y, et al. (2007) Sensory ciliogenesis in *Caenorhabditis elegans*: Assignment of IFT components into distinct modules based on transport and phenotypic profiles. Mol Biol Cell 18(5): 1554-1569.

40.   Lechtreck KF, Geimer S. (2000) Distribution of polyglutamylated tubulin in the flagellar apparatus of green flagellates. Cell Motil Cytoskeleton 47(3): 219-35.

41.   Suryavanshi S, Edde B, Fox LA, Guerrero S, Hard R, et al. (2010) Tubulin glutamylation regulates ciliary motility by altering inner dynein arm activity. Curr Biol 20(5): 435-40.

42.   Fouquet JP, Prigent Y, Kann ML. (1996) Comparative immunogold analysis of tubulin isoforms in the mouse sperm flagellum: Unique distribution of glutamylated tubulin. Mol Reprod Dev 43(3): 358-365.

43.   Edde B, Rossier J, Le Caer JP, Desbruyeres E, Gros F, et al. (1990) Posttranslational glutamylation of alpha-tubulin. Science 247(4938): 83-5.

44.   Sharma N, Bryant J, Wloga D, Donaldson R, Davis RC, et al. (2007) Katanin regulates dynamics of microtubules and biogenesis of motile cilia. J Cell Biol 178(6): 1065-1079.

45.   O'Hagan R, Piasecki BP, Silva M, Phirke P, Nguyen KC, et al. (2011) The tubulin deglutamylase CCPP-1 regulates the function and stability of sensory cilia in *C. elegans*. Curr Biol 21(20): 1685-1694.

46.   Kann ML, Soues S, Levilliers N, Fouquet JP. (2003) Glutamylated tubulin: Diversity of expression and distribution of isoforms. Cell Motil Cytoskeleton 55(1): 14-25.

47.   Pathak N, Obara T, Mangos S, Liu Y, Drummond IA. (2007) The zebrafish *fleer* gene encodes an essential regulator of cilia tubulin polyglutamylation. Mol Biol Cell 18(11): 4353-4364.

48.　Pugacheva EN, Jablonski SA, Hartman TR, Henske EP, Golemis EA. (2007) HEF1-dependent Aurora A activation induces disassembly of the primary cilium. Cell 129(7): 1351-63.

49.　Hori Y, Kobayashi T, Kikko Y, Kontani K, Katada T. (2008) Domain architecture of the atypical arf-family GTPase Arl13b involved in cilia formation. Biochem Biophys Res Commun 373(1): 119-124.

50.　Larkins CE, Aviles GD, East MP, Kahn RA, Caspary T. (2011) Arl13b regulates ciliogenesis and the dynamic localization of Shh signaling proteins. Mol Biol Cell 22(23): 4694-4703.

51.　Satish Tammana TV, Tammana D, Diener DR, Rosenbaum J. (2013) Centrosomal protein CEP104 (*Chlamydomonas* FAP256) moves to the ciliary tip during ciliary assembly. J Cell Sci 126(Pt 21): 5018-5029.

52.　Lee JE, Silhavy JL, Zaki MS, Schroth J, Bielas SL, et al. (2012) CEP41 is mutated in Joubert syndrome and is required for tubulin glutamylation at the cilium. Nat Genet 44(2): 193-199.

53.　Zhou C, Cunningham L, Marcus AI, Li Y, Kahn RA. (2006) Arl2 and Arl3 regulate different microtubule-dependent processes. Mol Biol Cell 17(5): 2476-2487.

54.　Wu Y, Dai XQ, Li Q, Chen CX, Mai W, et al. (2006) Kinesin-2 mediates physical and functional interactions between Polycystin-2 and Fibrocystin. Hum Mol Genet 15(22): 3280-92.

55.　Follit JA, Xu F, Keady BT, Pazour GJ. (2009) Characterization of mouse IFT complex B. Cell Motil Cytoskeleton 66(8): 457-468.

56.　Fan S, Hurd TW, Liu CJ, Straight SW, Weimbs T, et al. (2004) Polarity proteins control ciliogenesis via kinesin motor interactions. Curr Biol 14(16): 1451-1461.

57.　Sanchez de Diego A, Alonso Guerrero A, Martinez-A C, van Wely KH. (2014) Dido3-dependent HDAC6 targeting controls cilium size. Nat Commun 5: 3500.

58.　DiPetrillo CG, Smith EF. (2013) Methods for analysis of calcium/calmodulin signaling in cilia and flagella. Methods Enzymol 524: 37-57.

59.　Jin X, Mohieldin AM, Muntean BS, Green JA, Shah JV, et al. (2013) Cilioplasm is a cellular compartment for calcium signaling in response to mechanical and chemical stimuli. Cell Mol Life Sci .

60.　Collingridge P, Brownlee C, Wheeler GL. (2013) Compartmentalized calcium signaling in cilia regulates intraflagellar transport. Curr Biol 23(22): 2311-2318.

61.　Morgan D, Goodship J, Essner JJ, Vogan KJ, Turnpenny L, et al. (2002) The left-right determinant Inversin has highly conserved ankyrin repeat and IQ domains and interacts with calmodulin. Hum Genet 110(4): 377-384.

62.　Yasuhiko Y, Imai F, Ookubo K, Takakuwa Y, Shiokawa K, et al. (2001) Calmodulin binds to Inv protein: Implication for the regulation of Inv function. Dev Growth Differ 43(6): 671-681.

63.　Zhang H, Constantine R, Vorobiev S, Chen Y, Seetharaman J, et al. (2011) UNC119 is required for G protein trafficking in sensory neurons. Nat Neurosci 14(7): 874-880.

64.　Hubbert C, Guardiola A, Shao R, Kawaguchi Y, Ito A, et al. (2002) HDAC6 is a microtubule-associated deacetylase. Nature 417(6887): 455-458.

65. Zhang Y, Li N, Caron C, Matthias G, Hess D, et al. (2003) HDAC-6 interacts with and deacetylates tubulin and microtubules in vivo. EMBO J 22(5): 1168-1179.

66. Matsuyama A, Shimazu T, Sumida Y, Saito A, Yoshimatsu Y, et al. (2002) In vivo destabilization of dynamic microtubules by HDAC6-mediated deacetylation. EMBO J 21(24): 6820-6831.

67. Verhey KJ, Gaertig J. (2007) The tubulin code. Cell Cycle 6(17): 2152-60.

68. Fukushige T, Siddiqui ZK, Chou M, Culotti JG, Gogonea CB, et al. (1999) MEC-12, an alpha-tubulin required for touch sensitivity in *C. elegans*. J Cell Sci 112(Pt 3): 395-403.

69. Chu CW, Hou F, Zhang J, Phu L, Loktev AV, et al. (2011) A novel acetylation of beta-tubulin by san modulates microtubule polymerization via down-regulating tubulin incorporation. Mol Biol Cell 22(4): 448-456.

70. Kiemer L, Bendtsen JD, Blom N. (2005) NetAcet: Prediction of N-terminal acetylation sites. Bioinformatics 21(7): 1269-1270.

71. Kubo T, Yanagisawa HA, Yagi T, Hirono M, Kamiya R. (2010) Tubulin polyglutamylation regulates axonemal motility by modulating activities of inner-arm dyneins. Curr Biol 20(5): 441-5.

72. Kimura Y, Kurabe N, Ikegami K, Tsutsumi K, Konishi Y, et al. (2010) Identification of tubulin deglutamylase among *Caenorhabditis elegans* and mammalian cytosolic carboxypeptidases (CCPs). J Biol Chem 285(30): 22936-41.

73. Otto EA, Schermer B, Obara T, O'Toole JF, Hiller KS, et al. (2003) Mutations in INVS encoding Inversin cause nephronophthisis type 2, linking renal cystic disease to the function of primary cilia and left-right axis determination. Nat Genet 34(4): 413-420.

74. Olbrich H, Fliegauf M, Hoefele J, Kispert A, Otto E, et al. (2003) Mutations in a novel gene, NPHP3, cause adolescent nephronophthisis, tapeto-retinal degeneration and hepatic fibrosis. Nat Genet .

75. Bergmann C, Fliegauf M, Bruchle NO, Frank V, Olbrich H, et al. (2008) Loss of Nephrocystin-3 function can cause embryonic lethality, Meckel-Gruber-like syndrome, *situs inversus*, and renal-hepatic-pancreatic dysplasia. Am J Hum Genet 82(4): 959-970.

76. Otto EA, Trapp ML, Schultheiss UT, Helou J, Quarmby LM, et al. (2008) NEK8 mutations affect ciliary and centrosomal localization and may cause nephronophthisis. J Am Soc Nephrol 19(3): 587-592.

77. Cantagrel V, Silhavy JL, Bielas SL, Swistun D, Marsh SE, et al. (2008) Mutations in the cilia gene ARL13B lead to the classical form of Joubert syndrome. Am J Hum Genet 83(2): 170-179.

78. Altschul SF, Madden TL, Schaffer AA, Zhang J, Zhang Z, et al. (1997) Gapped BLAST and PSI-BLAST: A new generation of protein database search programs. Nucleic Acids Res 25(17): 3389-3402.

79. Hau J, Muller M, Pagni M. (2007) HitKeeper, a generic software package for hit list management. Source Code Biol Med 2: 2.

80. Lupas A. (1997) Predicting coiled-coil regions in proteins. Curr Opin Struct Biol 7(3): 388-393.

81. Brenner S. (1974) The genetics of *Caenorhabditis elegans*. Genetics 77(1): 71-94.

82.   Weimer RM. (2006) Preservation of *C. elegans* tissue via high-pressure freezing and freeze-substitution for ultrastructural analysis and immunocytochemistry. Methods Mol Biol 351: 203-221.

83.   Altun ZF, Herndon LA, Crocker C, Lints R, Hall DH. (2013) WormAtlas. 2013.

Chapter 4: Conclusion

4.1 Key Findings

This work supports and extends our understanding of the TZ, InvC, and doublet region in significant ways. I established that both Inversin and the Inversin compartment are conserved in *C. elegans*, and that the worm is a viable model to study this gene.

In my first paper (Warburton-Pitt et al., 2012), I characterized *nphp-2* and found that it is required for proper TZ placement. I also demonstrated that TZ genes are organized into two distinct genetic modules, and that *nphp-2* interacts with these in a cell-type specific manner. Other work in *C. elegans* and mammalian systems has corroborated this finding. I found that *nphp-2* is not required for the localization of TZ components; as ciliary anchoring is a function of the TZ, this suggests that anchoring defects in *nphp-2* mutants are not due to TZ assembly failure. I also found that *nphp-2* and the TZ gene *nphp-4* interact strongly to guide multiple aspects of cilia biology, including cilia placement and IFT.

In my second paper (Warburton-Pitt et al., 2014), I explored the relationship between *nphp-2* and doublet region associated genes. I found that these genes are also organized into two parallel genetic modules, interactions between which are modulated by *hdac-6* and *arl-3*. Additionally, I found that contrary to previous reports, UNC-119 localizes to the proximal cilium and not the TZ. I also demonstrated that ciliary glutamylation lies downstream of the action of doublet region-associated genes, and that glutamylation does not specify the localization of doublet region proteins. How the InvC and doublet region are initially established is unknown in any system. Our data rules out multiple possible mechanisms, including IFT, the UNC-119 shuttle, TZ, tubulin glutamylation, and microtubule ultrastructure.

Chapter 1 of this thesis is the first comprehensive review of the InvC to date,

summarizing over five years of work in the field. I introduced several hypotheses, including the hypothesis that the *C. elegans* ciliary "middle segment"/ doublet region is analogous to the mammalian doublet region and not to the mammalian InvC. I also proposed and explored many possible functions for the InvC. As a whole, this chapterwill help synthesize results from across multiple organisms to give a more complete and easy to understand overview of the field than was previously available.

4.2 Future Directions

With the advancement of the field, and the work presented herein, many, many unanswered questions and unexplored paths remain. Here, I discuss several immediate questions and possible experimental approaches. The function of the InvC is omitted, as it is thoroughly discussed in Chapter 1 (1.5 – The Function of the Inversin Compartment).

4.2.1 – InvC biogenesis

The single biggest mystery regarding the InvC is how it is initially established. While many possible mechanisms have been put forward, tested, and ruled out, I have no definitive answer to date. Currently, the only positive data that I have is from mammalian and *C. elegans* domain deletion experiments, which found that the calmodulin binding IQ and ninein homology domains of Inversin, and the EF-hand of NPHP-2 are required for ciliary targeting and InvC restriction (Shiba et al., 2009; Warburton-Pitt et al., 2014). Chapter 3 explores and discusses several other mechanisms in *C. elegans*, including IFT, TZ scaffolding/restriction, tubulin glutamylation, and microtubule ultrastructure. Many possible mechanisms remain unexplored, and further possible mechanisms remain unimagined. Here, I discuss several possibilities and experimental treatments in turn. An in-depth discussion of some of these is presented in

Chapters 1 and 3 (1.4.4 – Establishing the Inv Compartment and 3.5.8 – Origin of the Inversin

Compartment).

4.2.1.1 – Calcium signaling. The high intraciliary calcium concentration belies the importance of

calcium signaling in cilia biology (Reviewed in Masyuk 2014). Calcium can function signal

transduction and/or signaling cascades. As the earliest known determinant of the InvC, Inversin,

requires its calmodulin-binding IQ2 domain for restriction to the InvC, calcium signaling likely

plays a role in specifying the InvC (Shiba et al., 2009). NPHP-2 also requires its calcium binding

EF-hand for InvC localization (Warburton-Pitt et al., 2014). A significant difference exists

between the EF-hand of NPHP-2 and the IQ2 domain of Inversin: deletion of the EF-hand of

NPHP-2 results in a complete lack of ciliary localization, whereas deletion of the IQ2 domain of

Inversin results in a mislocalization of Inversin along the entire cilium. In both systems,

Inversin/NPHP-2 no longer localizes to the InvC. If calcium has a conserved role in the

specification of InvC restriction, then in *C. elegans*, non-InvC targeted NPHP-2 may be cleared

actively or passively out of the cilium through a non-conserved means. It is also possible that the

calcium-dependency of Inversin and NPHP-2 has diverged.

However, knowing that calcium-binding is required for localization does not allow us to

determine exactly how this is achieved. Inversin/NPHP-2 may localize based on pre-existing

calcium concentration gradients, or calcium may stabilize already InvC localized

Inversin/NPHP-2. In mammalian systems, calmodulin localizes throughout the cilium and is not

enriched in the InvC (Shiba et al., 2009); whether this population of calmodulin is all bound to

calcium, or if only small amounts of the calmodulin are bound to calcium, is unknown.

Inversin/NPHP-2 may also act as a calcium "sponge" at the base of the cilium, functioning to

maintain high intraciliary calcium and reducing leakage into the cytoplasm.

To clarify the complex link between calcium and the InvC, an experimental approach can be

taken. A calcium indicator can be used to determine if NPHP-2 is required to maintain ciliary

calcium levels or if a ciliary calcium micro-domain exists by comparing WT animals, *nphp-2*

mutants, and worms expressing NPHP-2-ΔEF. As the EF-hand is not required for IL localization of

NPHP-2, these new experiments should be performed across cell types to explore how cell

specific localization may be achieved. A calcium chelator can be used to determine if calcium is

required for the maintenance of the InvC (Mank and Griesbeck, 2008). It is difficult to determine

the role of calcium in establishment of the InvC as calcium cannot be completely removed

during development. Partial depletion of calcium in sensory neurons could be used instead using

a calcium reporter (Miyawaki et al., 1997). To avoid the problem of non-cilium-specific calcium

depletion, a cilia-specific depletion method should be used. Perforating the ciliary membrane

using OSM-9, a calcium TRP channel, may allow the excess calcium in the cilium to dissipate out

of the cell (Robert O'Hagan, Personal Communication). Additionally, if a ciliary targeting signal

could be identified, it could be fused to a calcium chelating protein, restricting the chelator to

the cilium. If no such targeting signal exists, then a portion of a cilia-targeted protein could be

substituted; for example, minimal targeting regions have been determined for ARL-13 (Cevik et

al., 2013).

4.2.1.2 – Membrane composition. Most cellular compartments have membranes with distinct

composition, suited for their specific task. The cilium possibly has several membrane

microdomains, including the periciliary membrane surrounding the cilium at the dendritic tip,

and the membrane of the cilium proper (e.g., Bae et al., 2009; Chih et al., 2011; Kaplan et al.,

2012). Multiple doublet region/InvC components are associated with membrane biology. ARL-13

is inserted into the membrane through a palmitoyl group (Cevik et al., 2010), NPHP-2 appears to

be enriched near the membrane (Warburton-Pitt et al., 2012), and HDAC-6 has a predicted FYVE

phosphatidylinositol 3-phostphate (PI3P) binding domain (Maureen Barr, Personal

Communication). The palmitoyl group of ARL-13 is required for doublet region restriction but not ciliary targeting, strong evidence that the membrane plays a role in localizing at least some InvC and doublet region components (Cevik et al., 2010). It is still possible that the membrane does not specify ARL-13 restriction, and that other membrane-associated factors are required. It is possible that specific membrane composition drives localization of InvC and doublet region components through these physical interactions. (It is also possible that these components regulate membrane composition; for a discussion of this, see 1.4.5 – Membrane Dynamics of the Inv Compartment.) The localization of NPHP-2 and UNC-119 have been examined in several combinations with PIP-associated gene mutants, including *age-1* (a PIP 3-kinase), *daf-18* (a PI3P 3-phosphatase), and *cil-1* (a PI(3,5)P 5-phosphatase), but these genes do not appear to be required (**Error! Reference source not found.**). The length of the UNC-119 territory was also easured in these mutants, but was not significantly altered compared to wild-type. However, this data does not rule out a role for membrane composition in InvC biogenesis, and does not touch upon membrane trafficking pathways.

As specific relevant phospholipids are not known, a broad approach needs to be taken. First, the localization of ARL-13, NPHP-2, UNC-119, and HDAC-6 should be determined in all mutants of PIP kinase and phosphatase genes expressed in ciliated neurons. As HDAC-6 may bind PI(3)P, one might predict that it HDAC-6 will mislocalize in *age-1* mutants if the membrane determines localization.

Second, fluorescent markers can be used to determine ciliary membrane composition and the role of the membrane in determining ciliary microdomains. Specific PIPs can be fluorescently labelled, including by 2XFYVE (labelling PI(3)P), AKT[PH domain](labelling PI(3,4,5)P_3 and PI(3,4)P_2), and PLCΔ[PH domain](labelling PI(4,5)P_2) (Bae et al., 2009). Sphingolipids rafts can be detected using BODIPY, which exhibits changes in emission wavelength depending on

concentration (Pagano and Chen, 1998). In addition to BODIPY tagging of cholesterol

(Holtta-Vuori et al., 2008), the cholesterol composition of the cilium can be determined using

dehydroergosterol, a fluorescent analog of cholesterol which functionally mimics cholesterol in

living cells (Mukherjee et al., 1998). An alternative is using a fluorescent protein reporter such as

Perfringolysin-O-domain D4::GFP, which preferentially labels cholesterol in lipid rafts (Johnson

et al., 2012; Ohno-Iwashita et al., 2004). A non-specific fluorescent marker, Laurdan/C-Laurdan,

changes its excitation wavelength depending on the fluidity of the surrounding membrane (Kim

et al., 2007; Parasassi et al., 1997). (C-Laurdan is more photostable and water soluble than

Laurdan.)

 If any of these membrane markers reveals a proximal cilium cilia membrane microdomain, that

marker could be colabelled with NPHP-2::GFP, ARL-13::GFP, GFP::UNC-119, and GT335

(anti-glutamylated tubulin antibody which marks doublet region microtubule doublets) to

determine the specific subciliary localization of the marker. This information could then be used

to select membrane pathway mutants to assay for localization of doublet region and InvC

components. In the case of cholesterol, a faster, though less definitive alternative to fluorescent

labelling would be to raise worms on cholesterol-deficient media, and then determine

localization of InvC and doublet region markers. Cholesterol depletion has previously been used

to explore the link between membrane biology, the transmembrane ciliopathy ortholog MKS-3,

and IFT (Juan Wang, personal communication). Analysis of other membrane components in such

a manner is not possible, as the other components are produced endogenously.

4.2.1.3 – The EVC Compartment.

As described in Chapter 1 (1.4.4 – Establishing the Inv Compartment), in mammalian cilia, there

exist two proteins, Ecv and Evc2, that localize to a region called the Evc compartment (EvcC),

laying in-between (or partially overlapping both) the TZ and the InvC (Dorn et al., 2012; Pusapati

et al., 2014). Evc and Evc2 physically interact, require each other for proper localization, and

positively regulate ciliary hedgehog signaling. Evc2 possesses a motif termed the W-peptide that

is required for restriction to the Evc compartment; the W-peptide binds to the calcium and

calmodulin binding complex EFCAB7-IQCE. When the interaction between Evc/Evc2 and

EFCAB7-IQCE is disrupted, Evc and Evc2 localize along the entire cilium. This is similar to the

calcium-dependence of Inversin/NPHP-2, which require calcium and calmodulin domains to be

restricted to the InvC (Shiba et al., 2009; Warburton-Pitt et al., 2014). Several questions arise: Is

the Evc/Evc2 complex required for InvC biogenesis or maintenance? Do InvC or TZ components

specify the EvcC? Evidence suggests that the Evc/Evc2 complex is not required for the

localization of Inversin or Arl13b, though the reverse has not been examined (Pusapati et al.,

2014); it maybe that EvcC components interact with both TZ and InvC proteins, restricting the

EvcC to the margin between these two larger compartments. Is the EFCAB7-IQCE complex

required for InvC biogenesis and does it play the same function in organizing both the InvC and

the EvcC? That both InvC and EvcC biogenesis requires proteins sharing domains is intriguing,

but this relationship has not been examined to date. Is the EvcC conserved in *C. elegans*, and can

C. elegans be used to study this novel compartment? A cursory search indicates that only

EFCAB7 may be conserved in *C. elegans* (T02G5.3), which possesses an X-box, the general cilia

gene promoter. The other EvcC components (IQCE, Evc, and Evc2) do not yield strong BLAST

matches. This suggests that while the EvcC itself is likely not conserved in *C. elegans*, the

mechanism that links a subciliary localization pattern to calcium may be present.

Regardless of whether the EvcC is present in *C. elegans* or is linked to calcium signaling, it is of

note that the cilium possess two distinct microcompartments, both adjacent to the TZ, both

regulated by calcium, and both functioning as signaling components (Wnt in the case of the InvC

and Hedgehog in the case of the EvcC). Further work in mammalian models is needed to explore

the relationship between these compartments.

4.2.1.4 – The Transition Zone.

The TZ and InvC are functionally linked, as demonstrated by SynDyf data presented in Chapters

2 and 3 (Figure 12, Figure 24). Several TZ and InvC components also physically interact, including

NPHP-2 and NPHP-4 in *C. elegans* (Andrew Jauregui, PhD Thesis), and Inversin and Nphp1,

Nphp5, and Ahi1 in mammalian systems (Sang et al., 2011). As the TZ is assembled early in

ciliogenesis, before the docking of the ciliary vesicle to the membrane, and the TZ acts as a gate

regulating ciliary traffic, it is possible that the TZ also functions to organize ciliary

compartmentalization (Williams et al., 2011). Indeed, in mammalian models, the coiled-coil

domain of Nphp3 is required for physical interaction with and targeting to the TZ prior to ciliary

import (Nakata et al., 2012).

Evidence in *C. elegans*, however, indicates that a role for the TZ in organizing the InvC is unlikely.

In TZ mutants, both NPHP-2 and ARL-13 were targeted and restricted to their respective

territories, indicating that the TZ is not even required for ciliary targeting of these proteins

(Figure 21, Figure 29, Figure 30). Since the TZ complex is formed of two redundant modules, it

may be possible that in TZ single mutants the second, unaffected module is sufficient for ciliary

targeting and territory restriction of NPHP-2 and ARL-13; however, in the *mks-3; nphp-4* double

mutant (in which both TZ modules are knocked out), NPHP-2 is still localizes to the InvC even in

cilia with severe placement defects (Figure 30). It was only possible to determine in the TZ was

strictly required for InvC localization of NPHP-2, and not whether the TZ played any role at all;

periciliary mislocalization of NPHP-2 may be due to either TZ defects or transgene

overexpression defects (

3.4.3 – NPHP-2 and ARL-13 do not require TZ- and doublet region-associated genes for ciliary targeting).

Because of the genetic redundancy of TZ, and the different roles each TZ protein plays in the complex, it might be that the *mks-3; nphp-4* double mutant does not represent a full TZ knockdown. *mks-3*, a transmembrane protein, is the furthest downstream gene in the MKS module (Williams et al., 2011); examining localization of NPHP-2 in an *mks-5; nphp-4* double mutant may be more informative because *mks-5* is the furthest known upstream MKS module gene. Additionally, the TZ may be required for NPHP-2 localization in a cell-specific manner: no cell-type specific localization analysis was undertaken in the *mks-3; nphp-4* mutants. This would not be surprising, as NPHP-2 appears TZ localized in IL2 cilia, and does not require the calcium binding EF-hand for proper localization in IL2 cilia (Warburton-Pitt et al., 2014).

4.2.1.5 – Glutamylation, acetylation and the target of hdac-6*.

Post-translational modification of tubulin and other proteins may also play a large role in establishing the InvC. Microtubules can be labeled for specific purposes by the addition of several moieties, via polyglutamylation and acetylation, among others (Verhey and Gaertig, 2007). Though the doublet region of amphid channel and phasmid cilia is polyglutamylated, experiments in Chapter 3 demonstrate that this polyglutamylation is likely to be downstream of the action of the InvC and doublet region (O'Hagan et al., 2011; Warburton-Pitt et al., 2014). However, I only examined the roles of *ccpp-1* (a deglutamylase) and *ttll-4* (a glutamylase); five other *ttll* genes are conserved in *C. elegans* (Robert O'Hagan, Personal Communication). *ttll-4* was chosen for the initial analysis because it can suppress *ccpp-1* ciliary degeneration in amphid channel and phasmid cilia, indicating that it is the reverse enzyme of *ccpp-1* in that cell type (O'Hagan et al., 2011). *ccpp-1* has other reverse enzymes in other cell types; whether these

regulate the localization of NPHP-2 in those cell-types is wholly unknown.

The genetic interactions between the doublet region SynDyf network and *hdac-6* strongly, though not strictly, suggest that acetylation plays a major role in the function of the InvC and doublet region. Because the targets of *hdac-6* are unknown, analysis is difficult. As *hdac-6* is a general antagonist to ciliogenesis, it is not surprising that NPHP-2, ARL-13, and UNC-119 all localize properly in *hdac-6* mutants. If acetylation of some target is required for proper InvC biogenesis, then localization defects would be evident in two conditions. First, overexpression of HDAC-6 should lead to a reduction in total acetylation levels of its target, possibly leading to InvC and doublet region localization defects. Second, once the target of HDAC-6 is found, then deleting it should also lead to localization defects.

Because trying to identify *hdac-6* targets has been fruitless due to the paucity of relevant data regarding acetylated ciliary proteins (Li et al., 2010), an unbiased approach must be taken. Initially, it should be established whether or not *hdac-6* is functioning as a deacetylase in cilia. This can be achieved by mutating a residue in the two active sites of HDAC-6, and then determining if inactive HDAC-6 can prevent suppression of Dyf defects. If HDAC-6 is not functioning as a deacetylase, its catalytic domains may only be functioning in binding of acetylated targets; this role can be tested by replacement of a residue in the active site to a bulky residue, preventing bending. Regardless of whether the deacetylase function of *hdac-6* is required for its ciliary activity, a screen for physical interactors of HDAC-6 can be performed. A physical interaction screen would provide valuable data in both *C. elegans* and mammalian studies; an alternative screen, a screen for suppression of *hdac-6* mediated suppression, would not be possible because of the number of unrelated Dyf genes that would be found (*hdac-6* suppression is specific to only the doublet region SynDyf network). A third, slightly biased, alternative would be to look for overlaps in the mammalian acetylome and genes possessing an

X-box or having higher expression in ciliated neurons (Blacque et al., 2005; Efimenko et al.,

2005). Candidates could then be tested for ciliary localization of the protein, and Dyf defects and

NPHP-2 mislocalization in the gene mutant.

4.2.1.6 – Extracellular/environmental interactions.

All of the previous discussions presuppose that the factors required for InvC organization all lay

within the cilium itself. In many mammalian cells, the cilia base is placed several microns within

the cell, and the membrane forms a circular invagination, called the ciliary pocket, around the

cilia base (Molla-Herman et al., 2010). This cilia pocket may mediate the span of the InvC

through interactions between the cilium and either the extracellular matrix filling the pocket, or

the plasma membrane forming the other side of the pocket. In *C. elegans* amphid neurons,

amphid cilia lie within the amphid pore, which is formed from the amphid sheath and socket

cells (Perkins et al., 1986). In the distal portion of the pore, cilia are bundled tightly and are in

close contact with the socket cell. The level of the transition between the socket and sheath

cells marks the transition between the doublet and singlet regions of the cilium; at this level,

cilia are still tightly bundled and closely associated with the glial cells. Further proximal, cilia are

spread out and are dissociated from the glial cells; here, they are primarily surrounded by

extracellular matrix filling the amphid pore. In both *C. elegans* and mammalian models, there

may be interactions between cilia and either the ECM or neighboring membrane. This is

supported by evidence in IMCD3 cells, which have cilia but no ciliary pocket, and have no strictly

defined InvC (Sang et al., 2011). In addition to the possibility of ECM-mediated ciliary

compartmentalization, in *C. elegans*, either sheath membrane or the membrane of nearby cilia

may mediate the size of the InvC; contact with other cilia may exclude InvC components such

that NPHP-2 localizes only in the proximal portion of the cilium where they are not bundled. If

extracellular interactions regulate ciliary compartmentalization, I predict that cilia placement

would correlate with both the length of the InvC (possibly patterned by ECM/sheath/other cilia) and the length of the doublet region (possibly patterned by sheath-socket transition).

4.2.2 – The role of Wnt signaling in *C. elegans* ciliated neurons

Mammalian Inversin has few established functions, including a well-characterized role in the regulation of Wnt signaling (Simons et al., 2005) (Discussed in 1.5.1 – Signal Transduction and Amplification). Canonical Wnt signal functions by derepressing β-catenin activity (Reviewed in Huang and He, 2008; MacDonald et al., 2009). An extracellular soluble Wnt ligand binds to the transmembrane receptor Frizzled. Frizzled then binds to and activates disheveled, which then recruits Axin and APC, which were bound to β-catenin; this, in turn, prevents them from binding GSK3β which phosphorylates beta-catenin; phosphorylated β-catenin is ubiquitinated and degraded. When Wnt ligand is present and the Axin/APC/GSK3β complex is dissociated, beta-catenin enters the nucleus, binds to TCF/LEF transcription factors, and induces transcription. Inversin interferes with this process by binding disheveled and targeting it for degradation; this prevents the activation of disheveled and then subsequent inactivation of the Axin/APC/GSK3β destruction complex. As a consequence of the downregulation of this pathway, a second Wnt induced pathway, the planar cell polarity pathway, is induced; as suggested by the name, the PCP functions in orienting cells that are part of two dimensional surfaces, including the orientation of cilia on these surfaces.

I did not explore this possible function of *nphp-2* in this work for two reasons. First, though the entire Wnt signaling pathway is present and does function in *C. elegans*, Wnt signaling has not been shown to function in ciliated neurons; establishing *C. elegans* as a viable model for ciliary Wnt signaling was beyond the scope of this project. Second, most of the mammalian work establishing Inversin as a Wnt modulator (Benzing et al., 2007; Lienkamp et al., 2010; Simons et

al., 2005) was completed before the localization of Inversin was characterized in detail (Hoff et

al., 2013; Nakata et al., 2012; Shiba et al., 2009; Shiba et al., 2010); thus, the models presented

in these earlier works are not compatible with the newer InvC complex model, as they draw

assumptions based on the previously believed cytosolic/cilia base localization of Inversin.

However, this avenue of research should continue to be explored in light of newer

advancements. NPHP-2 may physically interact with DSH-2 (shown in an uncontrolled yeast

two-hybrid experiment), tantalizing evidence that this pathway is conserved and functional

(Andrew Jauregui, PhD Thesis). It is difficult to analyze this pathway in *C. elegans* however, as all

three *dsh* genes (*dsh-1*, *dsh-2*, and *mig-5*) are required for viability, functioning in early

embryogenesis (Hawkins et al., 2005). *dsh-1* is expressed in unspecified neurons (McKay et al.,

2003), and has a second role in targeting ACR-16 to the post-synaptic region, which is required

for synaptic plasticity (Jensen et al., 2012). *dsh-2* is also reported to be expressed in unspecified

neurons, though no neuronal function has been reported (McKay et al., 2003). Both *mig-5* and

the *mom-5* Frizzled homolog are also reported to be expressed in the nerve ring, though

colabelling was not used (Hao et al., 2006; Wu and Herman, 2006).

An important future direction is to establish whether Wnt signaling is a downstream effect of

cilia functioning in *C. elegans*. To achieve this, it must be shown that in ciliated neurons, Wnt

signaling components are expressed, Wnt pathways are functional, Wnt pathway output can be

modulated by the cilium, and that Wnt components change localization and stability in response

to ciliary pathways. (1) To demonstrate that Wnt genes are expressed in ciliated neurons by

examining, in strains coexpressing a *daf-19* transcriptional reporter, transcriptional reporters of

all three Disheveled genes, all four frizzled genes, the Axin homologs *axl-1* and *pry-1*, the APC

homolog *apc-1*, the TCF homolog *pop-1*, and the β-catenin homolog *bar-1* (Harris et al., 2010).

(2) It should also be demonstrated that the Wnt pathway is active in ciliated neurons; this can

be achieved with use of a modified POPTOP system (Green et al., 2008). The POPTOP system

functions as readout of β-catenin activity. This system is viable in *C. elegans* and has been used

to study cell polarity (Green et al., 2008). (3) If the canonical Wnt pathway is functioning in

ciliated neurons, output of that pathway should be examined in various ciliary mutants, such as

nphp-2, TZ mutants, doublet region mutants, and mutants of the modulators *hdac-6* and *arl-3*.

Wnt output should also be examined in double mutants, as these processes may be regulated by

redundant pathways. In addition to Inversin, Nphp4 also has a demonstrated role in Wnt

modulation (Burckle et al., 2011); as *nphp-2* and *nphp-4* are redundant in ciliogenesis they may

also be redundant in Wnt modulation (though these pathways could be one and the same).

Additionally, to further refine the interaction between ciliary Wnt and ciliary pathways, Wnt

activation should be examined in worms expressing modified versions of NPHP-2, including the

N-terminal half, the C-terminal half, and full length missing the EF hand, D-box, and

SUMOylation signals; the D-box and SUMOylation signals in particular may play a role in Wnt

modulation as they be required for the targeted degradation of disheveled. (4) A final step

would be to examine the subcellular localization and intensity of Wnt components in different

ciliary mutants, which may reflect changing activation of the pathway by the cilium. (5) It may

also be desirable to examine physical interactions between Wnt components and ciliary

proteins. Though Inversin is known to physically interact with disheveled, other proteins may be

involved (Simons et al., 2005). Like NPHP-2, ARL-13 possesses a SUMOylation motif (which is

required for its function) (Li et al., 2012); additionally, PCP upregulation requires membrane

accumulation of disheveled (as opposed to the cytoplasmic disheveled targeted by Inversin).

This suggests that membrane associated-proteins may also modulate Wnt signaling. Establishing

C. elegans as a ciliary Wnt signalling model would provide valuable insight into control and

modulation of Wnt pathways.

4.2.3 – Regulating cilia placement

One of the earlier *nphp-2* phenotypes discovered was the misplacement of cilia (Warburton-Pitt et al., 2012). Using TZ fluorescent markers, it appeared that the bases of cilia were mispositioned, which prevented cilia from extending into the cilia pore and being exposed to the external environment. There were three possible defects that could lead to such a phenotype: dendritic extension defects, where the cilium is misplaced because of the failure of dendritic pathfinding, targeting, or tip anchoring pathways; ciliary anchoring defects, where the dendrite extends but the cilium cannot seat itself properly via interactions with neighboring cells or extracellular scaffolding; or glial cell defects, in which the cilium is anchored to glia or associated extracellular matrix, but the glia themselves are misplaced. These three possibilities are not mutually exclusive, and defects seen in different mutants may reflect these different underlying causes; this may also reflect the genetic redundancy which characterizes cilia genetics.

4.2.3.1 – Dendritic extension defects. Only the birth of amphid ciliated neurons is known in detail (Heiman and Shaham, 2009). After the final cell division and migration, the amphid cell body attaches to a site at the nose of the worm; this interaction is mediated by DEX-1, present on the neuronal membrane, and DYF-7, an ECM component. The anchoring site on the membrane is thought to be in association with the proto-cilium. Subsequently, the cell body migrates away from the nose, towards its final location within the nerve ring. As the cell body migrates, the physical attachment between the neuron and the ECM causes the membrane to stretch like taffy, elongating as the cell moves and forming the dendrite. Defects in the DEX-1/DYF-7 anchoring result in a cell body that has correctly migrated, but with a very short dendrite that does not extend more than a micron or two beyond the nerve ring.

Amphid cilia of *nphp-2* single and *nphp-2 nphp-4* double mutants only exhibit a slight

misplacement (3-5 microns) of cilia bases, which does not appear superficially similar to reported amphid Dex mutants (Figure 10). This suggests that *nphp-2* and TZ genes are not required for dendritic anchoring either singly or in combination. The mild misplacement defect may arise from alternative mechanisms; it may also represent defects in a hypothetical post-anchoring fine-tuning of cilia placement.

It is completely unknown whether phasmid dendrites are formed similarly. If they are not, the cell body may be placed prior to neurite outgrowth—cilia defects may perturb this outgrowth. Several ciliary genes that are part of the TZ and doublet region SynDyf networks, including *unc-119*, have been linked to neurite branching in *C. elegans*, and other SynDyf genes can be predicted to function in neurite pathfinding based on biochemical functions of their mammalian orthologs, including possible Wnt regulation by *nphp-2* (Ackley, 2014; Knobel et al., 2001; Zou, 2004).

Two striking pieces of evidence suggest both that phasmid dendrites form similarly to amphid dendrites and that ciliary components play a role in this process. First, overexpression of ARL-13 in *mks-5* mutants leads to a highly penetrant Dex phenotype in both amphids and phasmids (**Error! Reference source not found.**), similar in appearance to the reported Dex phenotype in *ex-1* and *dyf-7* mutants. These defects are not seen when ARL-13 is overexpressed in other *mks* mutant backgrounds; that this phenotype is only evident in *mks-5* mutants is unsurprising because of the role of *mks-5* as the master-patterning component of the MKS physical TZ module. Secondly, when determining the localization of NPHP-2 in an *mks-3; nphp-4* background, many animals exhibited a phasmid Dex phenotype, also similar to reported Dex phenotypes (Figure 30). In *mks-3; nphp-4* animals expressing CHE-13::YFP, cilia placement appears intermediate between a full Dex phenotype and the misplacement seen in *nphp-2* single mutants; this may suggest either overexpression of NPHP-2 as causing the Dex defect, or,

less likely, that overexpression of CHE-13 suppresses the defect.

Taken together, this data is suggestive of a link between dendritic extension and cilia genes, but is currently too insubstantial to draw firm conclusions.

4.2.3.2 – Ciliary anchoring defects. The subtle misplacement of cilia in cilia mutants may be due to failure of the cilium to position itself properly in relation to its external environs. Two regions of ciliated neurons are closely associated with anchoring: the TZ of the cilium, and the dendritic tip. I consider these in turn.

4.2.3.2.1 – TZ anchoring: Within a cilium at the TZ, the axoneme is linked to the membrane through a large complex composed in part of MKS and NPHP proteins (termed a "Y-Link" due to its appearance in early EM micrographs) (Perkins et al., 1986). The Y-links may interact with transmembrane proteins and phospholipids, which in turn can bind the ECM and neighboring cells; this direct attachment between the axoneme and its external milieu is what may determine cilia positioning. Components of other cilia compartments, including the basal body region, the periciliary membrane, and the InvC may also mediate physical interactions with the environment, though nothing is known of this. Additionally, a physical link between cilia and their environment is supported by recent evidence in male specific cilia indicates that intraciliary trafficking may be regulated by external ECM components, including *mec-5* and *mec-9* (Deanna DeVore, Personal Communication). Y-link organization is disrupted in many TZ mutants and in *nphp-2* mutants; this provides a plausible mechanism for cilia misplacement in these mutants (Warburton-Pitt et al., 2014). EM micrographs do not support or disprove this hypothesis, as a non-descript extracellular matrix surrounds the TZ region of the amphid bundle (no good quality phasmid EMs exist), in contrast with the aqueous, empty pore that surrounds the doublet and singlet regions (Perkins et al., 1986).

4.2.3.2.2 – Dendritic Tip Anchoring: Anchoring between the dendritic tip and the environment appears to be primarily mediated by tight junctions (Perkins et al., 1986). Both Nphp4 and Inversin localize to tight junctions in some mammalian tissue types, though these tight junctions are not in association with cilia (Delous et al., 2009; Nurnberger et al., 2002). In *C. elegans*, the orthologs NPHP-4 and NPHP-2 do not appear to localize to this region of the cell in most cell types, though a cursory examination shows that NPHP-2 may localize to this region in the ray cilia of male worms (**Error! Reference source not found.**). Ciliary proteins may function in this egion transiently during early stages of ciliogenesis, as this period of development has not been well characterized. At least one ciliary protein, ARL-13, has already been demonstrated to have a developmentally dynamic localization pattern, though in its case, localization still does not extend out of the cilium (Cevik et al., 2013). On the other hand, EMs of *nphp-2* mutants indicate that tight junctions are intact, and disruption of tight junctions has not been reported in any cilia mutant (Warburton-Pitt et al., 2014). Taken together, the weak evidence in support and the moderate evidence against this proposition suggest that dendritic tip anchoring is not an important mechanism of ciliary anchoring. To test this suggestion, (1) tight junction components should be identified in the various ciliomes (2) and mutants of these components tested for cilia placement defects, (3) EM micrographs should be obtained from a number of cilia mutants and carefully analyzed, (4) and tight junction markers should be examined in cilia mutants.

4.2.3.2.3 – InvC anchoring? A more speculative possibility is that the InvC itself mediates anchoring between the cilium and the environment. Though Inversin is an intracellular, soluble protein, it does localize to adherens junctions in some cell types, indicating that Inversin can mediate cell-cell interactions (Nurnberger et al., 2002). This hypothesis has not previously been suggested because the InvC is not yet formed at the time of cilia docking during early

ciliogenesis (Williams et al., 2011). However, the ciliary vesicle docking and cilia anchoring steps

of ciliogenesis may be in fact two separate steps. If anchoring occurs after elongation of the

axoneme begins (and thus after InvC biogenesis), it is possible the InvC can regulate final cilia

placement; deletion of *nphp-2* would thus lead to mispositioning defects.

An alternative is that TZ anchoring is not initially static; recent evidence in *Drospohila* shows that

the TZ is "pushed" or "extruded" into the cytoplasm after initial ciliogenesis by axonemal

extension (Basiri et al., 2014). If such TZ mobility also exists in *C. elegans*, it may be that the InvC

is providing the primary ciliary anchoring after the TZ begins to move. The mild displacement

defects seen in *C. elegans* TZ and *nphp-2* mutants is on the same order of magnitude as would

be expected if there were defects in this "TX extrusion" pathway; this is signinifcantly different

from the more severe dendritic extension defects on cilia placement.

4.2.3.3 – Glial cell defects. Two types of glial cells support amphid channel and phasmid cilia

(among other cilia types): the socket cell, which surrounds the distal end of the cilia bundle, and

the sheath cell, which surrounds the proximal portion of the bundle and the majority of the

length of the dendrite (Figure 2) (Perkins et al., 1986). These glial cells have very different

morphologies: the socket cell wraps around the bundle of cilia and forms tight junctions with

itself, and is covered by a thick layer of ECM continuous with the cuticle, while the sheath cell

surrounds all ciliated dendrites individually, as they are embedded in and form tight junctions

with it, forming a non-simply connected topology. Additional tight junctions connect the sheath

and socket cells for a given cilia bundle together. The junction between the sheath and socket

cells lies in the same plane as the doublet to singlet transition within cilia, providing the subtle

suggestion that these cells may influence (or be influenced by) cilia compartmentalization.

Strong evidence links cilia placement to these glial cells. *mks-3; nphp-4* double mutants exhibit

misplaced cilia (as described above); visualizing the sheath cell with F16F9.3 reveals that the

sheath cell is also misplaced, but is still attached correctly to the cilium. Even more remarkably,

visualizing the socket cell with MAGI-1 in the same *mks-3; nphp-4* double mutant reveals that

the socket cell is properly placed at the ciliary pore adjacent to the cuticle (Williams et al., 2010).

As neither *mks-3* nor *nphp-4* are expressed in any cells other than ciliated neurons, cilia

positioning may actually dictate sheath placement, instead of the supposed other way round.

mks-3 and *nphp-4* may convey signals (possibly from signals transduced by the cilium itself) into

the sheath cell that instruct the sheath where to position itself. The dissociation of the socket

and sheath cells may arise from four distinct possibilities. (1) *mks-3* and *nphp-4* may actually be

expressed in sheath and socket cells at levels that are not detectable using standard techniques.

(2) *mks-3* and *nphp-4* may function in cilia, transmitting signals to the sheath cell that it requires

to properly coordinate its interaction with the socket cell. (3) The sheath cell is born alongside

the ciliated neuron, binds the dendritic tip of the ciliated neuron, and travels with the dendrite

as it makes its way to the cilia pore; if the cilia are misplaced, then the sheath cell never comes

into contact with the socket cell and no junctions can form. (4) The tight junction between the

socket and sheath cells is weak and is simply too physically weak to hold the cells together when

any amount of tensile force is applied between them (the tight junction acting as a permeability

barrier instead of a structural role). Of these possibilities, all four are possible in the phasmid

organ, but only 1, 2, and 4 are possible in the amphid organ.

mks-3; nphp-4 is the only genotype that has been examined for ciliary defects; future work

should focus on examining the roles of the other TZ and doublet region genes in this phenotype.

Placement defects in doublet region mutants may arise from their defects in TZ organization,

which subsequently interfere with ciliated neuron-glia interactions.

4.2.4 – Are NPHP-2 cell body accumulations linked to membrane trafficking pathways?

Above (4.2.1.2 – Membrane composition) I discussed the possible roles of membrane trafficking pathways in the origin of the InvC.

In addition to InvC localization, NPHP-2L also localizes to puncta within the cell body (Warburton-Pitt et al., 2012). It was originally hypothesized that these puncta represented centriolar localization, as a large number of ciliary genes have alternate roles in cell cycle regulation (Andrew Jauregui, PhD Thesis). However, I saw that there were infrequently two to three NPHP-2L puncta in amphid and phasmid cilia, and upwards of 6-8 puncta in male specific neurons; this eliminates the possibility of centriolar localization. Instead, these accumulations are reminiscent of membrane trafficking microcompartments seen with Rab8 pathway markers (Kaplan et al., 2010). NPHP-2, the InvC and ciliary compartmentalization have all been associated with membrane biology (See 1.4.5 – Membrane Dynamics of the Inv Compartment).

Rab8 is a small GTPase that functions in ciliogenesis and regulation of traffic between endosomes and the periciliary membrane (Bae et al., 2006; Moritz et al., 2001 Nachury et al., 2007; Omori et al., 2008). Mammalian Rab8 has been physically and genetically linked to many ciliary components, including CEP290 (MKS-4), a predicted lipid binding protein that lies downstream of Rab8 function (Tsang et al., 2008); CC2D2A (MKS-6), which mediates vesicle trafficking (Tallila et al., 2008); and in worms, the BBSome, which links IFT-A and IFT-B and regulates multiple aspects of IFT machinery assembly and function (both CEP290/MKS4 and CCD2A/MKS6 are components of the TZ MKS module). RAB-8 is targeted to the basal body, and then binds to the BBSome, which transports it into the cilium (Nachury et al., 2007).

While *rab-8* mutants do not have any overt ciliogenic defects in *C. elegans* cilia, overexpression leads to amphid and phasmid dye-filling defects, suggesting that RAB-8 may act as an antagonist

of ciliogenesis (Kaplan et al., 2010). Additionally, RAB-8 overexpression leads to ODR-10 (a ciliary

receptor) trafficking defects in AWB cilia. UNC-101/AP-1, a clathrin coat component, is also

required for proper ODR-10 targeting and amphid/phasmid ciliogenesis. As in the cilia of

unc-119 mutants, cilia of *unc-101* mutants do not have singlet regions, and like *nphp-2* mutants,

unc-101 mutant cilia have microtubule patterning defects and alterations in ciliary

glutamylation. RAB-8 overexpression phenocopies these aspects of *unc-101* mutants (Kaplan et

al., 2010; Ou et al., 2007).

In addition to their ciliary localization, RAB-8 and UNC-101 also localize to puncta in the cell

body in both mammalian cell models and *C. elegans* ciliated neurons (Kaplan et al., 2010). In

C. elegans, colabelling reveals that these puncta do not overlap, but instead directly abut,

marking two separate regions that function in subsequent steps in the same membrane

trafficking pathway: UNC-101 functions in vesicle budding from the trans-golgi network, and

then *rab-8* functions in endosomal sorting. (This can be seen in the case of ODR-10, which

colocalizes with RAB-8, indicating that it accumulates here after leaving the TGN but before

being trafficked to the cilium). Whether NPHP-2L puncta localize to one of these compartments

is unknown. Such a role for NPHP-2/Inversin would not be surprising: like Inversin, Ahi1/JBTS3

acts as a nexus physically linking multiple TZ modules (Sang et al., 2011); Ahi1 also binds Rab8,

and may play a role in membrane trafficking (Hsiao et al., 2009).

Separate (or forked) cilia membrane trafficking pathways may exist; these pathways function in

parallel to IFT trafficking pathways. The Arl13b/INPP5E complex and IFT are required for

PC2/PKD-2 trafficking, but Rab8, NPHP-2, and Arl3 are not (Bae et al., 2009; Cevik et al., 2010;

Kaplan et al., 2010; Zhang et al., 2013); *rab-8* and *unc-101* are required for ODR-10 trafficking,

but IFT is not (Kaplan et al., 2010). ARL-13 and IFT do not function in NPHP-2 trafficking; whether

rab-8 and *unc-101* do is unknown (Warburton-Pitt et al., 2014). *nphp-2* and *arl-13* genetically

interact in *C. elegans*, which suggests that these genes have multiple functions (and function in separate pathways) or that they function in the same pathway before (*arl-13*) and after (*nphp-2*) it forks. Additionally, *rab-8* is not required for TAX-2 and TAX-4 trafficking in ASK or AWB cilia, whereas *nphp-2* is required; *rab-8* deletion can suppress *tax-4* cilia membrane extension defects however (Wojtyniak et al., 2013).

Membrane trafficking is a hugely complex field; the above discussion scratches it only with a microtome. The focus of the following proposed set of experiments is to determine the role of NPHP-2 in cilia membrane trafficking pathways. The above data suggest that NPHP2 may function in *rab-8*, but not *cil-1*/INPP5E membrane pathways. (1) First, double labeling between NPHP-2L, RAB-8, and UNC-101 will reveal if NPHP-2 localizes to one of the *rab-8* pathway puncta. This will determine if NPHP-2L functions in, or is shuttled by, this system. NPHP-2L may not overlap with the other markers; whether this NPHP-2L punctum lies in close association with the RAB-8 and UNC-101 compartments will help determine if NPHP-2 actually marks a separate step in the process. (2) Second, NPHP-2 localization should be examined in *rab-8* and *unc-101* single and double mutants. This will determine if NPHP-2 is trafficked by this pathway. (3) Third, the localization of known *rab-8* pathway cargo (including ODR-10) should be examined in *nphp-2* single mutants, and *nphp-2*, *rab-8*, *unc-101* double and triple mutants. (4) Fourth, as membrane composition has a critical role in trafficking, membrane composition in these mutants should be determined, using the markers proposed above (4.2.1.2 – Membrane composition). (5) Fifth, *unc-119* functions in trafficking of membrane-associated proteins (and can insert and remove them from the membrane), genetically interacts with *nphp-2* and the membrane-associated *cil-1* and *arl-3* (the former, but not the latter, required for PKD-2 trafficking), and phenocopies *unc-101* ciliogenesis defects. Whether *unc-119* functions in membrane trafficking has not been thoroughly explored; if *unc-119* has a role, the localization of *rab-8* pathway cargos and *cil-1*

pathway cargoes should be determined in *unc-119* mutants, and the localization of UNC-119

should be determined in *rab-8* and *unc-101* mutants.

Together, this set of experiments will greatly expand our understanding of ciliary membrane

trafficking and targeting, linking them to other aspects of cilia biology, and possibly assigning

function to *nphp-2* and *unc-119*.

4.2.5 – Ciliary protein shuttles (non-IFT methods of active transport)

As discussed in Chapter 1 (1.4.4 – Establishing the Inv Compartment), a set of three protein

trafficking shuttles is associated with the localization of ciliary proteins: the Unc119b, the Pde6d,

and the BART shuttles. There is strong evidence that these shuttles play key roles in cilia import

and dynamics of the ciliary membrane, though the mechanisms and genetics are largely

unknown.

The Unc119b shuttle has been thoroughly characterized (Wright et al., 2011). Briefly, (1)

Unc119b binds myristoylated cargo through a conserved hydrophobic binding pocket, (2) the

Unc119b-cargo complex is translocated into the cilium, (3) the GTPase Arl3-GTP binds to the

complex, (4) Rp2 binds Arl3-GTP and causes Arl3-GTP to hydrolyze its GTP, (5) Arl3-GDP induces

conformational changes in the binding pocket of Unc119b that cause it to release its cargo, (6)

and then C5orf30 binds empty Unc119b and escorts it out of the cilium (Figure 6). This overview

reveals the paucity of details needed to fully understand the Unc119b shuttle: What are the

cargoes of Unc119b? How/where does Unc119b bind its cargoes? Unc119b can remove acylated

proteins from the membrane; what sort of membrane can it remove them from (e.g.,

intracellular vesicles, MVBs, plasma membrane)? How is the complex translocated into the

cilium? How does Arl3-GDP revert to Arl3-GTP? What triggers Rp2? How is the Unc119b-C5orf30

complex exported from the cilium? Can Unc119b target its cargoes to specific subdomains of the

cilium? Can membrane composition alter the function of Unc119b?

Many components of the Unc119b shuttle are conserved in *C. elegans* and localize to the cilium, suggesting the worm may be a valid model to examine this shuttle system. *UNC119B/unc-119*, *ARL3/arl-3*, and *RP2/rpi-2* are conserved (Harris et al., 2010); C5orf30 and the only known Unc119b cargo (InvC restricted Nphp3) are not. However, two other cargoes of UNC-119 have been identified (GPA-13 and ODR-3, both myristoylated G-protein subunits), *arl-3* deletion suppresses defects in *unc-119* mutants, and the InvC progenitor *nphp-2* genetically interacts with *unc-119* (Warburton-Pitt et al., 2014; Zhang et al., 2011). Additionally, mutations in *cil-7*, which encodes a myristoylated protein, lead to a reduction in total neuronal UNC-119 fluorescence; this suggests that CIL-7 may not be a cargo but be a regulator of UNC-119 (Julie Maguire, Personal Communication).

Several experiments are possible: (1) Screen the *C. elegans* genome for predicted N-terminal myristoylated proteins, and cross-reference this list with genes containing an X-box. This list would constitute possible UNC-119 binding partners, and should not be longer than a few dozen genes. (2) Examine localization of these predicted binding partners in *unc-119* mutants. (3) Once two or three proteins have been identified that require *unc-119* for proper localization, then they can be used to dissect the *unc-119* shuttle; two or three proteins are required so that conclusions regarding the shuttle can be generalizable. Questions that can explored using UNC-119 cargo reporters include the roles of *rpi-2*, *arl-3*, and *nphp-2* in ciliary restriction and release of cargoes from UNC-119, the role of the TZ in ciliary translocation, and whether IFT is required. This experiment will hopefully resolve the conundrum of why *arl-3* deletion suppresses *unc-119* defects. The current model of Unc119b shuttle function predicts that *arl-3* defects should phenocopy *unc-119*; it may be that the shuttle and ciliogenesis roles of *unc-119* are separate. (4) The role of *unc-119* in singlet region biogenesis can also be explored: *unc-119*

mutants have defects in biogenesis or singlet region protein localization. *mec-12*, which encodes

an alpha-tubulin, is a likely candidate for this, as its mammalian ortholog is myristoylated.

C. elegans may also be a useful model to study the Pde6d protein shuttle. Pde6d is closely

related to Unc119b, and functions similarly: it binds farnysylated proteins through a

hydrophobic pocket, the shuttle-cargo complex is shuttle into the cilium and is bound by

Arl2/3/13, of which hydrolysis of Arl3-GTP triggers the release of the cargo (Humbert et al.,

2012). However, these details are not certain and I have drawn them largely through inference

and comparison with the Unc119b shuttle. Many of these components too are conserved in

C. elegans, including all three *arl* genes, *PDE6D/pdl-1*, and a possible cargo, *INPP5E/cil-1* (Bae et

al., 2009; Harris et al., 2010). Curiously, many of these components are specifically linked to

PKD-2 trafficking in male ciliated neurons, suggesting that this shuttle may function specifically

in these cell types. Initial proposed experiments regarding this shuttle serve to establish that it

does indeed exist, as opposed to the Unc119b experiments, which serve to clarify the

mechanism and targets. First, the epistatic interactions between these shuttle components

should be established by examining localization of components in mutant animals missing other

components. Second, the cargo binding pocket of PDL-1 should be altered such that it can no

longer bind farnysl groups; the localization of this mutant PDL-1 should be examined to

determine whether PDL-1 functions as a cargo shuttle or whether the binding pocket regulates

the function and localization of PDL-1. Third, the relationship between the various *arl*s that bind

PDL-1 is muddled; this model can be used to test the interactions and requirements of these *arl*s

by examining CIL-1 localization in the arl mutants (or PKD-2::GFP, as CIL-1::GFP is difficult to

construct), and animals with ARL constitutively bound to GTP or GDP. Fourth, bioinformatic

databases should be used to try to identify other pathway components, both upstream and

downstream from *pdl-1*. Large physical and genetic databases exist for both mammalian models

and *C. elegans*. Finally, as PKD-2 localization defects have been demonstrated to be largely due

to defects in extracellular vesicle pathways, and the biogenesis of these vesicles is intimately

tied to membrane biology, it would be unsurprising if the PDL-1 shuttle functioned in this

pathway, perhaps by loading membrane-associated proteins onto vesicle membranes.

The BART shuttle, also related to the Unc119b shuttle is almost completely uncharacterized

(Bailey et al., 2009; Sharer et al., 2002). BART (Binder of Arl2) is not conserved in *C. elegans*, so it

is unlikely that *C. elegans* would be a viable model to characterize this pathway. Additionally,

BART has not been associated with cilia and has only been associated with mitochondrial

transport and centrosomal processes.

4.2.6 – The TZ and doublet region may be dynamic

Several pieces of evidence suggest that ciliary protein localization and compartmental

composition are dynamic depending on developmental stage or environmental conditions,

including physical interactions between InvC and TZ proteins (Sang et al., 2011), localization of

ARL-13 in L1 stage worms (Cevik et al., 2013), and the role of *nphp-2* in cilia positioning

(Warburton-Pitt et al., 2014; Warburton-Pitt et al., 2012). Though this assessment appears

superficially facile, it is not necessarily obvious in *C. elegans*, as cilia form only on terminally

differentiated neurons, and likely do not go through the cycle of retraction and growth as do

cilia of other organisms (Perkins et al., 1986). Of note is the fact that ciliogenesis is plastic: in

che-2 mutants, which have no cilia, CHE-2 expression *at any time* in the animal's life, including

the adult stage, can rescue *che-2* mutant defects, allowing a functional cilium to grow (Fujiwara

et al., 1999). (See also 4.2.3 – Regulating cilia placement – InvC anchoring).

4.2.6.1 – Evidence 1: TZ localization of InvC and doublet region components. The first

suggestion that cilia are not static arose from physical interaction experiments. Work in

mammalian systems revealed that NPHP-2/Inversin and Nphp3 physically interact with

components of the transition zone (Sang et al., 2011; Andrew Jauregui, PhD Thesis). This is

somewhat peculiar as the localization of NPHP-2/Inversin and Nphp3 do not overlap with the TZ;

this may be explained by (1) transient localization, (2) low quantities of TZ localized protein, or

(3) developmental stage specific localization. Addressing the first possibility, it was found that

Nphp3 is targeted to the TZ before it is imported into the cilium; this was only observable when

certain domains of Nphp3 were deleted, causing it to accumulate at the TZ—Nphp3 TZ

localization was too transient to be visualized otherwise (Nakata et al., 2012). It is still unknown

when and why NPHP-2/Inversin interacts with TZ components, though it may also be for ciliary

targeting. NPHP-4 physically interacts with the N-term ankyrin repeats of NPHP-2 (Andrew

Jauregui, PhD thesis); an important experiment would be to determine the localization of the

N-terminal portion of NPHP-2 (this has only been done in specialized AWB cilia, where the

ankyrin repeat portion was targeted to the cilium but localized along all the AFD branches

[Wojtyniak et al., 2013]). The second possibility, that the quantities on InvC and doublet region

proteins residing at the TZ are too small to visualize, is not easily addressed. Several methods to

increase a possible dim signal include use of a sensitive confocal microscope, use of tandem GFP

tagged protein (e.g., NPHP-2::GFP::GFP::GFP), or use of anti-GFP antibodies (as multiple

antibodies can bind to a single target, whether the target be the protein of interest or the

primary antibody).

4.2.6.2 – Evidence 2: Doublet region protein localization is developmentally dynamic. A

surprising recent discovery by the Blacque Lab was that ARL-13 localization is not static through

development, and that during L1, ARL-13 localized along the entire phasmid cilium and

undergoes IFT (Cevik et al., 2013). It is unknown whether this represents an earlier stage of

ciliogenesis, or whether it reflects a different function of the cilium during that life stage. Little

time has been spent characterizing cilia in these early stage larvae; most features of the cilium,

including ultrastructure, ciliary protein and membrane composition, and IFT composition and

velocities are unknown, so interpretation of the ARL-13 result is difficult. I examined the

localization of NPHP-2 in L1 animals, and found that it was still restricted to the proximal cilium

(Warburton-Pitt et al., 2014). As ARL-13 is generally associated with microtubule doublets, it is

tempting to speculate that at this stage the entire cilia shaft is doublets, and that because the

InvC is not organized by ultrastructure, it appears similar to in adults. This question is rich with

possibility, and entails many further experiments and questions. In addition to the unknowns

outlined (ultrastructure and IFT) above, other salient aspects to investigate include

characterizing glutamylation, looking at localizations of TZ and doublet region proteins,

examining localization in conjunction in *dex-1* and *dyf-7* mutants (Heiman and Shaham, 2009),

looking at localization during embryogenesis, capturing a virtual time-lapse from L1 to L4 (made

by following an individual worm for only a few hours and then combining data from multiple

different staged worms together), and so on.

***4.2.6.3 – Evidence 3: Ciliary anchoring is mediated by* nphp-2.** (See also 4.2.3 – Regulating cilia

placement) *nphp-2* mutants exhibit misplaced cilia; because the InvC is not formed prior to

ciliary docking, InvC components cannot localize to the InvC and their localization may vary

depending on developmental stage. Ciliogenesis is a two-step process that begins with the

formation of a pericentriolar complex, which is followed by the binding of the ciliary vesicle, and

then extension of the TZ (Williams et al., 2011). At this point, the vesicle docks with the plasma

membrane, and then IFT begins and fully elongates the cilium. This model leads to several

questions: How does the ciliary vesicle identify the patch of membrane to which to will dock?

Are docking and anchoring synonymous or are they separate, temporally distinct steps? How

does an InvC component modulate cilium position when the InvC does exist prior to docking?

The second question suggests that Inversin may function in cilia anchoring after the formation of

the InvC, and does not entail dynamic, stage dependent localization. The third question, which

supposes that docking and anchoring are the same step, suggests that Inversin must localize to a

different part of the cilium during this early phase.

4.3 – Concluding Remarks

The primary cilium was once thought of as a functionless vestigial organelle. Further work

continually reveals hidden complexity in ciliary structure, composition, and function, yielding an

organelle that some have termed "the brain of the cell," an organelle that modulates processes

ranging from cell-cell adhesion to DNA damage response, from signal transduction to ECV

release, and from cell motility to mitosis.

Recent work has dissected TZ composition and layout using super-resolution microscopy,

revealing that the once thought to be homogenous TZ is in fact an intricately laid-out assembly.

Data suggests that this may be true for the InvC as well, possessing an Evc/Evc2

"micro-compartment", and membrane-associated and axoneme-associated complexes. A radical

interpretation may be that there is no distinct TZ and InvC, that they are one and the same, and

that the proximal ciliary localizations I observe are actually a gradient of continually varying

protein localizations, a striped compartment composed of many overlapping localization

patterns. The proteinaceous TZ Y-links have traditionally been used to delineate this

compartment, though whether all Y-links have identical composition, and whether Y-link

components can participate in other assemblies elsewhere is unknown.

The body of work characterizing the InvC fills in crucial holes in the grand picture, but as is

(happily) expected, has led to even more questions. How does it regulate aspects of ciliogenesis when it has yet to form at that stage? What sets up the InvC in the first place? Does it regulate biogenesis of the singlet region? How does it regulate IFT? How does it integrate all of the different functions ascribed to it? Are there even more ciliary micro-compartments that are still hidden to us? And finally, what is the relationship between the separate, yet inseparable, InvC and TZ?

4.4 – References

Ackley, B. D. (2014). Wnt-signaling and planar cell polarity genes regulate axon guidance along the anteroposterior axis in C. elegans. *Dev. Neurobiol.* **74,** 781-796.

Bae, Y. K., Kim, E., L'Hernault S, W. and Barr, M. M. (2009). The CIL-1 PI 5-phosphatase localizes TRP polycystins to cilia and activates sperm in C. elegans. *Curr Biol* **19,** 1599-607.

Bae, Y. K., Qin, H., Knobel, K. M., Hu, J., Rosenbaum, J. L. and Barr, M. M. (2006). General and cell-type specific mechanisms target TRPP2/PKD-2 to cilia. *Development* **133,** 3859-70.

Bailey, L. K., Campbell, L. J., Evetts, K. A., Littlefield, K., Rajendra, E., Nietlispach, D., Owen, D. and Mott, H. R. (2009). The structure of binder of Arl2 (BART) reveals a novel G protein binding domain: Implications for function. *J. Biol. Chem.* **284,** 992-999.

Basiri, M., Ha, A., Chadha, A., Clark, N., Polyanovsky, A., Cook, B. and Avidor-Reiss, T. (2014). A migrating ciliary gate compartmentalizes the site of axoneme assembly in drosophila spermatids. *Current Biology* **24,** 2622-2631.

Benzing, T., Simons, M. and Walz, G. (2007). Wnt signaling in polycystic kidney disease. *J. Am. Soc. Nephrol.* **18,** 1389-1398.

Blacque, O. E., Perens, E. A., Boroevich, K. A., Inglis, P. N., Li, C., Warner, A., Khattra, J., Holt, R. A., Ou, G., Mah, A. K. et al. (2005). Functional genomics of the cilium, a sensory organelle. *Curr Biol* **15,** 935-41.

Burckle, C., Gaude, H. M., Vesque, C., Silbermann, F., Salomon, R., Jeanpierre, C., Antignac, C., Saunier, S. and Schneider-Maunoury, S. (2011). Control of the wnt pathways by nephrocystin-4 is required for morphogenesis of the zebrafish pronephros. *Hum. Mol. Genet.*

Cevik, S., Hori, Y., Kaplan, O. I., Kida, K., Toivenon, T., Foley-Fisher, C., Cottell, D., Katada, T., Kontani, K. and Blacque, O. E. (2010). Joubert syndrome Arl13b functions at ciliary membranes and stabilizes protein transport in caenorhabditis elegans. *J Cell Biol* **188,** 953-69.

Cevik, S., Sanders, A. A., Van Wijk, E., Boldt, K., Clarke, L., van Reeuwijk, J., Hori, Y., Horn, N., Hetterschijt, L., Wdowicz, A. et al. (2013). Active transport and diffusion barriers restrict joubert syndrome-associated ARL13B/ARL-13 to an inv-like ciliary membrane subdomain. *PLoS Genet.* **9,** e1003977.

Chih, B., Liu, P., Chinn, Y., Chalouni, C., Komuves, L. G., Hass, P. E., Sandoval, W. and Peterson, A. S. (2011). A ciliopathy complex at the transition zone protects the cilia as a privileged membrane domain. *Nat. Cell Biol.* **14,** 61-72.

Delous, M., Hellman, N. E., Gaude, H. M., Silbermann, F., Le Bivic, A., Salomon, R., Antignac, C. and Saunier, S. (2009). Nephrocystin-1 and nephrocystin-4 are required for epithelial morphogenesis and associate with PALS1/PATJ and Par6. *Hum. Mol. Genet.* **18,** 4711-4723.

Dorn, K. V., Hughes, C. E. and Rohatgi, R. (2012). A smoothened-Evc2 complex transduces the hedgehog signal at primary cilia. *Dev. Cell.* **23,** 823-835.

Efimenko, E., Bubb, K., Mak, H. Y., Holzman, T., Leroux, M. R., Ruvkun, G., Thomas, J. H. and Swoboda, P. (2005). Analysis of xbx genes in C. elegans. *Development* **132,** 1923-1934.

Fujiwara, M., Ishihara, T. and Katsura, I. (1999). A novel WD40 protein, CHE-2, acts cell-autonomously in the formation of C. elegans sensory cilia. *Development* **126,** 4839-48.

Green, J. L., Inoue, T. and Sternberg, P. W. (2008). Opposing wnt pathways orient cell polarity during organogenesis. *Cell* **134,** 646-656.

Hao, L., Johnsen, R., Lauter, G., Baillie, D. and Burglin, T. R. (2006). Comprehensive analysis of gene expression patterns of hedgehog-related genes. *BMC Genomics* **7,** 280.

Harris, T. W., Antoshechkin, I., Bieri, T., Blasiar, D., Chan, J., Chen, W. J., De La Cruz, N., Davis, P., Duesbury, M., Fang, R. et al. (2010). WormBase: A comprehensive resource for nematode research. *Nucleic Acids Res* **38,** D463-7.

Hawkins, N. C., Ellis, G. C., Bowerman, B. and Garriga, G. (2005). MOM-5 frizzled regulates the distribution of DSH-2 to control C. elegans asymmetric neuroblast divisions. *Dev. Biol.* **284,** 246-259.

Heiman, M. G. and Shaham, S. (2009). DEX-1 and DYF-7 establish sensory dendrite length by anchoring dendritic tips during cell migration. *Cell* **137,** 344-355.

Hoff, S., Halbritter, J., Epting, D., Frank, V., Nguyen, T. M., van Reeuwijk, J., Boehlke, C., Schell, C., Yasunaga, T., Helmstadter, M. et al. (2013). ANKS6 is a central component of a nephronophthisis module linking NEK8 to INVS and NPHP3. *Nat. Genet.* **45,** 951-956.

Holtta-Vuori, M., Uronen, R. L., Repakova, J., Salonen, E., Vattulainen, I., Panula, P., Li, Z., Bittman, R. and Ikonen, E. (2008). BODIPY-cholesterol: A new tool to visualize sterol trafficking in living cells and organisms. *Traffic* **9,** 1839-1849.

Hsiao, Y. C., Tong, Z. J., Westfall, J. E., Ault, J. G., Page-McCaw, P. S. and Ferland, R. J. (2009). Ahi1, whose human ortholog is mutated in joubert syndrome, is required for Rab8a localization, ciliogenesis and vesicle trafficking. *Hum. Mol. Genet.* **18,** 3926-3941.

Huang, H. and He, X. (2008). Wnt/beta-catenin signaling: New (and old) players and new insights. *Curr. Opin. Cell Biol.* **20,** 119-125.

Humbert, M. C., Weihbrecht, K., Searby, C. C., Li, Y., Pope, R. M., Sheffield, V. C. and Seo, S. (2012). ARL13B, PDE6D, and CEP164 form a functional network for INPP5E ciliary targeting. *Proc. Natl. Acad. Sci. U. S. A.* **109,** 19691-19696.

Jensen, M., Hoerndli, F. J., Brockie, P. J., Wang, R., Johnson, E., Maxfield, D., Francis, M. M., Madsen, D. M. and Maricq, A. V. (2012). Wnt signaling regulates acetylcholine receptor translocation and synaptic plasticity in the adult nervous system. *Cell* **149,** 173-187.

Johnson, B. B., Moe, P. C., Wang, D., Rossi, K., Trigatti, B. L. and Heuck, A. P. (2012). Modifications in perfringolysin O domain 4 alter the cholesterol concentration threshold required for binding. *Biochemistry* **51,** 3373-3382.

Kaplan, O. I., Doroquez, D. B., Cevik, S., Bowie, R. V., Clarke, L., Sanders, A. A., Kida, K., Rappoport, J. Z., Sengupta, P. and Blacque, O. E. (2012). Endocytosis genes facilitate protein and membrane transport in C. elegans sensory cilia. *Curr. Biol.* **22,** 451-460.

Kaplan, O. I., Molla-Herman, A., Cevik, S., Ghossoub, R., Kida, K., Kimura, Y., Jenkins, P., Martens, J. R., Setou, M., Benmerah, A. et al. (2010). The AP-1 clathrin adaptor facilitates cilium formation and functions with RAB-8 in C. elegans ciliary membrane transport. *J. Cell. Sci.* **123,** 3966-3977.

Kim, H. M., Choo, H. J., Jung, S. Y., Ko, Y. G., Park, W. H., Jeon, S. J., Kim, C. H., Joo, T. and Cho, B. R. (2007). A two-photon fluorescent probe for lipid raft imaging: C-laurdan. *Chembiochem* **8,** 553-559.

Knobel, K. M., Davis, W. S., Jorgensen, E. M. and Bastiani, M. J. (2001). UNC-119 suppresses axon branching in C. elegans. *Development* **128,** 4079-92.

Li, Y., Wei, Q., Zhang, Y., Ling, K. and Hu, J. (2010). The small GTPases ARL-13 and ARL-3 coordinate intraflagellar transport and ciliogenesis. *J Cell Biol* **189,** 1039-51.

Li, Y., Zhang, Q., Wei, Q., Zhang, Y., Ling, K. and Hu, J. (2012). SUMOylation of the small GTPase ARL-13 promotes ciliary targeting of sensory receptors. *J. Cell Biol.* **199,** 589-598.

Lienkamp, S., Ganner, A., Boehlke, C., Schmidt, T., Arnold, S. J., Schafer, T., Romaker, D., Schuler, J., Hoff, S., Powelske, C. et al. (2010). Inversin relays frizzled-8 signals to promote proximal pronephros development. *Proc. Natl. Acad. Sci. U. S. A.* **107,** 20388-20393.

MacDonald, B. T., Tamai, K. and He, X. (2009). Wnt/beta-catenin signaling: Components, mechanisms, and diseases. *Dev. Cell.* **17,** 9-26.

Mank, M. and Griesbeck, O. (2008). Genetically encoded calcium indicators. *Chem. Rev.* **108,** 1550-1564.

McKay, S. J., Johnsen, R., Khattra, J., Asano, J., Baillie, D. L., Chan, S., Dube, N., Fang, L., Goszczynski, B., Ha, E. et al. (2003). Gene expression profiling of cells, tissues, and developmental stages of the nematode C. elegans. *Cold Spring Harb. Symp. Quant. Biol.* **68,** 159-169.

Miyawaki, A., Llopis, J., Heim, R., McCaffery, J. M., Adams, J. A., Ikura, M. and Tsien, R. Y. (1997). Fluorescent indicators for Ca2+ based on green fluorescent proteins and calmodulin. *Nature* **388,** 882-7.

Molla-Herman, A., Ghossoub, R., Blisnick, T., Meunier, A., Serres, C., Silbermann, F., Emmerson, C., Romeo, K., Bourdoncle, P., Schmitt, A. et al. (2010). The ciliary pocket: An endocytic membrane domain at the base of primary and motile cilia. *J Cell Sci* **123,** 1785-95.

Moritz, O. L., Tam, B. M., Hurd, L. L., Peranen, J., Deretic, D. and Papermaster, D. S. (2001). Mutant rab8 impairs docking and fusion of rhodopsin-bearing post-golgi membranes and causes cell death of transgenic xenopus rods. *Mol Biol Cell* **12,** 2341-51.

Mukherjee, S., Zha, X., Tabas, I. and Maxfield, F. R. (1998). Cholesterol distribution in living cells: Fluorescence imaging using dehydroergosterol as a fluorescent cholesterol analog. *Biophys. J.* **75,** 1915-1925.

Nachury, M. V., Loktev, A. V., Zhang, Q., Westlake, C. J., Peranen, J., Merdes, A., Slusarski, D. C., Scheller, R. H., Bazan, J. F., Sheffield, V. C. et al. (2007). A core complex of BBS proteins cooperates with the GTPase Rab8 to promote ciliary membrane biogenesis. *Cell* **129,** 1201-13.

Nakata, K., Shiba, D., Kobayashi, D. and Yokoyama, T. (2012). Targeting of Nphp3 to the primary cilia is controlled by an N-terminal myristoylation site and coiled-coil domains. *Cytoskeleton (Hoboken)* **69,** 221-234.

Nurnberger, J., Bacallao, R. L. and Phillips, C. L. (2002). Inversin forms a complex with catenins and N-cadherin in polarized epithelial cells. *Mol Biol Cell* **13,** 3096-106.

O'Hagan, R., Piasecki, B. P., Silva, M., Phirke, P., Nguyen, K. C., Hall, D. H., Swoboda, P. and Barr, M. M. (2011). The tubulin deglutamylase CCPP-1 regulates the function and stability of sensory cilia in C. elegans. *Curr. Biol.* **21,** 1685-1694.

Ohno-Iwashita, Y., Shimada, Y., Waheed, A. A., Hayashi, M., Inomata, M., Nakamura, M., Maruya, M. and Iwashita, S. (2004). Perfringolysin O, a cholesterol-binding cytolysin, as a probe for lipid rafts. *Anaerobe* **10,** 125-134.

Omori, Y., Zhao, C., Saras, A., Mukhopadhyay, S., Kim, W., Furukawa, T., Sengupta, P., Veraksa, A. and Malicki, J. (2008). Elipsa is an early determinant of ciliogenesis that links the IFT particle to membrane-associated small GTPase Rab8. *Nat. Cell Biol.* **10,** 437-444.

Ou, G., Koga, M., Blacque, O. E., Murayama, T., Ohshima, Y., Schafer, J. C., Li, C., Yoder, B. K., Leroux, M. R. and Scholey, J. M. (2007). Sensory ciliogenesis in caenorhabditis elegans: Assignment of IFT components into distinct modules based on transport and phenotypic profiles. *Mol Biol Cell* **18,** 1554-69.

Pagano, R. E. and Chen, C. S. (1998). Use of BODIPY-labeled sphingolipids to study membrane traffic along the endocytic pathway. *Ann. N. Y. Acad. Sci.* **845,** 152-160.

Parasassi, T., Gratton, E., Yu, W. M., Wilson, P. and Levi, M. (1997). Two-photon fluorescence microscopy of laurdan generalized polarization domains in model and natural membranes. *Biophys. J.* **72,** 2413-2429.

Perkins, L. A., Hedgecock, E. M., Thomson, J. N. and Culotti, J. G. (1986). Mutant sensory cilia in the nematode caenorhabditis elegans. *Dev. Biol.* **117,** 456-487.

Pusapati, G. V., Hughes, C. E., Dorn, K. V., Zhang, D., Sugianto, P., Aravind, L. and Rohatgi, R. (2014). EFCAB7 and IQCE regulate hedgehog signaling by tethering the EVC-EVC2 complex to the base of primary cilia. *Dev. Cell.* **28,** 483-496.

Sang, L., Miller, J. J., Corbit, K. C., Giles, R. H., Brauer, M. J., Otto, E. A., Baye, L. M., Wen, X., Scales, S. J., Kwong, M. et al. (2011). Mapping the NPHP-JBTS-MKS protein network reveals ciliopathy disease genes and pathways. *Cell* **145,** 513-528.

Sharer, J. D., Shern, J. F., Van Valkenburgh, H., Wallace, D. C. and Kahn, R. A. (2002). ARL2 and BART enter mitochondria and bind the adenine nucleotide transporter. *Mol. Biol. Cell* **13,** 71-83.

Shiba, D., Manning, D. K., Koga, H., Beier, D. R. and Yokoyama, T. (2010). Inv acts as a molecular anchor for Nphp3 and Nek8 in the proximal segment of primary cilia. *Cytoskeleton (Hoboken)* **67,** 112-9.

Shiba, D., Yamaoka, Y., Hagiwara, H., Takamatsu, T., Hamada, H. and Yokoyama, T. (2009). Localization of inv in a distinctive intraciliary compartment requires the C-terminal ninein-homolog-containing region. *J. Cell. Sci.* **122,** 44-54.

Simons, M., Gloy, J., Ganner, A., Bullerkotte, A., Bashkurov, M., Kronig, C., Schermer, B., Benzing, T., Cabello, O. A., Jenny, A. et al. (2005). Inversin, the gene product mutated in nephronophthisis type II, functions as a molecular switch between wnt signaling pathways. *Nat. Genet.* **37,** 537-543.

Tallila, J., Jakkula, E., Peltonen, L., Salonen, R. and Kestila, M. (2008). Identification of CC2D2A as a meckel syndrome gene adds an important piece to the ciliopathy puzzle. *Am. J. Hum. Genet.* **82,** 1361-1367.

Tsang, W. Y., Bossard, C., Khanna, H., Peranen, J., Swaroop, A., Malhotra, V. and Dynlacht, B. D. (2008). CP110 suppresses primary cilia formation through its interaction with CEP290, a protein deficient in human ciliary disease. *Dev. Cell.* **15,** 187-197.

Verhey, K. J. and Gaertig, J. (2007). The tubulin code. *Cell Cycle* **6,** 2152-60.

Warburton-Pitt, S.R.F., Silva, M., Nguyen, K.C.Q., Hall, D.H., Barr, M.M. "The *nphp-2* and *arl-13* genetic modules interact to regulate ciliogenesis and ciliary microtubule patterning in *C. elegans*" (Accepted, PLOS Genetics)

Warburton-Pitt, S. R., Jauregui, A. R., Li, C., Wang, J., Leroux, M. R. and Barr, M. M. (2012). Ciliogenesis in caenorhabditis elegans requires genetic interactions between ciliary middle segment localized NPHP-2 (inversin) and transition zone-associated proteins. *J. Cell. Sci.* **125,** 2592-2603.

Williams, C. L., Li, C., Kida, K., Inglis, P. N., Mohan, S., Semenec, L., Bialas, N. J., Stupay, R. M., Chen, N., Blacque, O. E. et al. (2011). MKS and NPHP modules cooperate to establish basal body/transition zone membrane associations and ciliary gate function during ciliogenesis. *J. Cell Biol.* **192,** 1023-1041.

Williams, C. L., Masyukova, S. V. and Yoder, B. K. (2010). Normal ciliogenesis requires synergy between the cystic kidney disease genes MKS-3 and NPHP-4. *J. Am. Soc. Nephrol.* **21,** 782-793.

Wojtyniak, M., Brear, A. G., O'Halloran, D. M. and Sengupta, P. (2013). Cell- and subunit-specific mechanisms of CNG channel ciliary trafficking and localization in C. elegans. *J. Cell. Sci.* **126,** 4381-4395.

Wright, K. J., Baye, L. M., Olivier-Mason, A., Mukhopadhyay, S., Sang, L., Kwong, M., Wang, W., Pretorius, P. R., Sheffield, V. C., Sengupta, P. et al. (2011). An ARL3-UNC119-RP2 GTPase cycle targets myristoylated NPHP3 to the primary cilium. *Genes Dev.* **25,** 2347-2360.

Wu, M. and Herman, M. A. (2006). A novel noncanonical wnt pathway is involved in the regulation of the asymmetric B cell division in C. elegans. *Dev. Biol.* **293,** 316-329.

Zhang, H., Constantine, R., Vorobiev, S., Chen, Y., Seetharaman, J., Huang, Y. J., Xiao, R., Montelione, G. T., Gerstner, C. D., Davis, M. W. et al. (2011). UNC119 is required for G protein trafficking in sensory neurons. *Nat. Neurosci.* **14,** 874-880.

Zhang, Q., Hu, J. and Ling, K. (2013). Molecular views of arf-like small GTPases in cilia and ciliopathies. *Exp. Cell Res.* **319,** 2316-2322.

Zou, Y. (2004). Wnt signaling in axon guidance. *Trends Neurosci.* **27,** 528-532.